Characterisation of the *Arabidopsis thaliana* leucine-rich repeat receptor kinase subfamily XII in immune signalling

Jack Rhodes

The Sainsbury laboratory, Norwich

September 2019

This thesis has been submitted for the degree of Doctor of Philosophy

Abstract

Plant cells employ cell surface-localised receptors in order to perceive perturbations in their environment. One such context, central to plant survival, is the recognition of potential pathogens through pattern recognition receptors (PRRs). Upon recognition of apoplastic molecular patterns indicative of danger, PRRs induce pattern-triggered immunity. These molecular patterns can be of non-self (pathogen-associated molecular patterns; PAMPs) or modified-self (danger-associated molecular patterns; DAMPs) origins. Recognition of many PAMPs is lineage specific due to the phylogenetically restricted distribution of the cognate receptors. In general, PRRs can be transferred between angiosperm genomes to confer PAMP-recognition and induce quantitative, broad-spectrum disease resistance. As such, non-crop genomes represent a potential reservoir of exploitable PRRs to engineer resistance. Currently, this approach is constrained by the limited number of characterised PRRs. With this in mind, I sought to characterise additional members of the leucine-rich repeat receptor kinase subfamily XII from *Arabidopsis thaliana*; a known PRR-containing clade. I generated a range of genetic resources to screen a range of pathogens for gain- or loss-of-resistance. Within this subfamily, I focused on MIK2, whose mutants show defects in pollen tube guidance, salt stress tolerance, cell wall integrity sensing, *Fusarium oxysporum* resistance and root skewing. Our data revealed that loss of *MIK2* leads to defects in basal ROS production and transcriptomic homeostasis. Moreover, we showed that *mik2* mutants are differentially affected in elicitor-induced reactive oxygen species production, revealing an undescribed elicitor-based dichotomy. Through this work, I identified the recently described DAMP SCOOP12 is a likely ligand for MIK2. Furthermore, analysis of transcriptional changes in *mik2* revealed a novel phytocytokine-like peptide, which is transcriptionally upregulated in *mik2*. The insights gained through this work further our understanding of how plants recognise and potentiate danger signals and integrate these into physiological responses.

Table of Contents

List of Publications 8
Acknowledgements 9
Abbreviations 10
General introduction 13
1.1 Abstract 13
1.2 Fundamentals of leucine-rich repeat receptor kinase signalling 13
1.2.1 Ligand-binding to LRR-RKs induces heterodimeric receptor complex formation 13
1.2.2 Signalling downstream of leucine-rich repeat receptor kinase complexes 15
1.3 Receptor kinases in sensing a cells local environment 18
1.3.1 Receptor kinases in development 18
1.3.2 Receptor kinases in reproduction 21
1.3.3 Receptor kinases as sensors of the abiotic environment 21
1.3.4 Receptor kinases as sensors of the biotic environment 22
1.3.5 Sensors of modified self 27
1.3.6 Receptor kinases as sensors of cell wall integrity 27
1.3.7 Concluding remarks 30
1.4 Regulation of LRR-RK receptor kinases 30
1.4.1 Inter-RK regulation 31
1.4.2 Regulation by kinase inhibitors 33
1.4.3 Regulation by localisation 34
1.4.4 Regulation of RKs by endocytosis 35
1.5 Evolutionary history of receptor kinases and its link with function 36
1.5.1 RKs are massively expanded in plant lineages 36
1.5.2 Expansion rates of RK subfamilies vary and are linked to biotic stress responces 36
1.6 Use of pattern recognition receptors in the field 37
1.7 Identification of PRRs 38
1.7.1 Forward genetics 38
1.7.2 Reverse genetics 39
1.7.3 Biochemical approaches 39
1.8 Concluding remarks 41
1.9 Aims of this thesis 41
Material and methods 42
2.1 Materials 42
2.1.1. Plant materials 42
2.1.2. Bacterial and fungal materials 44
2.1.3. Antibiotics 45

2.1.4. Antibodies 46
2.1.5 Peptides 46
2.1.6 *in silico* resources 47
2.1.7. Oligonucleotides 47
2.2 Methods 48
2.2.1 Molecular biology methods 48
2.2.2 Biochemistry methods 50
2.2.3 Transformation and transient expression 51
2.2.3 Physiological assays 52
2.2.4 Pathogen assays 54
Characterisation of the *Arabidopsis thaliana* leucine-rich repeat receptor kinase subfamily XII 58
3.1 Summary 58
3.2 Introduction 58
3.3 Results 61
3.3.1 LRR-RK subfamily XII from *Arabidopsis thaliana* 61
3.3.2 *XII2* expression appears to be root-specific 63
3.3.3 Is xup25 a PAMP recognised by *Arabidopsis*? 63
3.3.4 The cytoplasmic domains of most members of the *Arabidopsis* LRR-RK subfamily XII can induce early outputs indicative of PTI in *Solanaceae* 64
3.3.5 Generation of stable *Arabidopsis* transgenic lines expressing EFR:XII chimeras 67
3.3.6 Kinase activity of XIIa LRR-RKs is differentially required for ROS and calcium signalling 69
3.3.7 Gain of function in tomato 72
3.3.8 Loss of function in *Arabidopsis* 73
3.4 Discussion 83
3.4.1 Subfamily XIIa LRR-RKs as potential PRRs 83
3.4.2 Chimeric receptors as an approach to characterise cytoplasmic domain output 83
3.4.3 Quantitative differences in output – a potential for PRR engineering? 84
3.4.4 Kinase activity requirement for RK cytoplasmic domain function 84
3.4.5 Gain-of-resistance as an approach to identify novel PRRs 84
3.4.6 Merits and limitations *in planta* expression of RKs to assess function 86
3.4.7 Loss-of-function as an approach to identify novel PRRs 86
3.4.8 Concluding remarks 87
Phenotypic characterisation of *mik2* reveals roles in cell wall integrity perception, root growth, pathogen resistance and regulation of reactive oxygen species production 88
4.1 Abstract 88
4.2 Introduction 88
4.2.1 Cell wall integrity sensing 88
4.2.2 The role of ROS and regulation of RBOHD in plant immunity 89

4.2.3 *mik2* - a multifaceted mutant....91
4.3 Results....92
4.3.1 *MIK2* is required for responses to cellulose biosynthesis inhibition....92
4.3.2 *mik2* mutants display a root skewing phenotype....93
4.3.3 *mik2* mutants have impaired to salt stress tolerance....93
4.3.4 *mik2* mutants are more susceptible to *Fusarium oxysporum* infection....99
4.3.5 mik2 mutants exhibit impaired flg22-induced ROS production....99
4.3.6 MIK2 differentially regulates ROS production in response to diverse elicitors....100
4.3.7 Constitutive upregulation of background ROS in *mik2*....110
4.3.8 Late ROS production in *bak1* is *MIK2*-dependent....111
4.3.9 The *mik2 bak1* double mutant is dwarf....117
4.3.10 Precocious senescence in *mik2*....117
4.3.11 Transcriptomic perturbations in *mik2*....117
4.4 Discussion....125
4.4.1 Direct or indirect effects for MIK2....125
4.4.2 Cell wall integrity sensing....125
4.4.3 Root skewing....126
4.4.4 *Fusarium* resistance....126
4.4.5 MIK2 differently regulates ROS production in response to diverse elicitors....127
4.4.6 Why are the differential phenotypes ROS specific?....128
4.4.7 Transcriptomic changes....128
4.4.8 Involvement of the MDIS/MIK complex....129
The JRPs represent a novel family of phytocytokine-like peptides....130
5.1 Abstract....130
5.2 Introduction....130
5.2.1 'Self versus non-self' to the 'danger hypothesis' – the involvement of self in immune signalling....130
5.2.2 Modulation of plant immunity by phytocytokines....131
5.2.3 The role of small peptides in *mik2*....135
5.3 Results....136
5.3.1 Multiple genes encoding potential small secreted peptides are upregulated in *mik2*....136
5.3.2 JRP-like sequences are present in both *Rosid* and *Asterid* lineages....137
5.3.3 JRPs are transcriptionally upregulated by biotic stress....141
5.3.4 Exogenous JRP4 application induces BAK1-dependent, and SOBIR1-independent early immune responses....141
5.3.5 JRP4-induced ROS production is reduced in *mik2*....142
5.4 Discussion....146
5.4.1 JRPs - a novel family of phytocytokines?....146
5.4.2 JRP processing and release....146

5.4.3 The JRP perception mechanism 147
5.4.4 Could JRP peptides contribute to *mik2* phenotypes? 147
5.4.5 Concluding remarks 148
The Arabidopsis SCOOP12 peptide represents a putative ligand for MIK2 149
6.1 Summary 149
6.2 Introduction 149
6.3 Results 150
6.3.1 A subset of the *PROSCOOP* genes are transcriptionally responsive to elicitors 150
6.3.2 Responses to SCOOP12 are BAK1-dependent but SOBIR1-independent 151
6.3.3 Responses to SCOOP12 are MIK2-dependent 154
6.3.4 MIK2 confers responsiveness to SCOOP12 in *N. benthamiana* 156
6.3.5 SCOOP12 induces MIK2-BAK1 complex formation 156
6.3.6 MIK2 kinase activity is required for SCOOP12 responsivity 156
6.3.7 Sequences with a high degree of similarity to SCOOP12 are present within pathogen proteomes 157
6.4 Discussion 161
6.4.1 Is MIK2 the receptor for SCOOP12? 161
6.4.2 SCOOP12 as a phytocytokine 161
6.4.3 A SCOOP12-like motif is present in microbial proteins 162
6.4.4 The PROSCOOP family and MIK2 are both restricted to the *Brassicaceae* 163
6.4.5 To what extent can the role of MIK2 in SCOOP12 perception explain the diverse *mik2* phenotypes? 163
6.4.6 Concluding remarks 164
General Discussion 165
7.1 Identification of novel pattern recognition receptors to engineer resistance 165
7.1.1 Chimeric receptors 165
7.1.2 Heterologous expression 166
7.1.3 Loss-of-function. 167
7.1.4 Identification of PRR ligands 167
7.2 The role of MIK2 169
7.3 Why so many phytocytokines? 171
7.4 Outlook and summary 172
Bibliography 174
Appendices 213

List of Publications

Van der Does, D., Boutrot, F., Engelsdorf, T., **Rhodes, J.,** McKenna, J.F., Vernhettes, S., Koevoets, I., Tintor, N., Veerabagu, M., Miedes, E., et al. (2017). The Arabidopsis leucine-rich repeat receptor kinase MIK2/LRR-KISS connects cell wall integrity sensing, root growth and response to abiotic and biotic stresses. PLOS Genet. 13, e1006832.

Ikeuchi, M., and **Rhodes, J**. (2017). Latest Advances in Plant Development and Environmental Response: The Inaugural Cold Spring Harbor Asia Plant Biology Meeting in Japan. Plant Cell Physiol. 58, 1286–1290.

Acknowledgements

I would like to thank Cyril Zipfel for the opportunity to join the lab. Cyril's mentorship has guided my scientific and professional development over the last 4 years. I am exceptionally grateful that Cyril has encouraged me to develop and pursue my own ideas and interests throughout my PhD. I have always appreciated Cyril's investment in my progress and his professional and dynamic leadership.

I would like to thank all the Zipfel lab members for creating such a stimulating, rigorous and invigorating working environment. Your feedback has had a huge effect on my scientific development. I am especially thankful to Dieuwertje Van der Does for helping me to find my feet upon joining the lab and the Nick Holton, Freddy Boutrot, Kathrin Thor and Martin Stegmann for sharing their opinions, advice and expertise. Special thanks go to Lena Stransfeld, for her proficient organisation of the lab and sense of humour. I would like to thank Maria Derkacheva, Marta Bjornson and Kyle Bender for giving feedback on my thesis.

Thank you to Nick Talbot for hosting and supporting me in his lab for the past year. The Talbot lab has been incredibly welcoming, and I am grateful to all the lab for the fun, friendly and positive atmosphere. I would also like to thank Lars Østergaard for fruitful discussions during committee meetings.

I really valued being a TSLytherin, the student community at TSL provides a supportive and collegial atmosphere. I am especially fortunate for the friendships I developed with Jeoffrey George, Helen Brabham, Alicia Abarca and Jan Bettgenhaeuser during my time at TSL.

I am indebted to the support staff at TSL and the NRP horticultural services staff; their hard work has made my life considerably easier over the last 4 years.

I would also like to particularly thank Rosa Pérez, Patricia Olivares and Lucía Jordá for their support and friendship during my time at PlantResponse in Madrid.

I am grateful to BBSRC, The Gatsby Foundation, PlantResponce, The Genetics Society, The British Society for Plant Pathology and The Society for Industrial Chemistry for financially supporting my PhD.

Thank you to my family, especially Alice, for your love and support during this time.

Jack Rhodes,

The Sainsbury Laboratory, Norwich (September 2019)

Abbreviations

AM	ARBUSCULAR MYCORRHIZAL
ANJ	ANJEA
ANX	ANXUR
BAK1	BRI1-ASSOCIATED KINASE 1
BIK1	BOTRYTIS-INDUCED KINASE 1
BIR	BAK1-INTERACTING RECEPTOR-LIKE KINASE
BKI1	BRI1 KINASE INHIBITOR 1
BRI1	BRASSINOSTEROID INSENSITIVE 1
BRZ	BRASSINAZOLE
BUPS	BUDDHA'S PAPER SEAL
CASP	CASPARIAN STRIP MEMBRANE PROTEIN
CDPK	CALCIUM-DEPDEDENT PROTEIN KINASE
CEBiP	CHITIN OLIGOSACCARDIDE ELICITOR-BINDING PROTEIN
CEP	C-TERMINALLY ENCODED PEPTIDE
CEPR	CEP RECEPTOR
CERK	CHITIN ELICITOR RECEPTOR KIANSE 1
CIF	CASPERIAN STRIP INTEGRITY FACTORS
CLE	CLAVATA3/EMBRYO SURROUNDING REGION-RELATED
CLV1	CLAVATA1
COL-0	COLOMBIA
COR	CORONATINE
CORE	COLD SHOCK PROTEIN RECEPTOR
CRK	CYSTEINE-RICH RECEPTOR KINASE
CrRLK1L	*CATHARANTHUS ROSEUS* RLK1-LIKE
CuRe1	*CUSCUTA REFLEXA* RECEPTOR
DAB	3,3′-DIAMINOBENZIDINE
DAMP	DAMAGE ASSOCAIATED MOLECULAR PATTERN
DCB	2,6-DICHLOROBENZONITRILE
DORN1	DOES NOT RESPOND TO NUCLEOTIDES1
EFR	ELONGATION FACTOR TU RECEPTOR
EMS	ETHYL METHANESULFONATE
ENFOE	ENRICHED *FUSARIUM* OXYSPRUM EXTRACT
EPF	EPIDERMAL PATTERNING FACTOR
EPS	EXTRACELLULAR POLYSACCARIDE
ER	ERECTA

FER	FERONIA
FERE1	*FUSARIUM* ELICITOR REDUCED ELICITATION 1
FIR	FLS2-INTERACTING RECEPTRO KINASE
FLS2	FLAGELLIN SENSING 2
FLS3	FLAGELLIN SENSING 3
GFP	GREEN FLUORESCENT PROTIEN
GlcNAc	*N*-ACETYLGLUCOSAMINE
GPI	GLYCOSYLPHOSPHATIDYLINOSITOL
GSO1	GASSHO1
HERK1	HERCULES RECEPTOR KIANSE1
HSL2	HAESA-LIKE 2
IDA	INFLORESCENCE DEFICIENT IN ABSCISSION
IOS1	IMPAIRED OOMYCETE SUSEPTIBILITY
IRAK	INTERLEUKIN RECEPTOR-ASSOCIATED KINASES
ISX	ISOXABEN
LCO	LIPOCHITOOLOGOSACCARIDE
LIK1	LYSM-RLK1-INTERACTING KINASE
LORE	LIPOOLIGOSACCHARIDE-SPECIFIC REDUCED ELICITATION
LRR	LEUCINE-RICH REPEAT
LRX	LEUCINE-RICH EXTENSIN
LYK	LYSM-CONTAINING RECEPTOR-LIKE KINASE
LysM	LYSIN-MOTIF
MAPK	MITOGEN-ACTIVATE DPROTEIN KINASE
MDIS	MALE DISCOVERER
MIK	MALE DISCOVERER-INTERACTING RECEPTOR-LIKE KINASE
MLO	MILDEW RESISTANCE LOCUS O
NADPH	NICOTINAMIDE ADENINE DINUCLEOTIDE PHOSPHATE
NLP	NECROSIS AND ETHYLENE-INDUCING PEPTIDE 1-LIKE PROTEINS
OG	OLIGOGALACTURONIDES
PAMP	PATHOGEN ASSOCIATED MOLECULAR PATTERN
PBL	AVRPPHB SUSEPTIBLE 1-LIKE
PcBMM	*PLECTOSPHORELLA CUCUMERINA* PV. BMM
Pep	PLANT ELICITOR PEPTIDE
PEPR	PEP RECEPTOR
PIP	PATHOGEN-INDUCES PEPTIDE
PRC1	PROCUSTE1
PRK6	POLLEN RECEPTOR KINASE 6
PSK	PHYTOSULPHOKINE
PSKR	PHYTOSULPHOKINE RECEPTOR

PSY1	PLANT PEPTIDE CONTAINING SULFATED TYROSINE 1
PTO	*PSEUDOMONAS SYRINGAE* PV. *TOMATO*
PUB	PLANT U-BOX
PXY	PHLOEM INTERCALATED WITH XYLEM
RALF	RAPID ALKALINISATION FACTOR
RBOH	RESPIRATORY BURST OXIDATIVE HOMOLOG
RGF	ROOT GROWTH FACTORS
RGFR	ROOT GROWTH FACTOR RECEPTOR
RK	RECEPTOR KINASE
RLCK	RECEPTOR-LIKE CYTOPLASMIC KINASE
RLP	RECEPTOR-LIKE PROTEIN
RLU	RELATIVE LIGHT UNITS
ROS	REACTIVE OXYGEN SPECIES
RXEG1	RECEPTOR FOR XYLOGLUCAN-SPECIFIC ENDO-1,4-GLUCANASE 1
SAUR	SMALL AUXIN RESPONSIVE
SCOOP	SERINE-RICH ENDOGENOUS PEPTIDES
SERK	SOMATIC EMBRYOGENESIS RELATED RECEPTOR-LIKE KINASE
SGN3	SHENGEN 3
SIK1	SERINE/THREONINE KINASE 1
SOBIR1	SUPPRESSOR OF BIR1
SUB	STRUBBELIG
SYR1	SYSTEMIN RECEPTOR1
TDIF	TRACHAERY ELEMENT DIFFERENTIATION INHIBITORY FACTOR
TDR	TDIF-RECEPTOR
THE1	THESEUS1
TMM	TOO MANY MOUTHS
TXT	THAXTOMIN
WAK	WALL ASSOCIATED KINASE
Ws-2	WASSILEWSKJA-2
WUS	WUSCHEL
Xa21	*XANTHAMONAS ORYZAE* PR.*ORYZAE* RESISTANCE 21
XPS1	XANTHINE/URACIL PERMEASE FAMILY SENSING 1
ZIP1	*ZEA MAYS* IMMUNE SIGANLLING PEPTIDE

Chapter 1

General introduction

1.1 Abstract

The ability to perceive and transduce apoplastic stimuli across the plasma membrane is intrinsic to living organisms. Plants have evolved a suite of transmembrane receptor kinases to fulfil this function. Receptor kinases can bind extracellular ligands and activate downstream cytoplasmic signalling, resulting in cellular responses. They are fundamental to all aspects of plant biology with roles in development, cell fate determination, reproduction and defence. These functions are mediated by binding of endogenous and exogenous ligands present in the plant cells local environment. Here, I will provide an overview of our current knowledge of plant receptor kinase biology.

1.2 Fundamentals of leucine-rich repeat receptor kinase signalling

Receptor kinases consist of an apoplastic ectodomain connect via a single pass transmembrane α-helix to a conserved cytoplasmic kinase domain (Shiu and Bleecker, 2001*b*). They represent one of the largest gene families in plant genomes - ~2.5% of all *Arabidopsis thaliana* (here after *Arabidopsis*) protein encoding genes (Shiu and Bleecker, 2001*a*). Over recent years our understanding of how receptor kinases (RKs) function at the mechanistic level has increased substantially. This is especially true in regard to RKs with leucine-rich repeat (LRR) ectodomains, which represent approximal 50% of RKs (Gou *et al.*, 2010; Wu *et al.*, 2016; Fischer *et al.*, 2016; Xi *et al.*, 2019), and which I will focus upon in this text. These mechanistic insights have been guided by a synthesis of genetic, biochemical, and structural data (Hohmann *et al.*, 2017; Moussu and Santiago, 2019).

1.2.1 Ligand-binding to LRR-RKs induces heterodimeric receptor complex formation

Ectodomain interaction

LRR-RKs have bimodal distribution in ectodomain length and can be clustered into long and short ectodomain RKs (Xi *et al.*, 2019; Hohmann and Hothorn, 2019). The current paradigm dictates that ligand binding induces heterodimeric complex formation between a ligand-binding LRR-RK - with a long ectodomain - and a shape-complementary co-receptor, with a short ectodomain, frequently from the SERK family (SOMATIC EMBRYOGENESIS RELATED RECEPTOR-LIKE KINASE) (Ma *et al.*, 2016; Hohmann *et al.*, 2017). In almost

all cases the ligand acts as a molecular glue, physically interacting with the LRR motifs of both RKs. This mechanism is shared between numerous LRR-RKs despite recognising diverse ligands (She *et al.*, 2011; Sun *et al.*, 2013*b*,*a*; Santiago *et al.*, 2016; Zhang *et al.*, 2016*b*; Hohmann *et al.*, 2018*b*). In binary *in vitro* interactions, the ligand generally associates with receptor, but not the co-receptors (Hohmann *et al.*, 2017). However, the binding affinity can increase considerably when both the receptor and co-receptor are present (Santiago *et al.*, 2016). An exception is PHYTOSUFOKINE (PSK) perception. PSK binding induces allosteric changes to its receptor PSKR which stabilizes the island domain of the LRR for SERK-recruitment, with no physical PSK-SERK interaction (Wang *et al.*, 2015).

Whilst this model is well established for the binding of small ligands, the response to larger, folded, cysteine-rich peptides can also be SERK-dependent. The binding of the cysteine-rich peptides EPIDERMAL PATTERNING FACTORS (EPFs) to the ERECTA family (ERf) of LRR-RKs (along with the receptor-like protein TOO MANY MOUTHS (TMM)) enforce stomatal patterning (Geisler *et al.*, 2000; Nadeau and Sack, 2002; Shpak *et al.*, 2005; Hara *et al.*, 2007, 2009; Hunt and Gray, 2009; Kondo *et al.*, 2010; Sugano *et al.*, 2010; Abrash and Bergmann, 2010; Hunt *et al.*, 2010; Abrash *et al.*, 2011; Lee *et al.*, 2012). Interestingly, distinct EPFs are able to differentially promote or repress the stomatal lineage through the same ERf receptors in a SERK-dependent manner (Meng *et al.*, 2015; Zoulias *et al.*, 2018). Alignment of ER-EPF-TMM structure with resolved SERK-RK structures reveals that a hairpin loop of the EPF peptides would be at the hypothetical SERK interaction interface, potentially allowing SERK recruitment (Lin *et al.*, 2017).

The POLLEN RECEPTOR KINASE 6 (PRK6) recognises the LURE peptides which are also cysteine-rich (Takeuchi and Higashiyama, 2016). The PRK6 ectodomain binds to its ligands, the cysteine-rich LURE peptides, through the C-terminal loop of the LRR domain (Zhang *et al.*, 2017); this contrasts with other LRR-RKs which employ either the lateral or inner surfaces of the LRR helix for ligand binding (Hohmann *et al.*, 2017; Zhang *et al.*, 2017).

Much more ambiguity exists around the mechanistic basis of non-LRR-RK ligand binding, however, structural, genetic and biochemical data is beginning to answer some of these questions (Liu *et al.*, 2012; Hohmann *et al.*, 2017; Xiao *et al.*, 2019; Moussu and Santiago, 2019).

Whilst exceptions exist, in general, characterised LRR-RKs function through a conserved ligand-induced receptor-co-receptor ectodomain heterodimerisation mechanism (Hohmann *et al.*, 2017).

Cytoplasmic domain activation

The heterodimeric complex formation between ectodomains forces the cytoplasmic domains into proximity, which then facilitates a series of auto- and transphosphorylation events resulting in receptor activation (Wang *et al.*, 2008; Karlova *et al.*, 2009; Oh *et al.*, 2009; Yun *et al.*, 2009; Schulze *et al.*, 2010; Yan *et al.*, 2012; Perraki *et al.*, 2018). Chimeric receptors have revealed that the specificity of the signalling output is determined by the cytoplasmic domain of the ligand binding receptor (He *et al.*, 2000; Brutus *et al.*, 2010; Albert *et al.*, 2010; Hohmann *et al.*, 2018*b*).

It is remarkable that common SERK coreceptors are constituents of such diverse, often antagonistic, signalling complexes (Ma *et al.*, 2016; He *et al.*, 2018). This differential has been most extensively studied in the context of immune and brassinosteroid signalling which both rely on the BAK1/SERK3 (BRI1-ASSOCIATED KINASE 1) as a co-receptor (Li *et al.*, 2002; Chinchilla *et al.*, 2007). Interestingly, C-terminal tagging of BAK1 impairs its function in immune, but not brassinosteroid, signalling (Ntoukakis *et al.*, 2011). Furthermore, an allele of BAK1, *bak1-5*, with a point mutation in the kinase domain is specifically impaired in immune signalling, but not in brassinosteroid signalling or cell death control (Schwessinger *et al.*, 2011). Perraki *et al.* (2018) revealed that the dichotomy between these two pathways is encoded through a differential phosphocode on BAK1. This phosphocode is determined by specific residues within the cytoplasmic domain of ligand binding receptors.

Not all ligand-binding LRR-RKs are dependent upon SERK co-receptors. Genetic evidence suggests that sequence-related NIK/CIK/CLERK may fulfil similar functions (Hu *et al.*, 2018; Anne *et al.*, 2018; Cui *et al.*, 2018*a*; Ren *et al.*, 2019*a*); however structural data is still awaited. Additional LRR-RKs with short ectodomains, such as PRKs, have structural similarity to the SERKs, implying they could perform a similar function (Chakraborty *et al.*, 2018; Xi *et al.*, 2019).

Activation of receptor complexes triggers downstream signalling cascades, regulated by a plethora of cytoplasmic components to potentiate or suppress RK signalling.

1.2.2 Signalling downstream of leucine-rich repeat receptor kinase complexes

Receptor-like cytoplasmic kinases

Accumulating evidence shows that a diverse repertoire of RECEPTOR-LIKE CYTOPLASMIC KINASES (RLCKs) associate with LRR-RK complexes facilitating downstream signal transduction (Lin *et al.*, 2013; Liang and Zhou, 2018). RLCKs form part of the same monophyletic clade of kinases as RKs, but lack the transmembrane and extracellular domains (Shiu and Bleecker, 2001*a*). There are 147 RLCKs in the *Arabidopsis*

genome with specific RLCKs associating with defined LRR-RK complexes to confer downstream signalling. RLCKs are phosphorylated by RKs within the activated RK heterodimer (Liang and Zhou, 2018). This results in RLCK activation and subsequent phosphorylation of downstream signalling components and response executors (Liang and Zhou, 2018).

Within immune signalling the most notable players are BIK1 (BOTRYTIS-INDUCED KINASE1) and related PBLs (AVRPPHB SUSCEPTIBLE 1-LIKE), which act downstream of immune complexes to potentiate immune signalling (Lu *et al.*, 2010; Zhang *et al.*, 2010; Liu *et al.*, 2013*a*; Ranf *et al.*, 2014). Additional RLCKs have been shown to function

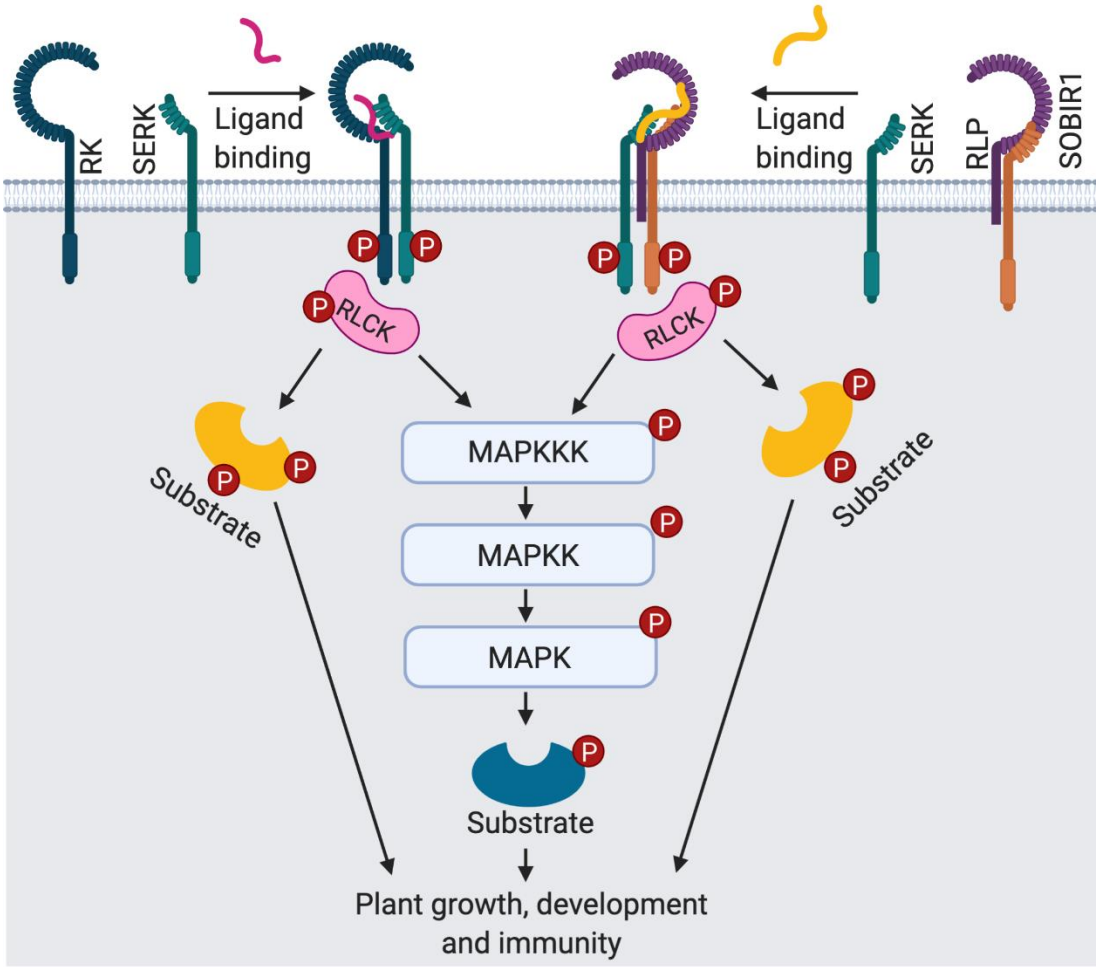

Figure 1. 1 A model of ligand-induced receptor activation and signal transduction in plants

Plasma membrane-localised LRR-RKs and LRR-RLPs facilitate the perception of endogenous and exogenous molecular patterns. RKs consist of an extracellular domain, transmembrane α-helix and cytoplasmic kinase domain. RLPs lack a cytoplasmic domain and form a constitutive interaction with SOBIR1, an adaptor RK. Ligand-binding induces heterodimerisation between the RK (or RLP-SOBIR1 complex) and a co-receptor RK, usually from the SERK family. This leads to phosphorylation and activation of the cytoplasmic kinase domains. RKs associate with and phosphorylate different cytoplasmic RLCKs upon complex activation. The cytoplasmic signal is then transduced via protein phosphorylation. This can be through the direct phosphorylation of substrates by RLCKs, however, activation of sequential MAPK cascades is shared downstream of many RK complexes. Phosphorylation of substrates regulates plant immunity, growth and development, either directly or through secondary signalling modules.

downstream of immune RK complexes but their roles are less pronounced, and potentially kinase activity-independent (Shi *et al.*, 2013; Sreekanta *et al.*, 2015; Kong *et al.*, 2016; Ren *et al.*, 2019*b*; Majhi *et al.*, 2019).

Interestingly, BIK1 accumulation is rate-limiting in immune signalling; as a consequence BIK1 is tightly regulated at a protein level (Monaghan *et al.*, 2014). In the resting state, BIK1 protein accumulation is positively regulated by heterotrimeric G proteins (EXTRA-LARGE GUANINE NUCLEOTIDE-BINDING PROTEIN 2, ARABIDOPSIS G-PROTEIN BETA SUBUNIT1 and ARABIDOPSIS G-PROTEIN GAMMA-SUBUNIT1/2) and phosphorylation by the mitogen-activated protein kinase kinase kinase kinases (MAP4Ks) SERINE/THREONINE KINASE1 (SIK1) and MAP4K4 (Liang *et al.*, 2016; Zhang *et al.*, 2018*a*; Jiang *et al.*, 2019*a*). Meanwhile, BIK1 accumulation is negatively regulated through the E3 ubiquitin ligases PLANT U-BOX 25/26 (PUB25/26), which target BIK1 for proteasomal degradation, and CALCIUM-DEPENDENT PROTEIN KINASE 28 (CPK28) (Monaghan *et al.*, 2014; Wang *et al.*, 2018*b*). BIK1 activity is negatively regulated through its dephosphorylation by PP2C38 (Couto *et al.*, 2016). Upon immune stimulation, activated BIK1 is protected from PUB25/26 ubiquitination and subsequent degradation (Wang *et al.*, 2018*b*). Moreover, PP2C38 is phosphorylated by MAP4K4 and dissociates from BIK1 allowing activated BIK1 accumulation (Couto *et al.*, 2016; Jiang *et al.*, 2019*a*). However, CPK28 activity is also enhanced allowing it to phosphorylate PUB25/26, which promotes their polyubiquitination of inactive BIK1 (Monaghan *et al.*, 2014; Wang *et al.*, 2018*b*). This leads to a decreased pool of inactive BIK1, curtailing further activation and thus regulating the amplitude of the immune response.

A number of direct BIK1 substrates have been identified including the NADPH oxidase, RBOHD; WRKY transcription factors; and calcium channels (Li *et al.*, 2014; Kadota *et al.*, 2014; Lal *et al.*, 2018; Tian *et al.*, 2019).

Other RLCKs shown or suggested to function downstream of RK complexes include the BR-SIGNALING KINASEs in brassinosteroid signalling, immunity and tapetum development (Tang *et al.*, 2008; Sreeramulu *et al.*, 2013; Majhi *et al.*, 2019; Chen *et al.*, 2019); and CONSTITUTIVE DIFFERENTIAL GROWTH 1 in brassinosteroid signalling (Kim *et al.*, 2011); SHENGEN1 in Casparian strip development (Alassimone *et al.*, 2016); LOST IN POLLEN TUBE GUIDANCE 1/2 in pollen tube guidance (Liu *et al.*, 2013*b*); NFR5-INTERACTING CYTOPLASMIC KINASE 4 in nodulation (Wong *et al.*, 2019) and CAST AWAY in organ abscission (Burr *et al.*, 2011).

Mitogen-Activated Protein Kinases

Another shared module downstream of RK complexes are MAPK cascades. A typical MAPK cascade contains 3 sequentially activated kinases (MAPKKK/MEKK→ MAPKK/MKK→ MAPK/MPK) (He *et al.*, 2018; Komis *et al.*, 2018). For a long time, the link between RK complexes and MAPK activation had remained enigmatic; however, RLCKs have been shown to activate MAPK cascades (Yamada *et al.*, 2016*a*; Yan *et al.*, 2018; Bi *et al.*, 2018). Moreover, MAPKs have been shown to phosphorylate MAPKKKs, creating a positive feedback mechanism (Bi *et al.*, 2018).

In immune signalling, two major MAPK cascades are activated in parallel MAPKKK3/MAPKKK5-MKK4/MKK5-MPK3/MPK6 and MEKK1-MKK1/MKK2-MPK4 suggesting a point of signalling divergence (Meng and Zhang, 2013; Bi *et al.*, 2018). Surprisingly, There is a high degree of convergence between MAPK cascades downstream of different RK signalling complexes – indeed MKK4/5-MPK3/6 are activated downstream of pathways controlling immunity, stomatal patterning, floral organ abscission, embryo patterning and pollen development (He *et al.*, 2018). It is still unclear how specificity is determined. Many MPKs substrates have been identified (He *et al.*, 2018).

RLCKs and MAPKs represent two of the key signal transduction pathways downstream of LRR-RK complexes. They can potentiate the signal from the receptor complex to orchestrate cellular responses. Having discussed the generalities of LRR-RK signalling I will move on to discussing the physiological roles of RKs in sensing the plant cell's local environment.

1.3 Receptor kinases in sensing a cells local environment

Plant cells must constantly monitor their surroundings in order to respond appropriately to local cues. In part this is facilitated by transmembrane RKs which can detect endogenous and exogenous signals. Perception of autocrine and paracrine signalling molecules enables cell-cell orchestration of developmental programmes, reproduction and environmental responses (He *et al.*, 2018). In addition, recognition of non-self molecules mediates interactions between plants and their biotic environment (Zipfel and Oldroyd, 2017). Due to the large number of RKs within plant genomes and the important functions they perform, an extensive literature exists implicating RKs in numerous biological functions. Here, I will discuss some prominent examples.

1.3.1 Receptor kinases in development

In *Arabidopsis*, a number of RKs regulate a diverse range of growth and developmental processes through the recognition of endogenous ligands (Matsubayashi, 2014; Olsson *et al.*, 2019*a*).

Leucine-rich repeat receptor kinases

Whilst most ligands perceived by LRR-RKs are proteinaceous, an exception is the brassinosteroid receptor BRI1 that recognises non-proteinaceous brassinosteroids (Li and Chory, 1997; Hothorn *et al.*, 2011; She *et al.*, 2011). Brassinosteroids regulate diverse responses including cell expansion, senescence, male fertility, induction of flowering, fruit ripening, and stress responses (Wang *et al.*, 2013; Planas-Riverola *et al.*, 2019).

The LRR-RK CLAVATA1 (CLV1)-type receptors, including CLV1 and BARELY ANY MERISTEM (BAM) 1/2/3 perceive peptides from the CLE (CLAVATA3/EMBRYO SURROUNDING REGION-RELATED) family. This signalling module spatially restricts the stem cell niche in order to control apical, floral and root meristem size (Leyser and Furner, 1992; Clark *et al.*, 1993, 1997; DeYoung *et al.*, 2006). In the context of apical meristem homeostasis, the primary ligand, CLV3, is excreted from apical cells and restricts the expression of the WUSCHEL (WUS) transcription factor which would otherwise promote stem cell fate, and meristem fasciation (Clark *et al.*, 1995; Fletcher *et al.*, 1999; Somssich *et al.*, 2016). This signalling module also plays roles in lateral root emergence, protophloem formation and anther development (Hazak and Hardtke, 2016).

Other members of the CLE family regulate cell fate through related RKs. The TDIF peptide (TRACHEARY ELEMENT DIFFERENTIATION INHIBITORY FACTOR) is independently derived from CLE41 and CLE44 and controls xylem differentiation through recognition by the LRR-RK PXY/TDR (PHLOEM INTERCALATED WITH XYLEM/ TDIF-RECEPTOR) (Ito *et al.*, 2006; Fisher and Turner, 2007; Hirakawa *et al.*, 2008; Etchells and Turner, 2010; Zhang *et al.*, 2016*b*; Morita *et al.*, 2016). The receptor complex regulates the expression of WUSCHEL-related HOMEOBOX transcription factors to control vascular proliferation and differentiation (Hirakawa *et al.*, 2010).

CLE peptides also act as systemic signals to negatively regulate global nodulation (in legumes) and mycorrhization through CLV1 orthologs *(e.g.* the SUNN-CLE module in *Medicago truncatula*) (Schnabel *et al.*, 2005; Reid *et al.*, 2011; Okamoto *et al.*, 2013; Imin *et al.*, 2018; Müller *et al.*, 2019).

The LRR-RK ERECTA and its paralog ERECTA-LIKE 1 recognise EPF1/2/9 in order to regulate ovule and stomatal patterning (Torii *et al.*, 1996; Shpak *et al.*, 2004, 2005; Kawamoto *et al.*, 2019). The EPF family consists of eleven members in *Arabidopsis*, six of which have been shown to interact with ERECTA family receptors (Shpak, 2013). ERECTA is also an important regulator of plant architecture.

LRR-RKs HAESA and HAESA-LIKE2 are able to promote cell wall weakening and cell separation in response to INFLORESCENCE DEFICIENT IN ABSCISSION (IDA) family

peptides (Jinn *et al.*, 2000; Butenko *et al.*, 2003; Stenvik *et al.*, 2008; Vie *et al.*, 2015*a*; Santiago *et al.*, 2016). This signalling module plays important roles in lateral root emergence, floral organ abscission and root cap sloughing (Kumpf *et al.*, 2013; Shi *et al.*, 2018).

EXCESS MICROSPOROCYTES 1 perceives the peptide TAPETUM DETERMINANT 1 in order to promote tapetum differentiation and thus controls male reproductive development (Jia *et al.*, 2008; Zheng *et al.*, 2019).

The LRR-RK SGN3/GSO1 (SHENGEN3/GASSHO1) is required for Casparian strip formation (Pfister *et al.*, 2014). The close homolog GSO2 plays a redundant role with SGN3/GSO1 in embryo cuticle development (Tsuwamoto *et al.*, 2007). SGN3/GSO1 and GSO2 are receptors for the CIF peptides (CASPARIAN STRIP INTEGRITY FACTORS) (Nakayama *et al.*, 2017; Doblas *et al.*, 2017; Okuda *et al.*, 2019).

CIF peptides were originally identified due to their requirement for tyrosine-sulfation for peptide activity (Komori *et al.*, 2009; Nakayama *et al.*, 2017; Doblas *et al.*, 2017). Sulfated precursor proteins share a conserved DY-motif that is required for tyrosine-sulfation (Komori *et al.*, 2009). These peptide families include the PSKs, ROOT GROWTH FACTORS (RGF)/ GOLVEN and PLANT PEPTIDE CONTAINING SULFATED TYROSINE 1 (PSY1) (Matsubayashi and Sakagami, 1996; Amano *et al.*, 2007; Matsuzaki *et al.*, 2010; Meng *et al.*, 2012; Whitford *et al.*, 2012).

PSK is a tyrosine-disulfated pentapeptide that promotes cell expansion and is recognised by the RKs PSK RECEPTOR1/2 (PSKR) (Matsubayashi and Sakagami, 1996; Matsubayashi *et al.*, 2006). RGFs are recognised by RGF RECEPTOR 1/2/3 (RGFR) in the root leading to increased abundance of the transcription factor PLETHORA, which promotes maintenance of the root stem-cell niche (Shinohara *et al.*, 2016; Song *et al.*, 2016; Ou *et al.*, 2016). PSY1 appears to positively regulate cell expansion in a similar manner to PSK; however, the perception mechanism remains unclear as the proposed receptor mutant still responds to PSY1 treatment (Mahmood *et al.*, 2014).

Non-leucine-rich repeat receptor kinases

Non-LRR-RKs also play roles in development. Examples include the *CATHARANTHUS ROSEUS* RLK1-LIKE (CrRLK1L) RK FERONIA (FER), which is able to recognise the RALF1 peptide (RAPID ALKALINISATION FACTOR) in order to regulate root growth, cell expansion and morphology (Haruta *et al.*, 2014; Li *et al.*, 2015). RALFs were named after their ability to induce alkalinisation of growth media when applied to cell cultures and were shown to inhibit growth (Pearce *et al.*, 2001). Interestingly a subset of RALF1 induced responses are BAK1-dependent, including growth inhibition, but not alkalinisation (Dressano *et al.*, 2017). The paralogous receptor, THESEUS1 (THE1), and it proposed ligand, the

peptide RALF34, have been shown to modulate lateral root initiation (Murphy *et al.*, 2016; Gonneau *et al.*, 2018).

1.3.2 Receptor kinases in reproduction

Leucine-rich repeat receptor kinases

To ensure successful fertilisation, pollen tubes require stimuli to guide them toward the synergid cells (Higashiyama and Yang, 2017). Related synergid cell derived LURE and XIUQIU cysteine-rich peptides promote pollen tube attraction (Okuda *et al.*, 2009; Takeuchi and Higashiyama, 2012; Zhong *et al.*, 2019). LUREs are perceived by the LRR-RK PRK6 (an additional receptor complex has been proposed which is discussed later), whilst the receptor for XIUQIUs remains unknown (Takeuchi and Higashiyama, 2016; Zhang *et al.*, 2017; Zhong *et al.*, 2019).

CrRLCK1L receptor kinases

Despite roles in development, CrRLK1L were originally described for their roles in reproduction. FER was the first member of the family to be cloned as a female fertility determinant (Rotman *et al.*, 2003; Huck *et al.*, 2003; Escobar-Restrepo *et al.*, 2007). In *fer* ovules, arriving pollen tubes overgrow upon reaching the synergid cell, which fails to rupture. It is proposed that FER interacts with the paralogous receptors HERK1/ANJ (HERCULES RECEPTOR KIANSE1/ANJEA) to carry out this function (Galindo-Trigo *et al.*, 2019). Other CrRLK1L receptors are required for male reproductive success (Boisson-Dernier *et al.*, 2009; Ge *et al.*, 2017). The pairs of paralogous receptors ANXUR1/2 (ANX) and BUDDHA'S PAPER SEAL1/2 (BUPS) are required to prevent premature pollen tube rupture through perception of RALF4/19 peptides – an autocrine signal (Mecchia *et al.*, 2017; Ge *et al.*, 2017). When the pollen tube approaches the synergid cell, female-derive RALF34 is able to displace RALF4/19 from the ANX/BUPS complex to impair pollen tube integrity and promote rupture.

Lectin S-domain receptor kinases

Plants also employ RKs to recognise and reject self during reproduction to promote outbreeding. In the Brassicaceae, the determinant genes underlying the S-locus (self-incompatibility) encode a pollen expressed cysteine-rich SP11/SCR peptides and a cognate stigmatic receptor kinase. Their interaction induces incompatibility signalling within the stigma papilla cells leading to rejection of self-pollen (Stein *et al.*, 1991; Nasrallah *et al.*, 1994). These receptors exhibit allelic diversity amongst *Brassicaceae* S-haplotypes (Schopfer *et al.*, 1999; Takayama *et al.*, 2000).

1.3.3 Receptor kinases as sensors of the abiotic environment

Several RKs have been implicated in response to abiotic stress; however, this remains one of the most poorly understood areas of RK signalling, potentially due to the diverse physiological

effects of abiotic stresses. RKs are involved in response to the hormone abscisic acid (ABA), however, the mechanism is still unclear. These include the LRR-RK GUARD CELL HYDROGEN PEROXIDE-RESISTANT1 which is required for ABA- and H_2O_2- induced stomatal closure (Sierla *et al.*, 2018). Moreover, RECEPTOR-LIKE KINASE1 is required for full ABA sensitivity, especially ABA-induced senescence (Lee *et al.*, 2011). In these contexts, the RKs may perceive secondary signals. Furthermore, the cle25 peptide has been shown to regulate stomatal aperture during drought (Takahashi *et al.*, 2018). Drought-induced root-expressed cle25 moves through the vasculature to induce ABA biosynthesis in the leaves through BAM LRR-RKs, resulting in stomatal closure. Indeed, cle9 has also been shown to induce stomatal closure, however in this context no long distance transport has been proposed and cle9/10 play a role in stomatal development through the HSL1 LRR-RK (Qian *et al.*, 2018; Zhang *et al.*, 2019)

The C-TERMINALLY ENCODED PEPTIDEs (CEPs) play a role in the regulation of nitrogen homeostasis through interaction with the cognate LRR-RK CEP RECEPTOR1/2 (CEPR1/2) in *Arabidopsis* (Taleski *et al.*, 2018). CEPs produced in roots under nitrogen starvation, they are then transported in the xylem to the shoot where they are perceived by CEPR1/2 (Tabata *et al.*, 2014). As a result, a phloem mobile protein is produced in the shoot, which acts as a systemic nitrogen starvation signal promoting nitrate uptake in nitrate-rich soil pockets (Ohkubo *et al.*, 2017). Interestingly, in legumes CEP peptides positively regulate nodule formation through the orthologous receptor COMPACT ROOT ARCHITECTURE2 - a further nitrogen homeostasis response (Imin *et al.*, 2013; Mohd-Radzman *et al.*, 2016).

PLANT ELICITOR PEPTIDE3 (Pep3), has been shown to promote salt tolerance via its cognate LRR-RK receptors PEP RECEPTOR1/2 (PEPR) (Nakaminami *et al.*, 2018). Other RKs have been implicated in salt stress tolerance including FER and CHITIN ELICITOR RECEPTOR KINASE1 (CERK1); the role of FER is discussed later in the context of cell wall integrity sensing whilst the mechanism of CERK mediated-tolerance is unknown (Espinoza *et al.*, 2017; Feng *et al.*, 2018).

1.3.4 Receptor kinases as sensors of the biotic environment

Central to plant survival is the ability to perceive and respond to pathogens. This mediated by either cell surface localised pattern-recognition receptors (PRRs) or cytoplasmic receptors (Jones and Dangl, 2006; Dodds and Rathjen, 2010; Cook *et al.*, 2015). These receptors can directly perceive the presence of the pathogens or discern pathogen-induced effects on the host. PRRs are either RKs or receptor-like proteins (RLPs) which are able to perceive apoplastic pathogen- or damage- associated molecular patterns (PAMPs or DAMPs) and transduce this signal into pattern-triggered immune (PTI) outputs (Zipfel, 2014; Saijo *et al.*, 2018).

Sensors of non-self

Leucine-rich repeat pattern recognition receptors

Many characterised PRRs have an LRR ectodomain. RK-PRRs include FLAGELLIN SENSING2 (FLS2), ELONGATION FACTOR-TU RECEPTOR (EFR), COLD SHOCK PROTEIN RECEPTOR (CORE), FLAGELLIN SENSING3 (FLS3), XANTHOMONAS ORYZAE PV. ORYZAE RESISTANCE 21 (Xa21) and XANTHINE/URACIL PERMEASE FAMILY SENSING1 (XPS1), which all perceive bacterial PAMPs and belong to the LRR-RK subfamily XIIa (Song *et al.*, 1995; Gómez-Gómez and Boller, 2000; Zipfel *et al.*, 2006; Mott *et al.*, 2016; Hind *et al.*, 2016; Wang *et al.*, 2016*a*). The subfamily XIIa is discussed in more detail in Chapter 3. In brief, these receptors bind short epitopes of microbial-derived molecules, such as the flagellin-derived 22-amino acid flg22, to induce receptor complex formation with BAK1 and active immune signalling (Felix *et al.*, 1999; Gómez-Gómez and Boller, 2000; Chinchilla *et al.*, 2007; Heese *et al.*, 2007; Sun *et al.*, 2013*b*).

RLPs lack the cytoplasmic domain of RKs and consist solely of an LRR ectodomain and transmembrane α-helix (or glycosylphosphatidylinositol (GPI) anchor). They are therefore dependent upon RKs to transduce signals across the plasma membrane. LRR-RLPs require the adapter SOBIR1 (SUPPRESSOR OF BIR1-1) for signal transduction (Liebrand *et al.*, 2013, 2014; Gust and Felix, 2014; Bi *et al.*, 2016). SOBIR1 forms a constitutive interaction with the LRR-RLPs through the GxxxG dimerization motif (Bi *et al.*, 2016). In effect the complex functions as a bimodular RK. However, RLP-SOBIR interactions have proved recalcitrant to *in vitro* biochemical and structural investigation (Hohmann and Hothorn, 2019).

The first PRR to be identified was a LRR-RLP, Cf-9, from Tomato which recognises the *Passalora fulva* (then *Cladosporium fulvum*) apoplastic effector Avr9 (Jones *et al.*, 1994). Subsequently, a number of LRR-RLPs have been identified which are responsible for the perception of (predominantly) fungal/oomycete apoplastic effectors which function as virulence factors when not recognised by the host (Boutrot and Zipfel, 2017). Interestingly, many characterised RLPs (although not all) mediate stronger, monogenic, 'gene-for-gene' resistance, rather than the quantitative resistance mediated by many RKs (Kruijt *et al.*, 2005; Liebrand *et al.*, 2013). Potentially, this is because most characterised RLPs recognise virulence factors, which specifically indicate pathogens, rather than benign organisms, facilitating the evolution of stronger responses.

Of note is the RLP23-SOBIR1-BAK1 receptor complex that perceives the nlp20 epitope of NECROSIS AND ETHYLENE-INDUCING PEPTIDE 1-LIKE PROTEINS (NLPs) (Böhm *et al.*, 2014; Albert *et al.*, 2015). This is of particular interest because NLPs are found in

bacterial, oomycete and fungal pathogens, all of which are perceived in an RLP23-depdendent manner.

Moreover, CuRe1, a tomato LRR-RLP is responsible for perception of an extract derived from the parasitic plant *Cuscuta reflexa* (Hegenauer et al., 2016). Transfer of CuRe1 into *Solanum pennellii*, conferred resistance against *C. reflexa*. Recently, a QTL for resistance to *Striga hermonthica* in rice has been mapped to an interval containing RLPs, suggesting RLPs may play a wider role in parasitic plant interactions (Beardon, 2018).

Furthermore, although most PRRs seem to perceive their ligands directly, examples of indirect recognition also exist. For example, the tomato LRR-RLP Cf-2 does not interact directly with the nematode elicitor Gr-VAP1 or the *P. fulva* apoplastic elicitor Avr2 but rather senses the inhibition imposed by these elicitor proteins on the host protease Rcr3 (Dixon *et al.*, 2000; Rooney *et al.*, 2005; Lozano-Torres *et al.*, 2012).

WALL-ASSOCIATED KINASE-LIKE pattern recognition receptors

Another class of RKs genetically involved in the perception of proteinaceous PAMPs are the WALL-ASSOCIATED KINASE-LIKE receptors (WAKL) – although ligand binding has never been demonstrated. *TaWAKL4/SBT6* (*SEPTORIA TRITICI BLOTCH6)* was shown to underlie resistance to *Zymoseptoria tritici* that is dependent upon the production of the apoplastic effector *avrSBT6* by the pathogen (Saintenac *et al.*, 2018).

Lysin motif pattern recognition receptors

Chitin (β-1,4-linked *N*-acetylglucosamine (GlcNAc) polymers) is the best characterised non-proteinaceous PAMP (Sánchez-Vallet *et al.*, 2015). Whilst chitin only makes a small proportion of fungal cell walls, is a potent elicitor when 6-8 sugar residues in length (Bozsoki *et al.*, 2017). Chitin perception is dependent upon LYK-family receptors (LYSM-CONTAINING RECEPTOR-LIKE KINASES) which have LysM (Lysin motif)-containing ectodomains. Within *Arabidopsis* three LYK-RKs have been implicated in chitin perception - CERK1/LYK1, LYK4 and LYK5 (Miya *et al.*, 2007; Wan *et al.*, 2008, 2012; Cao *et al.*, 2014; Erwig *et al.*, 2017; Xue *et al.*, 2019). The first chitin receptor to be identified was from rice, CEBiP (CHITIN OLIGOSACCHARIDE ELICITOR-BINDING PROTEIN), a GPI-anchored LysM-RLP (Kaku *et al.*, 2006). CEBiP forms a heterooligomer with *Os*CERK1 and both are required for chitin perception in rice (Shimizu *et al.*, 2010). Interestingly, in *Arabidopsis*, a LysM-RLP is not required for all chitin-induced responses, but is essential for chitin induced plasmodesmatal closure (Faulkner *et al.*, 2013; Cheval *et al.*, 2019).

LysM receptors are also required for lipochitooligosaccharide (LCO) perception (Oldroyd, 2013). Based on the same structural backbone as chitin, LCOs are acylated chitooligosaccharides with various functional group substitutions. LCOs act as bacterial- or

fungal-derived symbiosis signals (Nod-factors or Myc-factors respectively). They are important signals in the initiation of the legume–rhizobium and arbuscular mycorrhizal (AM) symbioses respectively (Oldroyd, 2013). LCO perception is important for early responses such as pre-symbiotic nuclear calcium spiking, but also AM-induced modification of root system architecture (Ehrhardt *et al.*, 1996; Chiu *et al.*, 2018).

Extracellular polysaccharide (EPS) mutants of the nodule forming bacteria *Mesorhizobium loti* are defective in nodule formation in *Lotus japonicus* (Kelly *et al.*, 2013). These mutants produce truncated EPS pentamers - rather than longer EPS polymers. A suppressor screen in *L. japonicus* identified a LysM-RK, EPS3, which appears positively regulate nodule formation in the presence of wild-type EPS, however, is able to inhibit nodule formation in the presence of truncated EPS (Kawaharada *et al.*, 2015). This demonstrates that LysM-RKs can be EPS receptors.

The LysM RK CERK1 also perceives bacterial cell wall-derived peptidoglycan, in association with GPI-anchored RLPs LYM1/LYM3 (Willmann *et al.*, 2011). Peptidoglycan is structurally similar to chitin except with alternating β-1,4-linked GlcNAc and N-acetylmuramic acid residues and peptide links between the polydimer backbones. CERK1 has been shown to be required for the perception of 1,3-β-*d*-glucans derived from fungal and oomycete cell walls (Mélida *et al.*, 2018).

It is apparent that LysM receptors are able to perceive a range of carbohydrate oligomers, potentially through context-dependent differential complex formation. In the majority of cases CERK1/LYK1 appears to be required for LysM-type receptor complex signalling. It is intriguing how the same receptors are able to mediate intuitively contradictory outputs of immunity and symbiosis.

Lectin S-domain pattern recognition receptor

LIPOOLIGOSACCHARIDE-SPECIFIC REDUCED ELICITATION/BULB -TYPE LECTIN S-DOMAIN RLK1-29 (LORE) is the RK responsible for perception of the bacterial metabolite 3-hydroxydecanoic acid, the active contaminant of lipopolysaccharide extracts (Ranf *et al.*, 2015; Kutschera *et al.*, 2019). LORE remains the only characterised PRR in this family and currently little is known about its function.

Pathogen exploitation of RK signalling

Interestingly, several examples have emerged of pathogens exploiting RK signalling by producing mimetic ligands to modulate host signalling as a virulence strategy. Plant parasitic nematodes have been shown to produce CLE, IDA and CEP peptides to manipulate the host (Wang *et al.*, 2005; Lu *et al.*, 2009; Mitchum *et al.*, 2012; Replogle *et al.*, 2013; Tucker and Yang, 2013; Ripke *et al.*, 2014; Eves-Van Den Akker *et al.*, 2016; Kim *et al.*, 2018).

Nematode-encoded CLE peptides are able to complement *Arabidopsis cle* mutants when expressed appropriately (Wang *et al.*, 2005, 2010). Moreover, the fungal pathogen *Fusarium oxysporum* has been shown to produce RALF peptides that are able to phenocopy host RALFs when applied exogenously (Masachis *et al.*, 2016). *Fusarium ralf* mutants fail to induce alkalinisation in tomato plants and have reduced virulence (Masachis *et al.*, 2016). Peptides with homology to RALFs have been described in multiple phytopathogen genomes (Thynne *et al.*, 2017). In addition, *Xanthomonas oryzae* produces a mimic of the endogenous PSY1 peptide in order to suppress host immunity and promote virulence, presumably through an RK that perceives PSY (Pruitt *et al.*, 2017). Interestingly *Oryza longistaminata* evolved a PRR, Xa21, that is able to specifically recognise the mimetic peptide RaxX and induce immunity (Pruitt *et al.*, 2017; Luu *et al.*, 2019).

Pathogens fight back

The importance of PRRs in plant immunity is highlighted by evolution of virulence factors that suppress PTI responses. *Pseudomonas syringae* injects effectors into host cytoplasm via a type-3 secretion system, these effectors are then able to influence host physiology. Unless mentioned otherwise the effectors discussed in this section are derived from *Pseudomonas syringae*. The effector HopB1 was found to cleave BAK1 to impair its function in PTI signalling (Li *et al.*, 2016). Interestingly, as BAK1 depletion leads to autoimmunity, HopB1 protease activity was specific to immune-activated BAK1, thus limiting *bak1*-induced autoimmunity (Yamada *et al.*, 2016*b*; Li *et al.*, 2016). Effectors not only allow us to understand pathogenesis, they can help our understanding of signalling mechanisms. HopAO1 was shown to be a tyrosine phosphatase that targets PRRs to impair their activation (Macho *et al.*, 2014). This revealed the importance of EFR Tyr836 in immune signalling. Studying the protease, AvrPphB, enabled the identification of BIK1 and the PBLs which function downstream of PRR complexes (Zhang *et al.*, 2010). HopF2, AvrPto and the E3 ligase AvrPtoB all target and inhibit the PRR complex (Shan *et al.*, 2008; Göhre *et al.*, 2008; Gimenez-Ibanez *et al.*, 2009; Zhou *et al.*, 2014). A conserved fungal effector, NIS1, targets BAK1 and BIK1 to fulfil its virulence function showing PRR complex targeting effectors are not restricted to bacterial pathogens (Irieda *et al.*, 2019).

Pathogens have also evolved to disguise PAMPs from the host. For example, fungal effectors ECP6 and SLP1 compete for binding of chitin oligomers with host immune receptors (De Jonge *et al.*, 2010; Mentlak *et al.*, 2012; Sánchez-Vallet *et al.*, 2013). Moreover, whilst the flg22 epitope of flagellin is evolutionarily constrained, bacteria glycosylate flagellin to disguise it from FLS2 (Buscaill *et al.*, 2019). In turn, hosts have evolved a glycosidase which is able to reveal the immunogenic epitope (Buscaill *et al.*, 2019).

1.3.5 Sensors of modified self

In addition to the perception of non-self, plants use receptor kinases in order to perceive modified-self as an indicator of danger, DAMPs. DAMPs can be classified as either primary or secondary (also known as phytocytokines) depending on whether they are passively or actively released by the host during infection (Gust *et al.*, 2017). This is discussed more extensively in Chapter 5.

In brief, these primary DAMPs are generally either cell wall components which are released during wounding, stress or pathogen invasion; or cytoplasmic components that are released into the apoplast following plasma membrane damage (Gust *et al.*, 2017). Several RKs are involved in the perception of primary DAMPs. WAK1 has been implicated in the perception of pectin-derived oligogalacturonides released during infection, although genetic evidence remains elusive (Brutus *et al.*, 2010).

The lectin RK, LecRK-I.9/DORN1 (DOES NOT RESPOND TO NUCLEOTIDES 1) is a plasma membrane localised receptor for extracellular ATP , while LecRK-I.8 is proposed as a receptor for extracellular NAD^+ (Choi *et al.*, 2014; Wang *et al.*, 2017*b*). High apoplastic concentrations of these cytoplasmic metabolites is indicative of wounding.

Secondary DAMPs, also known as phytocytokines, are plant-derived peptides that are produced, processed or secreted in responses to danger, such as pathogen invasion. Currently described phytocytokine receptors include the LRR-RKs PEPR1/2, RLK7 and SYR1, which perceive Pep, Pip and systemin peptides, respectively (Huffaker *et al.*, 2006; Yamaguchi *et al.*, 2006, 2010; Krol *et al.*, 2010; Hou *et al.*, 2014; Wang *et al.*, 2018*a*). These peptides are all proposed to amplify and potentiate immune signalling through pathways apparently conserved with LRR-RK PAMP receptors such as FLS2 and EFR.

Moreover, the rapid-alkalinisation factor RALF17 has been shown to induce immune responses through FER (Stegmann *et al.*, 2017).

1.3.6 Receptor kinases as sensors of cell wall integrity

Perception of cell wall integrity can be seen as part of a DAMP continuum (Wolf, 2017; Vaahtera *et al.*, 2019). Whilst considerable progress has been made in understanding cell wall integrity sensing in yeast, relatively little is known in plants. A suite of five transmembrane sensors – CELL WALL INTEGRITY AND STRESS RESPONSE COMPONENT1/2/3, MATING PHEROMONE-INDUCED DEATH PROTEIN2 (MID2) and MID2-LIKE PROTEIN 1 – represent a component in yeast cell wall integrity sensing, essential for survival under stress (Levin, 2011; Kock *et al.*, 2015). These proteins consist of a highly O-mannosylated, cell wall-embedded extracellular domain, single-pass transmembrane α-helix and small cytoplasmic domain. These sensors cluster during cell-surface stress and induce

MAPK cascades (Kock *et al.*, 2015). Due to the lack of homologs in plant genomes, structural analogy with RKs/RLPs made them promising candidates to fulfil the role (Monshausen and Haswell, 2013). Over the last decade considerable evidence has accumulated confirming a role for RLKs in perceiving cell wall integrity and actively integrating this into developmental and defence signalling pathways (Wolf, 2017). Below, I will attempt to outline our current understanding.

Wall-associated kinases

The wall-associated kinases (WAKs) form a 5-member RK subfamily in *Arabidopsis* with all members closely linked in a tandem repeat on chromosome 1 (He *et al.*, 1996; De Lorenzo *et al.*, 2011). WAK proteins have EPIDERMAL GROWTH FACTOR-like motifs in their ectodomain which facilitate the formation of strong interactions with non-methylesterified homogalacturonan and oligogalacturonides (OGs) *in vivo* and *in vitro,* in a calcium-dependent manner (Decreux and Messiaen, 2005). Short chain OGs have long been known to function as elicitors of DAMP triggered-immunity, alerting the plant to tissue injury (Davis *et al.*, 1986; Davis and Hahlbrock, 1987; Ferrari *et al.*, 2013). Brutus et al. (2010) provided evidence that WAK1 functions as an OG receptor using a domain swap approach with EFR. Interestingly, the WAK family were also shown to be required for cell elongation, potentially suggesting a feedback mechanism between cell wall integrity sensing and growth (Kohorn *et al.*, 2006).

Catharanthus roseus sub-family

CrRLK1L members have been described in each of the preceding sections, highlighting their fundamental role in plant biology. The *CrRLK1L* subfamily contains 17 RKs in *Arabidopsis* whose ectodomains have homology with malectin, an ER localised di-glucose binding protein within mammals (Schallus *et al.*, 2008; Lindner *et al.*, 2012). They are receptors for RALF peptides in complex with the GPI-anchored RLP LORELEI or its homologs (Haruta *et al.*, 2014; Stegmann *et al.*, 2017; Mecchia *et al.*, 2017; Ge *et al.*, 2017; Gonneau *et al.*, 2018; Xiao *et al.*, 2019).

THE1 was identified in an EMS screen in the cellulose-deficient *procuste1-1* (*prc1-1*) background (Hematy *et al.*, 2007). *prc1-1* mutants have reduced dark-grown hypocotyl elongation and ectopic lignification. However, these phenotypes are partially supressed in a *the1-1* background and enhanced in a *p35S:THE1* background, independently of cellulose biosynthesis (Hematy *et al.*, 2007). Together, this suggests that THE1 may be involved in the signalling of cellulose deficiency. Subsequently, THE1 has been shown to regulate a diverse range of responses to cell wall integrity stress imposed by the inhibition of cellulose biosynthesis (Denness *et al.*, 2011; Van der Does *et al.*, 2017; Engelsdorf *et al.*, 2018).

FER is required for the maintenance of cell wall integrity during salt stress (Feng *et al.*, 2018). Sensing of the salinity-induced cell wall softening is proposed to be dependent upon the interaction of FER with pectin in the cell wall (Feng *et al.*, 2018; Lin *et al.*, 2018). Immediately following salt stress cells in the elongation zone of the roots enter a quiescent phase, before eventually resuming growth after several hours (Geng *et al.*, 2013). FER-dependent signalling elicits cell-specific calcium transients, which are required to prevent elongation cell bursting upon growth recovery (Feng *et al.*, 2018). FER is also required for the second phase of the biphasic Ca^{2+} response upon mechanical perturbation of *Arabidopsis* roots, potentially via the CNGC14 calcium channel (Shih *et al.*, 2014). FER is also required for proper cell elongation in *Arabidopsis* roots and root hairs of *fer* mutants tend to be very short or burst (Duan *et al.*, 2010; Haruta *et al.*, 2014). This elongation was shown to be dependent on RAPID ALKALINISATION FACTOR 1 (RALF1), a secreted peptide which binds to FER, resulting in its activation and phosphorylation of downstream targets (Haruta *et al.*, 2014). One characterised phosphorylation target is H^+-adenosine triphosphatase 2, which then reduces its proton export rate, thus alkalising the apoplastic space and inhibiting cell elongation (Haruta *et al.*, 2014). Potentially all these phenotypes are unified through cell-surface stretch, potentially sensed in a FER-dependent manner.

The role of CrRLK1Ls in the control of cell integrity and bursting is a recurring theme. As discussed earlier, a lack of FER, ANJ and HERK1 at the filiform apparatus fails to induce pollen tube rupture and ANX1/2 and BUPS1/2 differentially regulate pollen tube integrity (Huck *et al.*, 2003; Boisson-Dernier *et al.*, 2009; Duan *et al.*, 2014; Mecchia *et al.*, 2017; Ge *et al.*, 2017; Galindo-Trigo *et al.*, 2019). In the context of the synergid cell filiform apparatus, FER/HERK1/ANJ are required for the localisation of the seven-pass transmembrane protein MILDEW RESISTANCE LOCUS O-LIKE7(MLO7)/NORTIA to the site of pollen tube arrival (Kessler *et al.*, 2010; Galindo-Trigo *et al.*, 2019). Interestingly, FER is also required for the relocalisation of paralogous MLO proteins to the site of hyphal penetration during mildew infection leading to the hypothesis that this localisation could be the result of CrRLK1L-dependent perception of cell wall invasion (Kessler *et al.*, 2010).

Recently, *crrlk1l* mutants have been shown to phenocopy higher order mutants of a family of apoplastic LRR-extensin proteins (LRX) (Draeger *et al.*, 2015; Mecchia *et al.*, 2017; Sede *et al.*, 2018; Fabrice *et al.*, 2018; Zhao *et al.*, 2018; Dünser *et al.*, 2019). These proteins have N-terminal LRRs and a variable C-terminal extensin domain which interacts strongly with cell wall carbohydrates (Draeger *et al.*, 2015; Herger *et al.*, 2019). LRX proteins directly interact with RALFs and are required for RALF perception (Mecchia *et al.*, 2017; Zhao *et al.*, 2018; Moussu *et al.*, 2019). LRX proteins have also been shown to co-immunoprecipitate with the

ectodomain of FER, and are required for salt stress tolerance (Zhao *et al.*, 2018; Dünser *et al.*, 2019). Potentially, LRX represent the nexus linking CrRLK1Ls, RALFs and the cell wall.

Leucine-rich repeat RLKs/RLPs

The LRR-RK STRUBBELIG (SUB) has controls tissue morphogenesis (Chevalier *et al.*, 2005), however, recently *sub* mutants haven been shown to be impaired in CBI-induced ROS accumulation, gene expression, lignification and callose deposition (Chaudhary *et al.*, 2019).

A pair of homologous LRR-RLKs, FEI1/2, are required for cell wall function under stress (Xu *et al.*, 2008). While the single *fei1* and *fei2* mutants have no obvious phenotype, the double mutant has impaired anisotropic root growth and lignin deposition under high sucrose and salinity conditions, phenotypes associated with defects in cellulose biosynthesis. The cell walls of *fei1/fei2* double mutants had significantly less cellulose content than wild-type roots (Xu *et al.*, 2008).

Brassinosteroid signalling is upregulated during cell wall weakening, specifically when there is impaired demethyleseterfication which prevents pectin cross-linking and results in softer cell walls (Wolf *et al.*, 2012*b*). RLP44 is genetically required for this upregulation, potentially by physically interacting with BRI1 to promote co-receptor complex formation (Wolf *et al.*, 2014; Holzwart *et al.*, 2018).

Moreover, the barrier surveillance mechanism employed to ensure Casparian strip contiguity is also a mechanism to monitor cell wall status through SGN3/GSO1 and its CIF ligands (Pfister *et al.*, 2014; Doblas *et al.*, 2017). (This is discussed in more detail in 1.4.3.)

Further work is required to understand the contribution of RKs to monitoring cell wall status and integrating this information into developmental and immune signalling programmes to regulate the dynamic cell wall matrix.

1.3.7 Concluding remarks

The work summarised here provides an overview of the emerging roles of RKs in diverse physiological processes. Plants employ RKs to perceive autocrine and paracrine stimuli; non-self; or homeostatic perturbations in order to coordinate development and defence. Hopefully this provides an impression of the diverse and elegant mechanisms that exist. However, due to the crucial role of these receptors they require tight regulation to ensure they are not aberrantly activated.

1.4 Regulation of LRR-RK receptor kinases

Earlier I touched upon the regulation of RK signalling, particularly at the level of downstream RLCKs. Here I will discuss further mechanisms employed to regulate receptor complex

function at the plasma membrane. It is vital that the plant is able to maintain tight control of these receptor complexes in order to prevent precocious signalling.

1.4.1 Inter-RK regulation

BAK1-INTERACTING RECEPTOR-LIKE KINASE

The LRR-RK BAK1-INTERACTING RECEPTOR-LIKE KINASE 1 (BIR1) was initially identified from a library of T-DNA mutants whose transcript levels were significant upregulated 48 h post-inoculation with *Pseudomonas syringae* pv. *maculicola* (Gao *et al.*, 2009). Mutation of *bir1* causes seedling lethality through enhanced cell death and constitutive defence responses which can be supressed by mutation of SOBIR1 (Gao *et al.*, 2009). BIR1 belongs to a family of four RKs in *Arabidopsis,* BIR1-4; all of these members are able to form constitutive interactions with BAK1 (Gao *et al.*, 2009; Ma *et al.*, 2017*a*). In the absence of BIRs (predominantly BIR1), BAK1 interacts promiscuously with SOBIR1, causing the constitutive activation of defence responses (Gao *et al.*, 2009). BIRs sequester BAK1 to prevent erroneous interactions with signalling partners (Ma *et al.*, 2017*a*; Hohmann *et al.*, 2018*a*). This is in accordance with the role of BIRs as negative regulators of RK signalling (Halter *et al.*, 2014; Blaum *et al.*, 2014; Hohmann *et al.*, 2018*a*). The affinity of the ligand-bound receptor, (*e.g.* flg22-bound FLS2) is sufficient to displace BIR to form a complex with BAK1 (Ma *et al.*, 2017*a*). Interestingly, the increase apoplastic pH during immune signalling appears to favour BAK1-BIR dissociation, thus potentiating immune signalling (Ma *et al.*, 2017*a*). BIR2 is the only member whose interaction with BAK1 appears to be stable at higher pH; concordant with its stronger role as a negative regulator of PRR signalling (PTI signalling induces apoplastic alkalinisation) (Halter *et al.*, 2014; Ma *et al.*, 2017*a*). Mutations in the BAK1 ectodomain which effect function in brassinosteroid signalling in fact strengthen the BAK1-BIR interaction, rather than directly effecting the BAK1-brassinosteroid-BRI1 interaction (Hohmann *et al.*, 2018*a*).

CATHARANTHUS ROSEUS RLK1-LIKE

The FER-RALF signalling module has been shown to regulate immune signalling (Stegmann *et al.*, 2017). A mutant screen for restoration of PTI signalling in the immunocompromised *bak1*-5 background identified a mutation in the S1P protease that processes a subset of RALF peptides (Srivastava *et al.*, 2009; Stegmann *et al.*, 2017). These processed RALF peptides are able to negatively regulate immune signalling by inhibiting FLS2-BAK1 complex formation. This response is FER-dependent. FER is proposed to act as a scaffold protein promoting FLS2-BAK1 complex formation. Another subset of RALF peptides, including RALF17, that lack the S1P recognition site are able to function antagonistically and promote immune signalling (Stegmann *et al.*, 2017).

In addition, a mutant screen for enhanced elicitor-induced immune marker gene expression isolated a mutation in ANX1 (Mang *et al.*, 2017). However, unlike FER, ANX1 and its paralog ANX2 are negative regulators of flg22-induced immunity (Mang *et al.*, 2017). ANX1 constitutively associates with FLS2 and BAK1; however, in the presence of flg22 the BAK1-ANX1 association increases. The flg22-induced ANX1/2 sequestration of BAK1 is proposed as the mechanism of negative regulation of PTI signalling. Given that FER and ANX1/2 have additional functions, it will be interesting to elucidate the potential roles of other CrRLK1L RKs and their RALF ligands in the regulation of immune receptor signalling.

FLS2-INTERACTING RECEPTOR KINASE

The ectodomain of the LRR-RK FIR (FLS2-INTERACTING RECEPTOR KINASE) was found to directly associate with the FLS2 in an *in vitro* LRR-RK ectodomain interactome (Smakowska-Luzan *et al.*, 2018). FLS2-BAK1 complex formation is significantly reduced in the *fir* mutant, which is reflected in reduced flg22-induced ROS production, gene expression and induced resistance. Thus, FIR positively regulates FLS2 signalling by facilitating FLS2-BAK1 complex formation (Smakowska-Luzan *et al.*, 2018).

APEX

The same LRR-RK ectodomain interactome study identified APEX as a central component of the interaction network (Smakowska-Luzan *et al.*, 2018). APEX associates with PEPR1/2 *in vivo* and *in vitro* and exhibits a dose-dependent effect on PEPR signalling, with impaired PEPR-signalling in over-expression and knock-out lines. *apex* mutants also show perturbations in FLS2 and BRI1 signalling with a promotion of FLS2-BAK1 complex formation and conversely reduced sensitivity to brassinosteroid (Smakowska-Luzan *et al.*, 2018). This suggests APEX plays a general role in LRR-RK signalling.

LYSM RLK1-INTERACTING KINASE 1

The LRR-RK LYSM RLK1-INTERACTING KINASE 1 (LIK1) was identified in a yeast-2-hybrid screen for interactors with CERK1 (Le *et al.*, 2014). The LIK1-CERK1 interaction was confirmed *in planta*. LIK1 negatively regulates chitin- and flg22-induced ROS production. Whilst LIK1 associates with CERK1, it is unclear if the effect it exerts is mediated directly through the PRR interaction.

IMPAIRED OOMYCETE SUSCEPTIBILITY1

The RK IMPAIRED OOMYCETE SUSCEPTIBILITY1 (IOS1) contains both LRRs and malectin-like motifs within its extracellular domain (Hok *et al.*, 2011). IOS1 differentially regulates resistance to pathogens. Initially it was identified as susceptibility factor for the oomycete pathogen *Hyaloperonospora arabidopsidis* (Hok *et al.*, 2011). Since it has been found to positively regulate *Pseudomonas syringae* resistance (Hok *et al.*, 2014; Yeh *et al.*,

2016). IOS1 interacts with FLS2, EFR, BAK1 and CERK1 to positively regulate PTI responses (Yeh *et al.*, 2016). It appears to promote FLS2-BAK1 complex formation (Yeh *et al.*, 2016). However, *IOS1* is required for some ABA-induced responses, potentially explaining the differential role in immunity (Hok *et al.*, 2014).

LecRK-VI.2

LecRK-VI.2 has been shown to interact with FLS2 and to positively regulate PTI responses (Singh *et al.*, 2012; Huang *et al.*, 2014). Surprisingly, AtLecRK-VI.2 overexpression in *Nicotiana benthamiana* confers enhanced flg22-induced ROS production, however, overexpression in *Arabidopsis* does not have this effect (Singh *et al.*, 2012; Huang *et al.*, 2014). The mechanism by which PTI responses are regulated is unclear and are not necessarily direct.

Cysteine-rich receptor-like kinases

CYSTEINE-RICH RECEPTOR KINASES (CRKs) contain DUF26 motifs within their ectodomains (Bourdais *et al.*, 2015). CRKs are transcriptionally induced biotic and oxidative stress; however, precise understanding of their function remains elusive (Bourdais *et al.*, 2015). Redundancy between CRKs has impaired genetic characterisation; however, over-expression of certain CRKs induces constitutive immunity and cell death (Chen *et al.*, 2003, 2004; Acharya *et al.*, 2007; de Oliveira *et al.*, 2016; Yadeta *et al.*, 2017; Lee *et al.*, 2017). CRK28 associates constitutively with BAK1 and can also be co-immunoprecipitated with FLS2 in a flg22-depdendent manner (Yadeta *et al.*, 2017). Overexpression of CRK28 enhances flg22-triggered PTI responses (Yadeta *et al.*, 2017). CRK36 also interacts with FLS2 (Lee *et al.*, 2017). CRK overexpression-induced cell death is dependent upon BAK1 (Yadeta *et al.*, 2017); however, contradictory results propose that upregulation of CRKs is responsible for cell death in *bak1* mutants (de Oliveira *et al.*, 2016). Recently, CRK2 has been proposed to directly regulate RBOHD activity through phosphorylation of its C-terminal in response to PAMP treatment (Kimura *et al.*, 2019). It is currently unclear whether CRKs are functioning to regulate RK signalling complexes or are functioning in parallel pathways.

RECEPTOR-LIKE PROTEIN 44

RLP44 has been shown to promote BRI1/PSKR1-co-receptor complex formation to positively regulate these signalling pathways to control vascular cell fate (Holzwart *et al.*, 2018). It is unclear how widely the effect is observed.

1.4.2 Regulation by kinase inhibitors

The BRI1 cytoplasmic domain interacts constitutively with a kinase inhibitor, BRI1 KINASE INHIBITOR1 (BKI1) (Wang and Chory, 2006; Wang *et al.*, 2014). BKI1 is phosphorylated

in response to brassinosteroid perception resulting in its dissociation from BRI1, thus BKI1 inhibits promiscuous activation of BRI1 (Jaillais *et al.*, 2011).

1.4.3 Regulation by localisation

RKs are not distributed homogeneously at the plasma membrane, but instead are restricted to specific domains (Yu *et al.*, 2019*a*). Localisation within micro-/nano- domains constrains RK interactions and plays an important role in regulating their function (Burkart and Stahl, 2017; Ott, 2017; Gronnier *et al.*, 2018). This localisation is determined by both lipid and protein plasma membrane constituents, as well as cytoskeletal and cell wall components (Gronnier *et al.*, 2018; McKenna *et al.*, 2019; Yu *et al.*, 2019*a*). Moreover, the dynamics, localisation and composition of these domains is modulated during signalling (Bücherl *et al.*, 2017; Liang *et al.*, 2018; Cui *et al.*, 2018*b*).

Whilst BRI1 and FLS2 share the BAK1 co-receptor, they localise to distinct nanodomains, which show different plasma membrane dynamics (Bücherl *et al.*, 2017). The lateral mobility of RK nanodomains is reduced during signalling. These effects are specific to the activated signalling pathway, rather than a general effect on the plasma membrane (Bücherl *et al.*, 2017). Recruitment into nanodomains was shown to promote signalling and inhibit endocytosis of the LYK3 receptor in *Medicago* during symbiosis signalling (Liang *et al.*, 2018). These correlations suggest and significant link between nanodomain properties and RK function.

Whilst some nanodomains are distributed across the cell surface, other RKs localise to specific subcellular locations (Hutten *et al.*, 2017; Burkart and Stahl, 2017; Gronnier *et al.*, 2018; Yu *et al.*, 2019*a*). The LRR-RK SGN3/GSO1 is expressed exclusively within endodermal cells where it localises adjacent to the equatorial CASP domain (Pfister *et al.*, 2014). It is required for CASP domain fusion to form the contiguous Casparian strip. GSO1/SGN3 recognises the steele-expressed CIF1/2 peptides to promote CASP domain expansion (Nakayama *et al.*, 2017; Doblas *et al.*, 2017). As the Casparian strip lignifies it impedes CIF diffusion from the steele towards the cortex. The SGN3-CIF-SERK complex is only able to successfully signal through the polarly-localised, cortex facing RLCK SGN1 (Alassimone *et al.*, 2016; Okuda *et al.*, 2019). This forms a 'barrier surveillance' system in which Casparian strip lignification is only promoted when its integrity is impaired, allowing CIF diffusion and co-localisation of all signalling components (Doblas *et al.*, 2017).

The RK ERL1 has been shown to preferentially localise in newly formed membranes at sites of cell division in order to perform its function in stomatal lineage determination (Qi *et al.*, 2017). Within pollen tubes the LURE-receptor, PRK6, is tip-localised and asymmetrically accumulates in favour of higher LURE concentrations – a response which proceeds the morphological turning of the pollen tube (Takeuchi and Higashiyama, 2016).

Plant cells form a symplastic continuum regulated by plasmodesmatal aperture; however, symplastic isolation is important in development and stress responses (Brunkard and Zambryski, 2017; Sager and Lee, 2018). Surprisingly, whilst most chitin-induced responses are CERK1-depdendent, plasmodesmatal closure is CERK1-independent and relies on distinct receptors LYK4 and LYM2 (Faulkner *et al.*, 2013; Cheval *et al.*, 2019). LYM2 and LYK4 are enriched within plasmodesmatal membranes. The LRR-RKs BAM1/2 also localise to plasmodesmatal membranes and are targeted by the viral effector C4 to inhibit the spread of RNA interference and promote viral pathogenesis (Rosas-Diaz *et al.*, 2018). BAM1/2 also positively regulate plasmodesmatal-mediated spread of miRNA involved in xylem development (Fan *et al.*, 2019). The recruitment of RKs to plasmodesmatal membranes under osmotic stress appears to be important for callose-mediated plasmodesmatal closure and lateral root development (Grison *et al.*, 2019). Moreover, the interactions between RKs has been shown to differ between the plasma membrane and the plasmodesmatal membrane, affecting their function (Stahl *et al.*, 2013).

1.4.4 Regulation of RKs by endocytosis

The delivery and retention of RKs within the membrane is tightly regulated. Endocytosis regulates RK accumulation and partitioning (Claus *et al.*, 2018). This affects signalling duration, amplitude and specificity (Claus *et al.*, 2018). Receptor-mediated endocytosis has been documented for many RKs. Notable examples include BRI1 (Russinova *et al.*, 2004; Geldner *et al.*, 2007), BAK1 (Russinova *et al.*, 2004), SERK1 (Kwaaitaal *et al.*, 2005), FLS2 (Robatzek *et al.*, 2006), EFR (Mbengue *et al.*, 2016), PEPR1 (Mbengue *et al.*, 2016; Ortiz-Morea *et al.*, 2016), CLV1 (Nimchuk *et al.*, 2011), CERK1 and LYK5 (Erwig *et al.*, 2017). Non-activated RKs have been shown to undergo constitutive cycling between the plasma membrane and the *trans*-Golgi network/early endosomes in a Brefeldin A-sensitive manner to regulate protein accumulation at the plasma membrane (Geldner *et al.*, 2007; Beck *et al.*, 2012). In contrast, ligand-induced receptor endocytosis occurs upon receptor complex activation, leading to multivesicular body/late endosome targeting and vacuolar degradation (Robatzek *et al.*, 2006; Beck *et al.*, 2012; Mbengue *et al.*, 2016; Ortiz-Morea *et al.*, 2016). Post-translational modifications play a key role in this process. BAK1 constitutively associates with the E3 ubiquitin ligases PUB12/13 which are phosphorylated by the activated BAK1 kinase domain to promote polyubiquitination of FLS2, stimulating its endocytosis (Lu *et al.*, 2011). PUB12/13 have subsequently been shown to regulate polyubiquitination of LYK5 and BRI1 to promote their endocytosis; however, BRI1 phosphorylates PUB13 directly (Martins *et al.*, 2015; Liao *et al.*, 2017; Zhou *et al.*, 2018).

1.5 Evolutionary history of receptor kinases and its link with function

1.5.1 RKs are massively expanded in plant lineages

The cloning of the first RK from maize created excitement due to its structural analogy to receptor-tyrosine kinases in metazoans that had already been shown to function as transmembrane receptors (Walker and Zhang, 1990). Phylogenetic analysis of RK kinase domains reveals they form a monophyletic clade with the *Drosophila melanogaster* gene PELLE and the INTERLEUKIN RECEPTOR-ASSOCIATED KINASES (IRAKs) found in mammals (Halfon *et al.*, 1995; Lemaitre *et al.*, 1996; Qiu *et al.*, 1998; Flannery and Bowie, 2010; Rhyasen and Starczynowski, 2015). PELLE and the IRAKs are cytoplasmic kinases that lack transmembrane domains. PELLE is the only member of this clade in *Drosophila* and four IRAKs are encoded in the human genome. This contrasts sharply with plants where the RK/PELLE/IRAK gene family has expanded massively (*e.g.* the *Arabidopsis*, rice and oak genomes encode 600, 977 and 1247 RKs, respectively) (Shiu and Bleecker, 2001*a*; Lehti-Shiu *et al.*, 2009; Gao and Xue, 2012; Fischer *et al.*, 2016; Plomion *et al.*, 2018). The asymmetry in RK abundance between eukaryotic genomes suggests the expansion within plants has been driven by positive selection to retain RK duplications.

A key innovation of plant RKs is the transmembrane structure. RK sequences with the canonical transmembrane structure have been identified in *Charophyceae* implying that this conformation predated the *charophyte*-land plant divergence, however all known RK kinases in chlorophyte genomes are cytoplasmic (Lehti-Shiu *et al.*, 2009; Delaux *et al.*, 2015; Nishiyama *et al.*, 2018; Han, 2019). It should be noted that not all plant RK kinases have transmembrane domains as RLCKs belong to this clade.

RK extracellular domains are diverse in their biochemistry enabling the binding of a wide range of ligands. It is likely that the canonical RK structure arose due to multiple fusion events between kinase domains and ancestoral RLPs (Lehti-Shiu *et al.*, 2009). This may have provided a source of innovation in signaling networks; linking novel inputs to exant response networks. This fusion is predicted to have occurred twelve times since the divergence of *Arabidopsis*, rice and poplar (Lehti-Shiu *et al.*, 2009). Interestingly, whilst the ancestral RK/PELLE/IRAK kinase was likely active, approximatly 20% of RKs in plants are predicted to be kinase-inactive based on sequence (Castells and Casacuberta, 2007; Gish and Clark, 2011).

1.5.2 Expansion rates of RK subfamilies vary and are linked to biotic stress responces

Whilst the RK family has expanded in plants, there is considerable variation in expansion rates between RK clades (Shiu *et al.*, 2004; Lehti-Shiu *et al.*, 2009; Sakamoto *et al.*, 2012; Fischer

et al., 2016). The rate of lineage-specific subfamily expansion correlates with RK function. Sub-families with defence-related functions show more rapid expansion (Hanada *et al.*, 2008; Lehti-Shiu *et al.*, 2009; Fischer *et al.*, 2016). This is hypothesised to be due to the dynamic evolutionary landscape created by host-pathogen co-evolution (Hanada *et al.*, 2008). There is a correlation between RK transcriptional responsivity to biotic stress and subfamily expansion rate (Lehti-Shiu *et al.*, 2009, 2012). For example the LRR-RK subfamily XI and subfamily XIIa contain a similar number of genes; however they show very different evolutionary signatures (Fischer *et al.*, 2016). Subfamily XI LRR-RKs - which perceive endogenous ligands - show ancient duplication and ortholog retention between genomes. However, LRR-RK subfamily XIIa - which contains PRRs - shows much more rapid evolution with recent expansion in parellel lineages (Fischer *et al.*, 2016).

Signatures of positive selection are enriched within the ectodomains of LRR-RKs, suggesting ectodomains are evolving faster than other domains (Fischer *et al.*, 2016). There is a positive correlation between the rate of LRR-RK subfamily expansion and evidence of positive selection. Indeed, lineage specific expanded subfamilies of LRR-RK showed a nearly 10-fold increase in positively selected codons (Fischer *et al.*, 2016). An example of this rapid evolution is the fixation of an adaptive allele of *FLS2* in *Arabidopsis* (Vetter *et al.*, 2012).

Taken together these evolutionary fingerprints can guide our interpetation of RK subfamily function, especially in attempting to identify clades of RKs that function in biotic stress tolerance, potentially functioning as PRRs.

1.6 Use of pattern recognition receptors in the field

Crop diseases significantly diminish agricultural productivity (Savary *et al.*, 2012). These losses can be mitigated through chemical controls, however, some of these have potential deleterious environmental consequences, resulting in restricted usage (Hillocks, 2012). Genetic resistance introduced through molecular breeding technologies can contribute to overcoming many of these issues (Dangl *et al.*, 2013). However, its application is limited by regulatory restrictions and public mistrust (Eckerstorfer *et al.*, 2019; Fernbach *et al.*, 2019). Conventional breeding programmes have long exploited natural variation in cell surface receptors to enhanced resistance, highlighting the value of extending elicitor recognition in commercial systems (Boutrot and Zipfel, 2017). I will now briefly explore the potential for transgenic deployment of PRRs in crop protection.

As many PAMPs are recognised by evolutionarily recent, lineage specific receptors, interfamily transfer of PRRs is a promising option in order to fortify crop genomes (Boller and Felix, 2009; Boutrot and Zipfel, 2017). Current evidence suggests that LRR-RK and LRR-RLP PRRs can be successfully transferred between families, even between monocots and

dicots, without the requirement to transfer any other signal transduction components (Lacombe *et al.*, 2010; Holton *et al.*, 2015; Schoonbeek *et al.*, 2015; Schwessinger *et al.*, 2015; Albert *et al.*, 2015; Lu *et al.*, 2015; Wang *et al.*, 2016*a*; Boschi *et al.*, 2017; Kunwar *et al.*, 2018). This makes their transfer a feasible and attractive approach.

Currently due to regulatory constraints, very few PRR transgenic plants have been tested under field conditions; however, under controlled conditions, PRRs from non-crop genomes have been used to confer quantitative, broad-spectrum disease resistance (Boutrot and Zipfel, 2017). Examples include the transfer of RLP23 from *Arabidopsis* into potato resulting in enhanced resistance to *Sclerotinia sclerotiorum* and *Phytophthora infestans* (Albert *et al.*, 2015) and ELICITIN RESPONSE, an LRR-RLP from *Solanum microdontum* that recognises *Phytophthora/Pythium* elicitin, also confers enhanced resistance to *P. infestans* in potato (Du *et al.*, 2015). Perhaps the best example is the *Brassicaceae* LRR-RK, EFR, which has been transferred into tomato, potato, rice and wheat to confer resistance to pathogens with an active elf18-epitope (Lacombe *et al.*, 2010; Holton *et al.*, 2015; Schoonbeek *et al.*, 2015; Schwessinger *et al.*, 2015; Lu *et al.*, 2015). Indeed, the resistance in potato and tomato has recently been confirmed in field trials (Boschi *et al.*, 2017; Kunwar *et al.*, 2018).

The success of these approaches has incentivised the identification of additional – family-specific – PRRs in order to engineer crop disease resistance.

1.7 Identification of PRRs

Below I will outline a range of biochemical and genetic approaches that have been employed to identify PRRs. Despite the identification of evolutionary signatures of PRR containing subfamilies, it remains a considerable challenge to identify novel PRRs and their cognate ligands. The limited number described stands testament to this (Boutrot and Zipfel, 2017).

1.7.1 Forward genetics

Within species natural variation has been used to map PRRs such as RLP1/RECEPTOR OF ENIGMATIC MAMP OF XANTHOMONAS (Jehle *et al.*, 2013), RLP32 (Fan, 2016), FLS3 (Hind *et al.*, 2016), VERTICILLIUM WILT DISEASE RESISTANCE PROTEIN1 (Fradin *et al.*, 2009), RESPONSIVENESS TO BOTRYTIS POLYGALACTURONASES1 (Zhang *et al.*, 2014), and RLP30 (Zhang *et al.*, 2013). This approach has been successful but relies on genomic resources, pre-existing genetically-determined phenotypic variation and, depending on the species, can be very costly in terms of time, plant growth and genotyping.

Where phenotypic diversity within a species is limited, introgression between species can augment variation. Eshed and Zamir (1995) introgressed regions of *Solanum pennellii* in the domesticated *S. lycopersicum* cv. *M82* genome (Chitwood *et al.*, 2013). *S. pennellii*'s insensitivity to csp22 (a 22-amino acid epitope of bacterial cold-shock protein) and the

phytocytokine systemin allowed the mapping and cloning of the cognate receptors, CORE and SYR1 (Wang *et al.*, 2016*a*, 2018*a*). Inversely the same introgression lines were used to identify CuRe1 in *S. pennellii* (Hegenauer *et al.*, 2016).

Mutagenesis screens can be used where no standing phenotypic variation exists. Indeed this approach was used to clone some of the first PRRs including the RLP Cf-9 and RK FLS2 (Jones *et al.*, 1994; Gómez-Gómez and Boller, 2000). Whilst ethyl methanesulfonate mutagenesis was used to identify FLS2, transposon-tagging was used to identify Cf-9 (Jones *et al.*, 1994; Gómez-Gómez and Boller, 2000). An advantage of this approach is having the ability to select the genetic background for the screen, for example they can contain genetically-encoded reporters. Prominent examples are LORE1 and DORN1 which were both identified through loss of cytoplasmic calcium influx in mutagenized Col-0^{AEQ} (Choi *et al.*, 2014; Ranf *et al.*, 2015). Indeed the effectiveness of this approach has been demonstrated multiple times *e.g.* identification of 57 *efr* mutants encoding 37 different alleles in an mutant screen for elf18-insensitivity (Nekrasov *et al.*, 2009).

1.7.2 Reverse genetics

With increasing understanding, we can begin to more accurately predict candidate receptors. Use of T-DNA insertional mutants lead to the identification of EFR, RLP23 and XPS1, which perceive bacterial elf18, nlp20 and xup25, respectively (Zipfel *et al.*, 2006; Albert *et al.*, 2015; Mott *et al.*, 2016). Moreover, RLK7, the receptor for the phytocytokine PIP1 was identified by screening mutants of RKs closely related to other phytocytokine receptors (Hou *et al.*, 2014). Similarly, CERK1 in *Arabidopsis* was identified through a screen of RLKs with ectodomain sequence similarity to the previously identified chitin binding RLP, CEBiP, in rice (Miya *et al.*, 2007).

Where stable mutants do not exist, transient approaches can be applied. A library of VIGs (virus induced gene silencing) constructs was used to silence every RK and RLP within the *N. benthamiana* genome to identify RXEG1 - an RLP conferring recognition of the *Phytophthora sojae* apoplastic effector XYLOGLUCAN-SPECIFIC ENDO-BETA-1,4-GLUCANASE 1 (Wang *et al.*, 2018*c*). This resource will undoubtedly prove fruitful in the identification of orphan ligands in *N. benthamiana* in the future.

1.7.3 Biochemical approaches

Genetic approaches are limited by receptor redundancy. Biochemical approaches can help overcome this limitation. A labelled ligand can be used to 'fish' for its receptor(s). This approach relies on a high ligand-receptor affinity, or the crosslinking of the ligand to the receptor, to enable co-purification. Several PRRs have been identified using labelled ligands, including PEPR1 and CEBiP which were identified using ^{125}I radiolabelled, photo-crosslinkable ligands (Ito *et al.*, 1997; Yamaguchi *et al.*, 2006; Kaku *et al.*, 2006). The

labelled ligands were applied to suspension cell cultures, crosslinked to the receptors by UV light, and subsequently identified from SDS-PAGE gels. Similar approaches can be applied using ligand labelled beads to purify the receptor (Petutschnig *et al.*, 2010). A limitation of these approaches in that they would struggle to identify low abundance receptors. In an attempt to overcome this a library of tobacco BY-2 cells has been generated overexpressing LRR-RKs in order to screen with labelled ligands, this has successfully been used to identify the RGF, CEP and CIF receptors (Tabata *et al.*, 2014; Shinohara *et al.*, 2016; Nakayama *et al.*, 2017; Shinohara and Matsubayashi, 2017).

Interestingly, in mammalian cell cultures CRISPR activation screens have been used to differentially overexpress endogenous candidate receptors in a population of cells (Chong *et al.*, 2018). A fluorescently labelled ligand was applied to the cell population which was subsequently sorted based of fluorescence. Fluorescent cells were predicted to be overexpressing the cognate receptor. They were then sequenced to identify which promoter regions the gRNAs were targeting. Whilst not applied to plant system this approach has advantages over cDNA over-expression libraries which are resource intensive to generate and maintain.

However, the approach can be taken fully *in vitro* with the use of recombinantly expressed receptor ectodomains to identify interactors. Gel filtration can be used to separate LRR-ectodomains, and bound peptide(s), from a peptide library pool, the associated peptide can then be identified using mass-spectrometry (Song *et al.*, 2016). This approach led to the independent discovery of the RGF receptors as well as rediscovering the HSL2-IDA and PXY-TDIF interactions. The recombinant ectodomains can also be bound to beads, this approach was used to identify a non-peptide agonist of CLE9-BAM1 interaction using a fluorescently labelled peptide and high-throughput microscopy (Shinohara and Matsubayashi, 2007; Shinohara *et al.*, 2019). One could also envisage a chip-based array approach to identify interaction in a high-throughput manner (Katz *et al.*, 2011; Szymczak *et al.*, 2018).

Many LRR-RKs and LRR-RLPs display ligand-induced complex formation with SERK co-receptors. Identification of RKs/RLPs which show ligand dependent interaction with BAK1 was used to identify CSPR, an RLP involved in the recognition of CSP22; however genetic evidence suggest this might not be the receptor (Saur *et al.*, 2016; Wang *et al.*, 2016*a*).

FER was identified as a candidate receptor for RALF1 through a RALF1-induced phosphoproteomics approach (Haruta *et al.*, 2014). This was possible due to the rapid ligand-induced phosphorylation of receptor cytoplasmic domains. As with all the aforementioned approaches, candidate receptors need to be confirmed using a variety of biochemical approaches to corroborate binding and confirm it is specific.

1.8 Concluding remarks

In summary, receptor kinases allow plant cells to respond to a plethora of environmental stimuli. In the case of leucine-rich repeat receptor kinases this appears to be through a generally conserved mechanism of ligand-binding induced receptor complex heterodimerisation. This induces cytoplasmic signalling via receptor-like cytoplasmic kinases and mitogen-activated protein kinase cascades to bring about diverse responses. Receptor kinases, and there signalling pathways are tightly regulated in order to prevent aberrant signalling activation. This is especially true in the case of pattern-recognition receptors where tight control of costly defence responses is essential. Further characterisation of RK signalling can help us to understand and manipulate how plants develop and respond to their environment.

1.9 Aims of this thesis

In this thesis I focus on the characterisation of the *Arabidopsis* leucine-rich repeat receptor kinase subfamily XII in immune signalling. This subfamily contains the pattern-recognition receptors FLS2, EFR, and XPS1, whose cognate ligands have been identified (Gómez-Gómez and Boller, 2000; Zipfel *et al.*, 2006; Mott *et al.*, 2016). Several members remain undescribed but represent putative, lineage-specific, PRRs. Using complementary gain- and loss-of-function approaches I attempt to identify novel PRRs within this family. Additionally, I focus on detailed characterisation of one member of this subfamily, MIK2, to investigate its role in immune homeostasis and response to diverse environmental stimuli.

Chapter 2

Material and methods

2.1 Materials

2.1.1. Plant materials

Arabidopsis thaliana

Wild type or mutant *Arabidopsis thaliana* (hereafter *Arabidopsis*) lines used in this study are in Col-0 (Columbia) or Ws-2 (Wassilewskija) backgrounds. Details of mutants are shown in Table 2.1 and transgenic lines are shown in Table 2.2.

For soil-grown plants seeds were sown directly on compost and plants were grown under controlled conditions: 21 °C; 10 h (short days) or 16 h (long days) photoperiod; 75% humidity.

In vitro growth was performed on Murashige and Skoog medium (MS; 4.41 $g.l^{-1}$; including vitamins) (Duchefa) supplemented with 1% sucrose. Seeds were vapour sterilized using chlorine gas for 5 h prior to stratification at 4 °C for at least 2 days. Subsequently plates were transferred to growth conditions: 22 °C; 16 h photoperiod.

Table 2. 1 *Arabidopsis* mutant alleles used in this study

Mutant allele	Ecotype	Publication	Identifier
sobir1-13	Col-0	(Leslie *et al.*, 2010)	SALK_009453
bak1-5	Col-0	(Schwessinger *et al.*, 2011)	
bak1-4	Col-0	(Kemmerling *et al.*, 2007)	SALK_116202
pepr1-1	Col-0	(Yamaguchi *et al.*, 2006)	SALK_059281
pepr2-3	Col-0	(Krol *et al.*, 2010)	SALK_098161
rbohd	Col-0	(Torres *et al.*, 2002)	
eds1-2	Col-0	(Falk *et al.*, 1999)	
sid2-1	Col-0	(Nawrath and Métraux, 1999)	
ndr1-1	Col-0	(Century *et al.*, 1997)	
bak1-1	Col-0	(Li *et al.*, 2002)	CS6125
bak1-3	Col-0	(Kemmerling *et al.*, 2007)	SALK_034523
irx1-6	Col-0	(Hernández-Blanco *et al.*, 2007)	
agb1-2	Col-0	(Ullah *et al.*, 2003)	CS6536
mik2-1	Col-0	(Wang *et al.*, 2016*b*)	SALK_061769
mik2-2	Col-0	(Van der Does *et al.*, 2017)	SALK_046987
mik2-3	Col-0	(Coleman *et al.*, 2019)	GABI_208H02

mik2-4	Ws-2		FLAG_518G04
efr-1	Col-0	(Zipfel *et al.*, 2006)	SALK_044334
fls2c	Col-0	(Zipfel *et al.*, 2004)	SAIL_691_C4
mik2-like-1	Col-0	(Van der Does *et al.*, 2017)	SALK_112341C
mik2-like-2	Col-0	(Van der Does *et al.*, 2017)	GABI_031G02
xii2-1	Col-0		SAIL_373_E04
xii2-4	Col-0		SALK_025037C
xii3-1	Col-0		SALK_101474
xps1-2	Col-0	(Mott *et al.*, 2016)	SALK_101668
xps1-3	Col-0		GABI_781A02
xps1-4	Col-0		GABI_544A06
xps1-5	Col-0	This publication	CRISPR-Cas9
xps1-6	Col-0	This publication	CRISPR-Cas9
xii5-1	Col-0		GABI_415H04
xii5-2	Col-0		SALK_150420
xii5-4	Col-0	This publication	CRISPR-Cas9
xii5-5	Col-0	This publication	CRISPR-Cas9
xii6-1	Col-0		SAIL_31_F02
xii6-2	Col-0		SAIL_837_D03
mdis1-2	Col-0	(Wang *et al.*, 2016*b*)	GABI_090F03
mdis2	Col-0	(Wang *et al.*, 2016*b*)	SALK_004879
pxl2-2/mik1	Col-0	(Fisher and Turner, 2007)	SALK_095005

Table 2. 2 Transgenic *Arabidopsis* lines used in this study

Transgene	Background	Publication
p35S::APOAEQUORIN	Col-0	(Knight *et al.*, 1991)
pUBQ10::APOAEQUORIN#8	Col-0	(Ranf *et al.*, 2014)
pUBQ10::APOAEQUORIN#31	Col-0	(Ranf *et al.*, 2014)
pBIK1::BIK1-HA	Col-0	(Liu *et al.*, 2013*a*)
p35S::RBOHD-FLAG	Col-0	(Kadota *et al.*, 2014)
p35S::MIK2-GFP	*mik2-1*	(Sharon and Sharon, 2015)
p35S::MIK2-GFP (kinase dead)	*mik2-1*	(Sharon and Sharon, 2015)
p35S::EFR-GFP	*efr-1*	(Macho *et al.*, 2014)

Solanaceous species

Nicotiana benthamiana was used for transient *Agrobacterium tumefaciens*-mediated transformation. Seeds were sown directly on compost and plants were grown under controlled conditions: 24 °C; 16 hours light and 8 hours dark (long days); 55% humidity. *Solanum lycopersicum* was grown under the same conditions for phenotyping. The Moneymaker background (LA3310) contains the introgression of the TOBACCO MOSAIC VIRUS 2 resistance gene (Solyc09g018220) for ease of growth. Transgenics lines generated in this study are listed in Table 2.3.

Table 2. 3 Transgenic tomato lines developed in this study

Transgene	AGI	Vector	Copy number	Identifier
XII3	AT3G47090	pEarleygate103	2	#4
XII3	AT3G47090	pEarleygate103	1	#12
XPS1	AT3G47110	pEarleygate103	2	#2
XPS1	AT3G47110	pEarleygate103	1	#4
XII6	AT3G47580	pEarleygate103	1	#2
XII6	AT3G47580	pEarleygate103	2	#6
XII5	AT3G47570	pEarleygate103	2	#1
XII5	AT3G47570	pEarleygate103	3	#4

2.1.2. Bacterial and fungal materials

Escherichia coli

E. coli strain DH10B (F- *mcrA* Δ(*mrr-hsd*RMS-*mcr*BC) Φ80*lac*ZΔM15 Δ*lac*X74 *rec*A1 *end*A1 *ara*D139 Δ(*ara leu*) 7697 *gal*U *gal*K *rps*L *nup*G λ- (Grant *et al.*, 1990)) was used for cloning purposes.

Agrobacterium tumefaciens

A. tumefaciens strain GV3101 was used in this study for transient transformation of *N. benthamiana* and stable transformation of *Arabidopsis*. GV3101 carries the helper plasmid pMP90 and is Rifampicin and Gentamycin resistant (Van Larebeke *et al.*, 1974; Koncz and Schell, 1986).

Pathogen isolates

Pathogen isolates used in this study are listed in Table 2.4.

Table 2. 4 Pathogen isolates used in this study.

Species/Strain	Source	Selection markers
Pseudomonas syringae pv. tomato DC3000 COR^{-}	(Bender *et al.*, 1987; Brooks *et al.*, 2004)	KAN RIF
Xanthomonas perforans pv. T4-4B	Brian Staskawicz (UC Berkley, USA)	RIF
Xanthamonas vesicatoria	PR biotech., ES.	
Botrytis cinerea strain CH94	PR biotech., ES.	
Sclerotinia sclerotiorum	PR biotech., ES.	
Plectosporella cucumerina BMM	Brigitte Mauch-Mani (Uni of Neuchatel, CH)	

2.1.3. Antibiotics

Stock solutions were stored at -20 °C, except for Rifampicin, which was stored at 4 °C (Table 2.5). Working concentration indicates the final concentration used in the selective media.

Table 2. 5 Antimicrobials used in this study.

Antimicrobial	Stock concentration	Working concentration
Carbenicillin (Carb)	100 mg.mL^{-1} in H_2O	100 µg.mL^{-1}
Gentamycin (Gen)	10 mg.mL^{-1} in H_2O	20 µg.mL^{-1}
Kanamycin (Kan)	50 mg.mL^{-1} in H_2O	50 µg.mL^{-1}
Rifampicin (Rif)	10 mg.mL^{-1} in methanol	50 µg.mL^{-1}
Spectinomycin (Spt)	100 mg.mL^{-1} in H_2O	50 µg.mL^{-1}
Nystatin	250 mg.mL^{-1} in H_2O	25 µg.mL^{-1}

2.1.4. Antibodies

Antibodies used in this experiment are listed with their respective dilution in Table 2.6.

Table 2. 6 Antibodies used in this study and their working dilutions

Target	Dilution	Secondary	Source
α-P44/42 MAPK	1:4,000	Rabbit	9101 (Cell Signalling)
α-RBOHD	1:1,000	Rabbit	AS15 2962 (Agrisera)
α-FLS2	1:1,000	Rabbit	(Schulze *et al.*, 2010)
α-BAK1	1:5,000	Rabbit	(Roux *et al.*, 2011)
α-pSer612 BAK1	1:2,000	Rabbit	(Perraki *et al.*, 2018)
α-BRI1	1:1,000	Rabbit	(Heese *et al.*, 2007)
α-GFP-HRP	1:5,000	-	sc-9996 HRP (Santa Cruz)
α-rabbit-HRP	1:10,000	-	A-0545 (Merck)

2.1.5 Peptides

Peptides were synthesised by EZbiolabs (NJ, USA) and diluted in ddH_2O before being stored at -20 °C (Table 2.7).

Table 2. 7 Synthetic peptides used in this study

Peptide	Amino acid	Reference
flg22	QRLSTGSRINSAKDDAAGLQIA	(Felix *et al.*, 1999)
elf18	acetyl-MSKEKFERTKPHVNVGTI	(Kunze *et al.*, 2004)
Pep3	ELKARGKNKTKPTPSSGKGGKHN	(Yamaguchi *et al.*, 2010)
SCOOP12	PVRSSQSSQAGGR	(Gully *et al.*, 2019)
JRP4	AMRPFPDPVDEIRLLFQALQRGPVRGSGRNGCTNIPRGSGRCHN	
nlp20	AIMYSWYFPKDSPVTGLGHR	(Böhm *et al.*, 2014)
xup25	LIPEGKVAVTTTQAATERKPLEQPR	(Mott *et al.*, 2016)

2.1.6 *in silico* resources

In silico resources used in this work are listed in Table 2.8.

Table 2. 8 *In silico* resources used in the study

Resource	Function	Reference
TMHMM2.0	Predicting transmembrane helices.	(Krogh *et al.*, 2001)
Genevestigator	Visualising RNA expression databases	(Zimmermann *et al.*, 2004)
iTOL	Phylogenetic tree visualisation	(Letunic and Bork, 2019)
UGENE	Alignments and phylogenies	(Okonechnikov *et al.*, 2012)
Benchling	*in silico* cloning/ sequencing alignments	Benchling [Biology Software]. (2019). Retrieved from https:benchling.com.
FIJI	Image analysis	(Schindelin *et al.*, 2012)
WEBLOGO	Creating sequence logos	(Crooks *et al.*, 2004)
Quantprime	Designing qPCR primers	(Arvidsson *et al.*, 2008)
SUBA4.0	Subcellular localisation predictor	(Hooper *et al.*, 2017)
Phytozome	Genomic resources	(Goodstein *et al.*, 2012)
eFP Browser	Visualising publicly available expression data	(Waese *et al.*, 2017)
Panther14.1	Gene Ontology enrichment analysis	(Mi *et al.*, 2019)
SignalP5.0	Predicting signal peptides	(Almagro Armenteros *et al.*, 2019)
BioRender	Figure drawing	Retrieved from https://biorender.com

2.1.7. Oligonucleotides

Oligonucleotides were ordered diluted to 100 µM (aqueous) and stored at -20 °C. These were further diluted to 10 µM in ddH_2O prior to use. Oligonucleotides are listed in Appendix table 1-2.

2.2 Methods

2.2.1 Molecular biology methods

Genotyping PCR

Genotyping PCRs were performed using REDEXTRACT-N-AMP™ PLANT TISSUE PCR KIT (Sigma Aldrich) following the manufacturers instructions. In brief, a small piece of leaf tissue was placed into 50 µl of REDEXTRACT-N-AMP™ extraction buffer and heated to 95°C for 10 min then diluted in 50 µl REDEXTRACT-N-AMP™ dilution buffer (1:1 dilution). 1 µl of the resultant DNA extract was then added to a 10 µl PCR mixture (50% (v/v) REDEXTRACT-N-AMP™ PCR reaction mixture, 0.4 µM forward primer, 0.4 µM reverse primer). The same PCR programme was used as for Qiagen *Taq* polymerase listed below.

Polymerase chain reaction (PCR)

PCRs were performed either using *TAQ* DNA POLYMERSE (Qiagen) or PHUSION® HIGH-FIDELITY POLYMERASE (New England Biolabs) (for high fidelity applications) according to the manufacturer's instructions. PCR programmes used for each application are outlined in Table 2.9 and 2.10.

Overlapping extension polymerase chain reaction was used to generate the chimeric receptors. In brief, primers were designed to amplify the respective fragments with an overlap of ~ 25 bp between adjacent modules (total primer length should not exceed 50 bp). The resultant PCR products were gel extracted and used as the template for subsequent PCR amplification with peripheral 3' and 5' primers (in this context always M13 Fw and M13 Rv primers) for 20 cycles using PHUSION® high-fidelity polymerase.

Table 2. 9 General Qiagen Taq touchdown PCR programme

Stage		Temp. (°C)	Time (sec)
Initial denaturing		95	60
35 cycles	Denaturing	95	20
	Annealing	58 → 53	20
	Extension	72	70 (~60 sec.kb^{-1})
Final extension		72	600

Table 2. 10 General Phusion® Taq touchdown PCR programme

Stage		Temp. (°C)	Time
Initial denaturing		98	60 sec
35 cycles	Denaturing	98	15 sec
	Annealing	58-> 53	20 sec
	Extension	72	30 sec.kb^{-1}
Final extension		72	600 sec

Gel extraction and plasmid purification

Gel extraction and plasmid purification were performed using MACHAREY-NAGEL NUCLEOSPIN® Gel and Plasmid kits respectively, according to the manufacturer's instructions.

RNA extraction and cDNA synthesis

Arabidopsis seeds were vapour sterilised, sown on ½ strength MS media, stratified and moved to growth conditions as previously descried. Three days later seedlings were transferred into transparent 24-well cell culture plates (Greiner Bio-One) containing 500 µL of liquid MS (2 seedlings per well). Seedlings were grown for a further 9 days. The day prior to elicitor treatment media was exchanged to avoid osmotic shock. Elicitor treatments were performed by addition of the MS media with or without the elicitor. 4 seedlings per sample were flash frozen in liquid nitrogen in 2 mL tubes and homogenised using 3mm glass beads in a SPEX CERTIPREP™ PULVERIZER AND CELL LYSER 2010 GENO/GRINDER (1500 RPM) whilst ensuring that the samples remained frozen.

Nucleic acids were extracted by the addition of 900 µL TRI reagent (Merck) and 200 µl chloroform followed by vigorous vertexing. Samples were subsequently centrifuged at 13,000 g for 20 min at 4 ºC after which 550 µl of the upper phase was transferred into a tube containing an equal volume of propan-2-ol (550 µl), mixed by inversion and allowed to stand at room temperature for 5 min whilst nucleic acids precipitated. The samples were spun again for 20 min at 4 ºC (13,000 g). The resultant pellet was washed in 500 µl 70% ethanol prior to drying.

Genomic DNA was removed by DNAse treatment using AMBION TURBO DNA-FREE KIT (ThermoFisher). Total RNA concentrations were measured using a nanodrop spectrophotometer.

2.5 µg of total RNA was then used to synthesise complementary cDNA using oligo$DT_{(18)}$ primers to anneal polyadenylated RNA using the REVERTAID FIRST STRAND CDNA SYNTHESIS KIT (ThermoFisher) according to manufacturer's instructions. The resultant cDNA was then diluted 20-fold prior to qPCR.

Quantitative PCR

qPCR was performed using LIGHTCYCLER® 480 SYBR GREEN I (Roche) according to manufacturer's instructions. In Brief, 4 µl of 20-fold diluted cDNA was added to 5 µl LIGHTCYCLER® 480 SYBR GREEN I MASTER MIX (Roche) with 0.5 µl of each forward and reverse primer (10 µM) creating a 10 µl total reaction volume. Analysis was performed in a CFX96 TOUCH REAL-TIME PCR DETECTION SYSTEM (Biorad).

Cloning

Goldengate modular cloning was performed using Type IIS restriction enzymes which cut outside their recognition site allowing seamless recombination (Weber *et al.*, 2011; Engler *et al.*, 2014). Appropriate modules were combined with 200 ng of the acceptor plasmid at a 2:1 molar ratio. The DNA was then combined with 1.5 µl cognate restriction enzyme (10 $U.\mu l^{-1}$, ThermoFisher), 1.5 µl T4 ligase buffer (NEB), 0.5 µl T4 ligase (400 $U.\mu l^{-1}$, NEB) and 1 µl 10x BSA (diluted 100X stock, NEB), the total reaction volume was then made up to 20 µl with ultrapure water. This reaction mixture was then incubated for 3 min at 37 °C and 4 min at 16 °C for at least 26 cycles, followed by heating to 50 °C and 80 °C sequentially to inactivate the enzymes. The resultant mixture was then transformed into *Escherichia coli* DH10β chemically competent cells (heat shock transformation – 50 sec at 42 °C) prior to appropriate selection and confirmation by sequencing.

Gateway entry cloning was performed using the pENTR™/D-TOPO® Cloning Kit (ThermoFisher) following the manufacturers instruction. GATEWAY™ LR CLONASE™ II ENZYME MIX (ThermoFisher) was then used to catalyse the *in vitro* recombination between an attL site-flanked entry clone and a destination vector (containing attR sites) to generate expression clones according to the manufacturer's instructions. The destination vector used was always pEARLEYGATE103 (Earley *et al.*, 2006). As pENTR-D-TOPO and pEARLEYGATE103 both have KAN resistance the entry clone was digested prior to recombination, where possible using MluI (New England Biolabs).

2.2.2 Biochemical methods

Immunoblotting assays

Plant tissue was ground in liquid nitrogen prior to boiling in 2x Laemmli sample buffer (4% SDS, 20% glycerol, 10% 2-mercaptoethanol, 0.004% bromphenol blue and 0.125 M Tris HCl; (10 $\mu l.mg^{-1}$ tissue)) for 10 min at 95°C. The samples were then spun at 13,000 g for 5 min prior to loading and running on SDS-PAGE gels of an appropriate concentration. Proteins were transferred onto PVDF membrane (ThermoFisher) (Wet transfer – overnight, 30 V; semidry transfer – 1.5 h, 25 V) and blocked for 1 h with 5% (w/v) fat-free milk powder in 1%

TBS buffer with 0.1% (v/v) Tween-20 (TBST) prior to incubation with appropriate antibodies in the same 5% milk buffer under gentle agitation.

Membranes were incubated with primary antibodies overnight at 4 °C or ~2 h at room temperature before being washed 3 times for 5 min in TBST. Subsequently membranes were incubated with the secondary antibody for ~1.5 h at room temperature. Membranes were washed 3 times in TBST for 15 min before detergent was removed by transfer to 1% TBS.

Western blots were developed using chemiluminescent PIERCE ECL PICO WESTERN BLOTTING SUBSTRATE (ThermoFisher) or SUPERSIGNAL™ WEST FEMTO MAXIMUM SENSITIVITY SUBSTRATE (ThermoFisher) and imaged with light-sensitive X-ray film (Super RX, Fujifilm) or with a LAS 4000 IMAGEQUANT SYSTEM (GE Healthcare). Staining of the blotted membrane with Coomassie Brilliant Blue was used to confirm loading.

Co-Immunoprecipitation

Fifteen to twenty seedlings were grown in wells of a 6-well plate for 2 weeks in liquid MS media with gentle agitation. The MS media was replaced the night before treatment. Seedling were treated with 1 μM elf18/SCOOP12 for 10 min before flash freezing. Tissue was ground and proteins extracted in 1:1 (v/v) powdered tissue:extraction buffer (50 mM Tris-HCl pH 7.5, 150 mM NaCl, 10% glycerol, 5 mM dithiothreitol, 1% protease inhibitor cocktail (Sigma Aldrich), 2 mM Na_2MoO_4, 2.5 mM NaF, 1.5 mM activated Na_3VO_4 and 1 % IGEPAL). For immunoprecipitation GFP-TRAP AGAROSE BEADS (ChromoTek) were incubated with extracts for 3 hr at 4 °C and washed 3 times in wash buffer (50 mM Tris-HCl pH 7.5, 150 mM NaCl, 10% glycerol, 5 mM dithiothreitol, 1% protease inhibitor cocktail (P9599, Sigma Aldrich), 2 mM Na_2MoO_4, 2.5 mM NaF, 1.5 mM activated Na_3VO_4 and 0.1 % IGEPAL) before adding Laemmli sample buffer and incubating for 10 minutes at 95 °C. Detection was carried out by SDS PAGE and western blots using α-BAK1 and α-GFP antibodies.

2.2.3 Transformation and transient expression

Transient expression in N. benthaminana

Agrobacterium tumefaciens GV3101 was used for all transient expression experiments, and were transformed by electroporation. 10 ml liquid L-media cultures containing the appropriate antibiotic were inoculated from a bacterial colony and grown overnight at 28 °C. Cultures were then spun-down (2500 g, 10 min) and resuspended in 10 mM $MgCl_2$ solution and the $O.D._{600}$ adjusted to 0.2. The subsequent bacterial suspension was then syringe infiltrated into *N. benthamiana* leaves at least 24 h prior to leaf disk collection for reactive oxygen and calcium measurements.

Transformation of Arabidopsis thaliana

Stable transgenic lines of *Arabidopsis thaliana* were generated using the floral dip technique (Clough and Bent, 1998). In brief 400 ml cultures of L-media were inoculated with from overnight cultures of *Agrobacterium tumefaciens* GV3101 containing the plasmid of interest growing in the presence of the appropriate antibiotics. These 400 ml cultures where then grown overnight, spun-down (2500 g) and resuspended in 200 ml 5% (w/v) sucrose solution. Immediately prior to dipping, 500 $\mu l.l^{-1}$ Silwet L-77 was added to the solution to decrease surface tension. Young flowering plants, with many immature inflorescence buds, were then dipped for 45 seconds prior to being covered and kept out of direct light for 24 h. Seeds were harvested and selected accordingly.

Transformation of Solanum lycopersicum (Performed by Matthew Smoker, TSL)

Transformation of tomato was performed by the tissue culture support team at TSL lead by Matthew Smoker. The method used was leaf disk transformation, as described by Horsch *et al.* (1985). Transformant explants were selected in tissue culture using 15 $mg.l^{-1}$ phosphinotricin. T1 transformants were screened for expression of the transgene as evidenced by a correctly sized band on an αGFP western blot, preferential lines were then copy number genotyped by IDNA GENETICS (Norwich, UK) using duplexed taqman qPCR to assay the quantity of the BAR selection marker from the pEarleygate103 vector used against a tomato housekeeping gene. Preferentially single copy transformants were selected.

2.2.3 Physiological assays

Reactive oxygen species measurement from leaf disks

Leaf disks were harvested from ~5-week-old *Arabidopsis* plants grown under short day conditions or 4-week-old *N. benthamiana* using a 4mm diameter biopsy punch (Integra™ Miltex™). Leaf disks were floated overnight on 100 µl of distilled water in white 96-well-plates (Greiner Bio-One). Prior to ROS measurement the water was removed and replaced with ROS assay solution (100 µM Luminol (Merck), 20 $\mu g.mL^{-1}$ Horseradish peroxidase (Merck)) with or without the addition of elicitors. Immediately following the addition of the assay solution light emission was measured from the plate using a HIGH RESOLUTION PHOTON COUNTING SYSTEM (HRPCS218, Photek) equipped with a 20 mm F1.8 EX DG ASPHERICAL RF WIDE LENS (Sigma Corp).

ROS burst from seedlings

Plate grown *Arabidopsis* seedlings were individually transferred into a sterile white 96-well-plate containing 150 µL full strength MS media, covered with a transparent lid and returned to growth conditions for an additional 5 days. The day before the ROS measurement the liquid MS media was replaced with 200 µl distilled water. Immediately before ROS measurement

the water was removed and replaced with L-012 ROS assay solution (0.5 µM L-012 (WAKO chemicals), 20 µg.ml^{-1} Horseradish peroxidase (Merck)) with or without the addition of elicitors. Photon emission was then measured as described previously.

DAB staining

3,3′-diaminobenzidine (DAB) staining was performed according to procedures described previously with modifications (de Oliveira *et al.*, 2016). Briefly, the excised plant tissues were immersed in DAB solution (1 mg.ml^{-1} DAB (MERCK) in 10 mM Na_2HPO_4 and 0.05% (v/v) Tween 20). Samples were vacuum-in filtrated and then incubated for the appropriate time. Subsequently, samples were transferred to DAB destaining solution (ethanol, acetic acid and glycerol in a ration of 3:1:1) and incubated in destaining solution at room temperature until complete destaining with replacement with fresh solution. Pictures were taken under a dissecting microscope with samples in 10% glycerol.

Measurement of cytoplasmic calcium concentration

Leaf disks were collected as described above, however, they were floated overnight in the dark in 20 µM coelenterazine (Merck). The following morning coelenterazine solution was replaced with 100 µl water and rested for a minimum of 30 min in the dark. Readings were taken in a VARIOSKAN^{TM} MUTIPLATE READER (ThermoFisher) using the injector to add 50 µl of 3x concentrated elicitor solution or mock. Seedlings were grown as described in the ROS assay and MS media was replaced with coelenterazine solution as described for leaf disks.

Conversion into cytoplasmic calcium concentration was performed using the formula below (Allen *et al.*, 1977; Knight *et al.*, 1991; Van Der Luit *et al.*, 1999; Mithöfer and Mazars, 2002)

$$[Ca^{2+}]_{Cytoplasmic} = \frac{\left\{\frac{\left(\frac{L_0}{L_{max}}\right)_1}{3} + \left[\frac{KTR\left(\frac{L_0}{L_{max}}\right)_1}{3}\right] - 1\right\}}{\left\{KR - \left[\frac{KR\left(\frac{L_0}{L_{max}}\right)_1}{3}\right]\right\}}$$

where L$_0$ = luminescence intensity per second

L_{max} = total amount of luminescence over the course of the experiment

KR = dissociation constant for the first Ca^{2+} ion to bind aequorin (2 x 10^6 M^{-1})

KTR = dissociation constant of the second Ca^{2+} ion to bind aequorin (55 M^{-1})

Values for KR and KTR were derived by Van Der Luit *et al.* (1999).

Seedling growth inhibition

Arabidopsis seeds were sterilised and sown on ½ MS plates prior to transfer to liquid MS media as described previously. Seedling were transferred individually into sperate wells of transparent 48-well tissue culture plates (Greiner Bio-One) containing 500 µl of liquid MS

media with/without elicitor addition. The plates were then transferred back to the growth conditions for an additional 10 days before seedlings were dried and weighed.

Relative lignification (performed by the Hamann Lab, NTNU, NO)

At 12 h after treatment, seedlings were harvested in 70% EtOH and stained for lignification using phloroglucinol-HCl as described (Denness *et al.*, 2011). For determination of lignin deposition in the root elongation zone, pictures were taken with a Zeiss Axio Zoom.V16 stereo microscope. Phlorogucinol-stained areas were quantified using ImageJ software and normalized to the total root area photographed, while the root length was kept equal in all images. The ratios obtained are plotted as fold change compared to Col-0.

Rosette growth under salt stress (performed by the Testerink lab, UVA, NL)

Soil-grown plants (11 h photoperiod; 22 ºC; 70% humidity) were transferred to pots which were saturated with 4 l of either 0 or 75 mM of NaCl solution. During the experiment, all plants were watered with rainwater from below. Conductivity measurements confirmed that salt levels stayed stable during the experiment. Four-week-old plants were harvested and dried at 68 ºC for 1 week to determine dry weight. Genotypes were randomised across trays using a randomized block design.

Root skewing/hypocotyl growth

Vapour-sterilised seeds were sown on square plates with MS medium; 1% sucrose; 0.8% agar (unless otherwise stated) supplemented with/without respective treatments. The seeds were stratified for 2 days at 4°C, and incubated for 9 days at 22°C under a 16 h photoperiod, in an upright position under a 10° angle relative to the direction of gravity. For dark-grown hypocotyl growth seedlings seeds were left in the light for several hours to promote germination, prior to being wrapped in foil. An exception to this is root angle in response to NaCl/Sorbitol treatment, here seedlings were germinated on media without treatment, 4-day-old seedlings were then transferred on to plates containing the treatment (75 mM NaCl; 150 mM sorbitol; or mock).

2.2.4 Pathogen assays

Spray infection with Pseudomonas syringae

Pseudomonas syringae cultures were grown over night in liquid KB media (20 $g.l^{-1}$ Peptone; 1.5 $g.l^{-1}$ K_2HPO_4; 1.5 $g.l^{-1}$ $MgSO_4 \cdot 7H_2O$; 1% glycerol (v/v)). Cultures were then spun down at 3,000g and the bacterial pellet was resuspended in 10 mM $MgCl_2$ solution and the OD_{600} adjusted to 0.2. Immediately prior to spray inoculation of 5-week-old plants 0.04% Silwet L-77 was added as a surfactant. Well-watered plants were then sprayed homogeneously sprayed with the inoculum and covered with a cloche for 3 days. On third day leaf disks were taken from the 3 youngest full expanded leaves form each plant and homogenised in 10 mM $MgCl_2$

using the Geno/grinder (2x 3 mm glass beads per sample, 1500 RPM). A dilution series was then generated in 10 mM $MgCl_2$ and plated onto KB media containing the appropriate antibiotics.

Alternatively, a qPCR based quantification of bacterial biomass was used (Ross and Somssich, 2016). In brief, total DNA was extracted using the FASTDNA SPIN KIT FOR SOIL (MP Biomedicals) according to the manufacturer's instructions. For qPCR measurement of the relative transcript abundance 15 ng of total DNA was used following the same protocol as outlined earlier. The abundance of *Pseudomonas* derived, *oprF* operon, DNA was then normalised to the plant derived DNA, *At4g26410*.

Xanthamonas infection

A *Xanthamonas vesicatoria* field isolate was used for inoculations belonging to PRB biotech. Bacterial lawns were grown on NGA media (13 $g.l^{-1}$ nutrient broth, 8 $g.l^{-1}$ glucose, 15 $g.l^{-1}$ agar) for 48 hours in the dark. The bacteria were subsequently resuspended in water to reach $O.D._{600}$=1.2. 3.5-week-old tomato plants were liberally spray inoculated and covered for 3 days to retain a high humidity. The cloche was then removed to allow the disease to progress. Plants were then assessed leaf by leaf to assess symptom severity.

To achieve more quantitative results, the pathogen *Xanthomonas perforans* T4-4B (previously known as *X. axonopodis pv. vesicatoria*) was used which has rifampicin resistance. *X. perforans* T4-4B was grown overnight in liquid NYGB media (5 $g.l^{-1}$ bacto-peptone, 3 $g.l^{-1}$ yeast extract, 2% (v/v) glycerol, 1 mM magnesium chloride) at 28 ^oC before being spun-down and resuspended in water to $O.D._{600}$ = 1.2. 0.008% Silwet L-77 was added immediately prior to dip inoculation. Inoculated plants were then left covered for 3 days and then uncovered for an additional 5 days prior to bacterial quantification. Bacterial growth was quantified by blending whole leaves in distilled water. The subsequent dilution series was then plated on NYGB media supplemented with rifampicin and nystatin and incubated at 28 ^oC for 2 days before colony counting.

Sclerotinia infection

Liquid Potato Dextrose Broth media (Fischer scientific) cultures were inoculated from fresh *Sclerotinia sclerotiorum* colonies growing on Potato Dextrose Agar plates (Fischer scientific). These were grown for 7 days at 24 ^oC with gentle shaking. Prior to inoculation the culture was blended and water was used to adjust the optical density to $O.D._{600}$ =0.6. Plants were spray inoculated and covered for 5 days before symptom scoring.

Plectosporella infection

Three-week-old soil-grown plants were spray inoculated with a suspension of 4 x 10^6 $spores.ml^{-1}$ (Delgado-Cerezo *et al.*, 2012; Jordá *et al.*, 2016). The progress of fungal infection

was quantified by qPCR as described earlier. Genomic DNA was isolated and primers were used which amplified the *Pc*BMM β-tubulin and *Arabidopsis* biomass was calculated using primers targeting UBC20 (AT5G25760) (Delgado-Cerezo *et al.*, 2012).

2.2.3 Statistical methods

Statistical analyses were performed using Graphpad Prism unless otherwise stated.

Graphical representations

Unless otherwise stated:

- Luminescence curves are plotted as the mean for each time point and error bars represent the standard error of the mean.
- Column data are plotted as scatter plots showing individual data points with a line representing the mean, and error bars representing a standard deviation.

In order to determine the likelihood that differences observed between sample means are reflective of differences between population means, a range of statistical analyses were performed. All these analyses are based on the null hypothesis that samples were drawn from populations with the same mean. P-values reported state the likelihood that, for the given sample size, the samples are drawn from populations with the same mean value.

Initially it was determined whether the data is normally distributed, and thus if parametric or non-parametric analyses should be applied to the data. A Kolmogorov-Smirnov test for normality was used to determine that probably that the data were taken from a population with a normal distribution.

If the assumption of normality was satisfied:

> In order to test for a significant difference between two sample means a two-way t-test was performed. If comparisons were made between multiple sample means a one-way Analysis of Variance (ANOVA) was performed. If the one-way ANOVA indicated, a significant probability that the data are taken from populations with different means ($p<0.05$), a multiple comparison post-hoc test was performed. To test for significant difference between multiple means a Tukey's post hoc test was performed. If multiple sample means are being compared to a single control mean, but not to each other, a Dunnett's Post hoc test was performed.

If the assumption of normality was not satisfied:

A Mann-Whitney test was used to compare two samples and a Kruskal-Wallis test was used to compare the multiple samples. If the Kruskal-Wallis test indicated a significant difference between sample populations a Dunn's multiple comparison test was used to identify which samples differed.

Chapter 3

Characterisation of the *Arabidopsis thaliana* leucine-rich repeat receptor kinase subfamily XII

3.1 Summary

Plants employ cell-surface localised receptors called pattern recognition receptors (PRRs) to perceive the presence of pathogen associated molecular patterns (PAMPs) and damage associated molecular patterns (DAMPs) in their environment. PAMP/DAMP perception induces pattern-triggered immunity (PTI) which promotes resistance to pathogens, thus promoting plant fitness. Therefore, plants have evolved numerous PRRs to recognise a diverse range of PAMPs/DAMPs. It is becoming apparent that the recognition of many PAMPs is lineage specific due to the limited phylogenetic distribution of their cognate receptors. Over the last decade, several PRRs have been transferred between plant species and families to confer PAMP recognition in plant otherwise blind to them, which increased broad-spectrum, quantitative disease resistance. As such, non-crop genomes represent an exploitable reservoir of PRRs that can be used to engineer disease resistance in crops. However, this approach is currently limited by the number of characterised, family-specific, receptors. Here, I aimed to characterise the *Arabidopsis thaliana* leucine-rich repeat receptor kinase subfamily XII as a promising source of PRRs. I demonstrate that the cytoplasmic domains of members of this family are able to produce outputs indicative of PTI. In light of these promising results, I generated genetic resources in *Arabidopsis thaliana* and tomato to enable the characterisation of the undescribed members of this receptor kinase clade using parallel loss-of-function and gain-of-function approaches in the context of disease resistance.

3.2 Introduction

Plants rely on passive and active defences in order to resist attack by pathogens (Dangl *et al.*, 2013; Cook *et al.*, 2015). Active defences depend upon the plants' ability to recognise the presence of the pathogen and to respond accordingly. To this end, plants employ both cell-surface and cytoplasmic immune receptors to detect the signatures of pathogen invasion (Cook *et al.*, 2015). Cell-surface pattern recognition receptors (PRRs) survey the apoplast for the presence of non-self elicitors (*i.e.* microbial derived) or modified-self (*i.e.* host derived) elicitor molecules (Saijo *et al.*, 2018). PRRs can be divided into two classes: i) receptor kinases

(RK), which consist of an apoplastic ligand binding domain, single pass transmembrane α-helix and a cytoplasmic kinase domain, and ii) receptor-like proteins (RLPs), which lack the cytoplasmic kinase domain and rely on adaptor RKs for signal transduction. In the current paradigm, PRRs perceive elicitor molecules which act as molecular glues to induce the recruitment of a shape complementary co-receptor (Hohmann *et al.*, 2017). This receptor complex activates downstream signalling – inducing, among other responses, reactive oxygen species (ROS) production, cytoplasmic calcium influx and defence gene expression - ultimately culminating in enhanced resistance.

Many of the RK-type PRRs that have been identified contain leucine-rich repeat (LRR) motifs within their ectodomains (Boutrot and Zipfel, 2017; Saijo *et al.*, 2018). LRR-RKs represent the largest family of RKs in plants, with 225 encoded in the *Arabidopsis thaliana* (hereafter *Arabidopsis*, unless indicated) genome (Shiu and Bleecker, 2001*b*; Gou *et al.*, 2010; Smakowska-Luzan *et al.*, 2018). Fourteen subfamilies have been defined within LRR-RKs based on the phylogeny of the kinase domain (Shiu and Bleecker, 2001*b*). LRR-RK subfamily XIIa, which contains the well-studied PRRs FLS2 and EFR, potentially represents a rich source of novel PRRs. The first cloned RK-type PRR, XANTHOMONAS ORYZAE PV. ORYZAE RESISTANCE 21 (Xa21), also belongs to subfamily XIIa (Song *et al.*, 1995). It originates from *Oryza longistaminata* and confers resistance to *Xanthomonas oryzae pv. oryzae* (*Xoo*) in rice (*O. sativa*). Xa21 functions as the receptor for sulphated RaxX peptide from *Xanthomonas* (Pruitt *et al.*, 2015; Luu *et al.*, 2019). RaxX is a virulence factor produced by *Xanthomonas* to mimic the host PSY1 peptide and consequently suppress host immunity (Amano *et al.*, 2007; Pruitt *et al.*, 2017). However, Xa21-mediated recognition of RaxX activates immune signalling, leading to host resistance (Pruitt *et al.*, 2017). Following the identification of Xa21, Gómez-Gómez and Boller (2000) cloned FLS2 (FLAGELLIN-SENSING 2) from *Arabidopsis*, a PRR which recognises an N-terminal 22-amino acid motif from flagellin, known as flg22 (Felix *et al.*, 1999). Both the receptor and the ligand are evolutionarily ancient and are conserved in plants and gram-negative bacteria, respectively (Boller and Felix, 2009; Han, 2019). This was followed by the identification of a related LRR-RK from *Arabidopsis*, EFR (EF-TU RECEPTOR), which recognises an 18-amino acid minimal epitope of bacterial elongation factor Tu known as elf18 (Kunze *et al.*, 2004; Zipfel *et al.*, 2006). However, unlike FLS2, EFR is restricted to *Brassicaceae* (Zipfel *et al.*, 2006; Lacombe *et al.*, 2010).

Since then, multiple PRRs have been identified from this family. These include XPS1 (XANTHINE/URACIL PERMEASE FAMILY SENSING 1) from *Arabidopsis* that perceives xup25, a 25-amino acid motif derived from a *Pseudomonas syringae* xanthine/uracil permease (Mott *et al.*, 2016). Other characterised members come from *Solanaceous* plants (Veluchamy

et al., 2014). The tomato (*Solanum lycopersicum*) LRR-RK FLS3 recognises an unrelated flagellin epitope, flgII-28 (Clarke *et al.*, 2013; Hind *et al.*, 2016). Meanwhile, the tomato LRR-RK CORE is the receptor for the highly conserved nucleic acid binding motif RNP-1 of bacterial cold-shock proteins (CSPs), specifically the 22-amino acid epitope csp22 (Felix and Boller, 2003; Wang *et al.*, 2016*a*).

The LRR-RK subfamily XIIa is the most expanded clade of LRR-RKs within land plant genomes (Fischer *et al.*, 2016; Dufayard *et al.*, 2017). The majority of these genes have arisen relatively recently through lineage specific expansions, indicative of the co-evolutionary arms race between host recognition and pathogen evasion. Furthermore, members of subfamily XIIa in *Arabidopsis thaliana* are all non-Arg/Asp-type protein kinases, a feature that has been correlated with immune function across eukaryotes (Dardick *et al.*, 2012). Taken together, this suggests that the LRR-RK subfamily XII represents a promising source of PRRs.

Whilst FLS2 is evolutionarily conserved, other receptors are lineage specific in their distribution, with lineages that lack cognate receptors being blind to the PAMPs. Interestingly, several examples show that these lineage-specific PRRs can be successfully transferred transgenically between plant species and families, leading to increased broad spectrum, quantitative disease resistance (Mendes *et al.*, 2010; Lacombe *et al.*, 2010; Afroz *et al.*, 2011; Bouwmeester *et al.*, 2014; Tripathi *et al.*, 2014; Holton *et al.*, 2015; Schoonbeek *et al.*, 2015; Schwessinger *et al.*, 2015; Du *et al.*, 2015; Albert *et al.*, 2015; Lu *et al.*, 2015; Hao *et al.*, 2016; Wang *et al.*, 2016*a*; Boschi *et al.*, 2017; Kunwar *et al.*, 2018). This is particularly well documented for EFR which has been transferred from *Arabidopsis* to *Nicotiana benthamiana*, tomato, potato (*S. tuberosum*), wheat (*Triticum aestivum*) and rice (Lacombe *et al.*, 2010; Holton *et al.*, 2015; Schoonbeek *et al.*, 2015; Schwessinger *et al.*, 2015; Lu *et al.*, 2015; Boschi *et al.*, 2017; Kunwar *et al.*, 2018). The success of this approach was surprising considering the millions of years of evolutionary divergence between *Brassicaceae* and the recipient plants (Kumar *et al.*, 2017), and indicate that PTI signalling components are functionally conserved across these plant families. Consistently, *Os*Xa21 and *At*EFR recruit homologous signalling components, suggesting functional conservation of immune signalling components downstream of distinct LRR-RK-type PRRs between monocots and dicots (Holton *et al.*, 2015). Therefore, the restricted phylogenetic distribution of many PRRs and the relative ease of their cross-species transfer makes PRRs in non-crop genomes an exploitable reservoir of immune receptors that can be used to engineer quantitative, broad spectrum disease resistance in crops (Boller and Felix, 2009; Boutrot and Zipfel, 2017). Notably, the transfer of EFR into potato and tomato provided significant control of diseases caused by the bacteria *Ralstonia solanacearum* and *Xanthomonas perforans* in field conditions (Boschi *et al.*, 2017; Kunwar *et al.*, 2018).

To test if additional *Arabidopsis* LRR-RK subfamily XII members play a role in PTI, potentially as PRRs, I used a chimeric receptor approach to assess if their cytoplasmic domains are able to activate PTI-like responses. I could show that the majority of this family are indeed able to induce PTI-like responses. Interestingly, my results in *Arabidopsis* and *N. benthamiana* however reveals surprising differences in the kinetics of PTI outputs. Having demonstrated functionality of the cytoplasmic domains in *N. benthamiana*, I transferred the uncharacterised LRR-RKs from *Arabidopsis* into tomato to test for a gain-of-resistance phenotype. In parallel, I generated and characterised higher order loss-of-function mutants in *Arabidopsis* to test if the loss of these genes would lead to enhanced disease susceptibility.

3.3 Results

3.3.1 LRR-RK subfamily XII from *Arabidopsis thaliana*

The LRR-RK subfamily XII consists of two clades, XIIa and XIIb, which contain 8 and 2 members in the Col-0 genome respectively, and which were numbered based on their position within the genome (coloured magenta and turquoise within the phylogeny respectively) (Fig. 3.1). With one exception, all subfamily XIIa RKs in *Arabidopsis* have long ectodomains, indicative of a function as ligand-binding receptor. The exception is *AT5G39390* which appears to have arisen from a recent duplication of *EFR*. It is only present in *A.* thaliana, it is not present in the closely related *A. lyrata* genome (Dufayard *et al.*, 2017). Unlike EFR which has 21 leucine-rich repeats, AT5G39390 has a short extracellular domain with only 1 LRR due to a large ectodomain deletion. This indicates that AT5G39390 may not function as a ligand-binding receptor. Interestingly, only two members of *Arabidopsis thaliana* LRR-RK subfamily XII are conserved outside *Brassicaceae* (Dufayard *et al.*, 2017). The well characterised *FLS2* receptor is present in all angiosperm lineages examined (Han, 2019), and *XII2* (*AT2G24130*) is conserved at least within the core eudicots (Dufayard *et al.*, 2017).

Figure 3. 1 Phylogeny of *Arabidopsis thaliana* and *Solanum lycopersicum* leucine-rich repeat receptor kinase subfamily XIIa and XIIb.

Phylogeny generated based on the alignment of the amino acid sequence of the kinase domain from the *A. thaliana* (blue) and *S. lycopersicum* (green) proteomes (Fischer *et al.*, 2016). Sequences were aligned using MUSCLE and a tree was generated using PhyML maximum likelihood with LG matrix. The tree was visualised using iTOL (Letunic and Bork, 2019). Subfamily XIIa = magenta, Subfamily XIIb = turquoise. Bold text indicates characterised proteins. The kinase domain of *A. thaliana* CrRLK1L FERONIA was used as an outgroup. Blue nodes represent >80% bootstrapping support (100 iterations performed)

3.3.2 *XII2* expression appears to be root-specific

Consultation of publicly available expression data suggests that *XII2* is highly induced by salt stress and is primarily expressed within root tissue (Ma *et al.*, 2006; Winter *et al.*, 2007; Kilian *et al.*, 2007; Aoki *et al.*, 2016) (Fig 3.2 a-b). Consistent with this, I was only able to clone *XII2* cDNA from RNA extracted from NaCl-treated seedling roots (75 mM NaCl for 6 h); no PCR product was obtained from untreated seedling RNA. Notably, a high resolution root transcription map shows *XII2* is predominantly expressed in BASIC LEUCINE-ZIPPER 6 (bZIP6) positive cells through a developmental time series (Fig. 3.2 c) (Brady *et al.*, 2007; Waese *et al.*, 2017). The bZIP6 transcription factor is a marker of phloem pole pericycle cell identity (Lee *et al.*, 2006; Brady *et al.*, 2007). It would be interesting to confirm this expression profile using reporter constructs and to explore the possibility of cell-type specific functions of XII2. *XII2* orthologs in poplar and tomato share this root specific expression (Wilkins *et al.*, 2009; Consortium, 2012; Waese *et al.*, 2017) (Fig. 3.2 d-e). Retention of both the coding sequence and its expression profile across evolutionary time scales suggests that both are under positive selection. Taken together, this data suggests that XII2 is recognising a PAMP from microbe(s) present in the rhizosphere – potentially upon phloem invasion. Alternatively, XII2 could recognise an endogenous peptide – potentially one that is involved in response to salt stress or phloem-mobile.

3.3.3 Is xup25 a PAMP recognised by *Arabidopsis*?

During the course of this project, Mott *et al.* (2016) identified a novel PAMP, xup25, derived from a xanthine/uracil permease family protein from *Pseudomonas syringae*. They used a bioinformatic approach to identify regions of the *Pseudomonas syringae* proteome that showed evolutionary signatures indicative of recognition by host immune receptors (McCann *et al.*, 2012). Having identified xup25, they employed a reverse genetic approach to identify XPS1, a member of LRR-RK subfamily XIIa, as its receptor (Mott et al., 2016). To confirm whether I could observe xup25-induced PTI outputs I performed luminol-based measurement of reactive oxygen species production. ROS production was measured by the authors but using a microtiter-plate based assay for peroxidase activity. Under our conditions, I was unable to observe xup25-induced ROS production, unlike the flg22 positive control (Fig. 3.3a). As several elicitors induce weak ROS production (*e.g.* cellobiose (Souza *et al.*, 2017)), I decided to measure cytoplasmic calcium influx. Like ROS production, I was unable to observe any xup25-induced cytoplasmic calcium influx; meanwhile the flg22 positive control produced a clear response (Fig. 3.3b). To test later responses, I assayed seedling growth in the presence of xup25 to determine whether I could observe the xup25-induced growth inhibition reported (Mott et al., 2016). There was no statistically significant difference in seedling mass between mock and xup25 treatments, unlike flg22 treatment which resulted significant in growth inhibition (Fig. 3.3c-d).

My results are in accordance with another recent publication that also failed to detect xup25-induced responses (Eckshtain-Levi *et al.*, 2018). One could envisage an environmental dependency to xup25 responses, for example governing *XPS1* expression. As I was unable to observe xup25 activity I was unable to verify whether this response was XPS1-depdendent.

3.3.4 The cytoplasmic domains of most members of the *Arabidopsis* LRR-RK subfamily XII can induce early outputs indicative of PTI in *Solanaceae*

Previous work has shown that the ectodomain of LRR-RKs confers ligand-binding specificity, whilst the cytoplasmic domain defines downstream signalling specificity (He *et al.*, 2000; Albert and Felix, 2010; Albert *et al.*, 2013; Holton *et al.*, 2015; Hohmann *et al.*, 2018*b*). To dissect ligand binding from downstream signalling function, chimeric receptors were generated with the transmembrane and cytoplasmic domain of each respective member of *Arabidopsis* LRR-RK subfamily XII fused to the EFR ectodomain (Fig 3.4a). The chimeric receptors were subsequently expressed in *N. benthamiana* using *Agrobacterium*-mediated transient expression. *N. benthamiana* lacks the cognate receptor for elf18. I exploited elf18-blindness in *N. benthamiana* to look for a gain of elf18-sensitivity in leaves transiently expressing the chimeric receptors (Fig 3.4 b). Initially, I used ROS production as an early output associated with immune signalling. *N. benthamiana* leaves transiently expressing GUS were unresponsive to elf18, however, transient expression of full length EFR was able to confer elf18 sensitivity and elicit ROS production (Fig. 3.4 c). The EFR:FLS2 chimeric receptor could also induce elf18-dependent ROS production. In order to determine the specificity of the response I created a chimeric receptor with the BRASSINOSTEROID INSENSITIVE1 (BRI1) transmembrane and cytoplasmic domain (Li and Chory, 1997). EFR:BRI1 did not confer elf18-induced ROS production (Fig. 3.4c). With the exception of EFR:XII2, all chimeric receptors from *Arabidopsis* LRR-RK subfamily XII induce ROS production in response to elf18 treatment (Fig. 3.4 c). I was unable to convincingly observe expression of the EFR:AT5G39390 chimera (Fig. 3.4 b); and excluded this RK from further analysis.

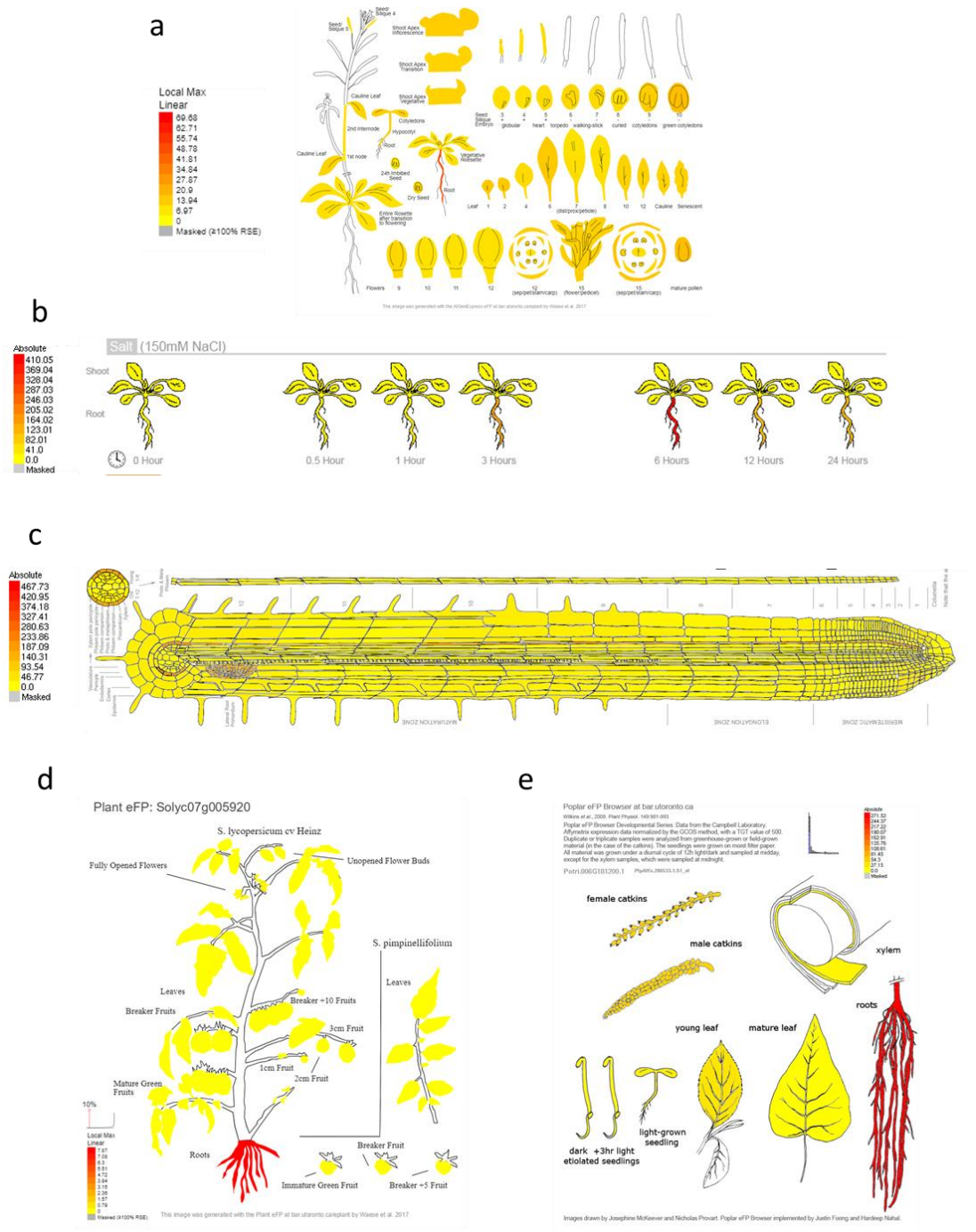

Figure 3. 2 Publicly available expression data showing the root specific expression profile of *XII2* and its orthologs

(a)Expression profile of *AT2G24130* in *Arabidopsis* (Schmidt *et al.* 2005) (b) Expression in response to salt stress (Kilian *et al.* 2007) (c) Root cell type specific expression profile of *AT2G24130 (Brady* et al. 2007) (d) Expression of the *XII2* ortholog *Solyc07g005920* in *S. lycopersicum* (e) Expression of *XII2* ortholog *Potri.006G181200* in *Populus trichocarpa.* All data taken from ePlant (Winter *et al.*, 2007; Fucile *et al.*, 2011; Waese *et al.*, 2017).

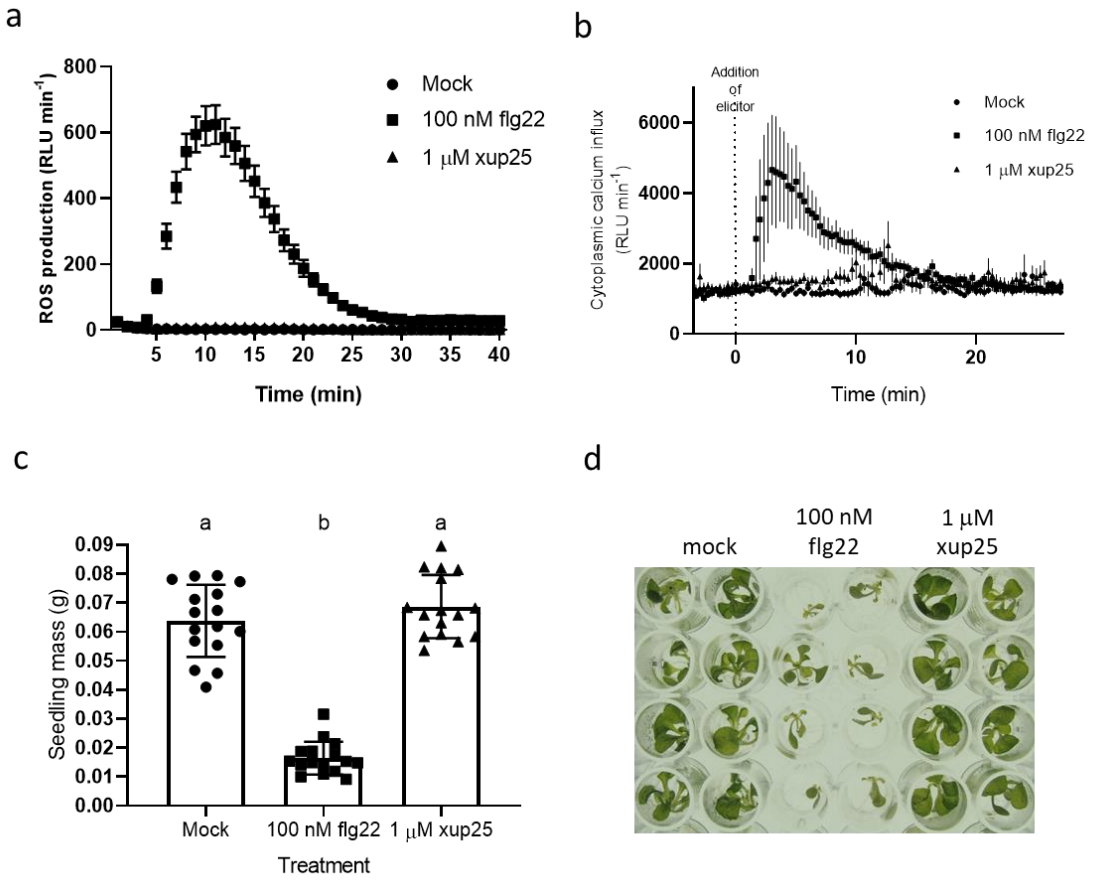

Figure 3. 3 Reanalysis of the PAMP xup25 in *Arabidopsis thaliana*

(a)Elicitor-induced ROS production in leaf disks from 5-week-old Col-0 rosettes. Mean ± S.E.M. (n=16) (b) Elicitor-induced cytoplasmic calcium influx in Col-0 seedlings expressing AEQUORIN. Mean value ± S.E.M. (n=8) (c,d) Seedling growth in the presence or absence of 1 µM xup25 and 100 nM flg22. Lower case letters represent significance groupings ($p<0.0001$) One-way ANOVA followed by Tukeys Post-hoc test. Error bars indicate S.D.

I repeated the transient expression in *N. benthamiana* lines stably expressing the cytoplasmic calcium reporter AEQUORIN (Segonzac *et al.*, 2011) and monitored elf18-induced changes in cytoplasmic calcium concentration. A similar trend was observed as for ROS production (Fig. 3.4 d).

Considered together these results suggest that the cytoplasmic domains of most members of LRR-RK subfamily XII from *Arabidopsis* are capable of inducing outputs indicative of PTI when expressed heterologously in *N. benthamiana*, supporting their proposed roles as PRRs.

3.3.5 Generation of stable *Arabidopsis* transgenic lines expressing EFR:XII chimeras

While the early responses of cytoplasmic calcium influx and ROS production in *N. benthamiana* are indicative of PTI, they are not sufficient to conclude the cytoplasmic domains are capable of inducing resistance to a pathogen. To address this question, I am generating stable transgenic *Arabidopsis* lines expressing the chimeric constructs in the *efr* background to perform elf18-induced resistance assays. This has proved challenging due to silencing of the transgene which has hampered my ability to obtain a complete set of stable transgenic lines.

Nevertheless, in the T1 generation I collected 4 leaf disks from 12 independent transgenic lines expressing each chimeric construct in the *efr* background. I observed intriguing differences in the kinetics and dynamics of elf18-induced ROS production (Fig. 3.5 a). As in transient expression in *N. benthamiana*, the chimeric receptors from subfamily XIIa were able to induce PTI-like ROS production, unlike the EFR:BRI1 chimera (Fig. 3.5 a-c). In addition to quantitative differences in cumulative ROS production, I observed that the kinetics of elf18-induced ROS production in the chimeric receptors differed. ROS production varied temporally; elf18-induced ROS production was delayed in EFR:XPS1 and EFR:XII6 expressing lines and more rapid in EFR:XII3 and EFR:XII5 relative to EFR:FLS2 (Fig 3.5 a,d). Caution should be taken when interpreting these results as the protein levels are unknown and the differences could be artefacts of chimera generation. More detailed characterisation of the lines is required in homozygous T3 lines with similar expression levels. Whilst I observed these differences in elf18-induced ROS production, flg22-induced ROS production did not appear to be affected, suggesting that the effect of chimera expression is specific to elf18 and does not generally affect elicitor-induced ROS (Fig 3.5 e).

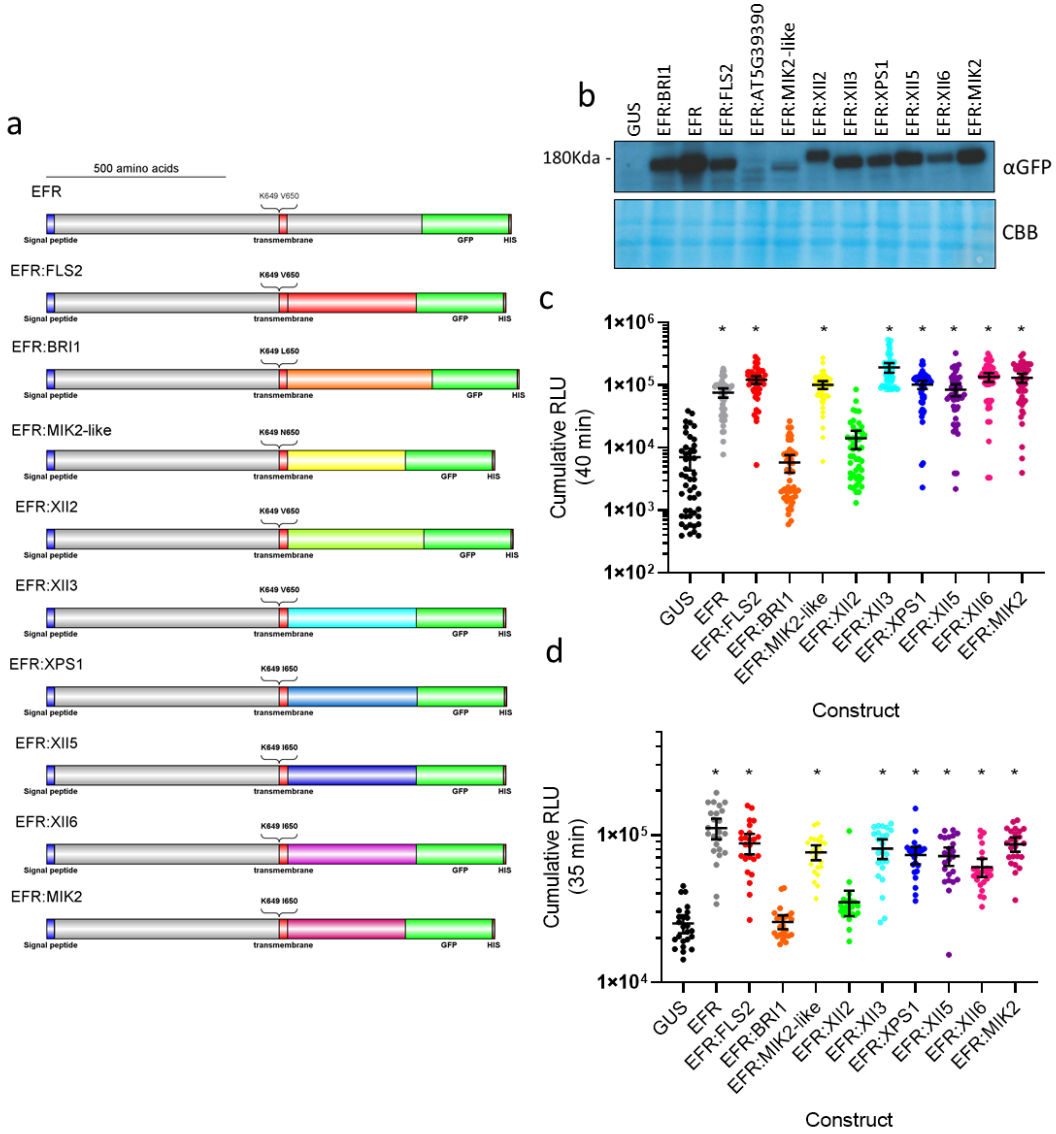

Figure 3. 4 Chimeric receptors with the ectodomain of EFR reveal the signalling outputs of the kinase domains from *At* LRR-RK subfamily XII in *N. benthamiana*.

(a) Models of the chimeric constructs generated. (b) Western blot showing the expression of the chimeric receptors transiently expressed in *N. benthamiana* (c) Cumulative 100 nM elf18-induced reactive oxygen species production in *N. benthamiana* leaf disks transiently expressing the chimeric receptors over 40 min. (d) Cytoplasmic calcium influx quantified as cumulative relative light emission induced by 100 nM elf18 application to *N. benthamiana/35S::AEQ* leaf disks transiently expressing the chimeric receptors.

Line represents the mean and error bars represent 95% confidence intervals. A one-way ANOVA indicated significant differences between groups. Consequently a Dunnett's multiple comparisons test was run to compare the mean of each population to the GUS negative control. * indicates a significant difference ($p<0.0001$) from the GUS negative control

The EFR:BRI1 chimera is unable to induce cytoplasmic calcium influx or ROS production, indicative of PTI. I wanted to test the ability of the chimera to activate elf18-induced brassinosteroid signalling. To this end, I assayed elf18-induced gene expression in *efr*/EFR and *efr*/EFR:BRI1 T2 segregating transgenic lines selected on phosphinothricin (PPT). I pre-treated plants with 2 µM brassinazole for 24 h to inhibit native brassinosteroid biosynthesis (Min *et al.*, 1999; Asami *et al.*, 2000, 2001; Nagata *et al.*, 2000). The brassinosteroid-responsive gene *SAUR15* (Nakamura *et al.*, 2003) was specifically induced by elf18 application in *efr/EFR:BRI1*, (Fig. 3.5 f), whilst the PTI marker gene *FRK1* (Asai *et al.*, 2002; Robatzek and Somssich, 2002) was specifically induced in *efr/EFR* (Fig. 3.5 g). Going forward it will be essential to repeat this assay and perform elf18-induced BES1-dephosphorylation to support the activation of brassinosteroid signalling (Yin *et al.*, 2002).

3.3.6 Kinase activity of XIIa LRR-RKs is differentially required for ROS and calcium signalling

To test whether kinase activity is required for subfamily XII function I generated kinase-dead versions of three characterised RKs, namely EFR (Zipfel *et al.*, 2006), FLS2 (Gómez-Gómez and Boller, 2000) and MIK2 (Wang *et al.*, 2016*b*; Van der Does *et al.*, 2017; Coleman *et al.*, 2019) distributed throughout the XII phylogeny. Kinase-dead variants were generated by mutating the catalytic aspartic acid to a neutral asparagine residue, thereby abolishing their kinase activity. The kinase-dead receptors were transiently expressed in *N. benthamiana.* The kinase-dead cytoplasmic domains of EFR* (* denotes kinase dead) and EFR:FLS2* were both able to elicit elf18-induced ROS, but with delayed peak ROS production and reduced cumulative ROS production compared to EFR and EFR:FLS2 (Fig. 3.6 a-b, d-e). A similar phenotype can be seen for cytoplasmic calcium influx in EFR* (Fig 3.6 c), however, elf18-induced cytoplasmic calcium influx was almost abolished in EFR:FLS2* (Fig. 3.6 f). This contrasts with MIK2 where mutation of kinase activity abolishes both ROS production and calcium influx (Fig. 3.6g-i). In all cases, the receptors with wild-type or mutated cytoplasmic domains accumulate to similar levels (Fig. 3.6 j). This points to a differential requirement for kinase activity in order to activate early PTI response, even amongst closely related RKs.

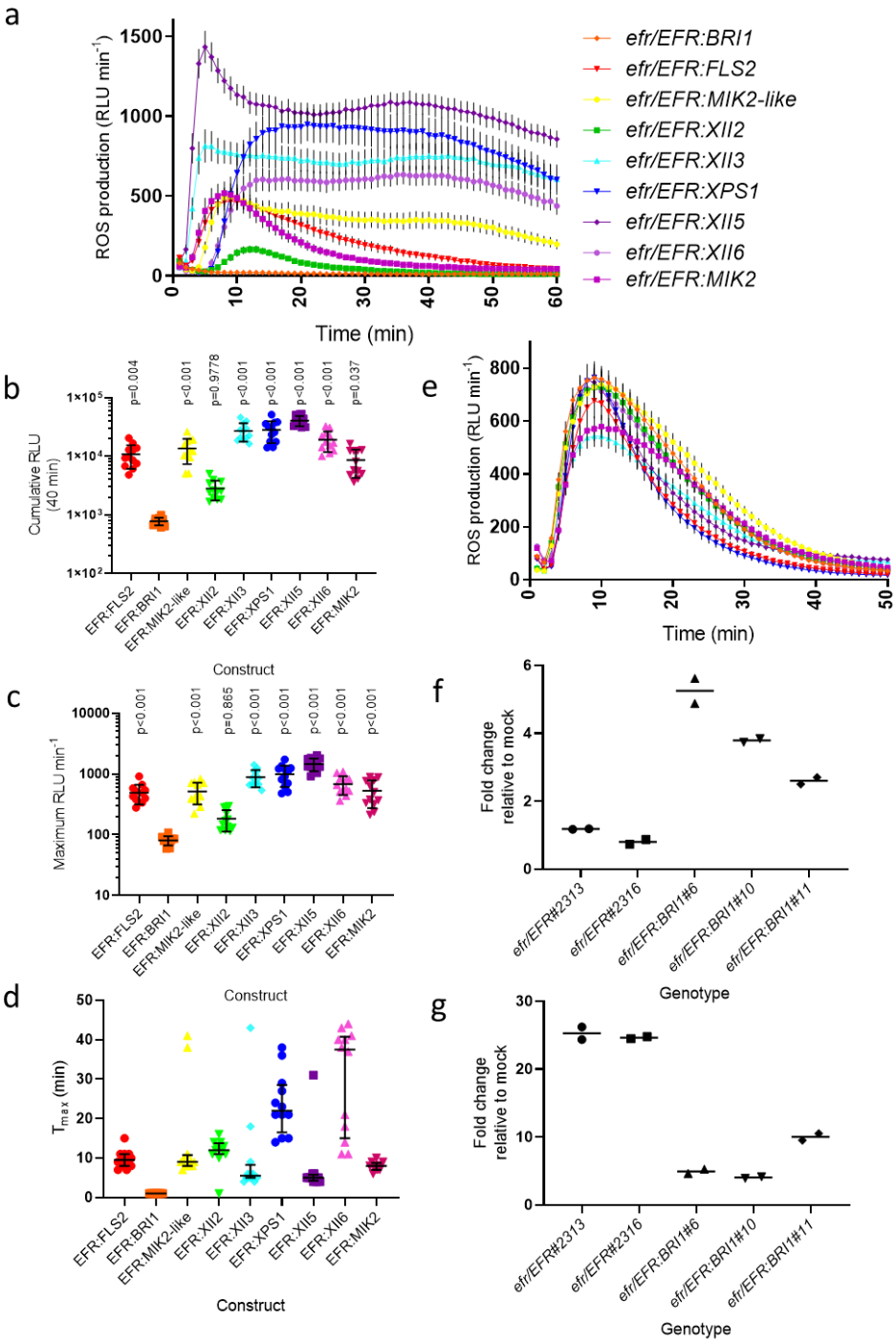

Figure 3. 5 Chimeric receptors with the ectodomain of EFR reveal the signalling outputs of the kinase domains from *At* LRR-RK subfamily XII when stably expressed in *Arabidopsis*.

(a) 100 nM elf18-induced ROS production in leaf disks from 5-week-old T1 plants. (b) Cumulative ROS production, (c) maximum ROS production per min and (d) time of peak ROS production from (a). (e) 100 nM flg22-induced ROS production in leaf disks from 5 week old T1 plants. Elf18-induced (d) *SAUR15* and (e) *FRK1* expression in T2 plants selected on PPT before transfer to liquid media. All plants were treated for 24 h with 2 µM brassinazole prior to 1 h treatment with 1 µM elf18 or mock.

All experiments performed once. (a,e) Values = mean (n=12), error bars = S.E.M. (b-c) Bar represents the mean and error bars represent S.D. A one-way ANOVA indicated significant differences between groups. A Dunnett's multiple comparisons test was run to compare the mean of each population to EFR:BRI1. (d) Bar represents median and error bars represent interquartile range.

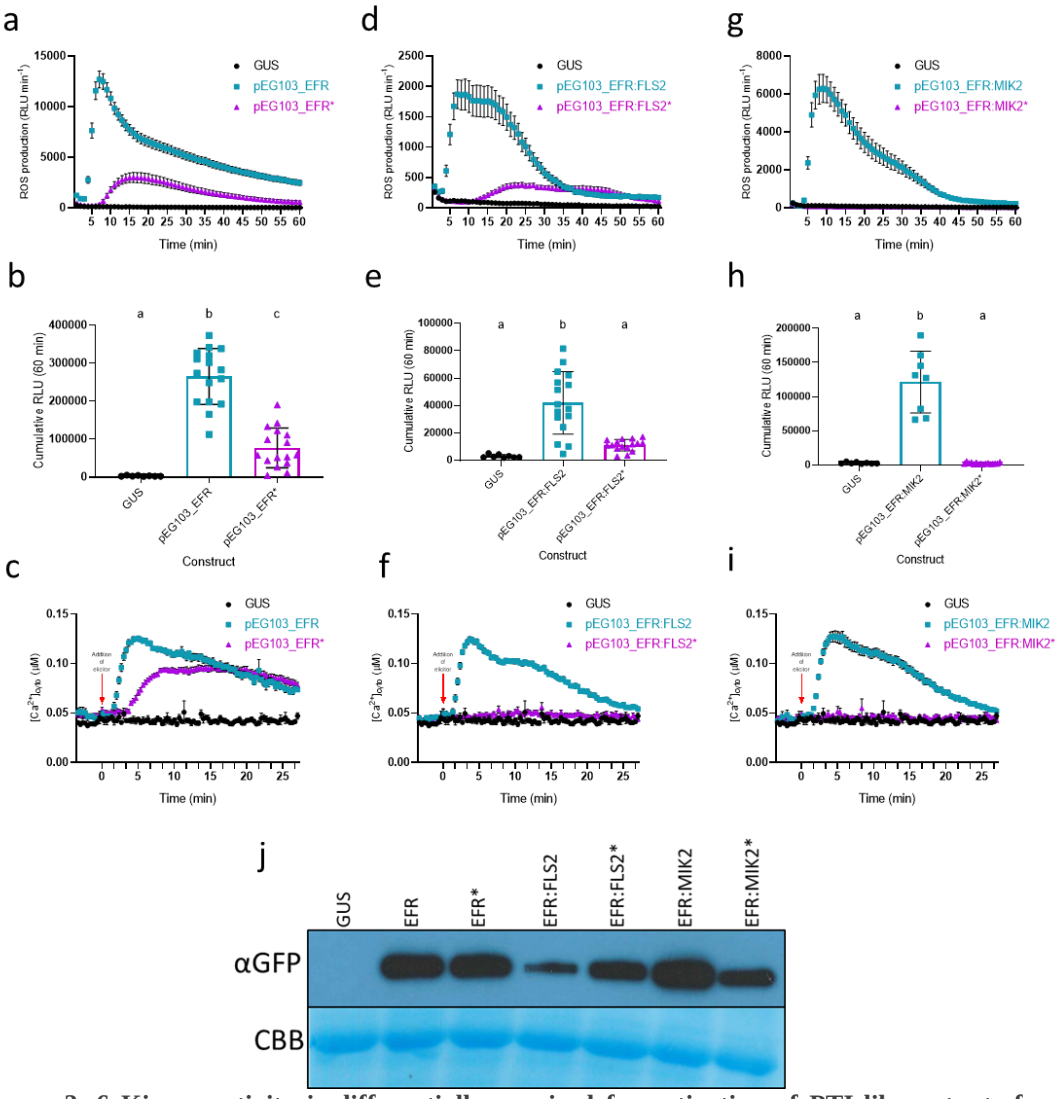

Figure 3. 6 Kinase activity is differentially required for activation of PTI-like outputs from subfamily XII kinase domains when transiently expressed in *N. benthamiana*

(a,d,g) 100 nM elf18-induced ROS production in leaf disks of *N. benthamiana* transiently expressing RK constructs. Mean value ±S.E.M. (n=16) Repeated 3 times with similar results. (b,e,h) Integrated ROS productions from (a,d,g) error bars represent S.D. Lower case letters represent significant groups as determined by Tukey's multiple comparisons test ($P<0.05$) (c,f,i) 100 nM elf18-induced cytoplasmic calcium influx in leaf disks of *N. benthamiana/35S::AEQ* leaf disks transiently expressing RK constructs (n=12) (j) Western blot confirming the expression of the RK constructs. Experiments were repeated 3 times with similar results.

3.3.7 Gain of function in tomato

EFR can be successfully transferred to tomato to confer elf18 sensitivity and quantitative, broad-spectrum disease resistance (Lacombe et al., 2010). EFR is a member of a clade of *Arabidopsis* LRR-RK subfamily XIIa genes, more similar to one another than any tomato RKs (Fig. 3.1). We hypothesised that this clade of RKs may be PRRs which perceive PAMPs which tomato has no receptor for, like EFR. Expression of these RKs in tomato may confer recognition of novel PAMPs in tomato, resulting in enhanced disease resistance. We therefore decided to express these RKs in tomato (the transformation was performed by Matthew Smoker and the TSL transformation support team). My confidence in this approach was bolstered by the functionality of the cytoplasmic domains in *Solanaceae* (Fig 3.4). The challenge with this approach is that the sources of putative PAMPs is unknown.

Transgenic tomato plants were generated using the pEarleygate103 expression vector (Earley *et al.*, 2006). Plants were selected based on RK accumulation assayed by western blot, and whenever possible single insertion events were selected (as determined by iDNA genetics, Norwich, UK). Where possible the two most promising lines were selected for further characterisation (Fig 3.7 a), unfortunately the second line expressing *XII3*, *XII3#4*, does not accumulate, potentially it has been silenced (Fig 3.7 b). *XII5#4* shows slight chlorosis in young leaves relative to other genotypes (Fig 3.7 a).

Initially, I spray inoculated four-week-old plants with *Sclerotinia sclerotiorum* - a necrotrophic fungal pathogen with broad host range (Moore, 1952). Disease symptom severity was assessed on a scale of 0 to 4 with 0 being asymptomatic and 4 being complete leaf necrosis or abscission (Fig. 3.8 a). The score was averaged over the second, third and fourth true leaves of the plant. There was no reproducible difference in disease symptom severity between any of the transgenic lines (Fig. 3.8 b). I also determined relative mass between genotypes following *S. sclerotiorum* infection. The heterogeneity within genotypes makes me reluctant to conclude anything from the statistically significant differences observed (Fig 3.8 c). Indeed, for the relative mass of *XII3#12* and *XPS1#2* there appears to be a bimodal distribution in relative mass (Fig 3.8 c). This could suggest that the infection is not homogeneous. An alternative hypothesis is that during tissue culture or transformation mutations affecting resistance or growth were introduced in these lines which are still segregating.

Subsequently I performed dip inoculation with *Xanthomonas campestris* pv. *vesicatoria* and scored symptom severity on a scale of 0 to 5 with 0 being asymptomatic and 5 being complete leaf necrosis or abscission. The line *XII5-1* had significantly reduced disease symptom severity compared to the Moneymaker control (Fig 3.9 a-c). However, this was not the case for the second independent transgenic line, *XII5-4* (Fig. 3.9 b). As with *Sclerotinia* infection, there is considerable heterogeneity in symptom severity within genotypes making it difficult

to draw conclusions. To gain more quantitative infection measurements I switched to using *Xanthomonas perforans* Race T4 (previously known as *X. axonopodis* pv. *vesicatoria*), which, due to rifampicin resistance, is more amenable to assaying bacterial growth through colony forming unit assessment on plates. One transformant from each line was selected in order to reduce the phenotyping workload and a previously published tomato line expressing EFR was included as a resistance control (Lacombe *et al.*, 2010). I was unable to replicate the enhanced resistance of *XII5-1* to *Xanthomonas campestris* pv. *vesicatoria* (Fig. 3.9 d). There was no significant difference between any of the transgenic lines (Fig 3.9 d), however, *XII3#12* and *XII6#1* showed statistically significant reductions in bacterial populations relative to the untransformed control (Fig 3.9 d). Surprisingly, I was unable to observe the published enhanced resistance in the EFR expressing (Fig 3.9 d) (Lacombe *et al.*, 2010). Upon further investigation, it became evident that the *EFR* transgene was silenced (data not shown). I have since reselected EFR-expressing plants that are elf18-responsive (Fig 3.9 e). It would be preferable to repeat *Xanthamonas* infection assays using a functional resistant control for comparison.

Finally, with the pathogen *Botrytis cinerea* strain CH94, I observed significantly reduced symptom severity in the *XII3#12*; however, I also observed that many of the lines appeared significantly more susceptible than the untransformed control (Fig 3.10). This experiment has only been performed once and requires repetition.

Taken together these results do not unambiguously identify a gain-of-resistance in any of the transgenic lines, however, some of the differences merit further investigation, especially the *Botrytis* infection. Moreover, the materials described represent a valuable resource for future characterisation.

3.3.8 Loss of function in *Arabidopsis*

In parallel with the gain-of-function studies in tomato, I sought to characterise the impact of loss of LRR-RK subfamily XII function on immunity in Arabidopsis. With this aim, T-DNA insertion lines were characterised for all the LRR-RK subfamily XII members (Table 2.1). The location of the insert was confirmed (T-DNA lines were preferentially selected with insertion within the ligand-binding ectodomain of the RK) and gene expression was analysed by qRT-PCR using primers spanning the intron within the cytoplasmic domain and normalised to *ACTIN7* (*AT5G09810)* (Fig. 3.11 a-b). I was only able to obtain Ct values under 30 in Col-0 for 3 genes, *XII3*, *XII5* and *XII6*, and of these only *XII6* seemed to show a reduction in RNA levels (Fig. 3.11 b). Given our current understanding of LRR-RK signalling, a major exonic disruption in the ectodomain of a ligand binding receptor should render it non-functional (Hohmann *et al.*, 2017). Therefore, I decided to perform semi-quantitative RT-PCR across the T-DNA insertion site in order to confirm transcript disruption and used *ACTIN7* as a loading

control (Fig. 3.11 c). For most of the T-DNA lines, I saw a loss of transcript, apart from *xps1-3*. This could be due to only a short fragment of the T-DNA inserting, or contamination of the cDNA with wild-type DNA. Moreover, the *xii3-1 ACTIN7* loading control shows weaker amplification than the other genotypes. This needs to be repeated in case the absence of *XII3* transcript in *xii3-1* is due to issues with *xii3-1* cDNA.

In order to tackle potential genetic redundancy between receptors, higher order mutants were generated. The LRR-RK XIIb RKs MIK2 and MIK2-like share 59% amino acid identity, the *mik2-1 mik2-like-2* double mutant has previously been published (Van der Does *et al.*, 2017). Subfamily XIIa members XII3, XII5 and XII6 all share >72% amino acid sequence identity and are tightly linked on chromosome 3 (all within a 187 Kb interval). I was able to identify a recombination event between *xii3-1* and *xii6-1*, however, as *XII5 and XII6* are only separated by 1.5 Kb, I used CRISPR-Cas9 mediated mutagenesis to knock-out *XII5* in the *xii3-1 xii6-1* background and generated 2 new *xii5* alleles with early stop codons (Fig. 3.12 a-c). In addition, I generated a quadruple *xii3 xps1 xii5 xii6* mutant to knock-out the entire cluster on chromosome 3, however, as this genotype has only recently been confirmed it is not included in all subsequent pathogen assays.

Initially I assayed susceptibility to *Pseudomonas syringae* pv. *tomato* DC3000 COR^- (*Pto* DC3000 COR^-) using a qPCR-based method (Ross and Somssich, 2016). Enhanced susceptibility of the *fls2, bak1-5* and, to a lesser extent, *efr* mutants was observable as increased *Pto* DNA relative to *Arabidopsis* (Fig 3.13). However, none of the other mutant lines tested showed any consistent differences in susceptibility compared to Col-0 (Fig. 3.13). *xii5-1* showed a tendency towards enhanced susceptibility, however, this was not reproduced in the triple mutant *xii3-1 xii5-3 xii6*-1 (Fig 3.13) .

As there is no reason to assume a cognate PAMP would be present in *Pseudomonas* I challenged the mutants with the fungal pathogen *Plectosphorella cucumerina* pv. *BMM* (*PcBMM*). *agb1-2* and *ixr1-6* were used as hyper- and hypo-susceptible controls respectively and I elected to exclude *fls2* and *efr* mutants from this analysis as their cognate PAMPs are not present within *PcBMM* (Gómez-Gómez and Boller, 2000; Zipfel *et al.*, 2006; Hernández-Blanco *et al.*, 2007; Delgado-Cerezo *et al.*, 2012). Interestingly, *bak1-5* is hypersusceptible to *PcBMM* suggesting the involvement of LRR-RKs/-RLPs in resistance (Jordá *et al.*, 2016).

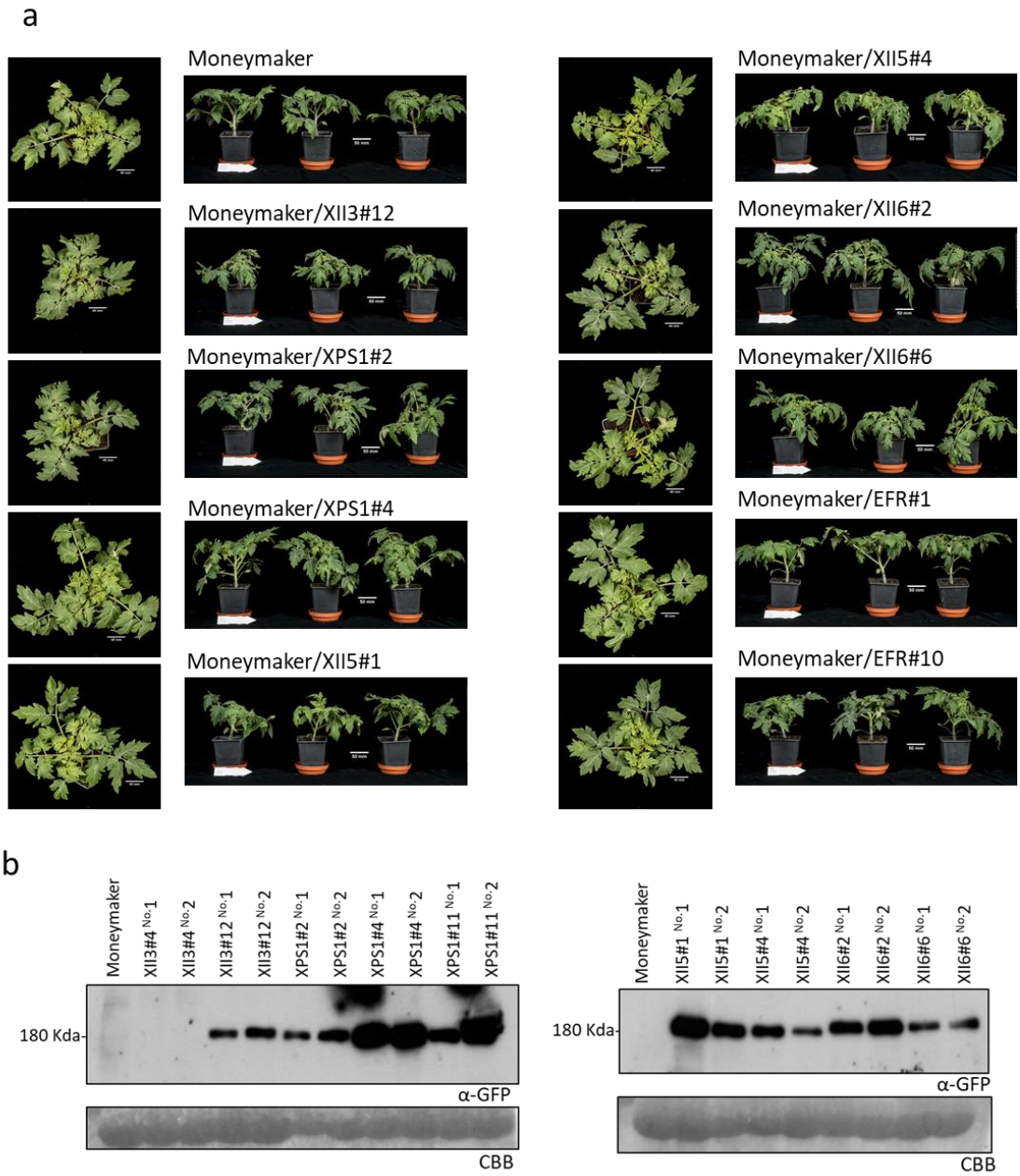

Figure 3. 7 Morphological documentation of transgenic tomato lines and elf18-induced ROS production

(a) Photographs of 32 day old tomato plants. (b) Western blots demonstrating the accumulation of the transgenes in tomato leaf tissue from 2 independent plants per genotype. CBB staining was used as a loading control

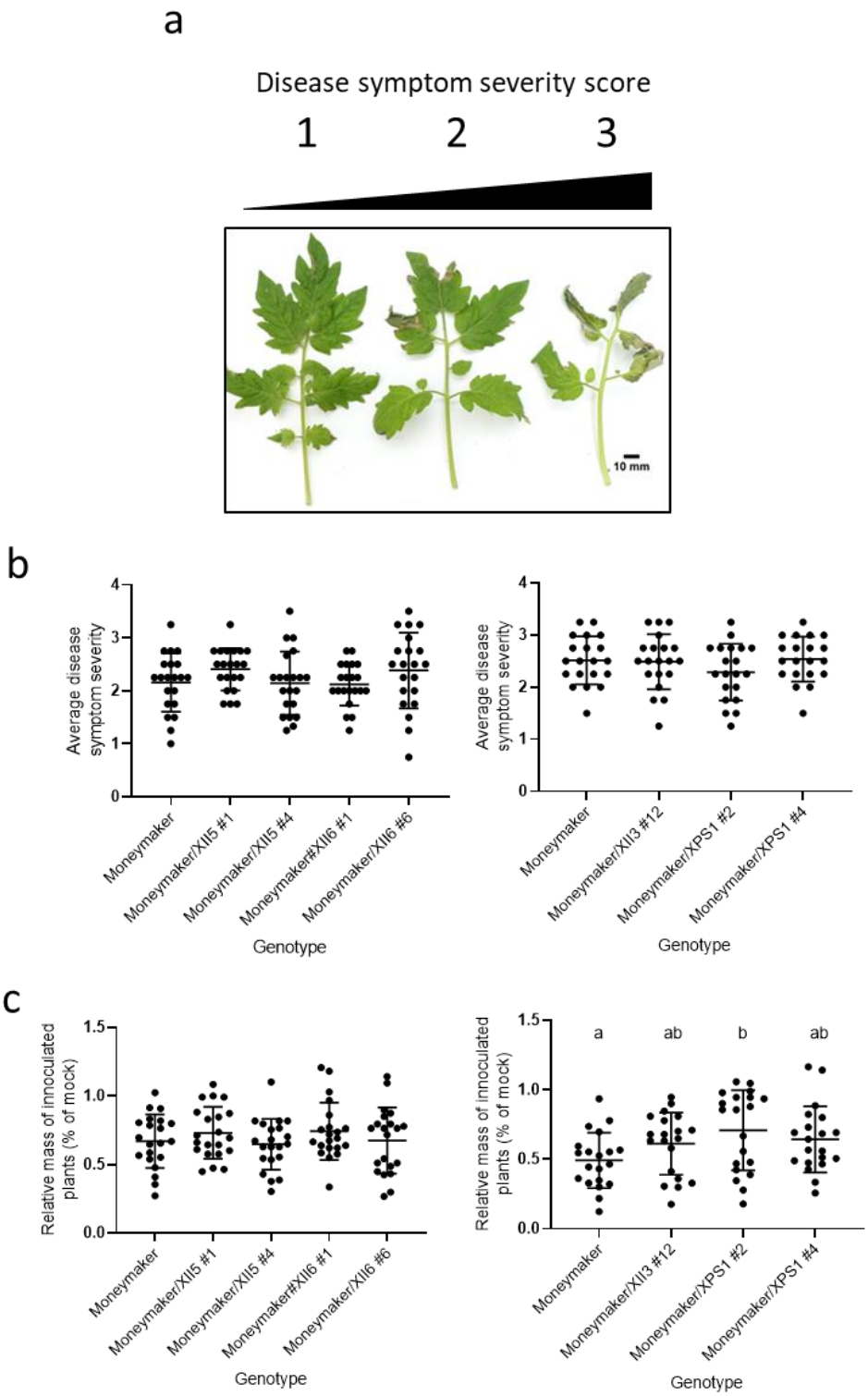

Figure 3. 8 Transgenic tomato infection with *Sclerotinia sclerotiorum*

(a) Disease scoring index used to quantify infection severity. (0 = asymptomatic (not shown) ; 1 = small lesions; 2 = large lesions; 3 = Majority of the leaf is necrotic; 4 = abscission/complete necrosis (not shown)). (b) represent two independent replicates of disease symptom severity scores following spray inoculation with S. sclerotiotum. (c) Mass of inoculated plants relative to mock treatment following S. sclerotiorum infection. Bars = mean., Error bars = S.D. Kruskal-Wallis tests were performed on the data and where a significant difference between genotypes was observed a Dunn's multiple comparisons test was performed to determine significance groups ($P<0.05$) denoted by the lower-case alphabet. Experiments were performed twice with similar results.

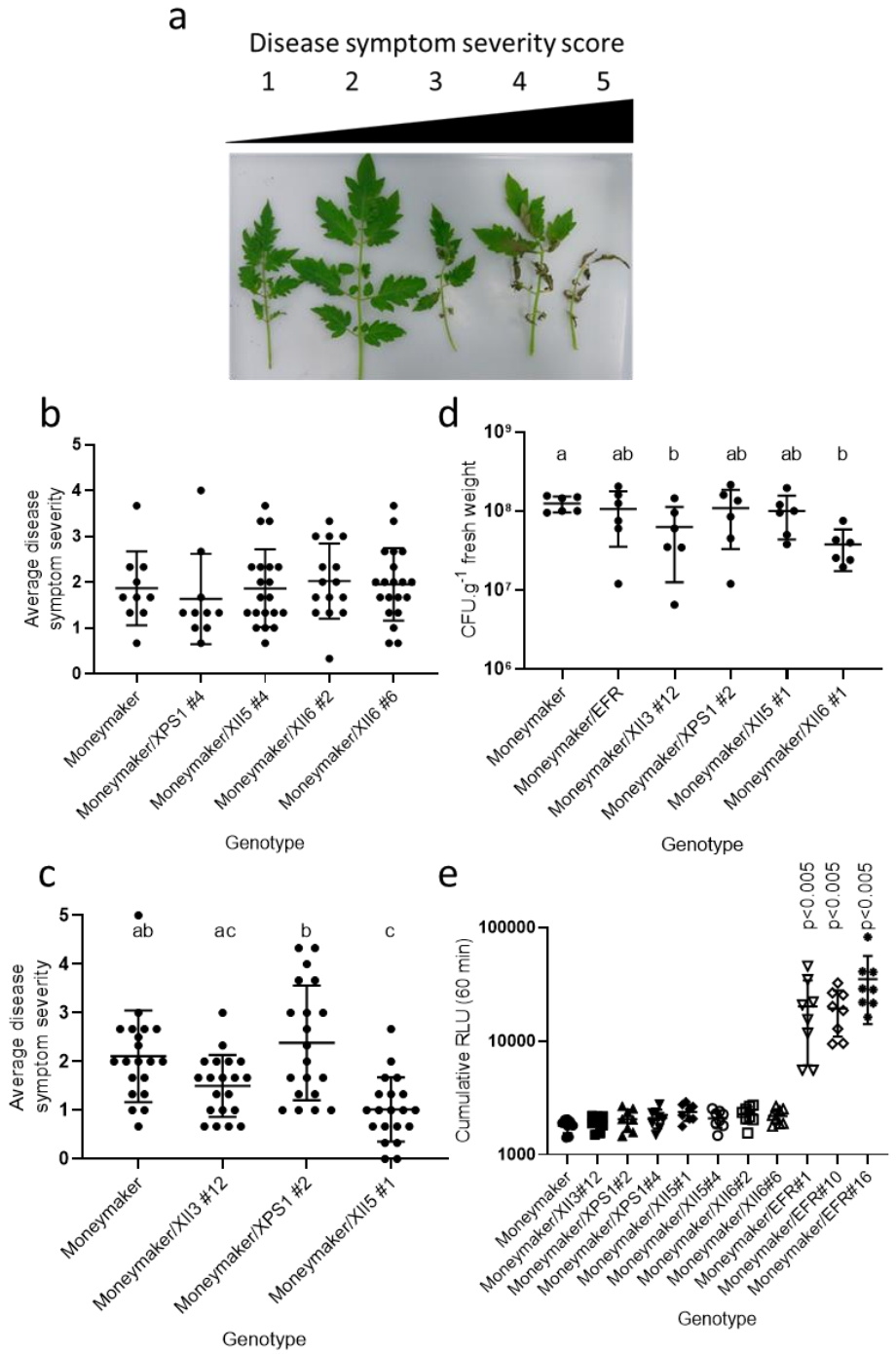

Figure 3. 9 *Xanthomonas* infection and reselection of elf18-sensitive transgenic tomatoes

(a) Disease scoring index used to quantify infection severity. (0 = asymptomatic (not shown) ; 1 = few lesions; 2 = many lesions; 3 = <50% of the leaf area necrotic; 4 = >50% of leaf area necrotic 5 = complete necrosis/abscission). (b,c) Disease symptom severity scores following spray inoculation with Xanthomonas campestris pv. vesicatoria (d) CFU following dip inoculation with X. perforans T4. Each value represents the mean of three technical replicates and represent the combined data from 3 biological replicates. (e) 1 μM elf18-induced ROS production in leaf disks from 32-day-old tomato plants

Lines = mean., Error bars = S.D. One way ANOVAs were performed on the data and where a significant difference between groups was observed a (c-d) Tukey's multiple comparisons test was performed to determine significance groups ($P<0.05$) denoted by the lower case alphabet or (e) a Dunnett's multiple comparison test compared to Moneymaker

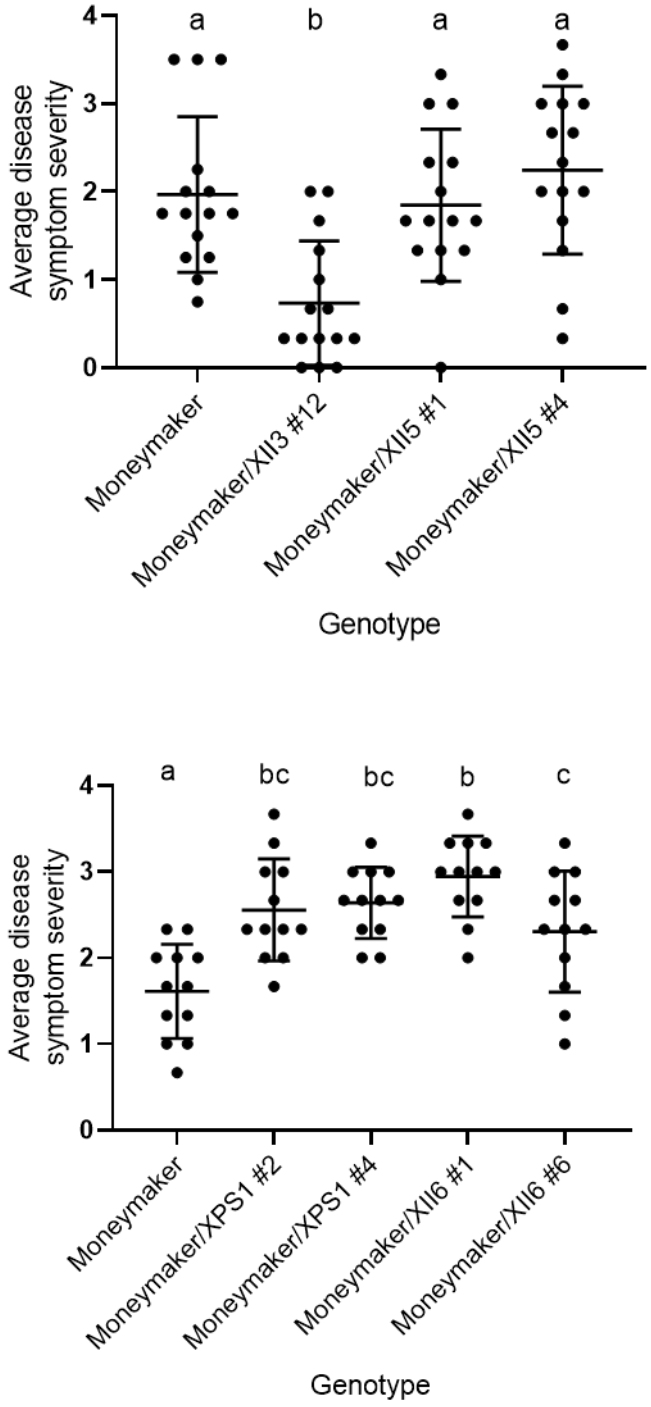

Figure 3. 10 Transgenic tomato infection with *Botrytis cinerea* strain CH94

Disease symptom severity scores following spray inoculation with *Botrytis cinerea* CH94. Each value represents an individual plant, averaged over 3 leaves. (Phenotyping performed by Rosa Perez, PRB,ES)

Lines = mean., Error bars = S.D. One-way ANOVAs were performed on the data and where a significant difference between groups was observed a Tukey's multiple comparisons test was performed to determine significance groups ($P<0.05$) denoted by the lower-case alphabet.

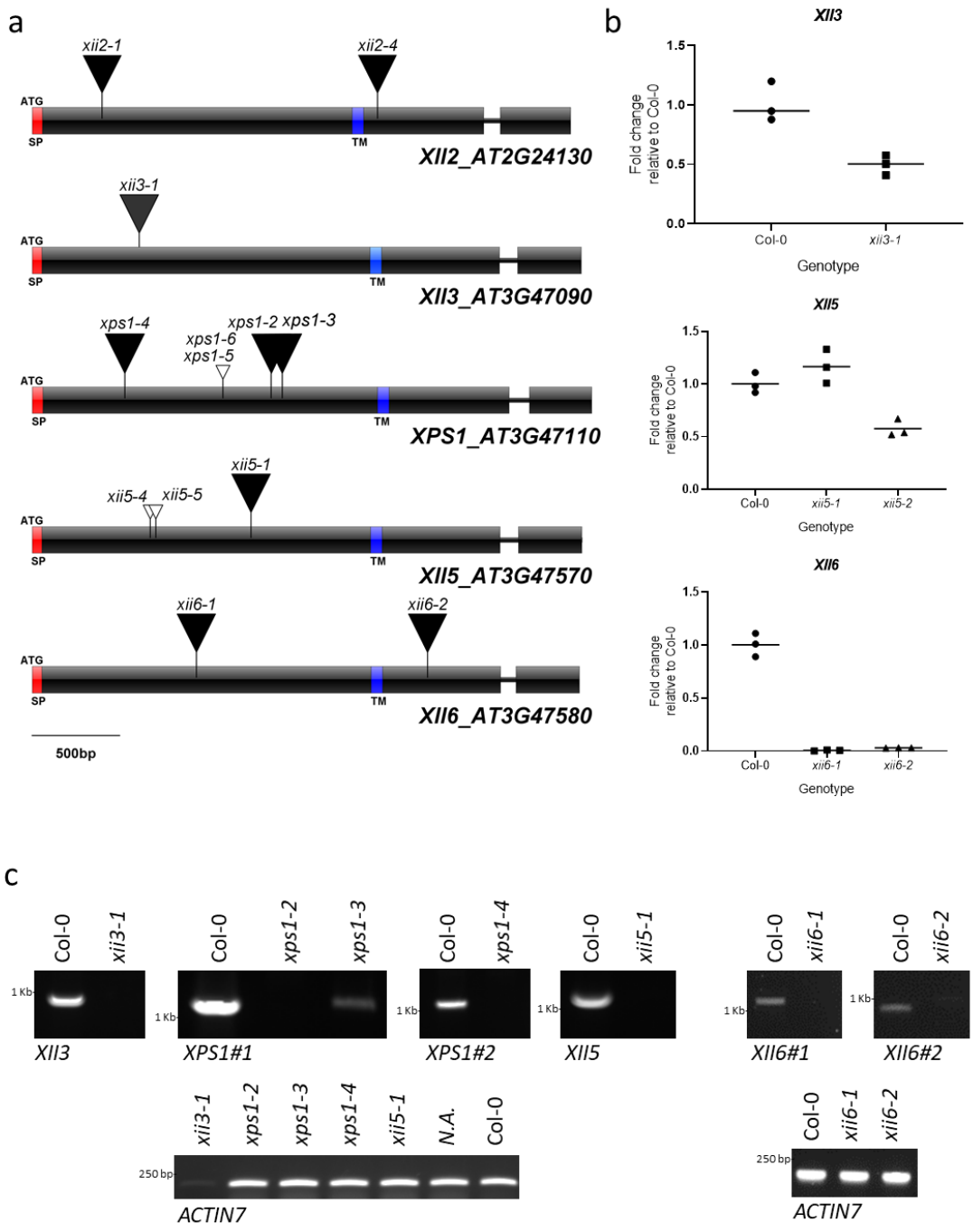

Figure 3. 11 Characterisation of *Arabidopsis* LRR-RK subfamily XII mutants

(a) Models showing the location of mutations within uncharacterised T-DNA (dark triangles) and CRISPR-Cas9-induced mutations (light triangles) (b) RT-qPCR based quantification of gene expression using primers spanning the C-terminal intron. The expression of all genes was shown relative to Col-0. Only those genes where a CT-value <30 were included. This experiment was performed once. The line represents the mean of the technical replicates. (c) RT-PCR using primers across the T-DNA insertion site and in ACTIN7 (AT5G09810) as a loading control. This experiment was performed once. *XII2* could not be detected by RT-PCR in untreated seedlings

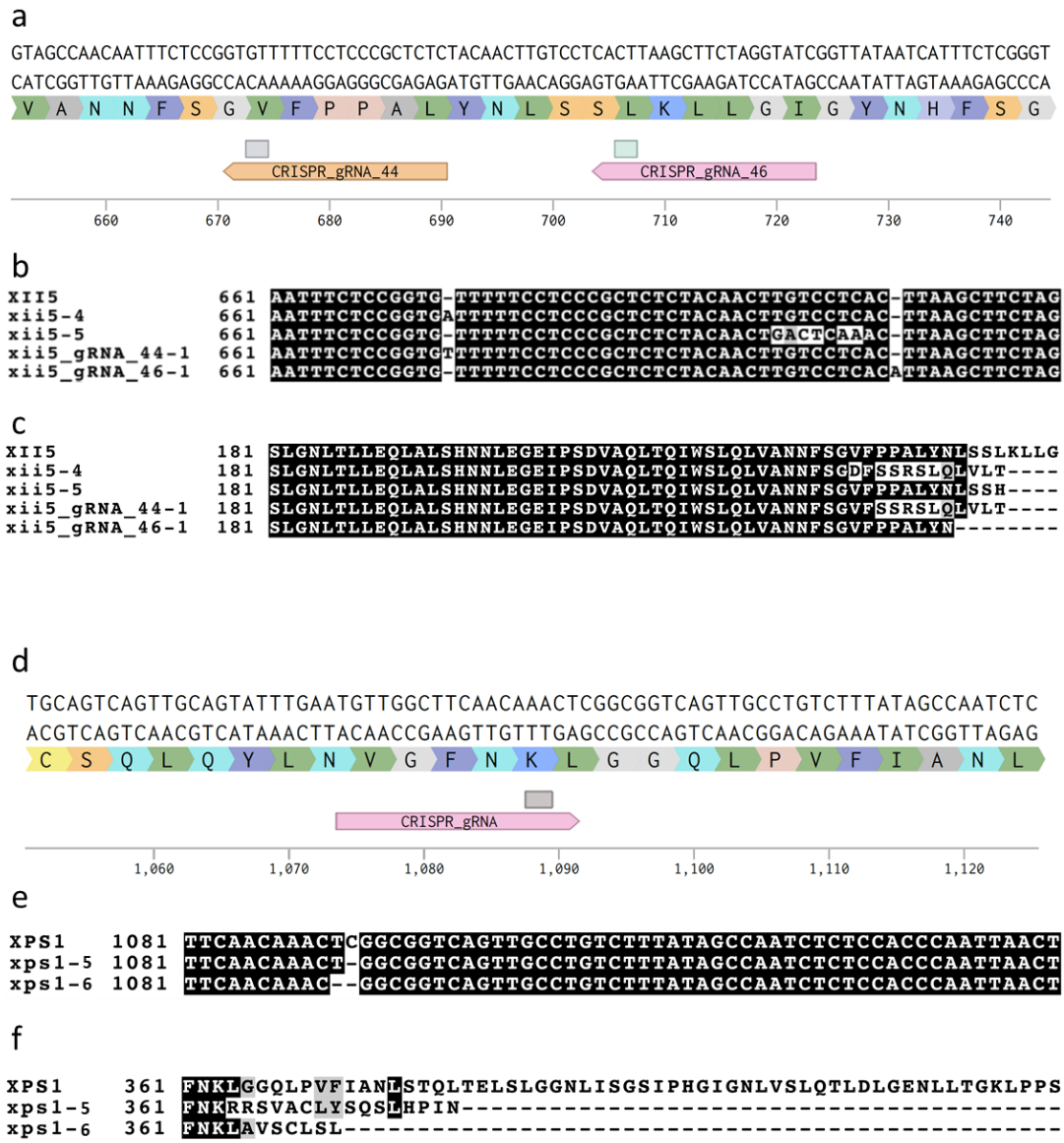

Figure 3. 12 Novel CRISPR-Cas9-induced mutations in *Arabidopsis* LRR-RK subfamily XII

(a,d) Genomic sequences of (a) *XII5* and (d) *XPS1* showing the site of the guide RNAs and the predicted site of double-stranded break formation (boxes). (b,e) Genomic sequences of the Col-0 and novel CRIPRS-Cas9-induced alleles of (b) *XII5* and (e) *XPS1* . (c,f) Amino acid sequences of the Col-0 and novel CRISPR-Cas9-induced alleles of (c) *XII5* and (f) *XPS1*. The last amino acid in the alignment is due to the gain of early stop codons.

Whilst the efficacy of the infection can be demonstrated by the controls, none of the initial mutants tested displayed a significant fungal biomass (Fig. 3.14 a). Repetition of the assay with the quadruple *xii3 xps1 xii5 xii6* mutants revealed that both lines showed an increase in fungal biomass, comparable with *bak1-5* (Fig 3.14 b). Whilst the difference biomass was not statistically significant; the difference is symptom severity scores is statistically significant (Fig 3.14 c-d). This result merits further investigation. It would also be interesting to repeat the assay with the *xii3 xii5 xii6* triple mutant to test whether this also has enhanced susceptibility, this was not done initially due to the timing of mutant generation.

As with the tomato assays no unambiguous loss-of-resistance has been identified in the *Arabidopsis* subfamily XII mutants assayed. The recent results showing enhanced susceptibility *PcBMM* in the quadruple mutants warrants further investigation.

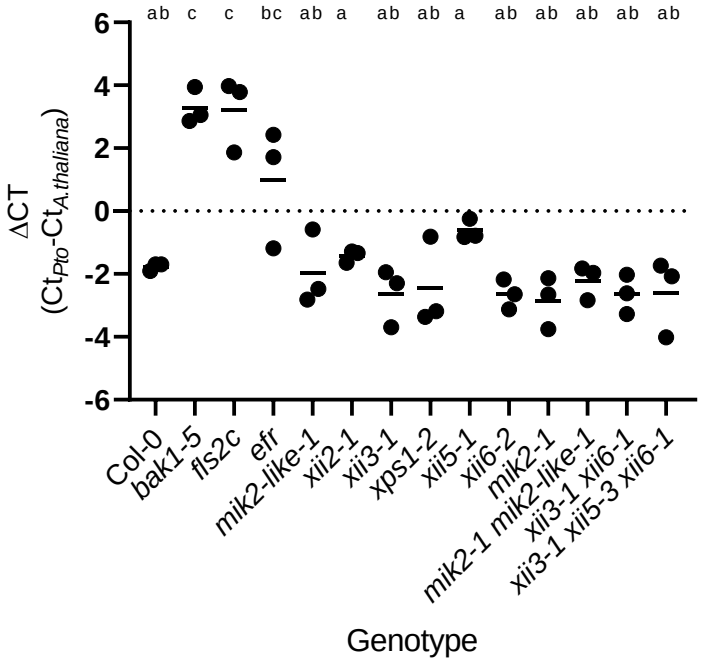

Figure 3. 13 Spray infection of *Arabidopsis thaliana* LRR-RK subfamily XII mutants with *Pseudomonas syringae* pv. *tomato* DC3000 Cor$^-$

(a) Quantification of bacterial biomass relative to plant biomass at 3 days post-infection with 10^8 CFU.ml^{-1} assessed using qPCR. Each value represents the mean of 3 technical replicates. One-way ANOVAs were performed on the data and where a significant difference between groups was observed a Tukey's multiple comparisons test was performed to determine significance groups ($P<0.05$) denoted by the lower case alphabet.

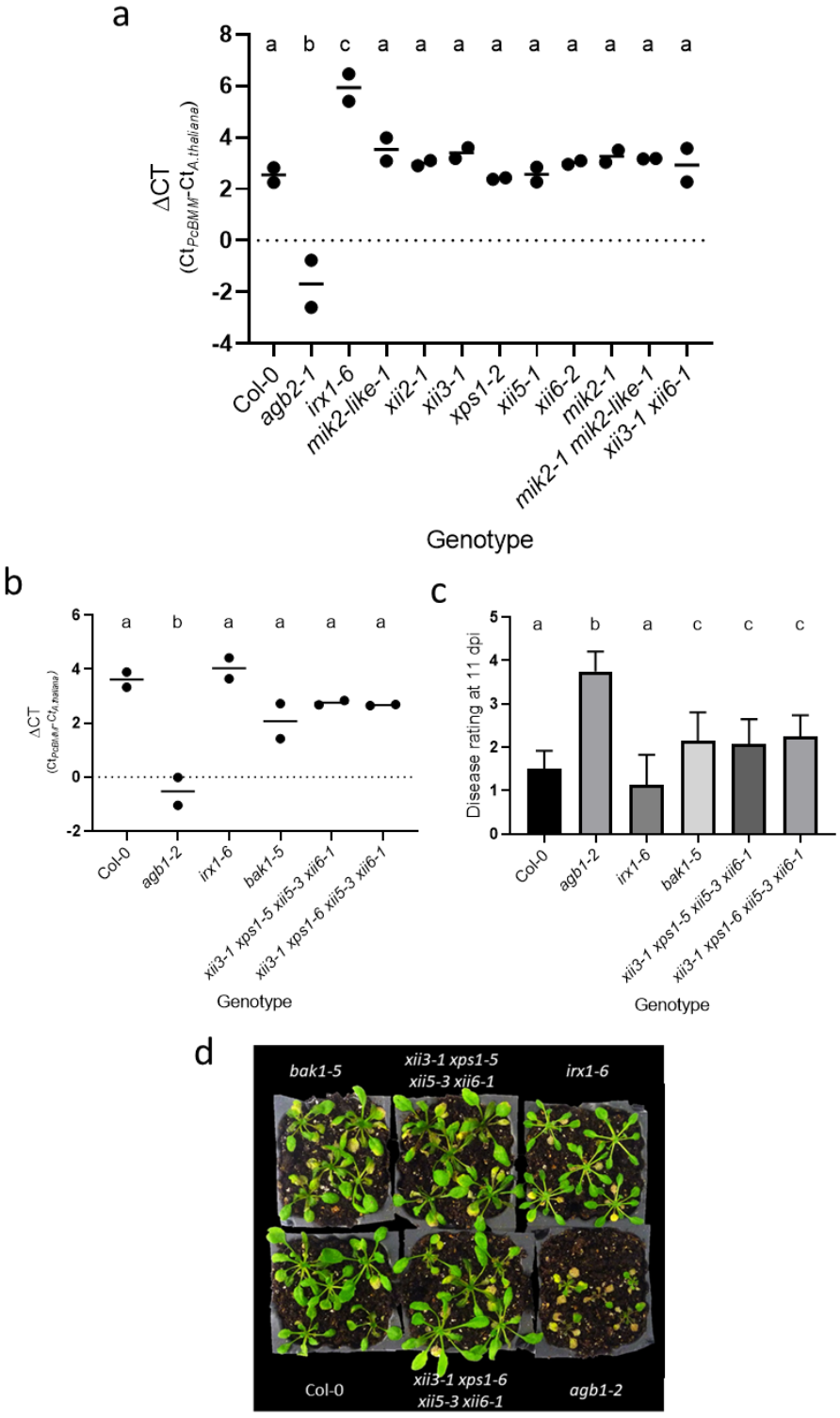

Figure 3. 14 Spray infection of *Arabidopsis thaliana* LRR-RK subfamily XII mutants with *Pc*BMM

Plants were spray inoculated with a suspension of $4x10^6$ spores.ml^{-1} *PcBMM* (a-b) Quantification of *Pc*BMM DNA relative to *Arabidopsis UBC21* at 5 D.P.I. assessed using qPCR. Values represent biological replicates from a pool of at least 4 plants (c-d) Photographs and disease symptom severity scores taken 11 D.P.I.. *agb1-2*, and *irx1-6* were included as susceptible and resistant controls respectively. One way ANOVAs were performed on the data and where a significant difference between groups was observed a Tukey's multiple comparisons test was performed to determine significance groups ($P<0.05$) denoted by the lower case alphabet. (b-d were performed by Lucia Jorda, UPM, ES)

3.4 Discussion

3.4.1 Subfamily XIIa LRR-RKs as potential PRRs

The LRR-RK subfamily XII contains multiple described PRRs. Uncharacterised genes in this subfamily represent a putative source of novel PRRs that can be explored using reverse genetic approaches. The work presented here provides evidence that LRR-RK subfamily XII cytoplasmic domains can induce responses indicative of PTI, further supporting the potential role of these RKs as PRRs. Moreover, it demonstrates that the cytoplasmic domains are functional in *Solanaceae* suggesting that these putative PRRs could be deployed in crops. The materials generated represent a valuable resource for further characterisation with diverse pathogens.

3.4.2 Chimeric receptors as an approach to characterise cytoplasmic domain output

The fact that the chimeric receptors were able to induce PTI-like responses indicates that the RKs may be PRRs. Nevertheless, I have still been unable to test elf18-induced resistance in stable transgenic lines, which would further support this. While the early responses such as ROS are indicative of PTI, they are not limited to PTI. Application of ligands to plants overexpressing RKs involved in development, such as HAESA/HAESA-LIKE 2, can also induce ROS production and cytoplasmic calcium influx (Butenko *et al.*, 2014; Olsson *et al.*, 2019*b*). Many other RKs activate ROS production; for example, SHENGEN3/GASSHO1 acts upstream of RBOHF in Casparian strip lignification (Lee *et al.*, 2013; Pfister *et al.*, 2014). Therefore, exogenous application of CIF peptides (the cognate ligands of SHENGEN3/GASSHO1), could lead to ROS production in any tissues expressing all signalling pathway components. Cytoplasmic calcium influx is a ubiquitous and sensitive response, not unique to PTI as it is induced in other RK signalling pathways (DeFalco *et al.*, 2010; Feijó and Wudick, 2018).

Moreover, by generating chimeric receptors with the EFR ectodomain, I am assuming SERK-dependency. The current paradigm implies that elf18 application will induce heterodimeric receptor complex formation between the EFR ectodomain and SERK ectodomain, bringing the cytoplasmic domains into proximity (Hohmann *et al.*, 2018*b*). SERK-dependency is a reasonable assumption because characterised members of LRR-RK subfamily XII are SERK-dependent (*e.g.* EFR, FLS2, FLS3, CORE and Xa21) (Chinchilla *et al.*, 2007; Roux *et al.*, 2011; Chen *et al.*, 2014*b*; Hind *et al.*, 2016; Wang *et al.*, 2016*a*). It is possible that some of these RKs recruit different co-receptors to activate signalling, thus the outputs generated by the chimeric receptors may not be representative of cytoplasmic domain outputs in the native RK configuration.

3.4.3 Quantitative differences in output – a potential for PRR engineering?

Assuming that the uncharacterised members of subfamily XII are PRRs, the differences in the ROS kinetics is intriguing as it suggests specificity in cytoplasmic domain outputs. Going forward, lines with comparable protein accumulation need to be tested to ensure that the differences observed are not an artefact of protein accumulation. Despite current evidence suggesting that signalling components are generally conserved, it is probable that PRRs have different affinities for them (Holton *et al.*, 2015). It would be of interest to investigate whether the stronger, sustained signalling outputs of some chimeric receptors, such as EFR:XII5, could translate into enhanced pathogen resistance. If this were the case it could provide a platform to optimise PRRs for improved pathogen resistance.

3.4.4 Kinase activity requirement for RK cytoplasmic domain function

The results presented here suggest that kinase activity is differentially required for the activation of ROS production and cytoplasmic calcium influx. In EFR:MIK2, kinase activity is essential for function, whilst it is only partly required for the functions of the EFR and FLS2 cytoplasmic domains in terms of early signalling outputs. However, the amino acid substitution could have caused structural perturbations in the cytoplasmic domain, independent of the loss of kinase activity. Whilst I tested expression of the construct, it could be important to demonstrate that this point mutation does not affect plasma membrane-localisation of the receptors.

Both EFR and FLS2 lack the highly conserved Arg/Asp motif within the cytoplasmic domain, which is present in MIK2. It would be interesting to test whether the mutation of this positively charged arginine alleviates the absolute requirement for kinase activity. It has been proposed that non-RD kinases have weaker kinase activity, and are less dependent upon it for their function (Schwessinger and Ronald, 2012). We must also remember that these experiments are overexpression in a heterologous system, which may affect functionality. This approach would have to be applied more widely to draw strong correlations about the kinase requirements of RKs. The kinase-independent function of RK cytoplasmic domains is highly relevant as ~20% of RKs lack residues essential for kinase function (Castells and Casacuberta, 2007).

3.4.5 Gain-of-resistance as an approach to identify novel PRRs

In general, the pathogen assays with tomato proved challenging. There was a huge amount a variability in disease severity within a genotype, and within individual plants. This heterogeneity precluded quantification of differences in infection severity, especially when

looking for a quantitative phenotype. It would be preferable to have larger sample sizes or more a quantitative measurement of pathogen growth, rather than assaying disease symptom severity.

One interpretation of the lack of a phenotype in any of the lines in response to *S. sclerotiorum* is that these receptors do not recognise a PAMP from this pathogen. It would be valuable to have a functional positive control, such as RLP23, which confers resistance to *Sclerotinia sclerotiorum* in potato (Albert *et al.*, 2015). This would demonstrate that under the inoculation conditions used cell-surface immunity can significantly affect resistance.

Pathogens also actively disguise and sequester PAMPs from host receptors to inhibit recognition (Mentlak *et al.*, 2012; Sánchez-Vallet *et al.*, 2013; Buscaill *et al.*, 2019). This could advocate in favour of the gain-of-function approach. Pathogens would probably be evolutionarily naïve to recognition by non-host PRRs and consequently not disguise the cognate PAMPs.

However, there is the possibility that the receptors are not functional in tomato. Whilst the work with the chimeric receptors suggests that the cytoplasmic domains of the receptors are functional in *Solanaceae*; it is still possible that the ectodomain of the receptor is not shape complementary to the orthologous co-receptor in tomato.

Further repetition of infection with *Botrytis* is required, preferably in more quantitative manner (such as measuring lesion diameter or fungal biomass). Nevertheless, in the assays performed, *XII3#12* showed a statistically significant reduction in *Botrytis cinerea* symptoms. The difference between *Sclerotinia* and *Botrytis* is unexpected as the pathogens are closely related so one might expect many molecular patterns to be conserved (Amselem *et al.*, 2011). Potentially this difference is due to the different inoculation techniques, with the *Botrytis* inoculum containing spores whilst the *Sclerotinia* inoculum consisted of homogenised mycelium. Larger fragments of homogenised mycelium may give the pathogen an advantage during establishment; rendering cell-surface activated defences ineffective, compared to the more vulnerable germinating spore.

It was surprising that I only saw the enhanced resistance to *Xanthomonas campestris* pv. *vesicatoria* in one of the two independent lines expressing *XII5*. This could be due to lower expression in the second line *XII5#4* (Fig 3.7 b). Furthermore, the phenotype was not observed in the more quantitative measurement of *Xanthamonas perforans* race T4 assay, where only the transgenic lines *XII6#1* and *XII3#12* showed a decrease in bacterial growth compared to the untransformed control. It is also possible that a PAMP may not be conserved between the two *Xanthomonas* species. Without the EFR resistant control it is difficult to interpret whether these differences in bacterial growth are what would be expected.

3.4.6 Merits and limitations *in planta* expression of RKs to assess function

The spatial resolution and level of expression can have an impact upon protein function. In the context of trying to identify a gain-of-function in the tomato lines overexpression could help amplify potentially weak quantitative differences in susceptibility; however, in the context of the chimeric receptors it may lead to inappropriate signalling outputs that would not occur if the RK was present at physiological levels. In addition there is the possibility that C-terminal tagging affects RK function (Ntoukakis *et al.*, 2011; Hurst *et al.*, 2018).

One of the major challenges that I faced in this project was the silencing of transgenes, especially in the *efr* background. The silencing of transgenes has been ascribed to two main mechanisms: 1/ RNA-directed DNA methylation (RdDM) leading to transcriptional gene silencing and 2/ posttranscriptional gene silencing in which mRNA is degraded (Sijen *et al.*, 2001). It has been widely noted that RdDM leads to hypermethylation of the viral 35S promoter resulting in silencing of gene expression (Scheid *et al.*, 1991; Kilby *et al.*, 1992). The RdDM machinery leads to the specific hypermethylation of genomic regions homologous to 24 nucleotide small RNA molecules resulting in heritable silencing of the methylated region (Matzke *et al.*, 2015). In transgenic plants small RNAs can be generated which map to the T-DNA and correlate with DNA hypermethylation and transgene silencing (Jupe *et al.*, 2019). Potentially problems with silencing can be reduced by using endogenous promoters which may be less prone to silencing, although empirical evidence for this is lacking. The severity of the problem may be exacerbated in the *efr-1* background which contains at least one *pROK2* T-DNA integration (Alonso *et al.*, 2003). *pROK2* contains a 35S promoter sequence, if 24 nucleotide sRNAs complementary to the 35S promoter are already being produced in this background it will lead to the *trans*-inactivation of the new 35S promoter integrations (Daxinger *et al.*, 2008). It may have been advantageous to use an *efr* mutant lacking this T-DNA (for example a CRISPR mutant or a SAIL mutant (Sessions *et al.*, 2002)). However, not all lines were silenced suggesting that other factors, such as the site of integration also play an important role in this process. An alternative vector could also have been used with an alternative promoter, such as an endogenous ubiquitin promoter, which may be less susceptible to silencing.

3.4.7 Loss-of-function as an approach to identify novel PRRs

No differences in susceptibility were observed between any of the single, uncharacterised LRR-RK subfamily XII mutants and Col-0, using either the bacterial pathogen *Pto* DC3000 *COR*$^{-}$ or the fungal pathogen *Pc*BMM. However, the quadruple subfamily XII mutant showed a quantitative enhancement in susceptibility to *PcBMM*, comparable with *bak1-5*. It would be

interesting to investigate this further to determine whether the triple *xii3 xii5 xii6* mutants also have the same phenotype. The cognate ligand for XPS1, xup25, is not present in *PcBMM* so it should not confer resistance (Mott *et al.*, 2016). It would be logical to test whether the quadruple mutants show weaker PTI induction in response to *PcBMM* extracts. This would support the recognition of a PAMP from *PcBMM*. The lack of phenotype in lower order mutants may be because the RKs are contributing additively to resistance through redundant perception of the same, or different PAMPs from *PcBMM*.

For the mutants that show no phenotype, this suggests that these RKs do not play a significant role in these pathosystems. Either they do not recognise a PAMP from these pathogens, or the recognition does not confer enhanced resistance to the host.

To overcome issues with small effects being masked by stronger players, for example FLS2 in *Pto* resistance, I am currently generating a complete knock-out of subfamily XIIa in the *fls2c efr cerk1-2* background (Miya *et al.*, 2007; Xin *et al.*, 2016). Hopefully this will remove background pattern recognition and potentially reveal more subtle differences.

3.4.8 Concluding remarks

None of the work presented here identifies a novel PRR within subfamily XII. However, the work with the chimeric receptors provides support for the hypothesis that they are PRRs. The expansion of 'EFR-like' receptors within *Brassicaceae* indicates that these receptors have been selectively retained, potentially due to the ability to recognise a pathogen (Fischer *et al.*, 2016).

In general, the resources generated in both tomato and *Arabidopsis* will prove valuable to the community in the attempt to characterise the remaining members of this family. They require further phenotyping with a diverse range of pathogens.

Chapter 4

Phenotypic characterisation of *mik2* reveals roles in cell wall integrity perception, root growth, pathogen resistance and regulation of reactive oxygen species production

Parts of this chapter have been published in a manuscript Van der Does *et al.* (2017), all figures that contain data that was not generated personally are indicated clearly in the figure legend.

4.1 Abstract

Plant cells actively perceive and respond to perturbations in their local environment through cell surface-localised receptors. In the context of stress responses, the signals recognised are molecular patterns indicative of danger. These can be non-self, pathogen-associated molecular patterns (PAMPs), or self-derived molecular patterns which are released or produced during stress or wounding, which can be damage-associated molecular patterns (DAMPs) or phytocytokines. Here, I report further characterisation of the leucine-rich repeat receptor kinase (LRR-RK) MIK2. Genetically, MIK2 is a key regulator of a diverse environmental responses. Indeed, *mik2* mutants are shown to have significantly impaired responses to biotic and abiotic stresses including cell wall damage, salt stress, resistance to *Fusarium* and biotic elicitors. Moreover, *mik2* mutants exhibit elevated RBOHD-dependent background reactive oxygen species (ROS) production, demonstrating a constitutive impairment in ROS homeostasis. Constitutive ROS dyshomeostasis is mirrored by transcriptomic perturbations in *mik2*. Most surprisingly, *MIK2* differentially regulates ROS production in an elicitor-dependent manner. Discriminating between highly conserved signalling pathways, *mik2* highlights an unexplained dichotomy in pattern recognition receptor signalling.

4.2 Introduction

4.2.1 Cell wall integrity sensing

Plant cells are surrounded by a wall, primarily consisting of complex carbohydrates (Keegstra, 2010). This wall provides mechanical strength to resist external and internal pressure, protects

against biotic and abiotic stresses, and represents the interaction interface with surrounding cells (Wolf *et al.,* 2012*a*). It is imperative that the plant cell wall integrity is maintained despite constant challenges imposed during cell expansion and stress (Wolf and Höfte, 2014). To this end the cell requires constant feedback about cell wall integrity in order to induce compensatory responses. Whilst we are still relatively naïve about how plants achieve this, an important role for receptor kinases (RKs) in cell wall integrity signalling is emerging (Wolf, 2017) (Discussed in Chapter 1).

In order to study cell wall damage in a controlled manner genetic or pharmacological cellulose biosynthesis inhibition is often used (Tateno *et al.*, 2016). Cellulose deficiency leads to dwarfism and reduced dark-grown hypocotyl elongation (Refrégier *et al.*, 2004). A genetic screen in the cellulose deficient *prc1-1* background identified a mutation in the receptor kinase *THESEUS1* (*THE1*) that was able to partially complement reduced dark-grown hypocotyl elongation, whilst not affecting cellulose biosynthesis (Hematy *et al.*, 2007). This suggested that RKs can play a role as cell wall integrity sensors. Recently, the LRR-RK STRUBBELIG was also shown to positively regulate responses to cellulose biosynthesis inhibition (Chaudhary *et al.*, 2019). Many cellulose biosynthesis inhibition-induced responses are reminiscent of immune responses (Hamann *et al.*, 2009; Denness *et al.*, 2011) (*i.e.* reactive oxygen species (ROS) production, jasmonic acid accumulation, lignin and callose deposition, defence gene expression, and growth inhibition). Indeed, as cell wall damage is part of the DAMP-triggered immune continuum, additional RKs presumably play undescribed roles in this fundamental process.

4.2.2 The role of ROS in plant immunity and the regulation of RBOHD

Induced apoplastic ROS production plays a key role in plant stress responses, including biotic interactions and cell wall damage (Waszczak *et al.*, 2018). Whilst their precise roles are poorly defined they contribute to important physiological processes including promoting the polymerisation of cell wall constituents, acting as secondary signalling molecules, and also directly functioning as antimicrobials (Waszczak *et al.*, 2018).

Intracellular ROS is primarily derived from chloroplasts, peroxisomes and mitochondria as by-products of electron transport chains and oxidative activity (Apel and Hirt, 2004). Their levels are elevated when these processes are perturbed during stress. Due to the harmful nature of these reactive molecules in living cells, mechanisms have evolved to maintain homeostasis including ROS scavenging enzymes such as catalases and ascorbate peroxidases as well as a reservoir of organic antioxidants, which are able to buffer ROS levels (Mittler, 2017).

In contrast apoplastic ROS in land plants is primarily generated through the dedicated enzymatic activity of plasma membrane-localised NADPH oxidases from the respiratory burst

oxidase homolog (RBOH) family. This family contains 10 members in *Arabidopsis thaliana* (Groom *et al.*, 1996; Torres and Dangl, 2005). RBOHs transfer electrons from cytosolic NADPH or FAD to apoplastic oxygen to form $O_2^{\bullet-}$. $O_2^{\bullet-}$ is subsequently converted to H_2O_2 either spontaneously, or through the catalytic activity of superoxide dismutase (Mittler, 2017). The 10 *Arabidopsis* isoforms are differentially expressed and have been implicated in diverse biological functions including defence, morphogenesis, reproduction, development, organ abscission and mechanosensing (Foreman *et al.*, 2003; Monshausen *et al.*, 2007; Takeda *et al.*, 2008; Müller *et al.*, 2009; Lee *et al.*, 2013, 2018; Boisson-Dernier *et al.*, 2013; Kaya *et al.*, 2014, 2015; Kadota *et al.*, 2015).

In the context of immunity, the most highly expressed isoform, RBOHD plays a dominant role, supported by RBOHF, and both contribute to ROS production induced by both cell-surface and cytoplasmic immune receptors (Torres *et al.*, 2002; Morales *et al.*, 2016). An important physiological function of RBOHD-derived ROS in immunity is pattern-triggered stomatal closure which is RBOHD-dependent (Mersmann *et al.*, 2010; Macho *et al.*, 2012). However, execution of stomatal closure in response to elevated CO_2 and ABA requires both RBOHD and RBOHF (Kwak *et al.*, 2003; Chater *et al.*, 2015). Pattern-triggered plasmodesmatal closure is also RBOHD-dependent (Cheval *et al.*, 2019).

In addition, RBOHD/F act downstream of cell wall damage where they are required for compensatory lignification (Hamann *et al.*, 2009; Denness *et al.*, 2011). In addition to local responses, RBOHD has been shown to play a crucial role in systemic signalling in response to a diverse range of both biotic and abiotic stresses (Miller *et al.*, 2009; Evans *et al.*, 2016).

Similar to their mammalian homologs, all RBOH enzymes have six transmembrane domains, FAD- and NADPH-binding sites and a functional oxidase domain (Kadota *et al.*, 2015). RBOHD, the best characterised member of the family, is tightly regulated at the post-transcriptional level through calcium-dependent and -independent mechanisms. The requirement of Ca^{2+} in RBOHD regulation was demonstrated by pharmacological experiments (Kadota *et al.*, 2004, 2014; Segonzac *et al.*, 2011; Ranf *et al.*, 2011). Ca^{2+} can bind to EF-hands within RBOHD to directly regulate its activity, but also activates calcium-dependent protein kinases, which have been shown to phosphorylate the N-terminus to promote its activity (Ogasawara *et al.*, 2008; Boudsocq *et al.*, 2010; Dubiella *et al.*, 2013).

Independent of calcium, the cytoplasmic kinase BIK1 and MAP4 kinase SIK1 have been shown to function downstream of immune RK complexes, phosphorylating distinct residues at the N-terminus of RBOHD to promote ROS production (Li *et al.*, 2014; Kadota *et al.*, 2014; Zhang *et al.*, 2018*a*). There appears to be a two-step regulation of RBOHD with initial, rapid BIK1-mediated phosphorylation, which is the proposed to prime RBOHD for calcium-

dependent regulation (Kadota *et al.*, 2015). However, substantial cross-talk exists between the two mechanisms: 1/cytoplasmic Ca^{2+} influx is impaired in *rbohd* mutants, 2/exogenous ROS application can induce calcium influx, and 3/calcium-dependent kinases regulate BIK1 stability (Ranf *et al.*, 2011, 2014; Li *et al.*, 2014; Monaghan *et al.*, 2014, 2015). Upon activation, RBOHD clustering and mobility within the membrane is increased (Hao *et al.*, 2014).

Reciprocal chimeric fusions between the N-terminal regulatory domain and the C-terminal catalytic domain of RBOHF and RBOHB showed that RBOHF function and localisation are determined in both elements of the protein (Lee *et al.*, 2013). Currently it is unknown whether the same is true for RBOHD function. Recently, CRK2-dependent phosphosites on the C-terminus of RBOHD have been proposed to regulate its function, suggesting that regulation occurs at both termini of the protein (Kimura *et al.*, 2019).

4.2.3 *mik2* - a multifaceted mutant

The leucine-rich repeat (LRR) RK MIK2 belongs to the subfamily LRR-RK XIIb, which is a poorly characterised clade of LRR-RKs. The only member – other than MIK2 – to be characterised is *OsXIK1*, which positively regulates resistance to *Xanthamonas* in rice through an unknown mechanism (Hu *et al.*, 2015). The LRR-RK subfamily XIIb is the second most expanded LRR-RK subfamily in angiosperm genomes with massive expansion in the apple, poplar, oak and soybean genomes (Zhou *et al.*, 2016; Fischer *et al.*, 2016; Plomion *et al.*, 2018). MIK2 has been implicated in processes including pollen tube guidance, salt stress tolerance, cell wall integrity sensing and response to a *Fusarium*-derived elicitor (Wang *et al.*, 2016*b*; Julkowska *et al.*, 2016; Van der Does *et al.*, 2017; Coleman *et al.*, 2019).

MIK2 was initially described as a component of a pollen-specific receptor complex for the synergid cell-derived LURE peptides – facilitating pollen tube guidance to the female reproductive organs (Wang *et al.*, 2016*b*). MIK2 (MALE DISCOVERER-INTERACTING RECEPTOR LIKE KINASE 2) was identified in a screen for interactors of MALE DISCOVERER1/2 (MDIS1/2). The LRR-RKs MDIS1/2 were previously isolated in a reverse genetic screen for male infertility conferred by kinase-dead, 'dominant negative' variants of pollen-expressed RKs. Wang *et al.* (2016*b*) also identified MIK1/PXL2, the receptor for CLE42 (Mou *et al.*, 2017), in the same yeast-two-hybrid screen and proposed that MDIS1/2 constitutively interact with the unrelated LRR-RKs MIK1 and MIK2 and synergistically perceive LURE peptides. Nevertheless, it must be noted that a back-to-back publication identified an alternative receptor, PRK6, which has since been confirmed by an independent group and the PRK6-LURE complex has been structurally resolved (Takeuchi and Higashiyama, 2016; Zhang *et al.*, 2017; Zhong *et al.*, 2019), which raises questions about the actual role of MIK2 in LURE perception.

Subsequently, *MIK2* (there named *LEUCINE-RICH REPEAT KINASE FAMILY PROTEIN INDUCED BY SALT STRESS*), was identified in a genome-wide association study for rosette growth under salt stress (Julkowska *et al.*, 2016). A SNP within the promoter of *MIK2* significantly associated with rosette growth under mild salt stress. Julkowska *et al.* (2016) went on to demonstrate a positive correlation between ecotype-dependent *MIK2* expression levels and salt stress tolerance.

Moreover, Coleman *et al.* (2019) showed that MIK2 is required for the perception of a *Fusarium* peptide fraction (EnFOE). In order to elucidate the perception mechanism, they identified a non-responsive mutant *fere1* (*FUSARIUM ELICITOR REDUCED ELICITATION 1*) using an EMS-mutagenised population of an aequorin calcium reporter line. The causal SNP mapped to an early stop in *MIK2*.

Here, I characterize *MIK2* as a key regulator of responses to cell wall damage. *mik2* mutants showed reduced defence gene expression, lignin deposition and jasmonic acid accumulation (Van der Does *et al.*, 2017). I show that *mik2* mutants show enhanced root skewing under control and salt stress conditions. The involvement of *MIK2* in rosette growth under salt stress, proposed by Julkowska *et al.* (2016), is confirmed in *mik2* mutants. Hypothesising that these phenotypes were linked by defects in cell wall integrity sensing, susceptibility to the cell wall damaging pathogen, *Fusarium oxysporum*, was assessed and *mik2* mutants were found to be hypersusceptible. However, a closer inspection of immune responses revealed that *MIK2* differentially regulates elicitor-induced ROS production, revealing a puzzling dichotomy. Furthermore, *mik2* mutants show constitutively elevated RBOHD-dependent ROS in the absence of treatment. This exposes a dyshomeostasis in *mik2*, which is reflected in transcriptomic perturbations. The transcriptome highlighted an overrepresentation of genes encoding extracellular and plasma membrane proteins involved in biotic and oxidative stress responses upregulated in *mik2*. Taken together, loss of *MIK2* function illustrates a nexus linking cell wall damage responses, salt stress tolerance, root growth, response to biotic elicitors, and disease resistance to ROS and transcriptomic homeostasis.

4.3 Results

4.3.1 *MIK2* is required for responses to cellulose biosynthesis inhibition

Prior to my arrival in the laboratory, a reverse-genetic screen of LRR-RK mutants was established to identify novel receptors involved in the perception of cell wall integrity perturbations. The pharmacological inhibitor of cellulose biosynthesis, isoxaben (ISX) was used to generate cell wall damage in a controlled manner. From this screen, one LRR-RK, MIK2, was identified as exhibiting impaired responses to ISX. MIK2 stood out as the only member of LRR-RK subfamily XII that showed consistently impaired ISX-induced

expression of the immune marker gene *CYP81F2* (Fig. 4.1 a). This response was not specific to ISX, but was shared with other cellulose biosynthesis inhibitors such as 2,6-dichlorobenzonitrile (DCB) and thaxtomin (TXT) (Fig. 4.1 b) (Hogetsu *et al.*, 1974; Scheible *et al.*, 2003; Bischoff *et al.*, 2009). However, mild osmotic stress caused by treatment with 400 mM mannitol did not induce *CYP81F2* expression in either Col-0 or *mik2-1* (Fig 4.1 b). Multiple alleles of *mik2* displayed impaired induction of the defence marker genes *FRK1*, *CYP81F2* and *AT1G51890* in response to ISX treatment, strengthening the genetic evidence (Fig 4.2 a; a model of all *mik2* alleles used is given in Fig. 4.1 c). *mik2-1* is also impaired in ISX-induced jasmonic acid accumulation and lignin deposition (Fig 4.2 b-c). Together, these data demonstrate that MIK2 is an important regulator of responses triggered by cellulose biosynthesis inhibition.

I did not find evidence of genetic redundancy between MIK2 and its paralog, MIK2-like, in ISX-induced gene expression (Fig 4.2 d). Moreover, I found no genetic evidence that other components of the MDIS-MIK complex (Wang *et al.*, 2016*b*) play any role in regulating cellulose biosynthesis inhibition-induced gene expression (Fig 4.2 e).

Taken together, these results show that *MIK2*, like *THE1* and *SUB*, is required for responses to cellulose deficiency, and, as such, genetically regulates cell wall integrity sensing.

4.3.2 *mik2* mutants display a root skewing phenotype

Serendipitously, whilst growing seedlings on vertical plates, Dr. Dieuwertje Van der Does noticed that *mik2* mutants display a leftward root skewing phenotype relative to Col-0 (Fig 4.3 a-d). Whilst considerable natural variation in root skewing has been observed, very little is known about the genetic architecture underlying these differences (Vaughn and Masson, 2011; Toal *et al.*, 2018). Many of the well-characterised root skewing mutants have defects in cortical microtubule organisation and consequential cellulose fibril orientation, but no such differences could be observed in *mik2-1* (Van der Does *et al.*, 2017). However, recent work has shown that defects in non-polar cell wall components can also lead to a root skewing phenotype comparable with *mik2* (Saffer *et al.*, 2017), which provides further support to a link between CW sensing and root growth angle.

4.3.3 *mik2* mutants have impaired to salt stress tolerance

Julkowska *et al.* (2016) identified a polymorphism within the promoter of *MIK2* significantly associated with natural variation in rosette growth under salt stress. Publicly available expression data shows that *MIK2* is upregulated transcriptionally in response to salt stress (Kilian *et al.*, 2007; Aoki *et al.*, 2016). *mik2-1* and *mik2-2* mutants show a reduction in rosette dry weight relative to mock under mild salt stress, confirming a role for MIK2 in salt stress tolerance (Fig 4.4 a).

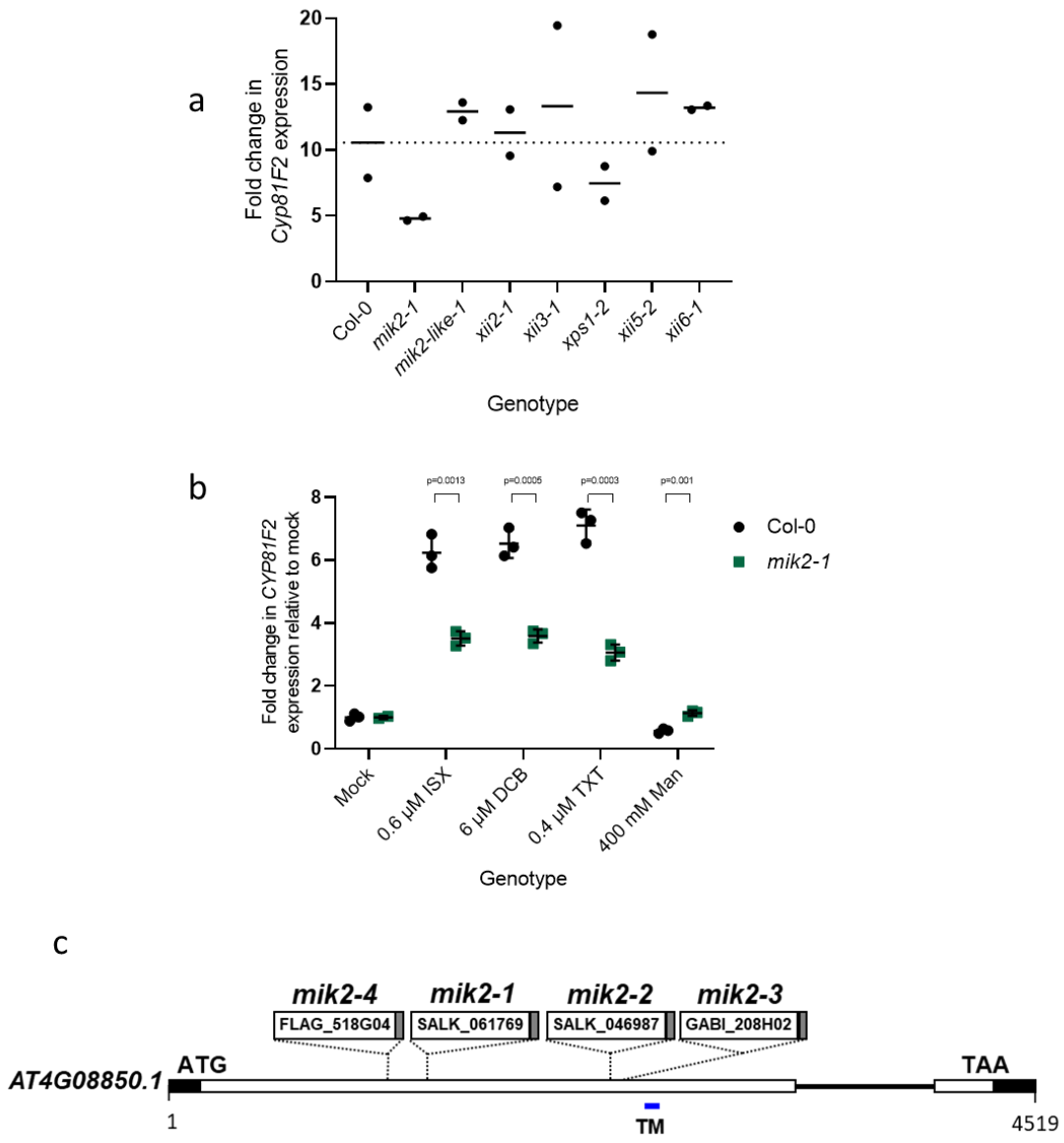

Figure 4. 1 MIK2 is a major regulator of marker gene expression induced by cellulose biosynthesis inhibition.

(a,b) Expression of the defence marker gene *CYP81F2* in *Arabidopsis* 13-day-old seedlings. Expression was normalised to *U-BOX (AT5G15400)* (a) Seedlings were treated with 0.6 µM ISX for 9 h treatment, expression is shown relative to mock. Data points are the mean of 3 technical replicates, 2 biological replicates per genotype and the line represents the mean. Dashed line represents the mean fold change in Col-0. (b) Seedlings were mock treated, or treated with 0.6 µM ISX, 6 µM DCB, 0.4 µM TXT, or 400 mM mannitol (Man) for 9 h. Data shown indicate 3 technical replicates. Error bars show S.D. Experiment was repeat 3 times with similar results (Other replicates were performed by D. Van der Does). P-values are derived from unpaired t-tests. (c) Gene models of *mik2* T-DNA alleles used in this study (Figure modified from F. Boutrot).

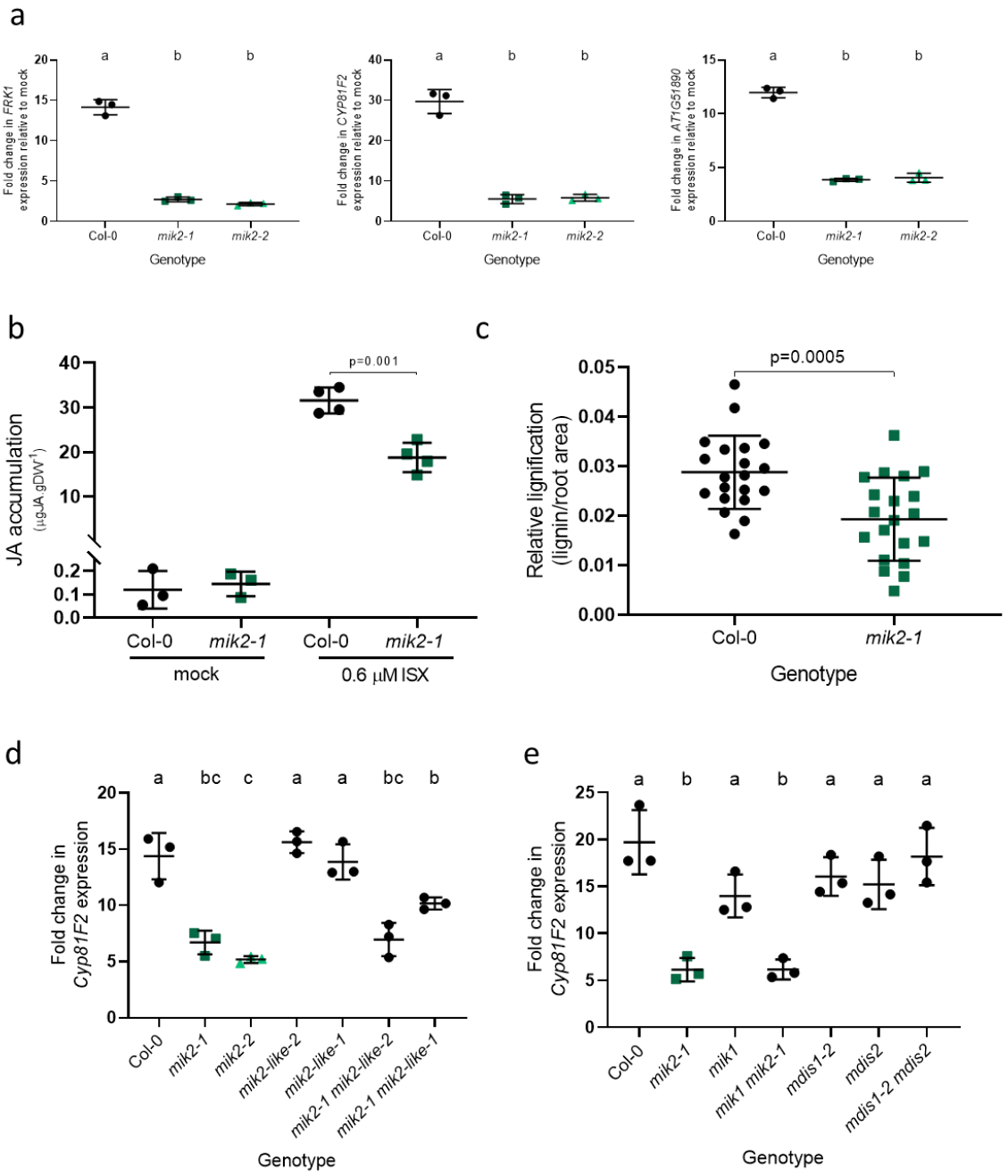

Figure 4. 2 MIK2 is a major regulator of multiple responses to cellulose biosynthesis inhibition unlike MIK2-like and other components of the MDIS/MIK complex

(a,d-e) Expression of the defence marker genes (a) *CYP81F2*, *FRK1* and *AT1G51890* in *Arabidopsis* 13-day-old seedlings treated with 0.6 µM ISX for 9 h treatment, relative to mock. Expression was normalised to *U-BOX (AT5G15400).* Data shown indicate 3 technical replicates. Experiment was repeat 3 times with similar results (Data for (a) from D. Van der Does) (b) Jasmonic acid (JA) accumulation in 6-day-old Arabidopsis seedlings, mock treated or treated with 0.6 µM ISX for 7 h. (Data from T. Hamann lab, NTNU, NOR). (c) Relative lignin deposition in root elongation zone in 6-day-old Arabidopsis seedlings, mock treated or treated with 0.6 µM ISX for 12 h determined by phloroglucinol-HCl staining. (Data from T. Hamann lab, NTNU, NOR). *CYP81F2* expression in 13-day-old seedlings treated with 0.6 µM ISX for 9 h treatment, relative to mock, normalised to *U-BOX (AT5G15400)* in mutants of (d) the *MIK2* homolog *MIK2-like* and (e) the *MDIS-MIK* complex (a-e) Error bars represent S.D., bar represents mean. (a,d-e) Lower case letters represent significance groupings ($p<0.05$) from one-way ANOVA followed by Tukeys Post-hoc test. P-values are derived from unpaired t-tests. (b-c) P-values are derived from unpaired t-test.

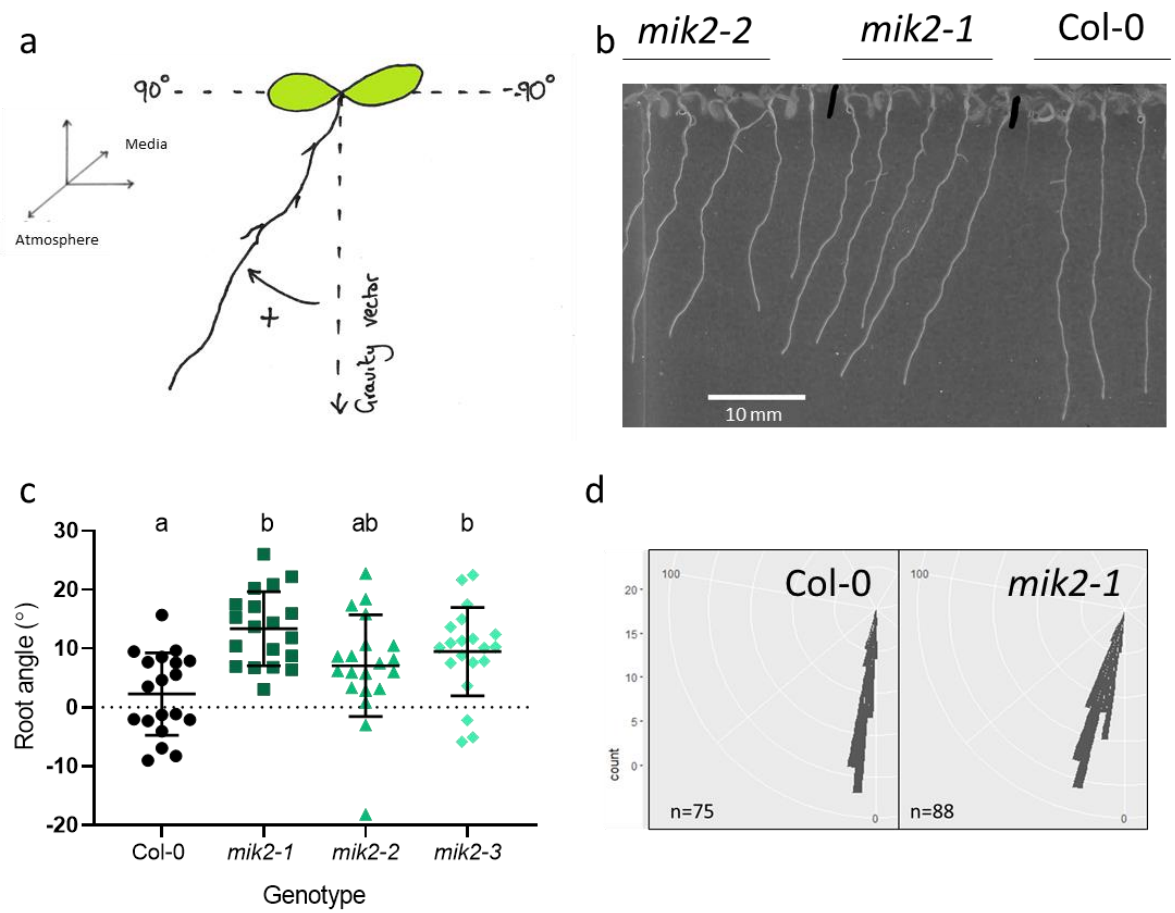

Figure 4. 3 The absence of MIK2 results in enhanced root skewing

(a) Diagrammatic representation of the root skewing demonstrating +ve values indicate skewing the left (clockwise) relative to the gravity vector whilst –ve values indicate skewing to the left. Angles were measured to the root tip. (b-d) Root skewing of 9-day-old seedlings grown in an upright position (10°) on MS +1% sucrose, 0.8% agar. Error bars represent S.D., bars represent the mean and lowercase letters represent significance groupings ($p<0.05$) from one-way ANOVA followed by Tukeys Post-hoc test.

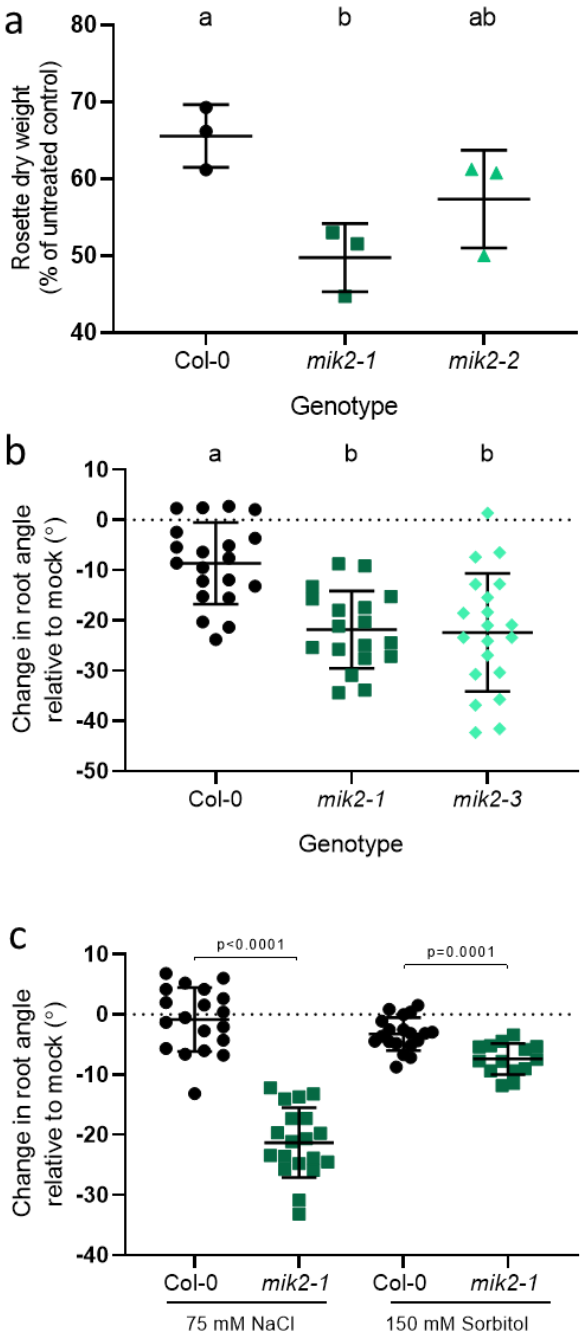

Figure 4. 4 The absence of MIK2 results in impaired rosette growth under NaCl stress and enhanced NaCl-induced root skewing

(a) Dry weight of soil-grown NaCl-treated plants as percentage of the dry weight of untreated plants. Data points represent the mean of independent experiments (each experiment n=20). A Freidman test indicated a significant difference between genotypes, lower case letter letters represent significant groupings based on Dunn's multiple comparison test ($p<0.05$). (b) Root skewing of 9-day-old seedlings grown an upright position (10°) on MS +1% sucrose, 0.8% agar relative to the addition of 75 mM NaCl. Error bars represent S.D., bars represent the mean and lower-case letters represent significance groupings from one-way ANOVA followed by Tukey's Post-hoc test ($p\leq0.0002$). (c) Ten-day-old Arabidopsis seedlings were grown in an upright position on ½ MS agar medium without sucrose, supplemented with or without 75 mM NaCl or 150 mM sorbitol. (n=20) Experiment repeated three times with similar results. P-values are derived from unpaired t-test. (Data for (a,c) from I. Koevoets UVA/WUR, NL).

It has previously been shown that salt stress causes rightward root skewing in Col-0 (Wang *et al.*, 2007); however, I observed that this change in root angle was more pronounced in *mik2* than Col-0 (Fig 4.4 b). The effect was much less when grown on sorbitol with the same osmotic potential, suggesting it is not due to the osmotic effect (Fig 4.4 c). These results show that *mik2* mutants are more sensitive to salt stress, supporting previous findings that natural variation in *mik2* expression governs salt stress tolerance.

4.3.4 *mik2* mutants are more susceptible to *Fusarium oxysporum* infection

Pathogens can cause considerable disruption to the cell wall during infection (Bacete *et al.*, 2018). As *MIK2* appears to positively regulate responses to cell wall damage - which overlap with immune responses – we sought to investigate whether *mik2* mutants are more susceptible to infection. As seen in chapter 3, *mik2* mutants do not show enhanced susceptibility to *Pseudomonas syringae* pv. *tomato* DC3000 *COR*$^{-}$ or *Plectosphaerella cucumerina* BMM (*Pc*BMM). In addition, it was previously found that *mik2* mutant plants are not affected in resistance against the powdery mildew species *Golovinomyces orontii* and *Erysiphe pisi* or to the downy mildew *Hyaloperonospora arabidopsidis* Noco2 (Humphry *et al.*, 2010; Van der Does *et al.*, 2017). Nevertheless, *mik2* mutants showed enhanced susceptibility to the hemibiotrophic fungal root pathogen *Fusarium oxysporum* isolate Fo5176 as shown by increased leaf chlorosis and whole plant decay (Fig 4.5 a-b).

Thus, *MIK2* appears to be differentially required for pathogen resistance. The enhanced susceptibility to *Fusarium* is consistent with the recent results from Coleman *et al.* (2019), which show that MIK2 is required for the perception of *Fusarium*-derived elicitor. This suggests that the difference is not due to cell wall integrity perception, but rather PAMP responsivity. This could either be due to impaired recognition of a PAMP or a secondary signal.

4.3.5 mik2 mutants exhibit impaired flg22-induced ROS production

Whilst MIK2 is required for cellulose biosynthesis inhibition and salt stress responses, it was logical to test other environmental stimuli. I decided to test PAMP responsivity in *mik2* (Sharon and Sharon, 2015; Coleman *et al.*, 2019). Humphry *et al.* (2010) identified MIK2 as part of a fungal pathogen-responsive regulon. This supports in house RNAseq data (generated by Dr Marta Bjornson), which shows that *MIK2* is upregulated by a plethora of biotic elicitors (Fig. 4.6 a). Moreover, Yadeta *et al.* (2017) demonstrated that MIK2 protein levels were significantly upregulated in the plasma membrane in response to flg22 treatment (Fig. 4.6 b). Together, these data suggest a role for MIK2 in response to biotic stimuli, in line with the recent finding that *MIK2* is required for the perception of a *Fusarium*-derived elicitor,

In order to test this, I first investigated whether *mik2* mutants exhibited perturbations in flg22-induced ROS production. *mik2* mutants showed a significant reduction in flg22-induced ROS production (Fig. 4.7 a) (This phenotype was first observed in Dr Milena Roux (2015)). An allelism test provided further evidence that the *mik2* mutation was causal (Fig 4.7 b). In order to test for redundancy between MIK2 and MIK2-like, the double mutant was phenotyped, it resembled *mik2* (Fig. 4.7 c). Whilst I observed a trend towards a stronger phenotype in the double mutant this was not statistically significant. Therefore, I decided to proceed with characterisation of the *mik2* single mutant.

To further understand the role of MIK2 in flg22-induced responses, I investigated other PTI outputs. However, I could not discern a difference in flg22-induced MAPK phosphorylation, seedling growth inhibition, or ultimately induced resistance (Fig. 4.8 a-c). No obvious differences in the protein levels of FLS2, BAK1 or RBOHD could be observed in the *mik2* mutant (Fig. 4.9 a-b). Moreover, neither flg22-induced FLS2-BAK1 complex formation nor phosphorylation of the downstream receptor-like cytoplasmic kinase BIK1 (visualised as BIK1-HA bandshift) appear to be impaired in *mik2* (Fig. 4.9 c-d). Therefore, MIK2 seems to specifically regulate the ROS response. However, because the difference is quantitative, the fact that it is not observed in other assays could also be a limitation of the threshold or sensitivity.

4.3.6 MIK2 differentially regulates ROS production in response to diverse elicitors

I decided to determine whether the *mik2* ROS phenotype was also apparent in response to other immune elicitors. Initially I tested the 18-amino acid Elongation Factor-TU derived epitope, elf18, which is recognised by EFR (Zipfel *et al.*, 2006). I observed impaired ROS production in *mik2* comparable to that observed with flg22 (Fig 4.10 a). I could confirm the impaired ROS production in *mik2-4* in the Wassilewskija (Ws-2) background (Ws-2 lacks a function FLS2 receptor and is thus blind to flg22, so the flg22 response cannot be tested (Gómez-Gómez *et al.*, 1999)) (Fig 4.10 d).

In order to test whether MIK2 also regulates ROS production triggered by LRR-RLP receptor complexes, I tested nlp20-induced ROS. Nlp20 is recognised by the RLP23-SOBIR1-BAK1 receptor complex (Albert *et al.*, 2015). There is also a reduction in nlp20-induced ROS production in *mik2,* suggesting that the phenotype is shared between LRR-RK and LRR-RLP receptors (Fig 4.10 b,e).

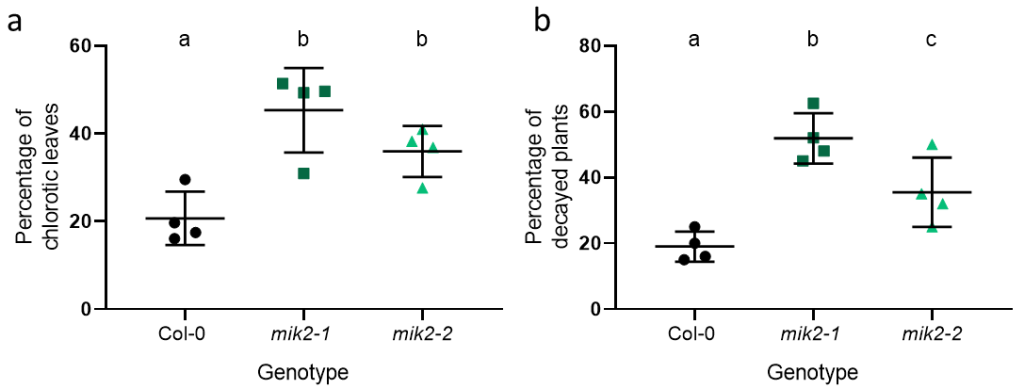

Figure 4. 5 MIK2 is required for resistance to the fungal root pathogen *Fusarium oxysporum*

Percentage of chlorotic leaves per plant (a), and percentage of decayed plants (b) after infection of the roots with *F. oxysporum* isolate *Fo5176*. (a) Chlorotic leaves per plant were determined 10 days after inoculation with *F. oxysporum*. (b) Decayed plants were determined 3 weeks after inoculation. Data points represent the mean of independent experiments, each consisting of 20-40 plants (a-b) The bars represent the average of four independent experiments, each consisting of n = 20–40 plants per genotype. Error bars represent S.D., bars represent the mean and lowercase letters represent significance groupings ($p<0.05$) following one-way ANOVA followed by Tukeys Post-hoc test. (Data from N. Tintor, UVA, NL).

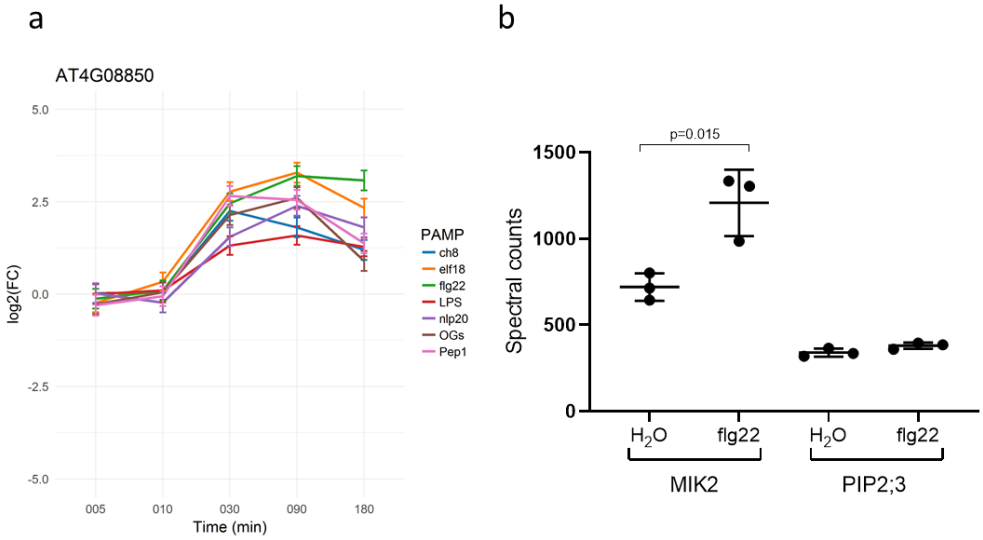

Figure 4. 6 MIK2 is induced at both the RNA and protein level in response to treatment with biotic elicitors

(a) Transcriptional response of *MIK2* to a range of biotic elicitors in whole seedlings over a time course (5 to 180 min). Ch8 = 1 µM chitooctaose, elf18 = 1 µM elf18, flg22 = 1 µM flg22, LPS = 1 µM 3-hydroxydecanoic acid, nlp20 = 1 µM nlp20, OG =100 µg.mL^{-1} oligogalacturonides (d.p. 14-16) , Pep1 = 1 µM Pep1. (Data from M. Bjornson). (b) Spectral counts from plasma membrane enriched fractions of four-week-old Arabidopsis plants sprayed with 10 µm flg22 peptide or water and rosette tissue harvested at 720 min. P-value derived from an unpaired t-test. PIP2;3 was included as a PM control (Data extracted from Yadeta *et al.* (2017)).

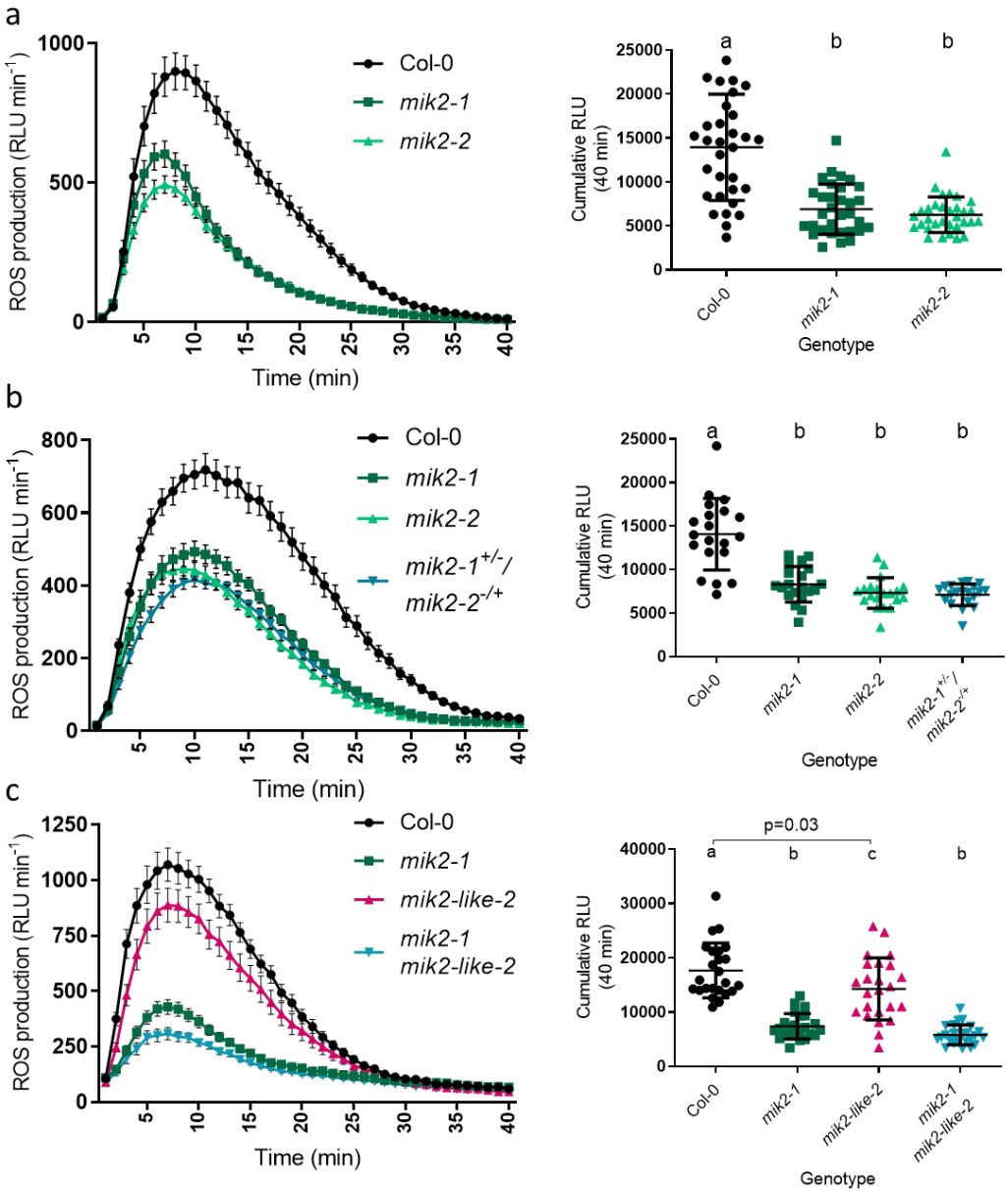

Figure 4. 7 MIK2 is required for a wild-type flg22-induced ROS response

(a-c) 100 nM flg22-induced ROS production from leaf disks taken from 5-week-old rosettes. Error bars on curves represent S.E.M. ((a) n=32; (b) n= 20; (c) n=24). Plots on the right show the integration derived from the plots on the left, horizontal lines show mean with S.D. Lowercase letters indicate significance groups based on one-way ANOVA followed by Tukey's Post-hoc test. (a,c) repeated at least three times with similar results (b) performed once. (Data for (b) from F. Boutrot)

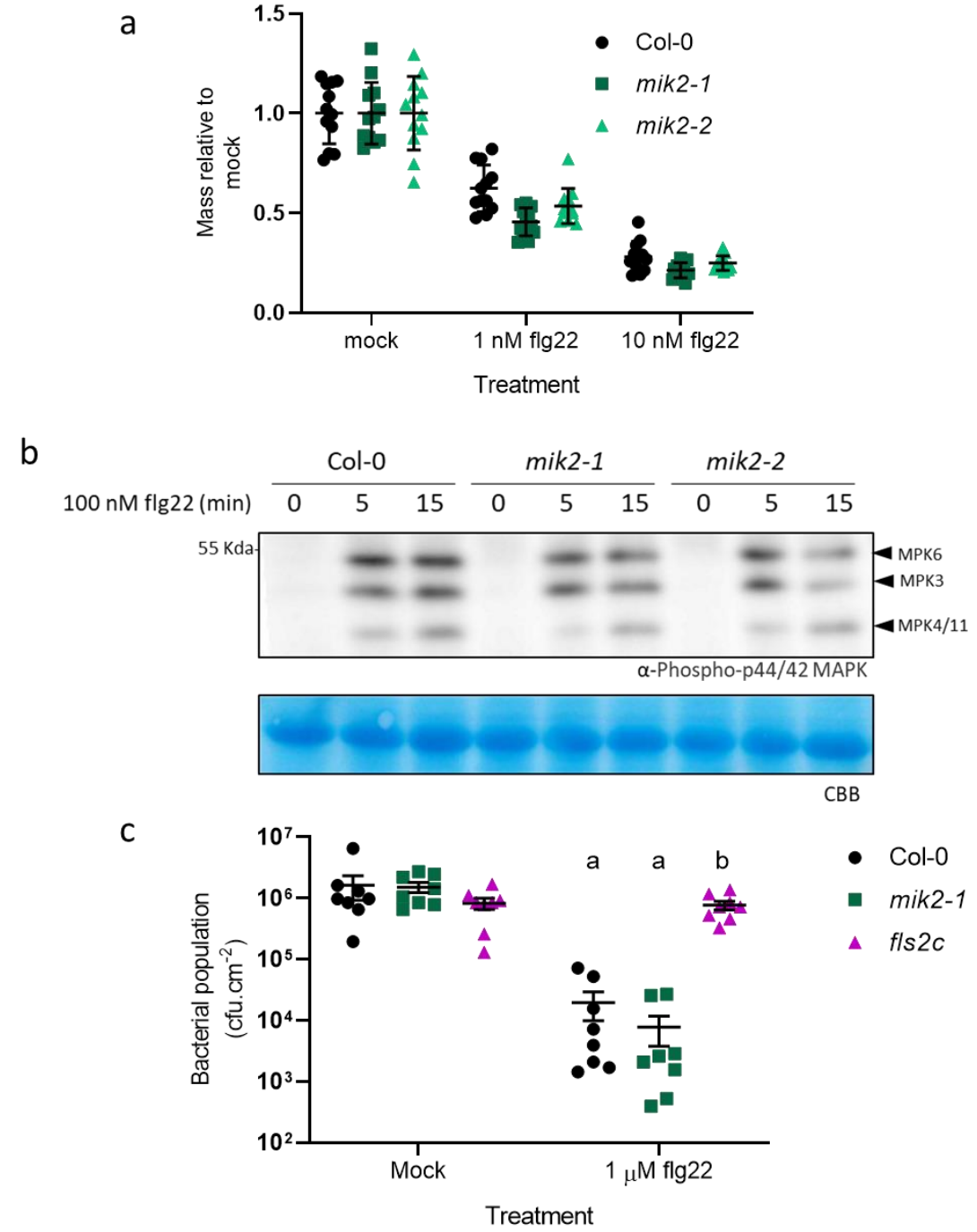

Figure 4. 8 MIK2 does not appear to be a regulator of other flg22-induced responses

(a) Mass of ten-day-old seedlings grown MS media with the addition of respective concentrations of flg22. Mass shown relative to mock. A two-way ANOVA found a significant effect of treatment $p<0.0001$; however, there was no significant interaction between genotype and treatment suggesting no significant difference in genotype response to flg22 ($p=0.1661$) so no multiple comparison was performed. (n=12). (b) 100 nM flg22-induced phosphorylation of MAP kinase in 12-day-old seedlings. CBB staining was performed as a loading control (c) 1 µM flg22 induced-resistance to *Pseudomonas syringae* pv. *tomato* DC3000 (*Pst* DC3000) in 4-week-old plants. Water or 1 µM flg22 were infiltrated one day prior to infiltration with *Pst* DC3000 ($O.D._{600}$ = 0.0002). The bacterial population was determined 3 days later. (Data for (c) from F. Boutrot). (a-c) Experiments were repeated at least three times with similar results.

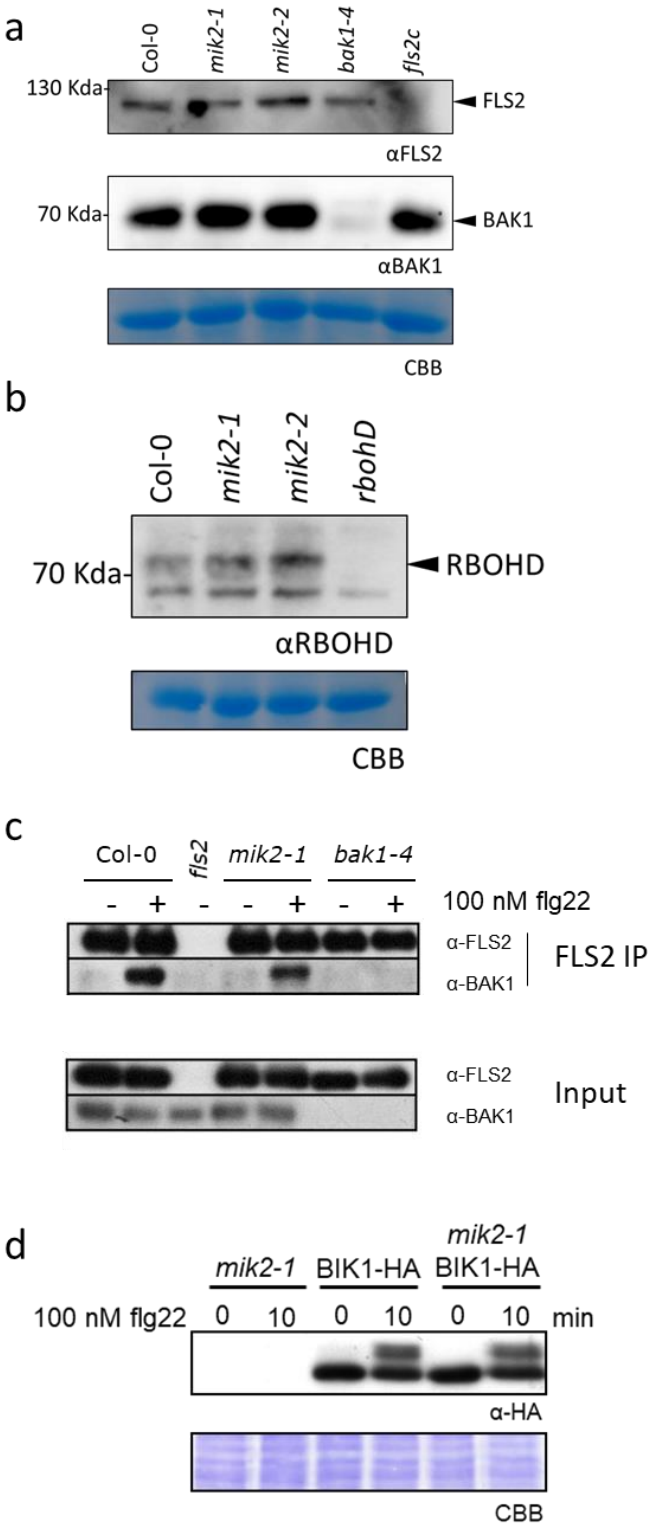

Figure 4. 9 Loss of MIK2 neither results in changes in FLS2, BAK1 or RBOHD accumulation nor affects FLS2-BAK1 complex formation and subsequent phosphorylation of the downstream RLCK BIK1.

(a-b) Protein levels in Col-0 and *mik2-1* 12-day-old seedlings. CBB staining of the membrane is shown as a loading control. (c) (Data from M. Roux) Co-Immunoprecipitation of BAK1 with FLS2 upon flg22 treatment in 13-day-old seedlings (d) (Data from F. Boutrot) flg22-induced bandshift in BIK1-HA in 14-day-old seedlings.

To investigate whether this reduction was specific to LRR-containing receptor complexes I tested response to 3-hydroxydecanoic acid, a bacterial metabolite recognised by the lectin S-domain receptor kinase LORE1 (Ranf *et al.*, 2015; Kutschera *et al.*, 2019). The 3-hydroxydecanoic acid-induced ROS response was also reduced in *mik2* showing that the phenotype was not specific to LRR-containing receptor complexes or to proteinaceous elicitors (Fig 4.10 c,f).

I then tested the function of MIK2 in ROS production triggered by DAMPs. Surprisingly, when testing the proteinaceous DAMP Pep3, pectin-derived oligogalacturonides (d.p. 14-16) and the cellulose-derived disaccharide cellobiose, I observed a surprising increase in elicitor-induced ROS production in *mik2* (Fig 4.11 a-f). This is particularly striking in the case of cellobiose where no ROS production could be previously measured in Col-0 or Ws-2 (Souza *et al.*, 2017); however, I observed a rapid peak in ROS production in *mik2* alleles (Fig 4.11 c,f). In addition to the elevated levels of ROS production in *mik2*, there is a temporal shift with ROS production peaking earlier, which is particularly evident in response to Pep3 (Fig 4.11 a). I selected Pep3 as a representative example of an elicitor whose ROS response is negatively regulated by *MIK2*, and assayed Pep3-induced PTI outputs. No difference in Pep-induced MAPK phosphorylation were observed (Fig 4.12 a). I observed a slight increase in Pep-induced seedling growth inhibition in one *mik2* allele at higher peptide concentrations (Fig 4.12 b). There was also no observable difference in *PEPR1* or *PEPR2* expression levels (Fig 4.12 c).

In order to assay ROS production in a more physiologically relevant context I performed DAB (3,3′-Diaminobenzidine) staining during *Pc*BMM infection. The role of RBOHD in pathogen-induced ROS production can be seen through the absence of brownish deposits in *rbohd* (Fig 4.13). However, there are no discernible differences between Col-0 and the *mik2* mutants. If this is pursued in future work a higher order PTI mutant (*i.e. bak1-5/bkk1-1/cerk1-2*) should be included in order to determine whether the ROS is due to recognition by cell surface receptors (Xin *et al.*, 2016).

Taken together, these results show that *MIK2* is differentially required for elicitor-induced ROS production. Despite testing biochemically-diverse elicitors, perceived by phylogenetically and biochemically diverse receptors, I am not able to identify a clear correlation with *MIK2* function. Currently, I am not able to define a mechanistic explanation for the dichotomy seen with *MIK2* acting as both a positive and negative regulator of elicitor-induced ROS production.

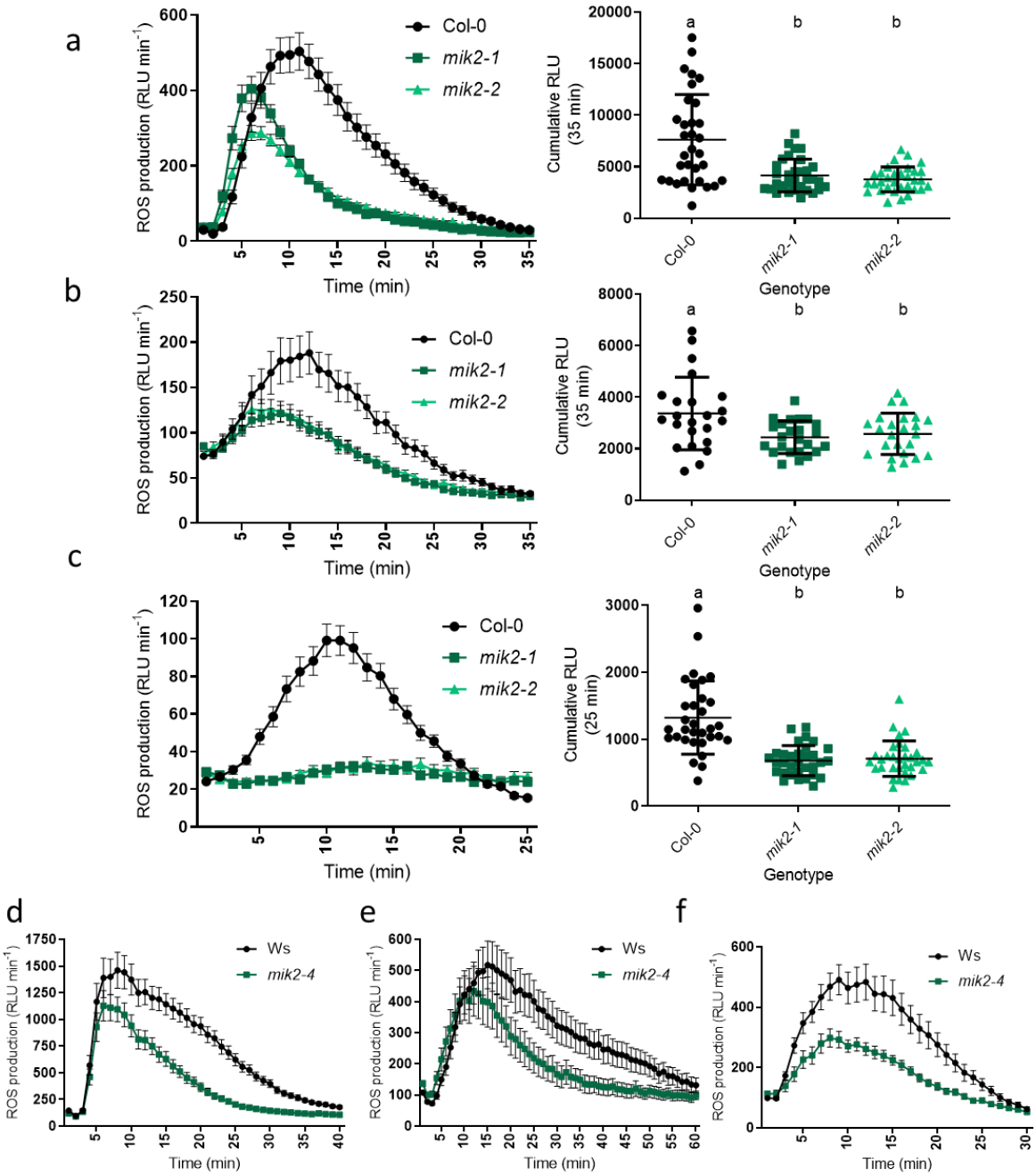

Figure 4. 10 *mik2* mutants have a reduced ROS response to the multiple elicitors

(a-f) Elicitor-induced ROS production from leaf disks taken from five-week-old rosettes. Error bars on curves represent S.E.M. Plots on the right show the integration derived from the plots on the left, horizontal lines show mean with S.D., lowercase letters indicate significance groups based on one-way ANOVA followed by Tukey's Post-hoc test. Treatment with (a,d) 100 nM elf18; (b,e) 1 µM nlp20 (c,f) 1 µM 3-hydroxydecanoic acid. (a-c) n=32; (d-f) n= 16. (a-c) Experiments have been repeated at least 3 times with similar results. (d-f) Experiments have been performed once.

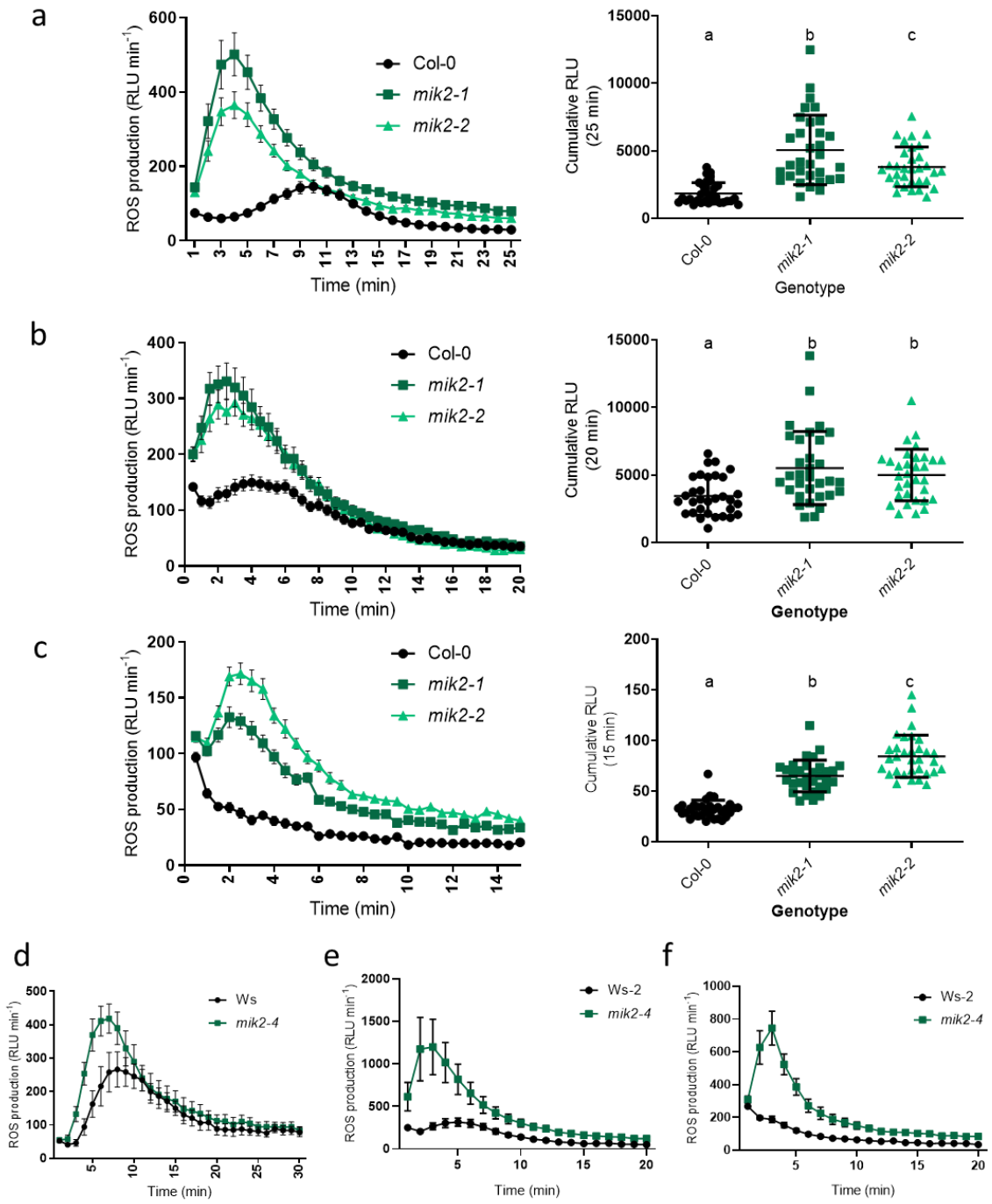

Figure 4. 11 *mik2* mutants differentially regulate elicitor-induced ROS responses

(a-f) Elicitor-induced ROS production from leaf disks taken from 5-week-old rosettes. Error bars on curves represent S.E.M. Plots on the right show the integration derived from the plots on the left, horizontal lines show mean with S.D., lowercase letters indicate significance groups based on one-way ANOVA followed by Tukey's Post-hoc test. Treatment with (a,d) 1 µM AtPep3; (b,e) 100 µg.ml^{-1} oligogalacturonides (c,f) 10 mM cellobiose. (a-c) n=32; (d-f) n= 16. (a-c) Experiments have been repeated at least 3 times with similar results. (d-f) Experiments have been performed once.

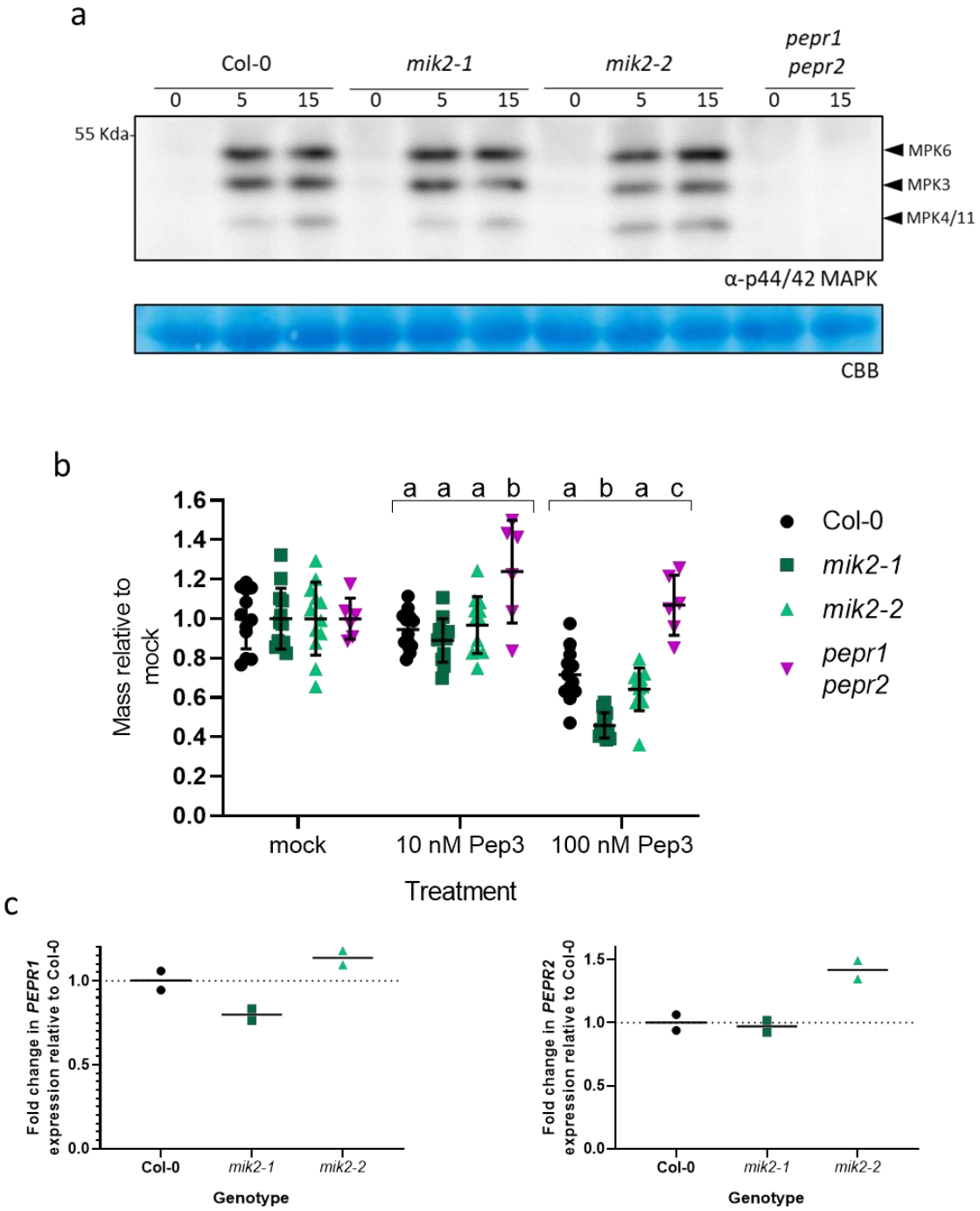

Figure 4. 12 MIK2 does not appear to be a regulator of Pep3-induced MAPK phosphorylation and seedling growth inhibition

(a) 100 nM Pep3-induced phosphorylation of MAP kinase in 12-day-old seedlings. CBB staining was performed as a loading control. (b) Mass of 10-day-old seedlings grown MS media with the addition of respective concentrations of Pep3. Mass shown relative to mock. A two-way ANOVA found a significant genotype-by-treatment interaction suggesting that the genotypes responded differently to the treatments. Lowercase letter represent significant groups from a Tukey's multiple comparison test performed within treatment groups ($p<0.01$) Error bars represent S.D., bar represent the mean. (c) *PEPR1/2* expression in 12-day-old seedlings grown in MS media assessed by qPCR. Bar indicates the mean. (a-b) Experiments were repeated three times with similar results. (c) Experiment was performed once.

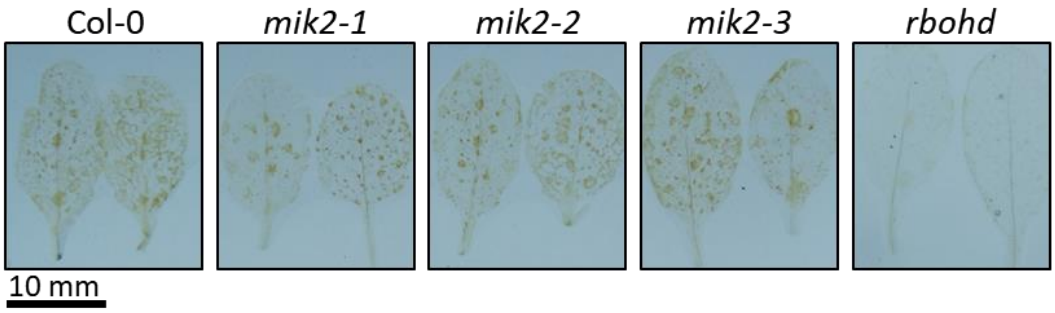

Figure 4. 13 DAB staining for ROS production during *Pc*BMM infection

Four-week-old plants were sprayed with and 4×10^6 spores ml^{-1} *Pc*BMM and then stained 48 hpi overnight with DAB.

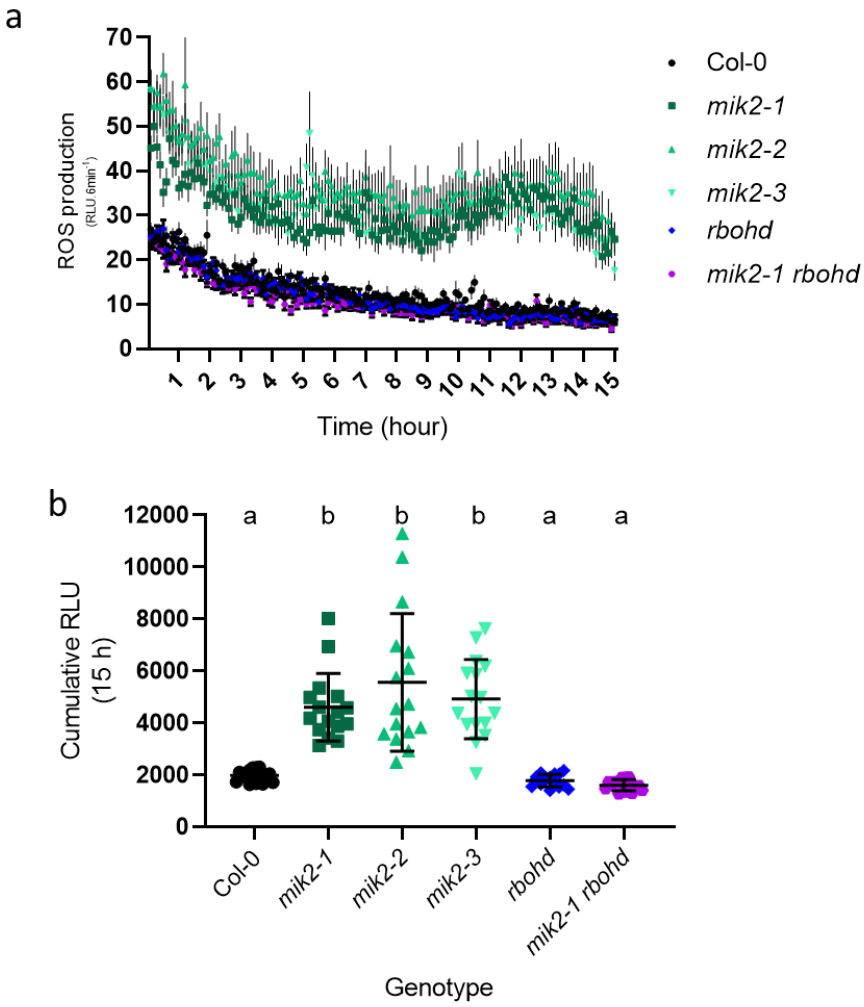

Figure 4. 14 MIK2 negatively regulates RBOHD-dependent background ROS production

(a-b) Background ROS production from leaf disks taken from 5-week-old rosettes measured using a luminol-based assay. (a) Error bars represent S.E.M.; n =16 (b) Integration of data from (a) Error bars represent S.D., lowercase letters represent significance groups based on Tukey's multiple comparison following a one-way ANOVA ($p<0.0001$).

4.3.7 Constitutive upregulation of background ROS in *mik2*

Intriguingly, whist performing elicitor-induced ROS assays it was observed that *mik2* mutants exhibit enhanced background ROS production with mock treatment when no elicitor was added (first observed by Dr. Freddy Boutrot). This phenomenon became striking when measured over longer time periods (Fig 4.14 a-b). Characterisation of this background ROS revealed that it was RBOHD-dependent (Fig 4.14 a-b). *MIK2-like* does not appear to show a redundant role with *MIK2* in negatively regulating background ROS production (Fig 4.15 a). I hypothesised that the *mik2* phenotype could be due to guarding by cytoplasmic receptors creating autoimmunity (Rodriguez *et al.*, 2016). However, impairing salicylic acid biosynthesis or mutating components required for the function of the two main classes of cytoplasmic immune receptors, EDS1 and NDR1, did not abolish the enhanced background ROS in *mik2* (Fig 4.15 b-c).

As the background ROS is RBOHD-dependent, I hypothesised that the phenotype could be due to the misregulation of an RK or RLP signalling pathway in *mik2*. As many of these receptors are dependent upon SERK coreceptors, I assayed the effect of *bak1* mutations on background ROS in *mik2*. Whilst not statistically significant, I reproducibly saw a quantitative reduction in background ROS in *mik2-1 bak1-5* compared to *mik2-1* (Fig 4.16 a). Conversely, I saw an increase in *mik2-1 bak1-4* and *mik2-4 bak1-1* relative to *mik2-1* and *mik2-4* respectively (Fig 4.16 b-c). Whilst *bak1-5* is a dominant negative point mutation that impairs the function of LRR-RKs containing the Tyr-VIa residue (Schwessinger *et al.*, 2011; Perraki *et al.*, 2018), *bak1-4* and *bak1-1* are null mutants that have weak autoimmunity and enhanced cell death (Li *et al.*, 2002; Kemmerling *et al.*, 2007; Heese *et al.*, 2007). This autoimmunity could explain the enhanced background ROS in *mik2-1 bak1-4* and *mik2-4 bak1-1*.

As *mik2* shows enhanced Pep-induced ROS production and *bak1*-null mutants are hypersensitive to Pep treatment (Yamada *et al.*, 2016*c*), I hypothesised that Pep-hyperresponsivity could underlie the enhanced background ROS. However, the background ROS was still apparent in the *mik2-1 pepr1-1 pepr2-3* triple mutant, suggesting this is not the case (Fig 4.16 d).

As these ROS measurements were all performed in leaf disks, I was keen to establish whether the wounding and cell wall damage generated during leaf disk collection was required for this enhanced background ROS. To test this, I performed ROS assays on seedlings grown in 96-well plates. There, I was still able to observe a significant increase in ROS production in *mik2-1* compared to Col-0 (Fig 4.16 e). In seedlings, ROS production in *mik2-1 bak1-4* was still enhanced relative to *mik2-1* and *mik2-1 bak1-5*, which were not significantly different (Fig 4.16 e-f). The background ROS production in *mik2* seedlings was also still RBOHD-dependent. DAB staining of *mik2-1 bak1-4* seedlings corroborates the enhanced ROS

observed by luminol-based measurements (Fig 4.16 e). However, no notable differences could be observed between Col-0 and *mik2* seedlings following DAB staining, potentially due to limited sensitivity, masking quantitative differences (Fig 4.16 f).

Taken together, these results show a constitutive enhancement in background ROS that is not dependent upon wounding during leaf disk collection. This ROS is dependent upon the NADPH oxidase RBOHD but appears to be independent of SA or cytoplasmic immune receptors. This ROS production is greatly enhanced by the loss of BAK1 but may be diminished in the *bak1-5* mutant background. This data points toward the dyshomeostasis of a BAK1- and RBOHD-dependent LRR-RK or LRR-RLP signalling pathway(s) in *mik2*, which does not appear to be PEPR-based.

4.3.8 Late ROS production in *bak1* is *MIK2*-dependent

All the elicitor-induced ROS production shown so far has immediately followed elicitor addition. Whilst performing ROS assays with *bak1* mutants, which show reduced elicitor induced ROS production, I serendipitously observed a strong second ROS burst in *bak1* mutants relative to their respective wild-type (Fig 4.17 a-b). As expected, *bak1* mutants show reduced elf18-induced ROS production in the first 60 min (Fig 4.17 a), however, after the first hour a second ROS response was observed in *bak1*-null mutants (Fig 4.17 b). Notably, this response was observed in all T-DNA *bak1* null backgrounds tested (*i.e. bak1-1, bak1-3, bak1-4*), but not in *bak1-5* (Fig 4.17 b-c). I was keen to test the effect of *mik2* loss-of-function on this second ROS response in *bak1*. As expected, within the first hour flg22-induced ROS was reduced in *mik2-1* and *bak1-4* (Fig 4.17 d). An additive effect of the two mutations can be seen with the weak ROS response in *mik2-1 bak1-4* (Fig 4.17 d). After 2 h, ROS production in *bak1-4* increases again, peaking approximately 3-4 h after elicitor addition. However, this response was not observed in the *mik2-1 bak1-4* background, revealing it is MIK2-dependent. This MIK2-depdendency is also observed in response to elf18 (Fig 4.17 e-f). flg22 and elf18 both induce reduced initial ROS bursts in *mik2* (Fig 4.7; Fig 4.10 a,d), to investigate whether this is responsible for the abolition of the second ROS burst in *mik2 bak1*, I assayed Pep3-induced second ROS burst. Despite early Pep3-induced ROS being enhanced in *mik2-1* (Fig 4.10 a), the second ROS burst - still apparent in *bak1-4* - was abolished in *mik2-1 bak1-4* (Fig 4.18 a). Furthermore, the same trend can be seen with chitin (Fig 4.18 b), despite the receptor complex being SERK-independent (Shan *et al.*, 2008; Schwessinger *et al.*, 2011).

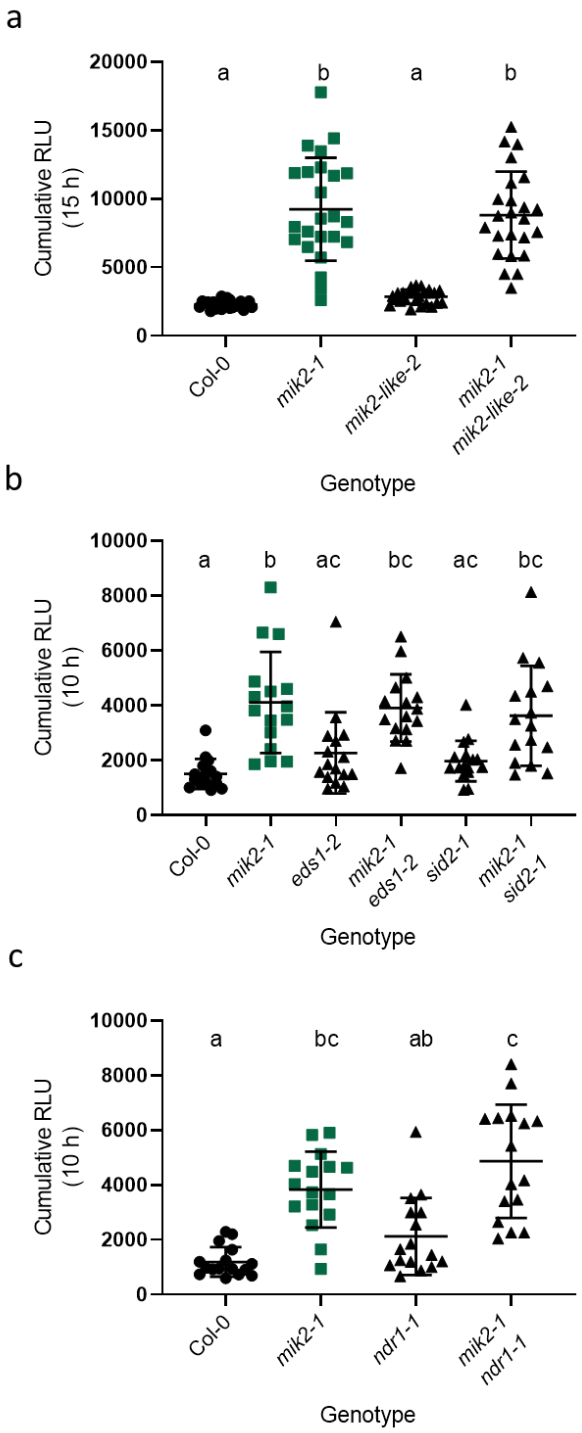

Figure 4. 15 Background ROS in *mik2* does not show redundancy with MIK2-like and is NDR1-, EDS1-, andSID2- -independent .

(a-c) Background ROS production from leaf disks taken from 5-week-old rosettes measured using a luminol-based assay. (a) n=24, (b-c) n=16

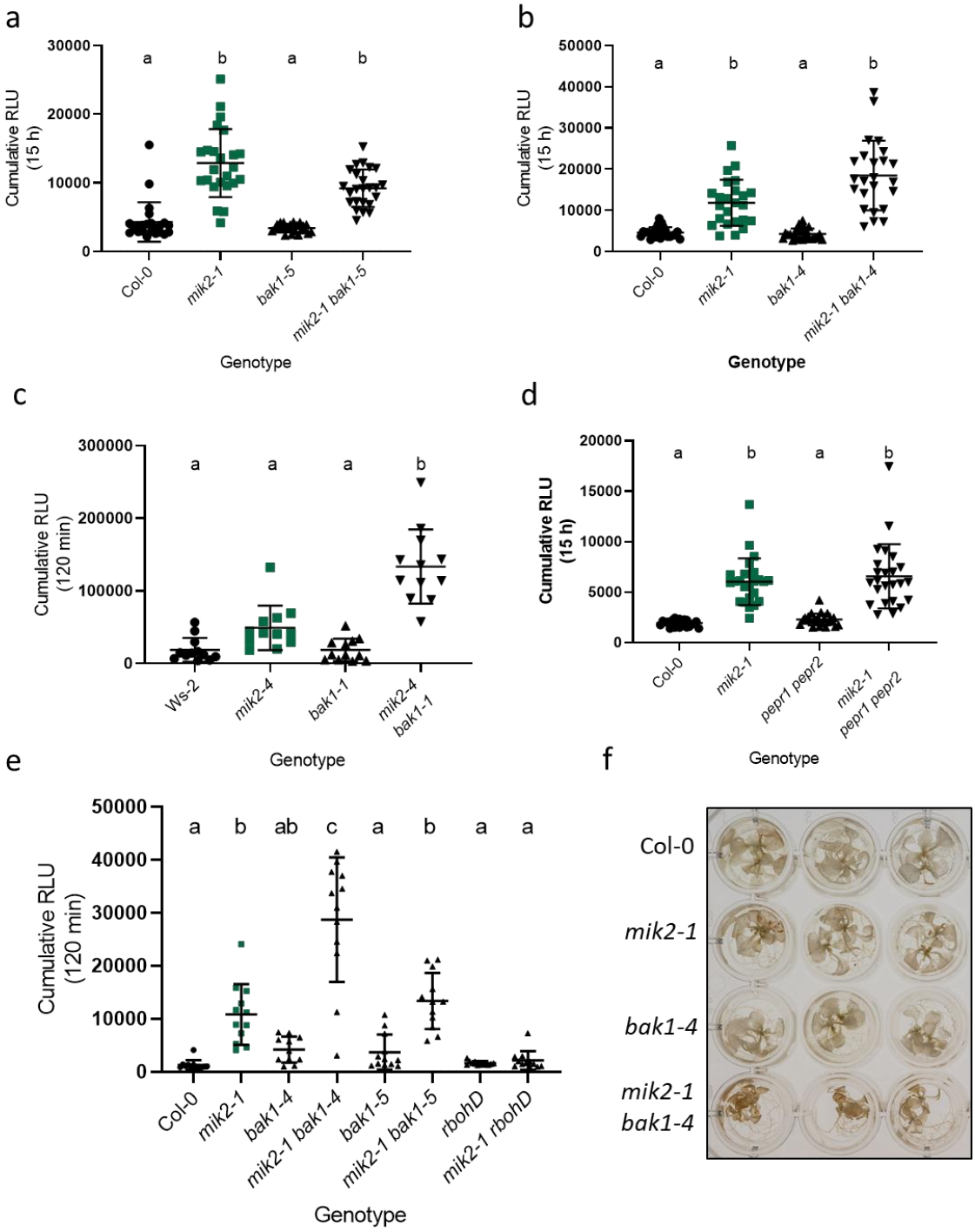

Figure 4. 16 Background ROS in *mik2* is enhanced in *bak1-4*

(a-d) Background ROS production from leaf disks taken from 5-week-old rosettes measured using a luminol-based assay. (a-b,d) n = 24 (c) n=12. (e) ROS production from 9-day-old seedlings measured using L-012. n =12. (f) DAB staining for ROS production in twelve-day-old seedlings. Lowercase letters represents significant groups (a-d) Error bars represent S.D. Lowercase letters represent significance groups based on Tukey's multiple comparison following a one-way ANOVA.

In an attempt to determine whether this response was due to the sustained PAMP presence throughout the experiment, I made use of the competitive inhibitor of elf18 signalling, elf12 (Kunze *et al.*, 2004). After 30 min of 100 nM elf18 application the solution was exchanged for either 10 mM elf12 or 100 nM elf18. I was able to observe the enhanced ROS in *bak1*-null mutants following both treatments (Fig 4.18 c-d). I observed a reduction in the *bak1* second ROS burst following elf12 treatment, relative to continued elf18 treatment (Fig 4.18 c-d). While this experiment is not conclusive it points towards the late peak being independent of sustained elicitor treatment and may be indirectly dependent on elf18 signalling. The majority of EFR has been endocytosed within 1 h of elf18 treatment, however, little is known about how long endocytosed EFR remains signalling active (Mbengue *et al.*, 2016), this could mean the second ROS burst is induced by EFR signalling complexes formed before elf12 treatment. EFR endocytosis is impaired in *bak1* mutants which also perturbs interpretation of the results (Mbengue *et al.*, 2016).

Due to the timing, I hypothesised that the second ROS response could be the result of elicitor-induced production, processing or secretion of a phytocytokine that acts as a secondary signal. *bak1* mutants may: 1/ produce more of this secondary signal, or 2/ be hypersensitive the secondary signal. Yamada *et al*. (Yamada *et al.*, 2016*c*) reported that *bak1* null mutants were hypersensitive to Pep treatment, in a PEPR-dependent manner. They proposed this guards against depletion of BAK1 by pathogen effectors during infection. *Propeps* are also transcriptionally upregulated and processed upon biotic elicitor treatment (Bartels *et al.*, 2013; Yamada *et al.*, 2016*c*). Therefore, I decided to investigate whether the enhanced second ROS burst in *bak1-4* was PEPR-dependent. The second ROS response to flg22 was comparable in *bak1-4* and *bak1-4 pepr1-1 pepr2-3* suggesting it is PEPR-independent (Fig 4.18 e).

These results describe a novel late ROS response in *bak1* null mutants, which is not apparent in *bak1-5*. This response is conserved between diverse elicitors and may contribute to a mechanism guarding against pathogen-mediated BAK1 depletion. This response appears to be MIK2-dependent. Potentially this could be due to the release of a phytocytokine that's perception is MIK2-depdendent.

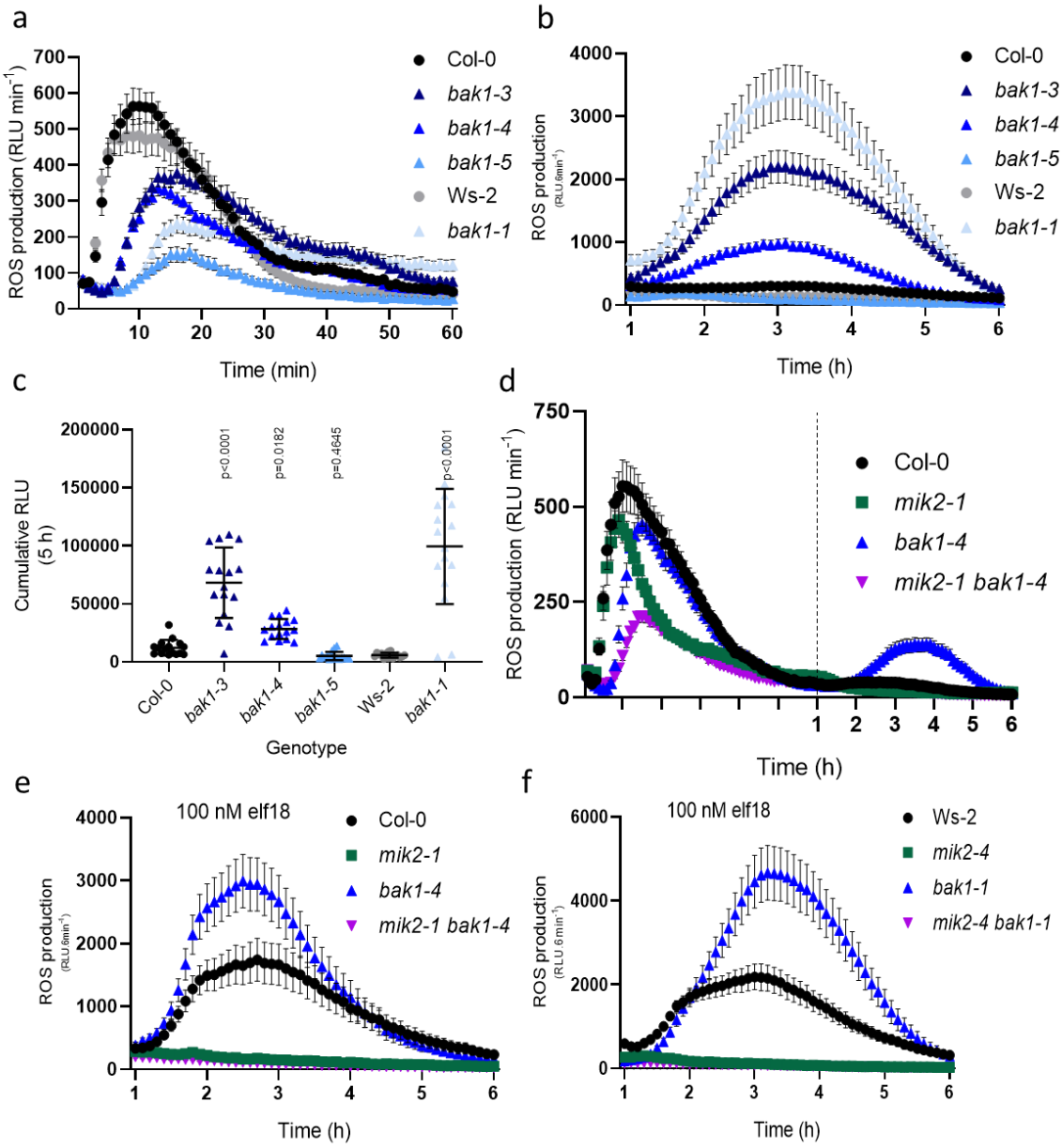

Figure 4. 17 Late second ROS production in *bak1* is *mik2*-depdendent

(a-b) ROS measurement after the addition of 100 nM elf18 in leaf-disks of 5-week-old *Arabidopsis* leaf disks n=16 (a) first 60 min; (b) 60-360 min after elicitor addition (c) Integration of the data in (b), bar = mean, error bars = S.D. P-values are derived from Dunnetts's multiple comparison or t-test relative to the respective wild-type control (d) 100 nM flg22-induced ROS production in leaf disks from 6-week-old rosettes. (n=24). (e,f) 100 nM elf18-induced ROS production in leaf disks from 5-week-old rosettes. (b,e-f) The first 1st hour after elicitor addition has been removed to aid visualisation. (a-b,e-f) Error bars represent S.E.M.

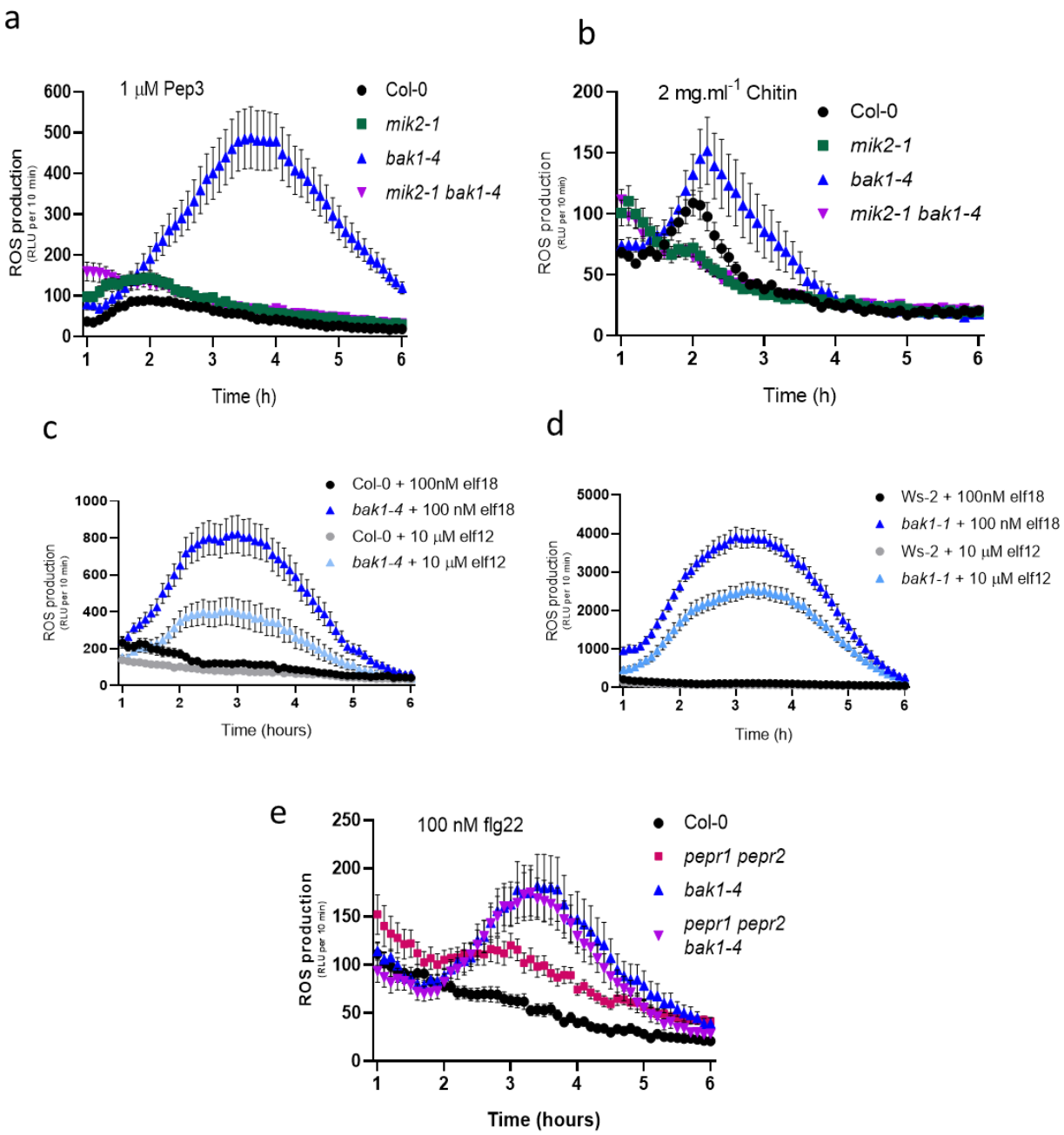

Figure 4. 18 Late second ROS production in *bak1* is *mik2*-depdendent in response to multiple elicitors, is not abolished by treatment with the competitive inhibitor elf12 and is PEPR-independent

(a) 1 µM Pep3-, (b) 2 mg.ml^{-1} Chitin and (e) 100 nM flg22-induced ROS production in leaf disks from six-week-old rosettes. (c-d) Initial 100 nM elf18 treatment was replaced after 30 min with the indicated treatment of 100 nM elf18 or 10 mM elf12. Error bars represent S.E.M. (n=24). The first 1 h after elicitor addition has been removed to aid visualisation.

4.3.9 The *mik2 bak1* double mutant is dwarf

Interestingly, I observed that the *mik2-1 bak1-4* double mutant shows rosette dwarfing (Fig 4.19 a). Whilst the *bak1*-null mutants have been shown to have a mild dwarfing phenotype (Li *et al.*, 2002; He *et al.*, 2007), there appears to be a strong epistatic interaction between *mik2-1* and *bak1-4*. This is also the case in the Ws-2 ecotype (Fig 4.19 b-c). The effect appears to be unique to *bak1*-null mutations as *mik2-1 bak1-5* does not show this phenotype, nor does mutation of *mik2* in *rbohD* which also has an autoimmune phenotype (Kadota *et al.*, 2014) (Fig 4.20). Due to the role of BAK1 in brassinosteroid perception, I wanted to establish whether the dwarf phenotype could be due to a hyposensitivity to this hormone. Accumulation of the brassinosteroid receptor BRI1 (Li and Chory, 1997) is similar between Col-0 and *mik2-1* (Fig 4.21 a). *bak1-4* clearly had reduced hypocotyl growth on 0.2 μM brassinazole (BRZ) due to reduced brassinosteroid sensitivity (Fig 4.21 b) (Asami *et al.*, 2000). Whilst *mik2* alleles showed no significant difference from Col-0 when grown on BRZ they did show slightly enhanced hypocotyl elongation under mock conditions. Therefore, they appear to have a slightly higher relative sensitivity to BRZ treatment (Fig 4.21 c-d). However, there was no significant difference between the sensitivity of *bak1-4* and *mik2-1 bak1-4*, implying that the double mutant is not more sensitive to BRZ, and thus has comparable brassinosteroid-sensitivity with *bak1-4* (Fig 4.21 d). Moreover, Col-0, *mik2-1* and *mik2-2* all showed the characteristic root curling when grown on 5 nM brassinolide (in the presence of 2 μM BRZ), whilst *bak1-4* exhibited impaired brassinolide sensitivity evident as root waving, comparable with *mik2-1 bak1-4* (Fig 4.21 e). Taken together, this indicates that *mik2-1 bak1-4* is as sensitive to brassinosteroids as the *bak1-4* single mutant, suggesting that the dwarfism is not the result of impaired brassinosteroid sensitivity. The cause of the increased dwarfism observed in *mik2 bak1-4* thus remains to be determined.

4.3.10 Precocious senescence in *mik2*

It also became apparent in older plants (greater than six-week-old rosettes) that there was a mild, but noticeable precocious senescence in *mik2*. This phenotype was documented but not investigated any further (Fig 4.22). Pep signalling has been shown to positively regulate senescence (Gully *et al.*, 2015); however, the phenotype appears to be still present in the *mik2-1 pepr1-1 pepr2-3* triple mutant (Fig 4.20). The cause of the precocious senescence observed in *mik2* remains to be determined.

4.3.11 Transcriptomic perturbations in *mik2*

As it became apparent that *mik2* mutants display many constitutive phenotypes, including the enhanced background ROS, it became of interest to investigate whether this was reflected in transcriptomic perturbations in *mik2-1*. To this end, microarray analysis was performed by Dr. Dieuwertje van der Does on thirteen-day-old seedlings grown in MS media. There was a

strong and significant downregulation of *MIK2* transcripts in *mik2-1* relative to Col-0 as would be expected (Fig 4.23 a). A selection of the genes differentially expressed in *mik2-1* based on the microarray was confirmed using qRT-PCR (Fig 4.23 b-e). In order to determine clusters of genes differentially expressed in *mik2*, I performed Gene Ontology (GO) enrichment (Mi *et al.*, 2019). Taking a commonly used cut-off of ≥4-fold change, I selected all genes differentially expressed in *mik2-1*. I searched for GO term enrichment under the categories 'Cellular component' for localisation and 'Biological process' for function. Strikingly, *mik2*-upregulated genes (n=97; Appendix table 3) are significantly enriched in genes whose protein products are predicted to be extracellular or plasma membrane-localised (Fig 4.24 a). In parallel, there was a significant under-representation of upregulated genes with intracellular and organelle specific annotations (Fig 4.24 b). Many of the *mik2* phenotypes seem to point to misregulation of the extracellular/plasma membrane environment; the transcriptome supports that conclusion.

When GO enrichment analysis was performed on the upregulated genes based on 'biological function' clusters involved in biotic interactions, defence and reactive oxygen species are enriched (Fig 4.24 c). This is in line with the many phenotypes of *mik2* mutants in defence-related and constitutive ROS production.

No GO term clusters were significantly enriched in the downregulated genes (>4-fold relative to Col-0) either for localisation or function, likely due to the smaller number of genes (n=24; Appendix table 4)).

I was particularly interested in whether these transcriptomic perturbations were downstream of the enhanced background ROS production in *mik2*, and the signalling components I had found to affect it – namely RBOHD and BAK1. Accordingly, I selected *WRKY30* as a marker gene, because it is amongst the most significantly upregulated genes in *mik2* and has been used as a reporter gene previously (Souza *et al.*, 2017). WRKY30 is upregulated in *mik2* compared to WT, and qRT-PCR shows that this upregulation is maintained in *mik2 rbohd*, *mik2-1 bak1-4* and *mik2-1 bak1-5* relative to *rbohd*, *bak1-4* and *bak1-5*, respectively (Fig 4.24 d). Although *WRKY30* is only one marker gene, this suggests that the enhanced background ROS is either genetically downstream or parallel to the transcriptomic perturbations.

The transcriptome reveals perturbations in the *mik2* mutant in keeping with the phenotypes observed in the mutant. These transcriptomic perturbations appear to be upstream of some of the phenotypes observed, therefore, further characterisation of these transcriptomic difference may prove fruitful in understanding the role of *mik2*.

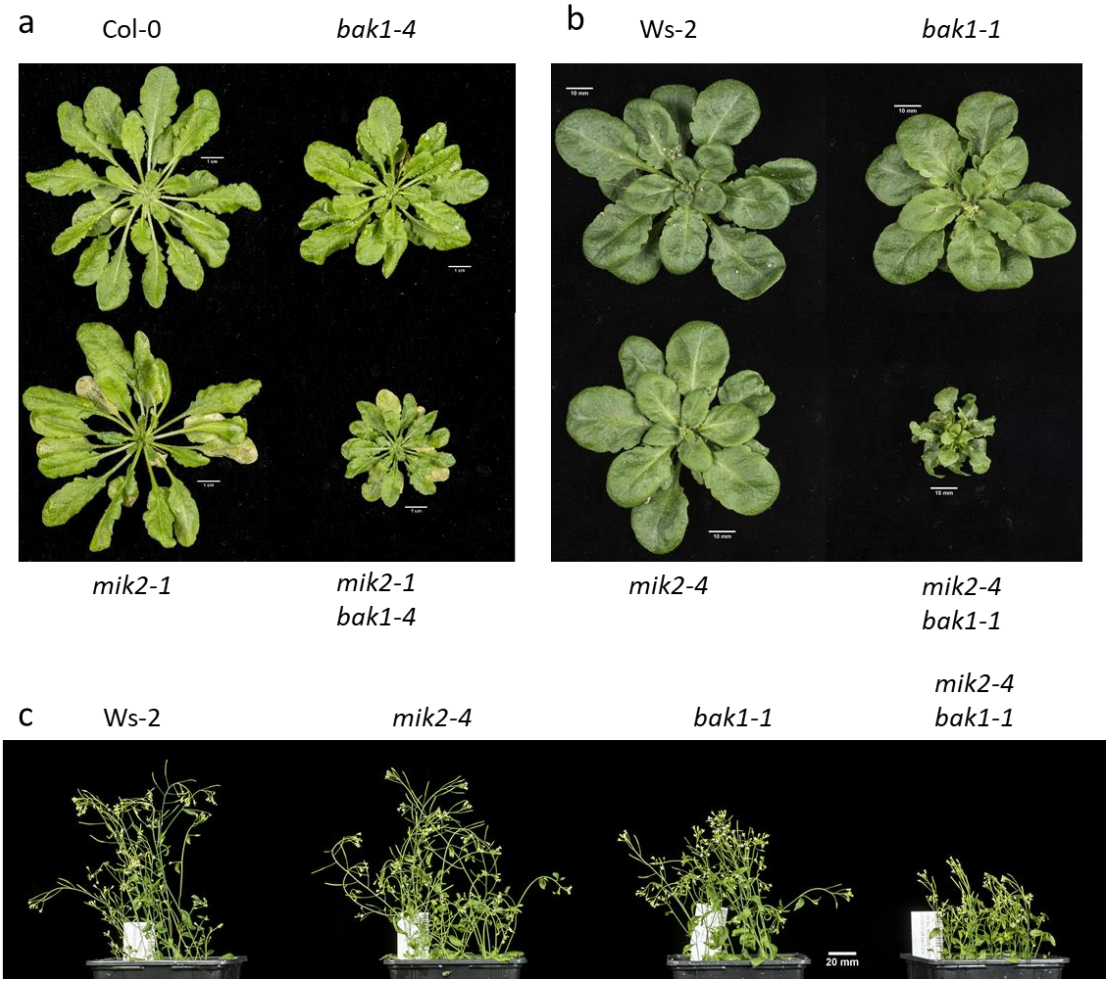

Figure 4. 19 Dwarf rosette and inflorescence phenotypes in *mik2 bak1* double mutants.

(a-b) Rosettes of (a) 8-week-old and (b) 5-week-old plants grown under short day conditions. (c) 7-week-old inflorescences grown in long-day conditions

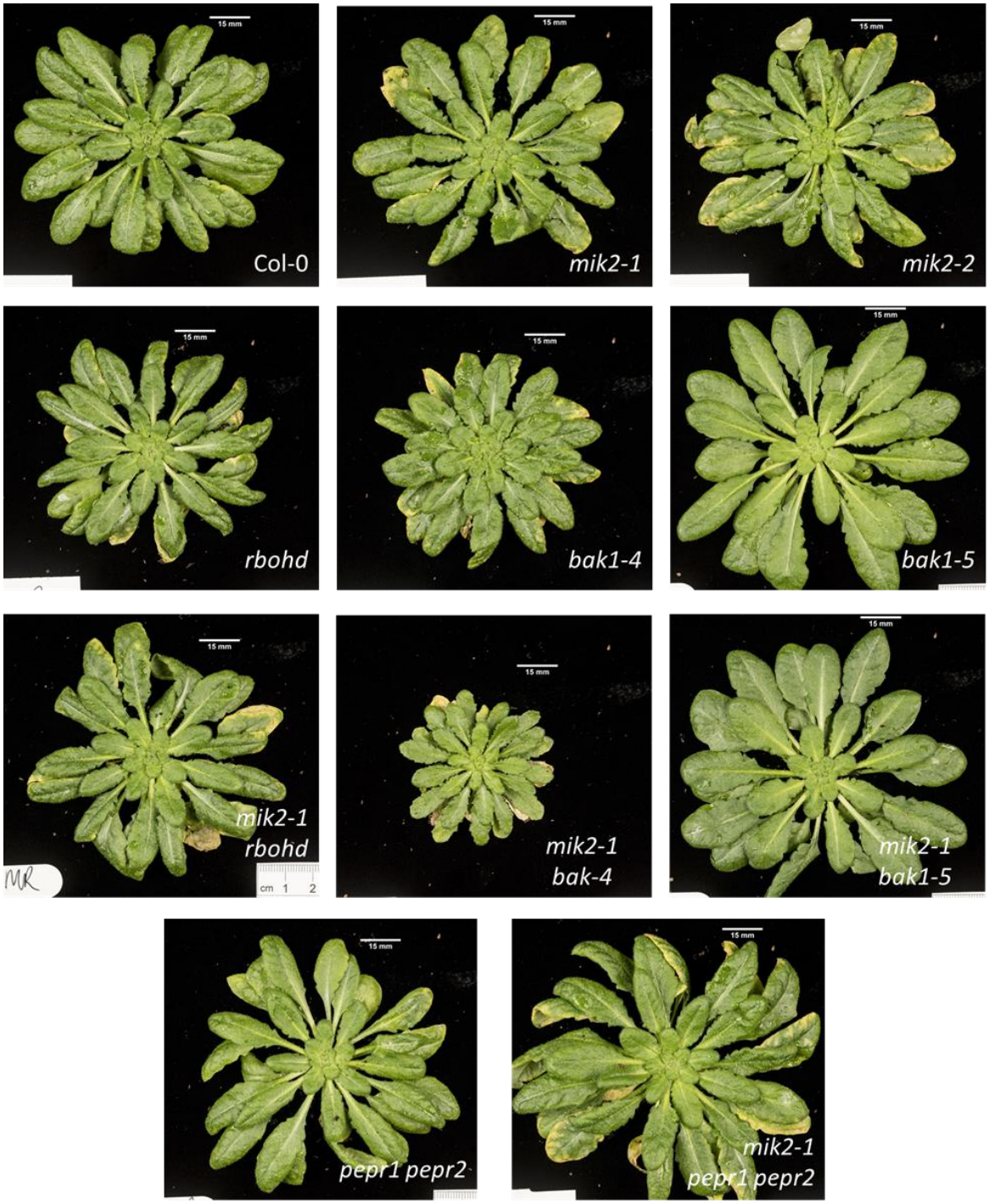

Figure 4. 20 Reduced rosette growth is specific to *mik2-1 bak1-4*

Images of 8-week-old rosettes grown under short-day conditions

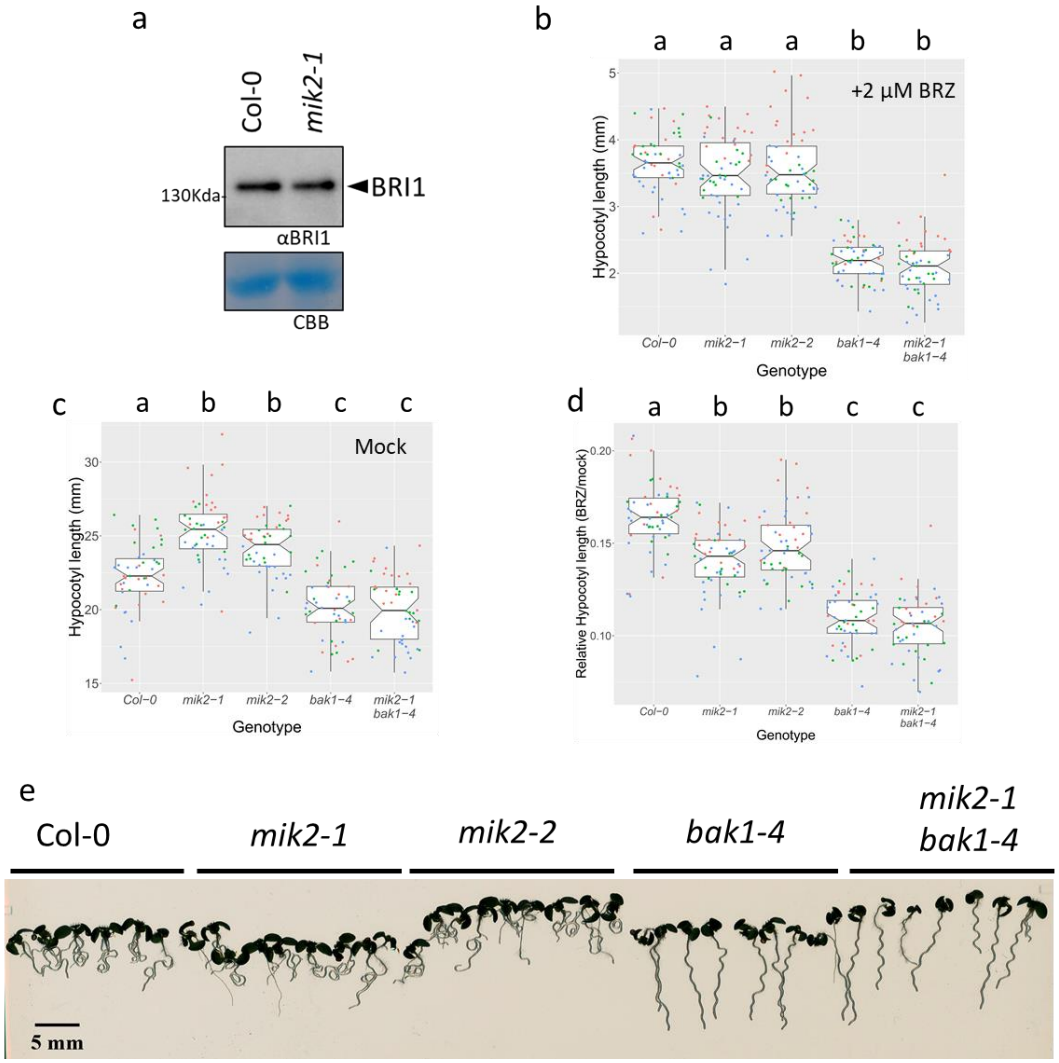

Figure 4. 21 *mik2* mutants do not show an impairment in brassinosteroid sensitivity

(a) BRI1 protein levels in Col-0 and *mik2-1* 12-day-old seedlings. CBB staining of the membrane is shown as a loading control. (b-e) 7-day-old seedlings grown on ½ MS + 1% sucrose (b-c) Dark-grown hypocotyl length in the (b) presence and (c) absence of 2 µM brassinazole (BRZ). (d) Relative root growth 2 µM BRZ length/ mock length. (e) Root growth of 7-day-old seedlings in the presence of 2 µM BRZ and 5 nM brassinolide. Blue, green and red dots represent biological replicates.

Figure 4. 22 *mik2* mutants show precocious senescence

Eldest 11 leaves from 7-week-old rosettes grown under short day conditions.

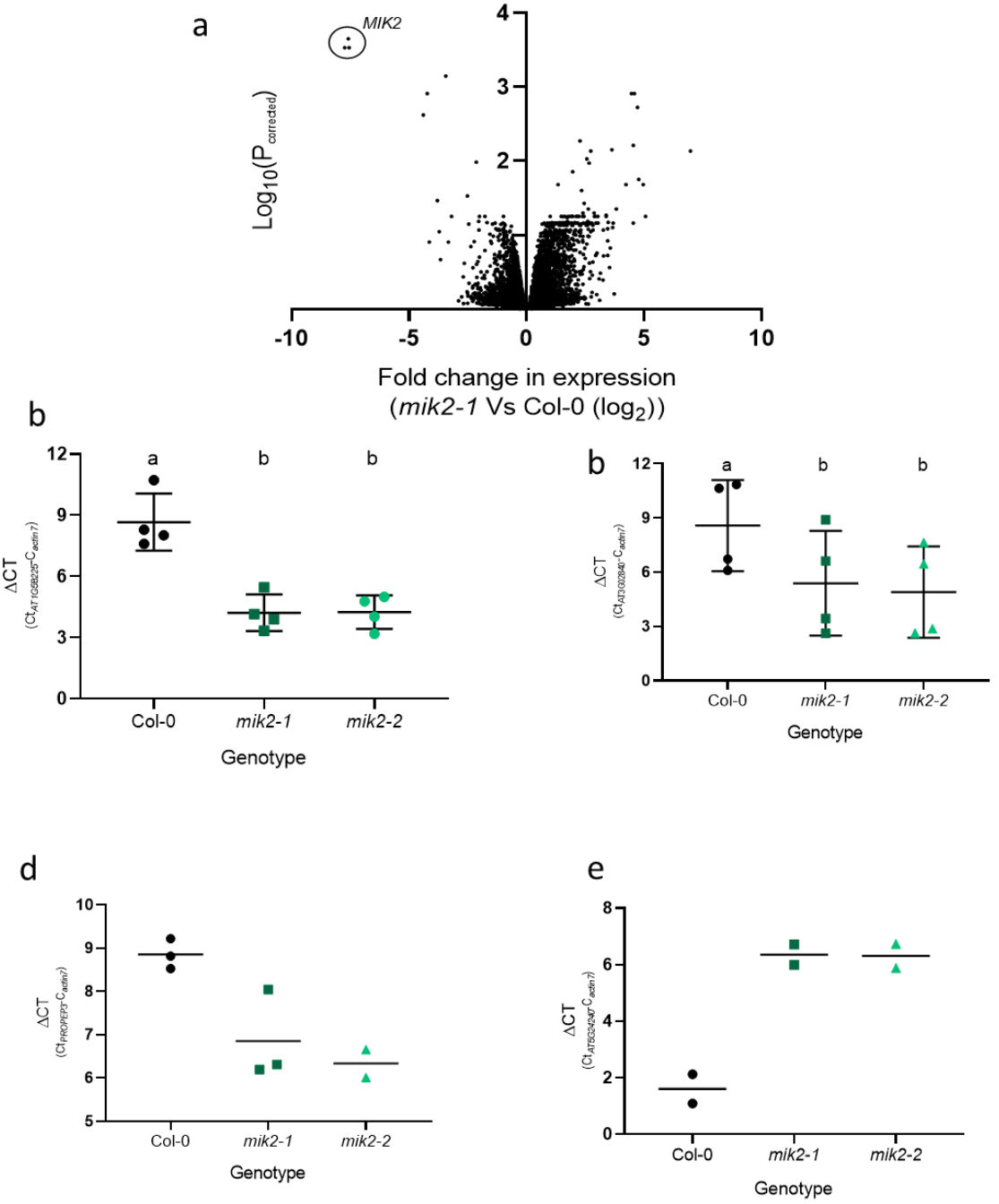

Figure 4. 23 Transcriptomic perturbations in *mik2*

(a) Volcano plot showing the transcriptomic perturbations in *mik2-1* Vs Col-0 in 13-day-old seedlings grown in MS media. Microarray analysis was performed using the Agilent-012600 microarray (Data from D. Van der Does). (b-e) Expression of selected genes from the *mik2* microarray data in 12-day-old seedlings grown in MS media assessed by qPCR. Bars represent mean, where shown error bars represent the S.D.. Lowercase letters represent significance groups ($p<0.03$) from a Tukey's multiple comparison test following a repeated measures ANOVA. (b) *AT1G58225;* (c) *AT3G02840;* (d)*PROPEP3* and (e) *AT5G24240*.

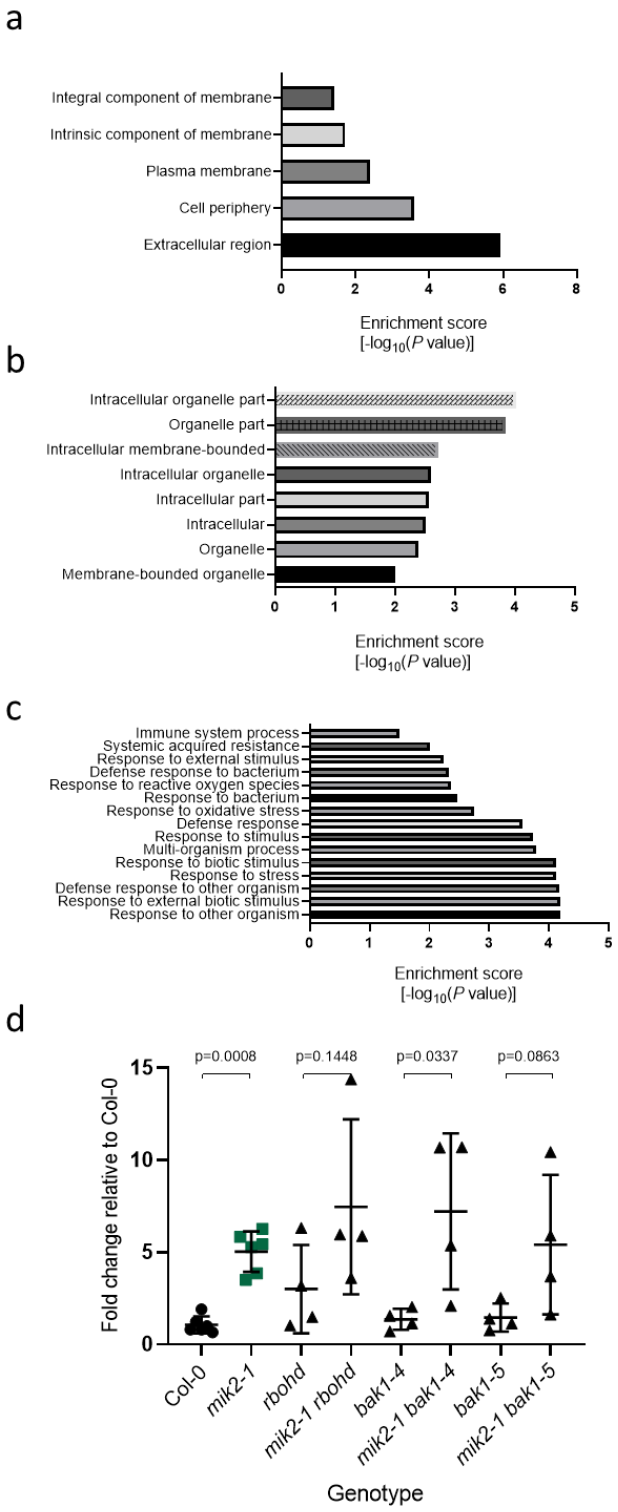

Figure 4. 24 Characterisation of the *mik2* transcriptomic perturbations

(a-c) All genes with >4 fold upregulation (n=97) were entered into the PANTHER14.1 to perform Gene ontology (GO) enrichment analysis to identify functional clusters significantly upregulated in *mik2*. The x-axis indicates the enrichment scores [–log10 (P value)] (the P value indicates the possibility of significant enrichment based on a false discovery rate on >0.05) for each GO item on the y-axis. (a-b) Analysis based on the cellular component: (a) overrepresented (b) underrepresented GO terms (c) analysis based on biological function (d) *WRKY30* expression in 12-day-old seedlings grown in MS media assessed by qPCR. Bar indicates the mean and error bars represent the S.D. P values are derived from t-tests.

a

AGI	Log$_2$ (Fold change *mik2*/Col-0)	Subfamily Sakamoto *et al.* (2012)	Name
AT4G23310	**12.80**	**DUF26**	***CRK23***
AT4G23150	**10.43**	**DUF26**	***CRK7***
AT4G04510	**7.10**	**DUF26**	***CRK38***
AT4G23280	**6.10**	**DUF26**	***CRK20***
AT5G38250	5.86	LRK10L2	
AT4G23140	**5.44**	**DUF26**	***CRK6***
AT4G04500	**5.44**	**DUF26**	***CRK37***
AT5G01550	5.33	L-LEC	*LECRK-VI.3*
AT1G79680	4.92	WAK	*WAKL10*
AT4G11890	**4.68**	**DUF26 singleton**	***ARCK1***
AT4G11470	**4.62**	**DUF26**	***CRK31***
AT1G66460	4.32	RLCKVI	
AT1G65790	4.31	SD1a	*ARK1*
AT5G60900	4.13	SD2b	*RLK1*
AT4G23230	**3.85**	**DUF26**	***CRK15***
AT5G20690	3.74	LRRIII	*PRK6*
AT5G24100	3.53	LRRIII	
AT5G12000	3.48	RLCKIXb	
AT3G45860	**3.48**	**DUF26**	***CRK4***
AT4G23220	**3.39**	**DUF26**	***CRK14***
AT1G21240	3.39	WAK	*WAK3*
AT2G19190	3.29	LRRIa	*FRK1/SIRK*
AT1G35710	3.27	LRRXIIb	*MIK2-like*
AT1G61550	3.22	SD1b	
AT4G04490	**3.13**	**DUF26**	***CRK36***
AT1G74360	2.95	LRRXb	*NILR1*
AT1G51890	2.94	LRRIa	
AT3G08870	2.86	L-LEC	*LECRK-VI.1*
AT3G45330	2.86	L-LEC	*LECRK-I.1*
AT4G23160	**2.86**	**DUF26**	***CRK8***
AT5G47850	2.84	CR4L	*CCR4*
AT1G16150	2.71	WAK	*WAKL4*
AT2G18470	2.70	PERK	*PERK4*
AT5G65600	2.69	L-LEC	*LECRK-IX.2*
AT1G51620	2.64	LRRIa	
AT5G35390	2.58	LRRIII	*PRK1*
AT4G17660	2.56	RLCKVIIa	
AT1G51820	2.47	LRRIa	*SIF4*
AT1G14370	2.47	RLCKVIIa	*PBL2*
AT1G61360	2.47	SD1b	
AT5G01560	2.42	L-LEC	*LECRKA4.3*
AT5G01540	2.39	L-LEC	*LECRK-VI.2*
AT1G61420	2.37	SD1b	
AT3G18810	2.35	PERK	*PERK6*
AT1G53420	2.34	LRRVIII-2	
AT1G34420	2.34	LRRXc	
AT3G42880	2.33	LRRIII	*PRK3*
AT4G23190	**2.32**	**DUF26**	***CRK11***
AT4G18250	2.29	LRK10L2	
AT2G30940	2.24	RLCKV	
AT4G23260	**2.23**	**DUF26**	***CRK18***
AT2G31880	2.17	XI-2	*SOBIR1*
AT1G67520	2.13	SD1a	
AT4G21380	2.13	SD1a	*ARK3*
AT2G32800	2.09	L-LEC	*LECRK-S.2*
AT5G38240	2.07	LRK10L2	
AT3G16030	2.06	SD1a	*RFO3/CES101*
AT5G58940	2.05	RLCKIV	*CRCK1*
AT5G01950	2.05	LRRVIII-1	
AT1G51800	2.03	LRRIa	*IOS1*
AT1G16110	2.02	WAK	*WAKL6*
AT4G23210	**2.02**	**DUF26**	***CRK13***
AT5G38210	2.01	WAK LRK10L1	*LRK10L3*

b

Name	Locus Identifier	FC
RLP43	AT3G28890	12.63
RLP7	AT1G47890	9.57
RLP20	AT2G25440	7.96
RLP41	AT3G25010	6.01
RLP23	AT2G32680	5.27
RLP28	AT2G33080	3.70
RLP49	AT4G13900	3.52
RLP21	AT2G25470	3.27
RLP53	AT5G27060	3.05
RLP38	AT3G23120	3.02
RLP40	AT3G24982	2.94
RLP56	AT5G49290	2.75
RLP46	AT4G04220	2.72
RLP42	AT3G25020	2.72
RLP39	AT3G24900	2.67
RLP52	AT5G25910	2.65
RLP11	AT1G71390	2.60
RLP48	AT4G13880	2.60
RLP44	AT3G49750	2.56
RLP35	AT3G11080	2.52
RLP50	AT4G13920	2.18

c

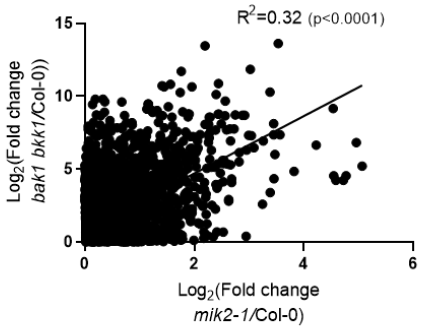

d

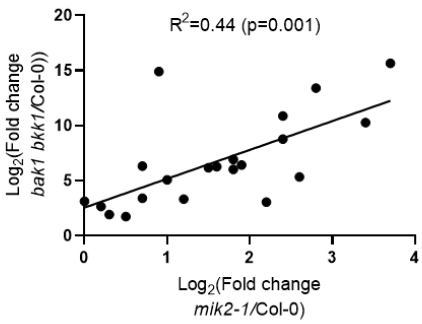

Figure 4. 25 RK and RLP encoding genes upregulated in *mik2-1* and comparisons with the *bak1 bkk1* transcriptome

(a) RKs and (b) LRR-RLPs transcriptionally upregulated >4 fold in *mik2-1* relative to Col-0. Bold highlights members of the DUF26/cysteine-rich RKs. (c-d) Correlation between (c) whole transcriptome and (d) *CRKs* transcriptionally upregulated in both *mik2* and *bak1/bkk1*.

4.4 Discussion

4.4.1 Direct or indirect effects for MIK2

The plethora of phenotypes in *mik2* raises the question whether *mik2* effects are a direct, or indirect consequence of MIK2 absence at the plasma membrane. MIK2 has the characteristics of a ligand-binding receptor with a long ectodomain containing 23 leucine-rich repeats and has a cytoplasmic domain capable of inducing 'PTI-like' responses when coerced into proximity with BAK1 (Chapter 3). No member of LRR-RK XIIb has been characterised extensively; however, closely related receptors in LRR-RK subfamily XIIa and XI are ligand-binding receptors recognising short proteinaceous ligands. The potential for MIK2 to act as a ligand-binding receptor is discussed further in Chapter 6.

MIK2 could also play a direct role as a regulator by physically interacting with receptor complexes to control their function. Current work is establishing an important role for higher order macromolecular RK complexes which play important roles in governing RK signalling (discussed in Chapter 1). However, this seems unlikely as the receptor complexes are biochemically very diverse.

Many RKs have to be tightly regulated to ensure homeostasis and prevent cell death (He *et al.*, 2007; Kemmerling *et al.*, 2007; Gao *et al.*, 2009; Domínguez-Ferreras *et al.*, 2015). The absence of MIK2 at the plasma membrane could alter the availability or interactivity of MIK2-associated proteins, which are themselves responsible for the phenotype. This remains a hypothesis.

Moreover, many of the genes differentially expressed in *mik2-1* encode proteins involved in biotic and oxidative stress responses, suggesting that some of the these differentially-expressed genes are responsible for the phenotypes observed and merit further investigation. However, this does not explain how this differential steady-state transcriptome arose in *mik2.*

4.4.2 Cell wall integrity sensing

The important role of *MIK2* in controlling the responses to cellulose biosynthesis inhibition have been confirmed (Engelsdorf *et al.*, 2018). Counterintuitively, Engelsdorf *et al.* (2018) found that PEPR signalling negatively regulates responses to cellulose biosynthesis inhibition. Potentially the enhanced ROS response to Pep in *mik2* could be linked to impaired cell wall integrity sensing in *mik2*. It would be interesting to see the response to cellulose biosynthesis inhibition in a *mik2-1 pepr1 pepr2* mutant to see whether it resembles either *mik2-1* or *pepr1 pepr2* which have impaired or enhanced responses, respectively.

The most parsimonious hypothesis would be that MIK2 acts as a positive regulator by recognising a phytocytokine that is released during cellulose biosynthesis inhibition, thus

amplifying the response. However, we cannot exclude the possibility that the impaired cell wall integrity sensing is a pleiotropic effect due to the absence of MIK2.

4.4.3 Root skewing

Whilst there is well documented natural variation in root skewing, little is known about the underlying mechanistic basis (Vaughn and Masson, 2011; Toal *et al.*, 2018). Root skewing is a complex trait, considerably influenced by the environment, phytohormones, stress, and the precise chemistry of the growth substrate (Buer *et al.*, 2000; Qi and Zheng, 2013; Yang *et al.*, 2015; Schultz *et al.*, 2017; Swarbreck *et al.*, 2019). Many well-described skewing mutants are defective in the alignment of cortical microtubules, and subsequently cellulose fibril co-alignment, resulting in helical growth. Helical growth combined with thigmotropic interactions with the solid media is believed to result in deviation in root growth angle from the vertical (Rutherford and Masson, 1996). However, microtubule alignment was indistinguishable in *mik2-1* vs Col-0 (Van der Does *et al.*, 2017), suggesting another mechanism underlies the root skewing phenotype. There is a link between salt stress, Na^+/K^+ balance and root skewing, but again there is no clear mechanistic understanding (Shoji *et al.*, 2006; Schultz *et al.*, 2017).

The RK FERONIA also has a role regulating root skewing, however, *fer* mutants skew to the right, and the mechanistic basis of this is still unclear (Shih *et al.*, 2014).

Going forward, it would be interesting to test whether *mik2-1 rbohd* mutants also have a root skewing phenotype or whether root skewing is dependent upon the elevated background ROS.

4.4.4 *Fusarium* resistance

Initially we hypothesised that the enhanced susceptibility to *Fusarium oxysporum* was because of the impaired cell wall integrity perception. However, the recent finding of Coleman *et al.* (2019) implies that MIK2 is required for the perception of a *Fusarium*-derived elicitor or potentially for the perception of an endogenous ligand released upon treatment with the *Fusarium* extract (Discussed further in Chapter 6). This could explain why other necrotrophic pathogens such as *Pc*BMM do not have a *mik2* phenotype. It is interesting that susceptibility phenotypes were not observed with any of the other pathogens tested given the perturbed response to multiple elicitors in *mik2* (Humphry *et al.*, 2010; Van der Does *et al.*, 2017). Multiple explanations for this discrepancy exist; it may be due to the balance between hypo- and hyper-sensitivity to different elicitors. However, no difference in flg22-induced resistance was observed (Fig 4.08 C). It is also possible that as the difference in elicitor responses appears to be ROS specific, as RBOHD-derived ROS does not play a significant role in all pathosystems (Morales *et al.*, 2016). Another explanation is that the constitutive expression

of defence genes or ROS accumulation in *mik2* may mask any enhanced susceptibility in *mik2*. Finally, it may simply be that MIK2 plays an important role in resistance to root, but not foliar pathogens. Discriminating among these possibilities is another avenue for future work in this project.

4.4.5 MIK2 differently regulates ROS production in response to diverse elicitors

The dichotomy revealed in elicitor-induced ROS is intriguing. Taking flg22 and Pep as illustrative examples, their signalling pathways to activate RBOHD are thought to be highly conserved (Couto and Zipfel, 2016; Saijo *et al.*, 2018). Both form ligand-induced PRR-BAK1 complexes, both induce the phosphorylation and activation of the cytoplasmic kinase BIK1, the same BIK1-depdendent phosphosites are required for RBOHD activation, and both induce cytoplasmic calcium influx (Lu *et al.*, 2010; Liu *et al.*, 2013*a*; Sun *et al.*, 2013*b*; Kadota *et al.*, 2014; Tang *et al.*, 2015). There have been some suggestions of differential requirements for intracellular calcium store between FLS2 and PEPR signalling (Ma *et al.*, 2017*b*). This highlights the possibility that the calcium-dependent regulation of RBOHD is differentially affected in *mik2.* In the future it would be important to test the calcium responses in *mik2* as assayed by Coleman *et al.* (2019). There is also the possibility that other mechanisms of RBOHD regulation could differentially effect Pep- and flg22- induced ROS production, including SIK1, CRK2- or PBL13-mediated phosphorylation (Lin *et al.*, 2015; Zhang *et al.*, 2018*a*; Kimura *et al.*, 2019). The role of SIK1, CRK2 and PBL13 in Pep-induced responses has not been reported. It is possible that the same mechanism is responsible for the differential elicitor-induced ROS and the background ROS. Levels of RBOHD in *mik2* and Col-0 are comparable implying that difference is caused by post-translational regulation (Fig 4.09 b). However, we cannot exclude the possibility that constitutive RBOHD-dependent ROS production levels are equivalent between *mik2* and Col-0 and there is impaired sequestration/detoxification of ROS in *mik2.*

Very few genetic components have been described that differentially regulate responses to elicitors. Interestingly, it has recently been reported that BIK1 whilst positively regulating RK-PRR signalling, negatively regulates RLP-PRR signalling, which is probably mediated by differential preference for RLCKs (Wan *et al.*, 2019). I saw the same trend of reduced flg22-induced ROS in *mik2* in response to both flg22 and nlp20 (Fig 4.7 a; Fig 4.10 b,e). Moreover, jasmonic acid perception is required for Pep1-induced ROS production, but not for flg22 or elf18-induced ROS production, however, this difference could be mediated by the expression levels of PEPR1, moreover, there was no reported difference in jasmonic acid levels in *mik2* (Van der Does *et al.*, 2017; Holmes *et al.*, 2018). However, no known dichotomy based on

receptor/ligand phylogeny, biochemistry, function or downstream signalling correlates with the differential responses seen in *mik2.*

4.4.6 Why are the differential phenotypes ROS specific?

It is of note that differential elicitor-induced phenotypes seen in *mik2* seem to be ROS specific. It may be that the constitutive ROS observed in *mik2* is relevant to this phenotype. This could 'prime' some weaker responses, such as those induced by cellobiose, whilst having the opposite effect on stronger responses that may saturate RBOHD activity in Col-0. On the other hand, it is possible that the effect of *mik2* is not specific to elicitor-induced ROS production, but rather that ROS is the only phenotype where the quantitative difference is in the dynamic range of the assay. Some of the assays many not have been sensitive enough to detect quantitative differences.

It would also be interesting to quantify PTI phenotypes that are RBOHD-dependent such as elicitor-induced plasmodesmal and stomatal closure (Mersmann *et al.*, 2010; Macho *et al.*, 2012; Cheval *et al.*, 2019). However, resistance to *Pst* DC3000 *COR*$^{-}$ was not impaired in *mik2* upon spray infection, which suggests that stomatal immunity is not impaired (Chapter 3). Whilst never tested, one can hypothesise that PTI-induced lignification is RBOHD-dependent (Chezem *et al.*, 2017). Going forward it could be illuminating to test whether flg22- and Pep-induced lignification is differentially affected in *mik2*. This could mirror the impaired cellulose biosynthesis inhibition-induced lignification in *mik2* (Fig 4.02 c)

4.4.7 Transcriptomic changes

The transcriptomic perturbations in *mik2* suggest a form of autoimmunity due to the steady-state upregulation of biotic stress responsive genes. It would be interesting to investigate whether some of the genes differentially regulated in *mik2* are responsible for the phenotypes observed; especially, as many of them are located in the apoplast or plasma membrane, including many RKs and RLPs (Fig 4.25 a-b). Indeed, it is important to consider that the effects seen in *mik2* may be pleiotropic effects due to autoimmunity. Many genes have previously been incorrectly characterised as negative regulators of immunity due to autoimmunity caused by guarding (Rodriguez *et al.*, 2016).

The transcriptome is reminiscent of *bak1 bkk1*-silenced plants (de Oliveira et al., 2016) (Fig 4.25 c). De Oliveira et al. (2016) propose that the upregulation of *CRK*s is responsible for the autoimmunity in *bak1 bkk1*. Many of the same *CRK*s are upregulated in *mik2* (Fig 4.25 d). Potentially there is an additive effect in the *mik2 bak1* double mutant (although not as strong as in *bak1 bkk1*) which results in the dwarf phenotype. Endoplasmic reticulum glycosylation pathways supress *bak1 bkk1* cell death (de Oliveira et al., 2016); it would thus be interesting to test whether *mik2* phenotypes are also dependent upon these.

Although the upregulation of *WRKY30* in *mik2* is not RBOHD-dependent, it would be interesting to know what the global effect on the *mik2* transcriptome would be if elevated background ROS was abolished. This would advance the goal of deciphering the hierarchy between the transcriptional changes and elevated basal ROS, in *mik2* mutants.

4.4.8 Involvement of the MDIS/MIK complex

Under the conditions used, I have found no evidence that other components of published LURE peptide receptor complex, MDIS1/2 and MIK1 (also known as PXL2), are genetically implicated in the *mik2* phenotypes studied here. It may be that there are other genetically related receptors that are fulfilling the role of MDIS1/2 and MIK1 in the tissues studied. Additionally, MIK2 may be a constituent of different receptor complexes in the different tissues and physiological contexts.

Nevertheless, due to the publication of an alternative receptor, PRK6, supported by an independent study and structural data (Takeuchi and Higashiyama, 2016; Zhang *et al.*, 2017; Zhong *et al.*, 2019), it is possible that the MDIS-MIK complex is not part of the LURE receptor. Moreover, it is highly surprising that two LRR-RKs which are phylogenetically distantly related, MIK1/PXL2 and MIK2, can play a partially redundant role within the receptor complex. Recent structural data has also identified CLE42 as a ligand for MIK1/PXL2 (Mou *et al.*, 2017), which is consistent with the ligands of closely related receptors.

In conclusion, genetically, *MIK2* is a key regulator of many environmental responses. However, it is also required to maintain ROS and transcriptional homeostasis. Further work is required to gain insight into the mechanistic basis of these phenotypes and the relationship between them. It remains to be seen whether they arise due to loss of an undiscovered MIK2-ligand signalling pathway or whether MIK2 is ‘guarded’ and its absence results in autoimmunity, which may itself generate the *mik2* phenotypes. Either or both explanations could explain the *mik2* phenotypes.

Chapter 5

The JRPs represent a novel family of phytocytokine-like peptides

5.1 Abstract

Plants employ small apoplastic peptides, known as phytocytokines, to potentiate and modulate immune signalling through cell-surface localised receptor complexes. These peptides have been shown to both positively and negatively regulate plant immunity, analogous to metazoan pro- and anti-inflammatory cytokines. Plant genomes encode hundreds of short open reading frames with the potential to function as phytocytokines, yet relatively few have a described function. Here I report the identification of a novel family of endogenous peptides, tentatively named JRPs. These peptides are transcriptionally induced by biotic and oxidative stress. Sequence similarity suggests that JRPs are present in both *Asterid* and *Rosid* lineages. Notably, exogenous JRP4 application results in BAK1-dependent but SOBIR1-independent immune outputs, indicating that JRPs are perceived by an LRR-RK. Taken together these data suggest that JRPs represent a conserved family of signalling peptide with phytocytokine properties.

5.2 Introduction

I will use this opportunity to provide a summary of current knowledge and paradigms in damage-associated molecular pattern signalling in plants followed by a concise introduction to the research questions addressed.

5.2.1 'Self versus non-self' to the 'danger hypothesis' – the involvement of self in immune signalling

Plants employ a sophisticated, multi-layered innate immune system to guard against microbial invasion (Jones and Dangl, 2006; Cook *et al.*, 2015). The ability to recognise a threat is key to mounting a successful immune response. In the mid twentieth century the concept of 'self versus non-self' discrimination first arose in metazoan systems and over the following fifty years was refined into the 'stranger model' (Burnet, 1941; Janeway, 1992; Medzhitov and Janeway, 2002). This stated that microbial-derived molecules (foreign, non-self) could act as immunogenic triggers, whilst host-derived molecules could be tolerated by the immune system. The term pathogen-associated molecular pattern (PAMP) was coined to refer to the

non-self molecules that were recognised by the immune system (Medzhitov and Janeway, 1997).

However, this model failed to consider that self-derived molecules can also elicit similar immune responses, but in the absence of foreign elicitors. This lead Matzinger (1994, 2002) to propose the 'danger model', which proposes that the immune system has evolved to recognise molecules indicative of danger, independent of their origin. Self-derived immunostimulatory molecules are known as damage-associated molecular patterns (DAMPs). Many DAMPs are recognised by the same classes of cell surface receptors as PAMPs, and signal through conserved pathways (Saijo *et al.*, 2018). This suggests that the immune system has evolved to recognise both DAMPs and PAMPs as 'danger' signals.

Intuitively, many DAMPs are passively released during stress, wounding and infection through physical and/or chemical damage; the action of pathogen derived hydrolyses; or cell death-induced release (Gust *et al.*, 2017). In the context of the plant cell wall, these include oligogalacturonides and cellobiose derived from cell wall polymers (Ferrari *et al.*, 2013; Souza *et al.*, 2017). However, the abundance of cytoplasmic molecules in the apoplast also indicates tissue disruption. These include, but are not limited to eATP, eNAD(P), HMGB3 and glutamate (Zhang and Mou, 2009; Chivasa *et al.*, 2009; Choi *et al.*, 2014, 2016; Wang *et al.*, 2017*b*; Toyota *et al.*, 2018). Collectively, these are known as primary DAMPs.

A second class of proteinaceous DAMPs, recently termed phytocytokines, are actively synthesised, processed, and/or released upon wounding or danger perception (Luo, 2012; Gust *et al.*, 2017). They act as a feedback mechanism to modulate immune signalling through cell surface-localised receptor kinases (Segonzac and Monaghan, 2019).

5.2.2 Modulation of plant immunity by phytocytokines

Amplification of immune signalling thorough positive feedback

Tomato SYSTEMIN was the first signalling peptide to be identified in plants, representing a watershed moment in plant signalling research (Pearce *et al.*, 1991; Ryan and Pearce, 1998). SYSTEMIN is synthesised as 200-amino acid precursor, PROSYTEMIN, which is then proteolytically processed to release the biologically active 18-amino acid epitope SYSTEMIN (McGurl and Ryan, 1992). SYSTEMIN has been proposed to act as a mobile signal to elicit paracrine signalling in response to herbivore attack and thus amplify and transduce the herbivory signal (Ryan and Pearce, 1998). Despite its early identification, its receptor, the leucine-rich repeat receptor kinase (LRR-RK) SYR1 (SYSTEMIN RECEPTOR1), has only recently been cloned (Wang *et al.*, 2018*a*).

Many, but not all, characterised phytocytokines consist of a ~20 amino acid mature peptide released from longer precursor proteins (known as proproteins; or preproproteins if they also

contain an amino-terminal signal peptide). They are usually part of protein families, which in certain cases redundantly bind the same receptor complex (Matsubayashi, 2014; Segonzac and Monaghan, 2019). They are rich in serine, proline and glycine residues, similar to their growth-related counterparts (Hou *et al.*, 2019). Generally they are transcriptionally induced during immune signalling (Hou *et al.*, 2019; Segonzac and Monaghan, 2019).

The archetypal phytocytokines are PLANT ELICITOR PEPTIDES (Peps) (Bartels and Boller, 2015). Peps are derived from the carboxyl ~20-amino acids of approximately 100-amino acid Propep proteins. *Arabidopsis thaliana* (*Arabidopsis* hereafter unless stated) contains 8 paralogous Peps that exhibit diverse expression patterns, with 3 of them being strongly induced by biotic and wounding stress (Bartels *et al.*, 2013). However, exogenous application of any Peps induces immune signalling, promoting resistance to a broad range of bacterial, oomycete and fungal pathogens, as well as herbivores (Huffaker *et al.*, 2006; Yamaguchi *et al.*, 2010; Flury *et al.*, 2013; Liu *et al.*, 2013*a*). Pep1-8 can all be perceived by PEP RECEPTOR1 (PEPR1) in Col-0, with PEPR2 also contributing to the recognition of Pep1/2 (Yamaguchi *et al.*, 2006, 2010; Krol *et al.*, 2010; Tang *et al.*, 2015). Propeps, like PROSYSTEMIN, lack a canonical signal peptide and were thought to be released from the cell upon wounding. Propep1 associates with the tonoplast membrane and is cleaved by METACASPASE4, enabling its release in damaged cells (Hander *et al.*, 2019; Shen *et al.*, 2019). METACASPASE4 is activated by the prolonged elevation of calcium levels in damaged cells. Nevertheless, total disruption may not be required because Pep3 release into the apoplast can be promoted by treatment with isoxaben (a cellulose biosynthesis inhibitor) and Pep2, potentially suggesting a feedforward loop in Pep signalling (Yamada *et al.*, 2016*b*; Engelsdorf *et al.*, 2018).

In terms of their perception, Peps act as molecular glue to induce heterodimerisation between PEPR1/2 and SERK (SOMATIC EMBRYOGENESIS RECEPTOR KINASE) co-receptors, and signal through a shared pathway with PAMP receptors FLS2 (FLAGELLIN SENSING 2) and EFR (ELONGATION FACTOR TU RECEPTOR) (Schulze *et al.*, 2010; Roux *et al.*, 2011; Liu *et al.*, 2013*a*; Tang *et al.*, 2015; Couto and Zipfel, 2016). Intriguingly, some Peps also have C-terminal extensions, which block receptor complex formation *in vitro*, where they act as competitive inhibitors (Tang *et al.*, 2015); however, the biological relevance of this has yet to be demonstrated.

Pep3 induces salt stress tolerance, and the loss of the PEPR1 receptor results in a significant decrease in salinity tolerance (Nakaminami *et al.*, 2018). The shared role in biotic and abiotic stress tolerance contributes to the idea of danger perception, rather than specificity to biotic stress. The function of Peps as positive regulators of innate immunity is conserved across angiosperms; for example, *Zm*Pep1 (an ortholog in maize) is able to induce resistance to the

fungal pathogens *Cochliobolus heterostrophus* and *Colletotrichum graminicola* (Huffaker *et al.*, 2011; Lori *et al.*, 2015).

In a similar manner, two additional families of peptides that amplify immunity have recently been identified: PAMP-INDUCED PEPTIDES (PIPs) and SERINE-RICH ENDOGENOUS PEPTIDES (SCOOPs), which contain 11 and 14 members, respectively, in the Col-0 genome (Hou *et al.*, 2014; Vie *et al.*, 2015*b*; Gully *et al.*, 2019). Unlike SYSTEMIN and Peps, SCOOPs and PIPs both have canonical signal peptides. Both PIPs and SCOOPs induce pattern-triggered immune (PTI) responses and enhance resistance to bacterial and fungal pathogens (Hou *et al.*, 2014; Gully *et al.*, 2019). PIP1 has been shown to amplify flg22-induced defences (Hou *et al.*, 2014; Olsson *et al.*, 2019*b*). In both peptide families, the active epitope is encoded towards the C-terminal of the preproprotein. Whilst homologs of PIP1 can be found in many monocot and eudicot genomes (Hou *et al.*, 2014), the SCOOP family seems to be *Brassicaceae* specific (Gully *et al.*, 2019). PIP1 is perceived by the receptor RLK7 from the LRR-RK subfamily XI; however, the receptor for the SCOOP peptides awaits characterisation (Chapter 6). Nevertheless, both are BAK1-dependent (BRASSINOSTROID INSENSITIVE1-ASSOCIATED RECEPTOR KINASE 1/SERK3), a co-receptor for many LRR-RKs (Hou *et al.*, 2014; Gully *et al.*, 2019).

In addition to signalling peptides, many antimicrobial peptides are produced during biotic stress and wounding (Campos *et al.*, 2018). The best known of which belong to the conserved CYSTEINE-RICH SECRETORY PROTEIN, ANTIGEN 5, AND PATHOGENESIS-RELATED-1 (CAP) superfamily. These have long been used as markers of immunity and sequester sterols to inhibit microbial growth (Gamir *et al.*, 2017). In addition to restricting pathogen growth, the 11-amino acid C-terminus of the PR1 protein was shown to accumulate in tomato in response to wounding and methyl jasmonate treatment (Chen *et al.*, 2014*a*). This peptide known as CAPE1 was shown to activate PTI-like responses through a yet unknown receptor (Chien *et al.*, 2015). This provides an interesting example of a peptide fulfilling a duel role of direct antimicrobial activity and immune amplification.

Some phytocytokines appear to induce distinctive responses, such as *ZEA MAYS* IMMUNE SIGNALLING PEPTIDE 1 (ZIP1), which surprisingly is unable to induce ROS production or MAPK phosphorylation (Ziemann *et al.*, 2018). However, it can induce salicylic acid accumulation and subsequent papain-like cysteine protease activity, which cleaves the precursor PROZIP1 leading to the release of active ZIP1, creating a positive feedback loop.

Modulation of immune signalling through phytocytokines

Rapid alkalinisation factors

RAPID ALKALINISATION FACTOR (RALF) peptides are best characterised for their roles in apoplastic alkalinisation, reproduction and growth regulation through *CATHARANTHUS ROSEUS* RECEPTOR KINASE 1-LIKE receptors (Murphy and De Smet, 2014). A mutation in the RALF-processing protease, S1P, results in PAMP hypersensitivity (Stegmann *et al.*, 2017). PAMP treatment resulted in the rapid cleavage and apoplastic release of RALF23. RALF23 was then able to inhibit PRR-dependent responses by impairing PRR-BAK1 complex formation. It does this through binding to FER, which in the absence of RALF23 acts as a scaffold to promote PRR-BAK1 complex formation. Conversely, the majority of RALF peptides lack the S1P cleavage site, including RALF17. RALF17 induces immune signalling in a FER-dependent manner. Thus, one clade of peptides has antagonistic roles in immune signalling, similar to what is seen with EPIDERMAL PATTERNING FACTORS in stomatal spacing (Zoulias *et al.*, 2018).

Sulfated peptides in the modulation of immune signalling

PHYTOSULFOKINES (PSKs) are a family of sulfated pentapeptides that promote cell expansion and growth through the LRR-RKs PSKR1/2 and the SERK co-receptors (Matsubayashi and Sakagami, 1996; Matsubayashi *et al.*, 2002, 2006; Stührwohldt *et al.*, 2011). Surprisingly, given their role in growth promotion, PSK expression is upregulated during immune signalling where they appear to play a role in negative cross talk with PRR-triggered responses (Igarashi *et al.*, 2012). The exact mechanism is unclear, but involves the negative regulation of salicylic acid signalling, either through enhancement of jasmonate or auxin signalling (Igarashi *et al.*, 2012; Mosher *et al.*, 2013; Mosher and Kemmerling, 2013). This can have inverse outcomes in pathology with PSK signalling impairing necrotophic, or promoting biotrophic pathogen growth respectively (Mosher *et al.*, 2013).

Another sulfated peptide, PLANT PEPTIDE CONTAINING SULFATED TYROSINE 1 (PSY1) has been shown to have overlapping functions with PSKs (Amano *et al.*, 2007; Mosher *et al.*, 2013; Mosher and Kemmerling, 2013). Recently the biotrophic pathogen *Xanthomonas oryzae* pv. *oryzae* has been shown to produce a quasi-identical mimic of PSY1 as a virulence factor to supress immunity (Pruitt *et al.*, 2017; Luu *et al.*, 2019). In the host-pathogen co-evolutionary arms race, rice has evolved a receptor which is able to differentiate this peptide, RaxX21, from the endogenous PSY1, to elicit immune responses (Song *et al.*, 1995; Pruitt *et al.*, 2015; Luu *et al.*, 2019).

IDA-like peptides

The INFLORESCENCE DEFICIENT IN ABSCISSION (IDA) peptide promotes floral organ abscission through a pair of homologous LRR-RKs HAESA/HSL2 (Jinn *et al.*, 2000; Butenko *et al.*, 2003; Stenvik *et al.*, 2008; Santiago *et al.*, 2016). In addition, peptides from the IDA family have been implicated in cell separation during lateral root emergence and root cap sloughing (Kumpf *et al.*, 2013; Shi *et al.*, 2018). There are 7 paralogs of IDA in *Arabidopsis* and two of these, IDL6 and IDL7, are strongly upregulated by biotic elicitors (Vie *et al.*, 2015*b*, 2017; Wang *et al.*, 2017*a*). Co-treatment with IDL7 impaired flg22-induced ROS production and supressed defence gene expression (Vie *et al.*, 2017) whilst IDL6 promoted pectin degradation and susceptibility to *Pseudomonas syringae* (Wang *et al.*, 2017*a*). Whilst initially paradoxical, *Pseudomonas syringae* has been shown to trigger HAESA/HSL2-dependent cauline leaf abscission (Patharkar *et al.*, 2017). Potentially the upregulated IDL peptides could be promoting this abscission, which is proposed to be a defence mechanism.

In conclusion, in the context of immunity many propeptides are transcriptionally upregulated to fulfil roles in sustaining and potentiating the danger signal. Whilst many of these exist, it should not be assumed that all upregulated peptides positively regulate immunity. Plants dynamically regulate their autocrine and paracrine signalling network in order to insure proportionate responses to the presence of danger to maximise fecundity. Moreover, these peptides are distributed in a heterogeneous cellular landscape where the presence (or absence) of corresponding cell surface receptors defines the ability to perceive and respond to these stimuli. Teasing apart the relative contributions of these multimeric peptide families will be challenging, especially due to the potential considerable cross-talk between different peptides. This is much better explored in vertebrate immunity where a plethora of both pro- and anti-inflammatory cytokines provide a biological precedent for such a complex, context-dependent network of immunomodulatory stimuli (Lin and Leonard, 2019).

5.2.3 The role of small peptides in *mik2*

Mutants of the LRR-RK *mik2* exhibit constitutively elevated ROS production that is dependent upon the NADPH oxidase RBOHD, and is reduced in the *bak1-5* background (Chapter 4). In addition, *mik2* mutants show differentially perturbed elicitor-induced ROS production. Transcriptomic differences in *mik2* are enriched in upregulated genes that encode apoplastic or plasma membrane proteins, and proteins with roles in biotic stress (Chapter 4). Taken together, these results could indicate constitutive aberrant activation of SERK-dependent RK signalling pathway(s) in *mik2*.

I hypothesised there could be a continual upregulation of a phytocytokine in *mik2*. To investigate this, I identified transcripts of small proteins upregulated in *mik2*. This revealed a number of candidate phytocytokines. Here, I describe the preliminary characterisation of a

family of four peptides (hereafter named JRPs), which appear to function as phytocytokines. JRPs are transcriptionally responsive to a range of biotic elicitors and synthetic JRP4 induces *BAK1*-dependent, SOBIR1-independent, early immune outputs when applied exogenously. Together, my data identifies the JRPs as a novel family of phytocytokine that is perceived in a *BAK1*-dependent manner.

5.3 Results

5.3.1 Multiple genes encoding potential small secreted peptides are upregulated in *mik2*

As an approach to investigate potential aberrant regulation of RK signalling modules in *mik2*, I decided to look for candidate phytocytokines transcriptionally upregulated in *mik2*. All annotated <150-amino acid sequences lacking predicted transmembrane domains were extracted from the Araport11 proteome (Krogh *et al.*, 2001; Cheng *et al.*, 2017). Where corresponding probes were present on the microarray, expression data was gathered for these transcripts in *mik2-1* relative to Col-0. I did not include the requirement for a signal peptide as several characterised phytocytokines, including PROSYSTEMIN and PROPEP lack canonical signal peptides (McGurl and Ryan, 1992; Hander *et al.*, 2019; Almagro Armenteros *et al.*, 2019).

To evaluate the likelihood of these sequences representing novel phytocytokines additional information was gathered on each of the genes:

1/ The localisation of the peptides was predicted using SUBA4.0 (Hooper *et al.*, 2017).

2/ The C-terminal amino acid was identified for each of the sequences. It has been proposed that C-terminal amino acid His/Asn residues are required for peptide binding with the conserved 'RxR' motif in LRR-RK subfamily XI (*e.g.* Pep-PEPRs and IDA-HAESA); however, recent work has questioned the universality of this finding (Song *et al.*, 2016; Okuda *et al.*, 2019).

3/ The number of cysteine residues was calculated to determine if the peptides were likely to for disulphide bridges, important determinants of tertiary structure (Matsubayashi, 2014). Peptides with multiple cysteine residues are known as cysteine-rich peptides.

4/ Transcriptomic response of the genes to NaCl, isoxaben, and flg22 were gathered (Feng *et al.*, 2015; Gigli-Bisceglia *et al.*, 2018).

The 30 genes, meeting these criteria, with the strongest upregulation in *mik2-1* are shown in Table 5.1. This list includes the known phytocytokines PROPEP3, PROPIP1 and IDL6 as well as the antimicrobial peptide ARACIN1 (Neukermans *et al.*, 2015; Bartels and Boller, 2015; Vie *et al.*, 2015*b*). However, the list also includes proteins highly unlikely to be recognised

by cell-surface receptors (*e.g.* AT5G65080/MADS AFFECTING FLOWERING 5 a paralog of FLOWERING LOCUS C (Ratcliffe *et al.*, 2003)). However, some of the candidate phytocytokines merited further investigation. Within the list of candidates, I identified two similar sequences (AT2G31335 and AT1G06135; 47% amino acid identity), which have predicated apoplastic localisation, two cysteine residues, and are short (<70-amino acids).

5.3.2 JRP-like sequences are present in both *Rosid* and *Asterid* lineages

A. thaliana Col-0 contains two additional sequences with similarity to AT2G31335 and AT1G06135. All together, these were named JRP1-4 according to their position within the genome (JRP1/AT1G06135; JRP2/AT1G06137; JRP3/AT2G31335; and JRP4/AT2G31345). JRP3 has a truncated hydrophobic signal peptide (Fig 5.1 A). The JRPs are conserved within *Brassicaceae* with the four *Arabidopsis* proteins representing four clades of JRPs (Fig 5.1 B). Due to the single exon and short length of JRPs, there is an increased risk they will be overlooked during proteome annotations which are optimised to avoid false positives (Zhou *et al.*, 2013). There are no conserved tyrosine residues, suggesting the peptide is not sulfated; however, there are proline residues which could be hydroxylated or arabinosylated (Fig 5.1 a) (Matsubayashi, 2014). JRP4 was used as a reference to identify similar sequences in *Viridiplantae* proteomes. Similar sequences were found across *Pentapetalae* proteomes within proteins in *Asterid* genomes, such as *Solanum tuberosum* and *Daucus carota*, as well as the *Rosids* (which contains *Brassicaceae*) these lineages diverged ~117 million years ago (Fig 5.2) (Kumar *et al.*, 2017). Interestingly, there seems to be a hydrophobic C-terminal extension on many of the proteins which has been lost in *Brassicaceae* (Fig 5.2). The two cysteine residues show 100% conservation in all the sequences (Fig 5.2).

Gene identifier	Fold Change in *mik2*	Signal peptide (signalP 5.0)	Predicted localisation (SUBA4)	Length (a.a.)	Cysteine residues	Induced by ISX (9 h) (Gigli-Bisceglia et al. 2018)	Induction by salt stress (4 h) (Feng *et al.* 2015)	Induction by flg22 (90 min) (Marta Bjornson)	C-terminal amino acid	Description (TAIR)
AT1G58225	31.1	Y	extracellular	143	2	0.0	0.8	5.0	L	
AT1G51915	11.0	Y	extracellular	67	9		6.0	4.6	P	cryptdin protein-related
AT1G51913	10.5	Y	extracellular	77	9	1.1	2.8	5.3	M	cryptdin protein-related
AT5G46770	9.5	N	plasma membrane	133	4			0.4	I	
AT1G51920	7.1	Y	extracellular	78	8	-0.6	1.2	5.7	P	
AT2G31335	**6.4**	**N**	**extracellular**	**60**	**2**			**4.4**	**G**	**JRP3**
AT1G36622	5.8	Y	extracellular	74	0	0.1	2.7	5.4	G	
AT4G14450	5.8	N	plastid	125	1	0.7	11.4	5.5	V	
AT5G55460	5.4	Y	extracellular	109	8		0.7	0.9	N	Lipid-transfer protein
AT3G15534	5.2	N	mitochondrion	68	8	-1.9	18.0	1.7	R	
AT5G52740	5.0	N	cytosol	118	7		0.2	0.9	S	Copper transport protein family
AT4G21840	4.8	N	cytosol	143	6	0.8	12.5	2.8	K	methionine sulfoxide reductase B8
AT5G05300	4.7	Y	extracellular	102	1		3.1	4.2	T	IDA-like 6
AT1G59865	4.6	N	plasma membrane	115	3		0.7	1.3	S	
AT5G04238	4.5	N	cytosol	64	1		0.8	0.9	V	
AT1G06135	**4.5**	**Y**	**extracellular**	**69**	**2**			**1.3**	**G**	**JRP1**
AT5G65080	4.2	N	nucleus	117	0	-0.2	0.8	-0.1	K	MADS-box transcription factor family protein
AT2G03933	4.1	Y	extracellular	75	8				Y	Encodes a defensin-like (DEFL) family protein
AT3G43170	4.1	N	peroxisome	133	3				L	
AT2G30810	3.9	Y	extracellular	106	12				P	Gibberellin-regulated family protein
AT5G55430	3.9	N	nucleus	149	11		2.0	0.0	Y	
AT5G36925	3.8	N	nucleus	76	3	0.0	11.0	6.7	P	ARACIN1
AT1G24145	3.8	Y	extracellular	128	2	0.1	0.5	4.2	H	
AT5G59080	3.7	N	nucleus	135	1	0.0	0.2	-0.1	Y	
AT5G64905	3.6	N	vacuole	96	2	2.3	17.6	6.9	N	elicitor peptide 3 precursor (Propep3)
AT4G28460	3.6	Y	extracellular	72	0		9.9	3.9	H	PROPIP1
AT4G01535	3.5	N	plasma membrane	137	3			3.2	P	
AT1G19610	3.5	Y	extracellular	78	9	0.2	1.9	1.9	C	PDF1.4
AT1G48070	3.5	N	plasma membrane	144	2		0.1	0.0	E	Thioredoxin superfamily protein
AT3G15518	3.4	N	plastid	106	4	1.3	4.2	5.2	V	

Table 5. 1 Thirty most-highly upregulated transcripts in *mik2-1* encoding proteins <150-amino acids in length, without predicted transmembrane domains.

Bold highlights the JRP peptides. Red indicates either predicted extracellular localisation or canonical signal peptide. Magenta represents maximum fold change in expression.

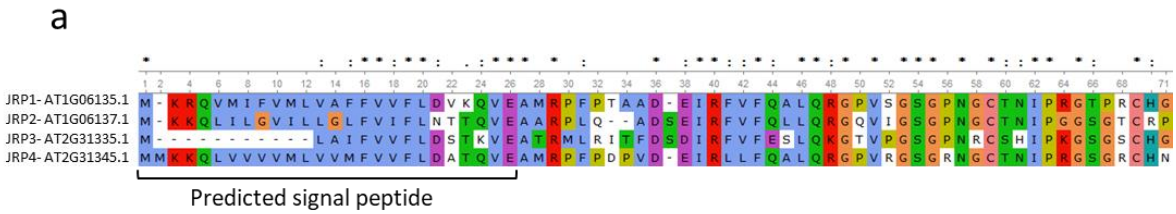

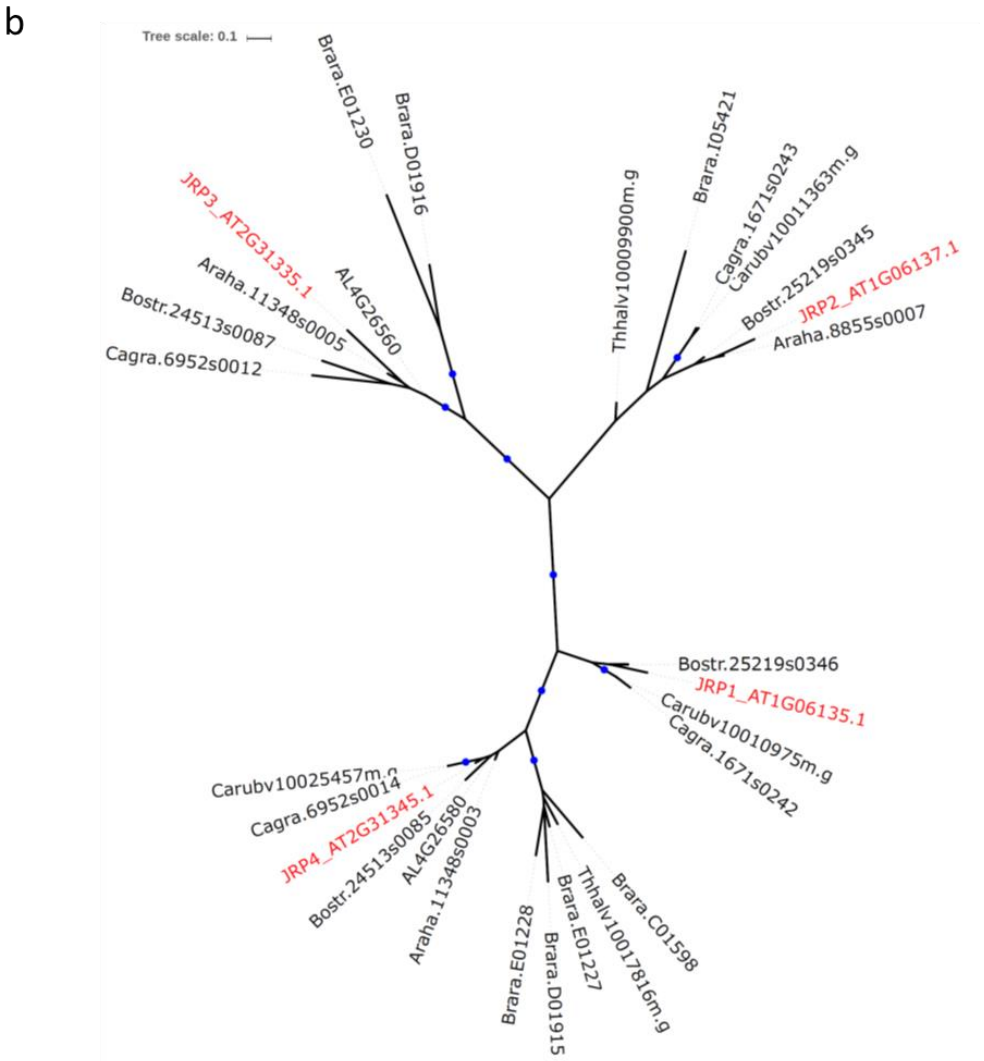

Figure 5. 1 JRP sequences in *Brassicaceae*

(a) Alignment of 4 JRP paralogs in the *Arabidopsis* proteome using MUSCLE. Consensus mode = ClustalW, Colouration = ClustalX (b) Phylogeny of JRPs sequences in the *Brassicaceae* identified using BLAST against the PHYTOZOME12.1.6 proteome database (Comparison matrix: BLOSUM62, E-value threshold < $1e^{-1}$) using JRP4 as the reference sequence. Sequences were aligned using MUSCLE and a tree was generated using PhyML maximum likelihood with LG matrix. Red indicates *Arabidopsis thaliana* proteins. The tree was visualised using iTOL (Letunic and Bork, 2019). Blue dots represent >80% bootstrapping support (100 iterations performed)

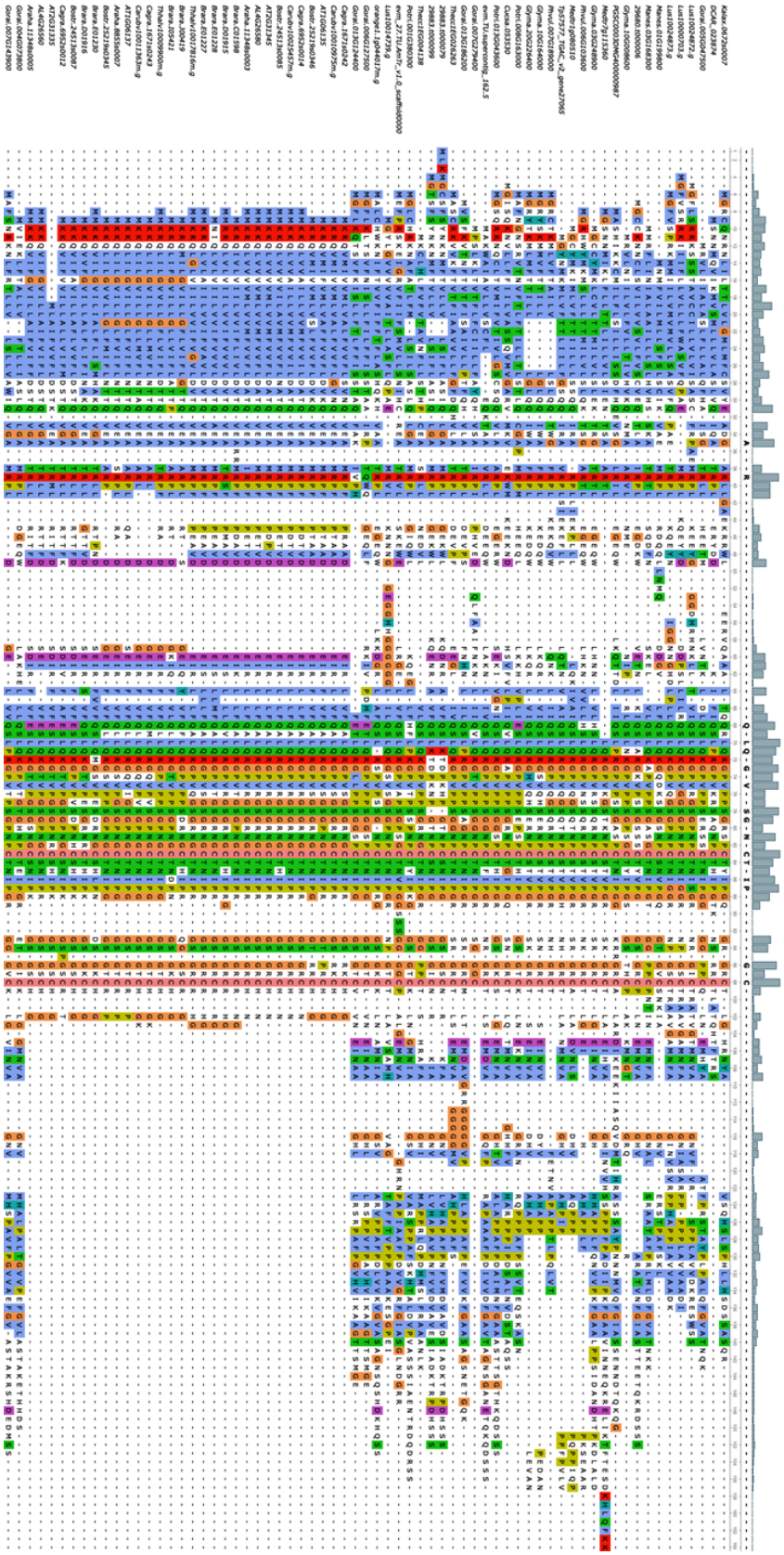

Figure 5. 2 JRP sequences from Viridiplantae

Sequences were identified from the PHYTOZOME12.1.6 proteome database (Comparison matrix: BLOSUM62, E-value threshold < $1e^{-1}$) and were aligned using MUSCLE. Consensus sequence definition was strict 75% conservation. Colouration = ClustalX .

5.3.3 JRPs are transcriptionally upregulated by biotic stress

JRP1, *JRP3* and *JRP4* show transcriptional responsivity to a range of biological elicitors (Fig 5.3 A). *JRP4* shows the strongest induction, whilst elicitor-induced *JRP3* transcript accumulation peaked later. Publicly available RNAseq data shows that *JRP*s are responsive to biotic and oxidative stress, as well as to abscisic acid (Fig 5.3 B). The *JRP*s – especially *JRP1* and *JRP4* – are upregulated during infection with fungal pathogens *Botrytis cinerea* and *Colletotrichum incanum*, but also the endophyte, *C. tofieldiae* (Hiruma *et al.*, 2016). *JRP4* is also upregulated during phosphate starvation, which is interesting as phosphate homeostasis is interconnected with immune signalling (Castrillo *et al.*, 2017). *Pseudomonas* also upregulates *JRPs*, although not to the same extent as flg22. Most of the transcript variability appears to be due to environmental perturbations as the *JRP*s show low expression across anatomical locations (Fig 5.3 C). Due to its strong transcriptional response to elicitors, I selected JRP4 for further characterisation.

5.3.4 Exogenous JRP4 application induces BAK1-dependent, and SOBIR1-independent early immune responses

To further probe the role of JRP4, it was desirable to investigate the effect of exogenous peptide application. The predicted signal peptide was removed and the subsequent C-terminal 43-amino acid sequence was synthesised.

Initially, to determine whether the peptide had biological activity cytoplasmic calcium influx was tested. JRP4 induced a rapid influx of cytoplasmic calcium, comparable to flg22 (Fig 5.4 a-b). To investigate whether JRP4-induced cytoplasmic calcium influx was dependent upon BAK1, calcium influx was measured in *bak1-4*. Loss-of-BAK1 resulted in reduced, temporally delayed cytoplasmic calcium influx in response to JRP4, again consistent with what was observed with flg22 (Fig 5.4 a-b).

To test if JRP4 can also trigger other immune outputs, I characterised JRP4-induced MAPK phosphorylation and ROS production. JRP4 can induce MAPK phosphorylation comparable with nlp20 in Col-0 (Fig 5.4 c) (Böhm *et al.*, 2014). It could also induce transient ROS production characteristic of pattern-triggered immune responses (Fig 5.4 d-e).

SOBIR1 (SUPPRESSOR OF BIR1) is an LRR-RK, which forms a constitutive interaction with LRR- receptor-like proteins (RLPs) and is required for their function (Liebrand *et al.*, 2013, 2014). To investigate whether JRP4 perception is mediated by an LRR-RLP, SOBIR1-dependency was tested. JRP4-induced MAPK phosphorylation and ROS production are comparable between Col-0 and *sorbir1-13*, in contrast to what observed with nlp20 (Fig 5.4 c-e) which is recognised by the RLP23-SOBIR1-BAK1 complex (Albert *et al.*, 2015). This demonstrates SOBIR1-independence, suggesting that JRP4 is not recognised by an LRR-RLP.

The BAK1-dependency described earlier was corroborated by the abolition of JRP4-induced ROS production in *bak1-5* (Fig 5.4 d-e). However, JRP4 still induced MAPK phosphorylation in *bak1-5*, which is probably due to signalling through other SERKs (Fig 5.4 c). Indeed, phosphorylation of MAPKs can also be seen following nlp20 treatment despite its receptor complex being BAK1-dependent (Schwessinger *et al.*, 2011; Albert *et al.*, 2015).

JRP4 can induce weak but significant seedling growth inhibition (Fig 5.4 f) showing it is able to induce long-term as well as rapid immune responses.

Taken together these results suggest that JRP4 is a biologically active peptide, recognised via an LRR-RK and capable of inducing SERK-dependent outputs indicative of PTI when applied exogenously.

5.3.5 JRP4-induced ROS production is reduced in *mik2*

Returning to the initial hypothesis, I wanted to test whether JRP4-induced ROS was affected in the *mik2* mutant. JRP4-induced ROS was reduced in all *mik2* alleles tested in both the Col-0 and Ws-2 backgrounds. Notably the ROS response was much stronger in the Ws-2 ecotype, relative to Col-0 (Fig 5.5 a-d). The striking decrease in JRP4-induced ROS in *mik2* lead me to test whether *mik2* mutants were still responsive to JRP4. MAPK phosphorylation was comparable in Col-0, *mik2-1*, and *mik2-2* (Fig 5.5 e). This suggests that *mik2* mutants are still able to respond to JRP4. Thus, while MIK2 seems to be involved for JRP4-induced ROS production, it is unlikely to be the JRP4 receptor.

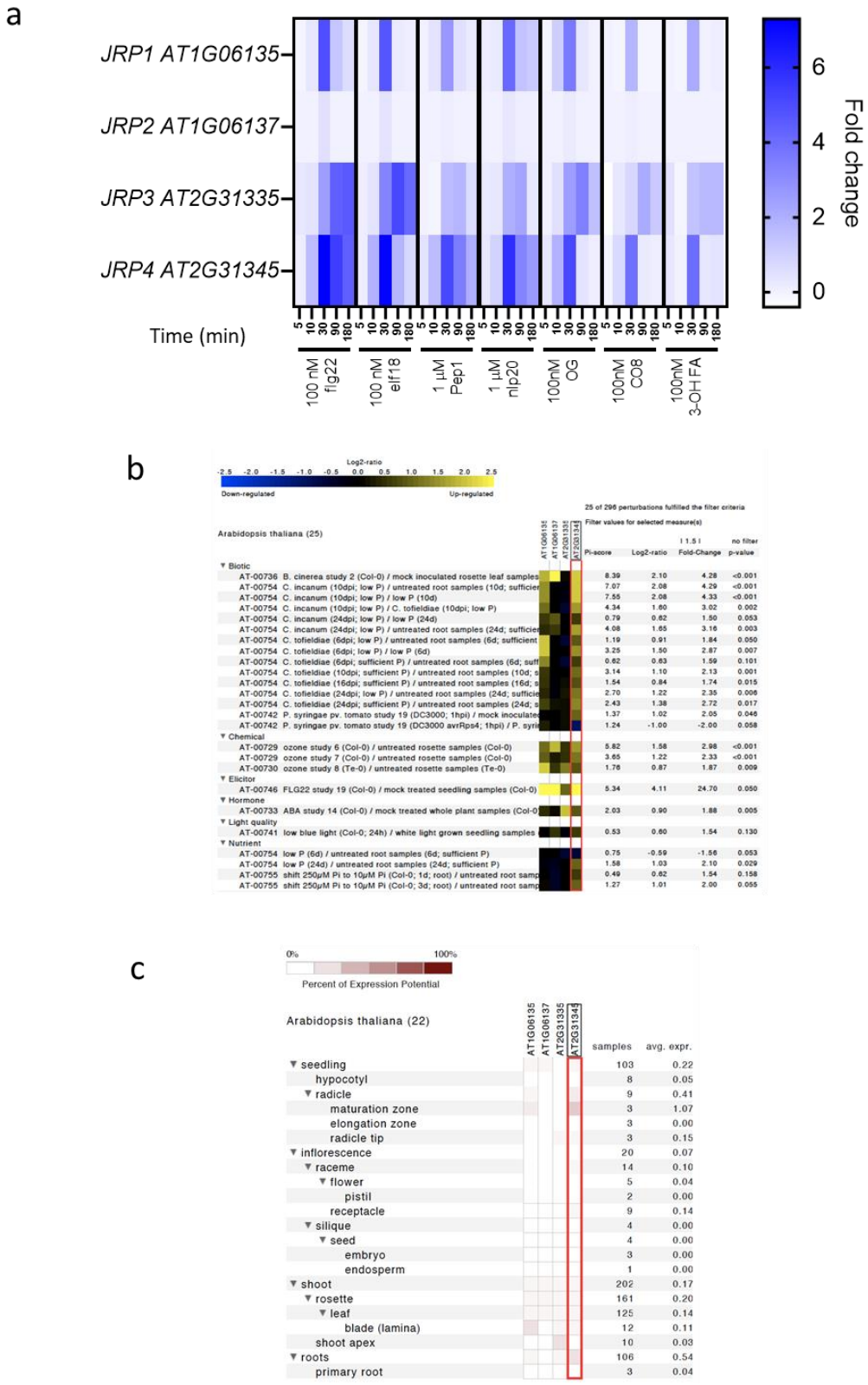

Figure 5. 3 Expression of *JRPs* in *Arabidopsis*

(a) Transcriptional response of *Arabidopsis JRP*s to a range of biotic elicitors in whole seedlings over a time course (5 to 180 min) relative to 0 min. Ch8 = 1 µM chitooctaose, elf18 = 1 µM elf18, flg22 = 1 µM flg22, 3-OH FA = 1 µM 3-hydroxydecanoic acid, nlp20 = 1 µM nlp20, OG =100µg/mL oligogalacturonides d.p. 14-16 , Pep1 = 1 µM Pep1. (Data from M. Bjornson). (b) Treatments under which *JRP4* shows >|1.5| fold change in expression. (c) Expression of *Arabidopsis* JRPs based on anatomy. (b-c) taken from Genevestigatgator (Zimmerman *et al.* 2004) **.**

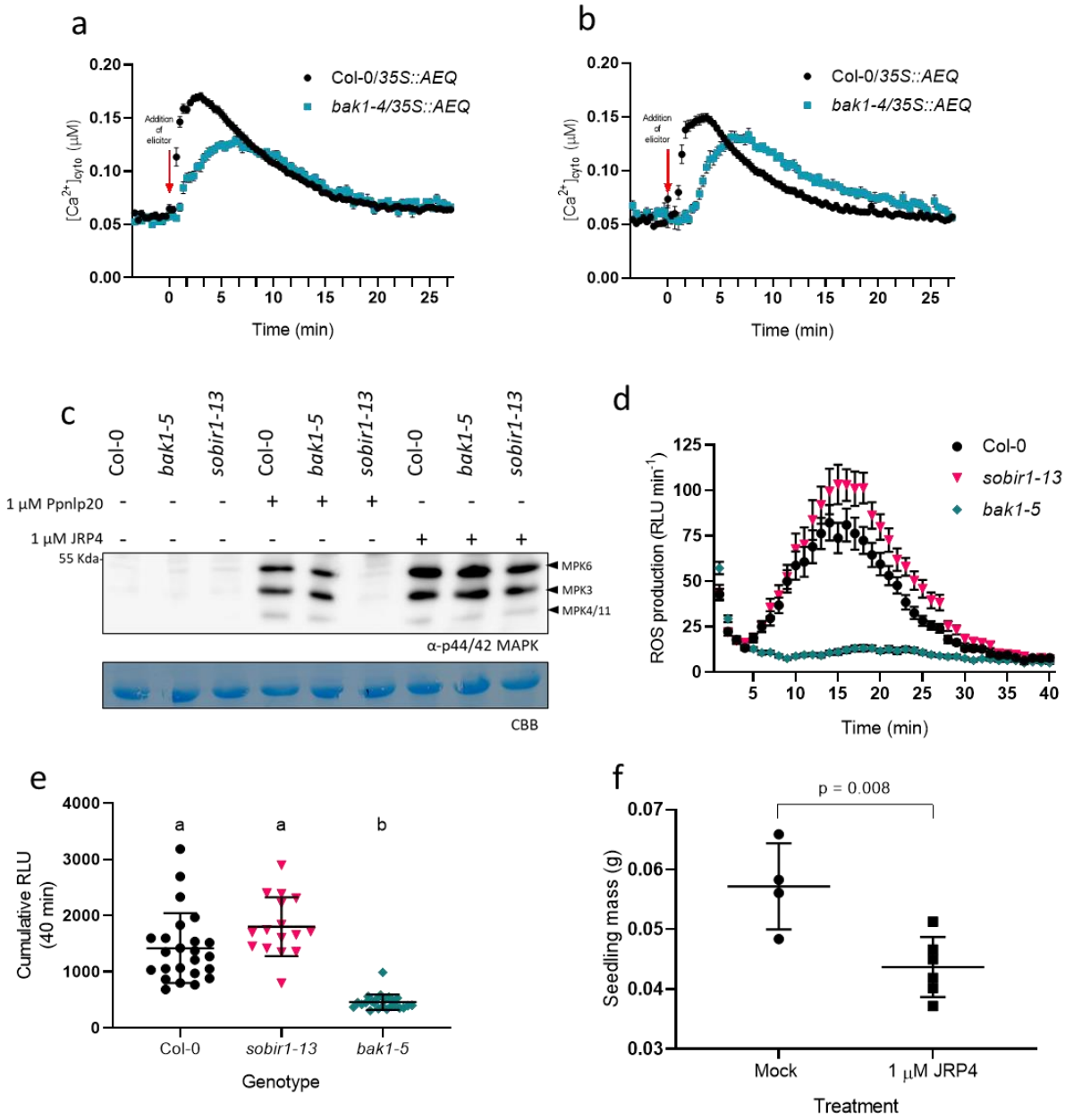

Figure 5. 4 JRP4 can induce PTI-like responses that are BAK1-dependent and SOBIR1-independent

Change in cytoplasmic calcium concentration in response to (a) 1 µM JRP4 or (b) 100 nM flg22 in seven-day-old seedlings. Calcium concentration was calculated using the method developed by Knight *et al.* (1991). (n=8) This experiment was performed once. (c) 1 µM JRP4- or Ppnlp20-induced phosphorylation of MAP kinases in twelve-day-old seedlings. CBB staining was performed as a loading control. This experiment was performed twice. (d) 1 µM JRP4-induced ROS production in leaf disks taken from five-week-old rosettes. (Col-0 n=24; *bak1-5/sobir1-13* n=16) (e) Integration of data from (d), lowercase letters indicate significance groups based on one-way ANOVA followed by Tukey's Post-hoc test. (f) Mass of ten-day-old seedlings grown MS media in the presence or absence of 1 µM JRP4. p-value derived from a t-test. (This experiment was performed once) (a-b,d) Error bars on curves represent S.E.M. (e-f) Bar represent the means, error bars show S.D.

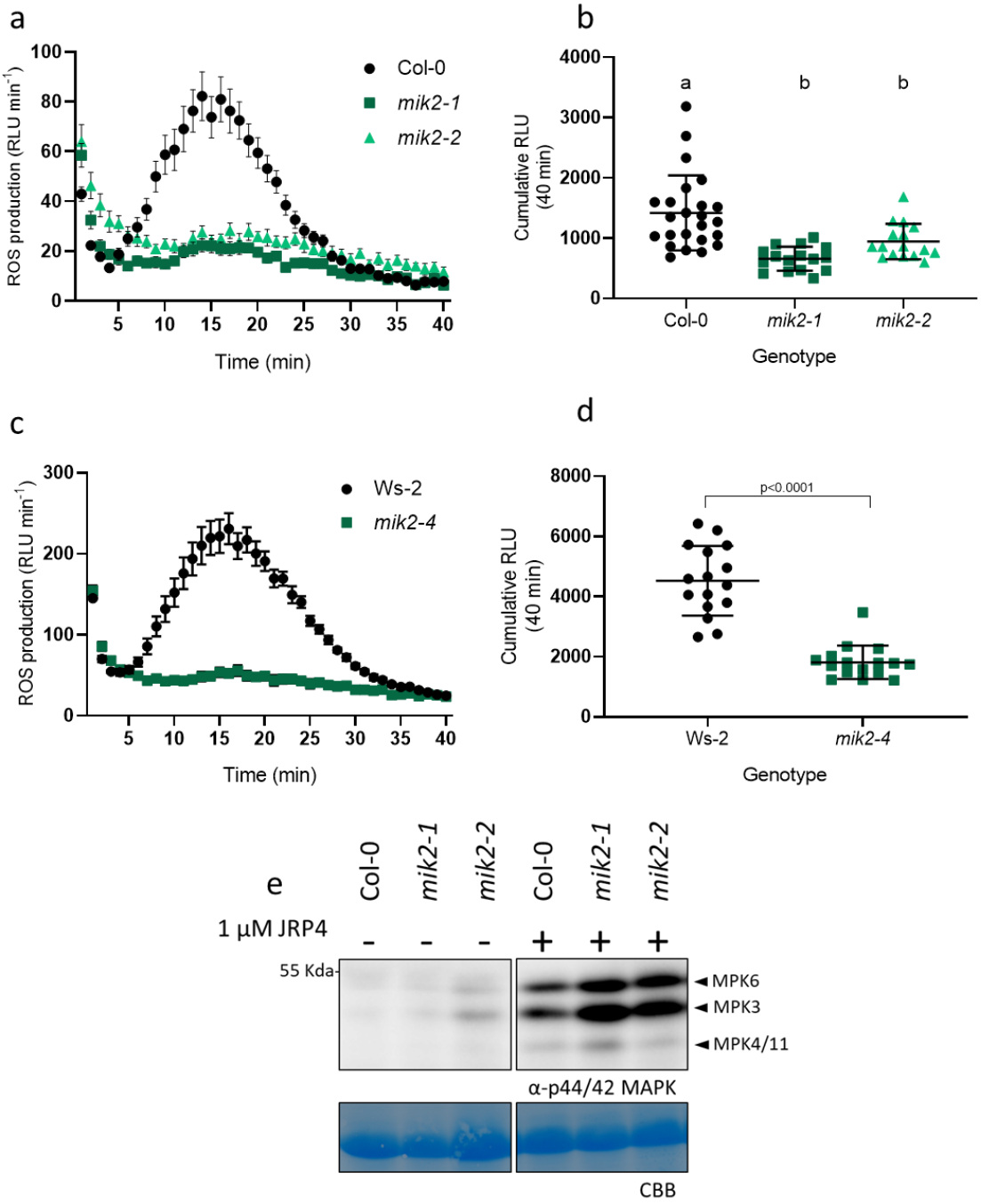

Figure 5. 5 JRP4-induced ROS production, but not MAPK activation, is MIK2-dependent

(a,c) JRP4-induced ROS production from leaf disks taken from five-week-old rosettes. Error bars on curves represent S.E.M. (n≥16). (b,d) Integration of the data from (a,c) respectively. Bars represent the mean, error bars represent S.D., lowercase letters indicate significance groups based on one-way ANOVA followed by Tukey's Post-hoc test, p-value derived from t-test. (e) 1 µM JRP4-induced phosphorylation of MAP kinases in twelve-day-old seedlings. CBB staining was performed as a loading control. The mock and treated samples are on the same membrane and have been separated to remove intervening lanes for reader convenience. This experiment has been repeated twice.

5.4 Discussion

5.4.1 JRPs - a novel family of phytocytokines?

JRPs represent a clade of small, (potentially) secreted peptides that are transcriptionally induced by biotic stress. Exogenous JRP4 application induces early signalling outputs indicative of immunity. Expression data suggest that *JRPs* are primarily responsive to biotic and oxidative stress. Taken together, this suggests that the JRPs may function as phytocytokines (Gust *et al.*, 2017). It remains to be established whether other JRPs can induce similar responses.

MAPK phosphorylation, cytoplasmic calcium influx and ROS production are not unique to immune signalling. Other peptides such, as IDL6, are induced during immune signalling, elicit MAPK phosphorylation, ROS production and cytoplasmic calcium influx, yet negatively regulate immunity (Butenko *et al.*, 2014; Wang *et al.*, 2017*a*; Vie *et al.*, 2017; Olsson *et al.*, 2019*b*). Future work needs to establish whether JRPs are required for, and sufficient to, induce pathogen resistance. Indeed, compared to other elicitors, JRP4-induced seedling growth inhibition and ROS production are relatively weak (Chapter 4). It might be valuable to look at JRP-induced transcriptomic changes to determine whether it resembles those of other elicitors to elucidate its function.

JRPs appear to be evolutionarily conserved. It would be interesting to test whether JRP4 is able to induce responses in distantly related plants such as *Fabaceae* or *Solanaceae*, which would suggest that the perception mechanism is also conserved.

5.4.2 JRP processing and release

The synthetic peptide ordered was the full length, minus the signal peptide. There is no evidence to suggest this is the peptide that is released into the apoplast *in planta*. JRPs may be synthesised as PREPROJRPs. Going forward it would be interesting to create a labelled peptide to study the maturation process. Whilst we can see that JRPs are transcriptionally upregulated in response to biotic elicitors, it would be interesting to see if proteolytic processing or apoplastic secretion was also induced (Yamada *et al.*, 2016*b*; Stegmann *et al.*, 2017; Engelsdorf *et al.*, 2018). This would further support their potential role as phytocytokines. Previous studies have used high sequence conservation to predict to the biologically active minimal motif; however, the JRP amino acid sequence seems conserved throughout. The C-terminal is ‘SGP-rich’ similar to PEP, IDA, CLE, PIP, SCOOP and CEP peptide families (Hou *et al.*, 2014; Gully *et al.*, 2019). This is quite distinct from the more hydrophobic N-terminus of the peptide (Fig 5.1 a). In the future, it would be worth identifying the minimal motif. It is of note that there are two cysteines in the C-terminus with 100% conservation in all *Brassicaceae* JRPs, which may form a disulphide bridge.

In addition, whilst JRPs do not show anatomically distinct expression profiles, it is possible that they are expressed within specific cell types. It may be profitable to characterise JRP promoters to further understand their activity.

5.4.3 The JRP perception mechanism

The BAK1-dependency of JRP4-induced ROS and calcium responses, combined with the SOBIR1-independence, suggests that JRP4 is recognised by a LRR-RK (Liebrand *et al.*, 2014; Hohmann *et al.*, 2017). Several approaches could be used to identify a putative JRP4 receptor – 1/ a forward-genetic screen; 2/ reverse-genetic screening of candidate mutants; or 3/ a biochemical approach.

A forward genetic approach could screen for a loss-of-response to JRP4 in a mutagenized population, for example using cytoplasmic calcium influx as the readout (Ranf *et al.*, 2012; Choi *et al.*, 2014). However, given our current understanding of RK signalling, we could screen a library of candidate LRR-RK T-DNA mutants in order to identify non-responsive lines, which would alleviate the need for mapping. However, genetic redundancy in receptors could hamper both approaches. A biochemical approach could overcome this by using 1/ a labelled peptide *e.g.* Biotin-JRP4 or 2/ pulling down BAK1-GFP +/- JRP4 treatment. This approach could identify candidate receptors to follow up genetically. It must be ensured that the labelled peptide is still active, and the label is not cleaved prior to recognition. Only a small percentage of the total BAK1 pool will be involved in the BAK1-JRP4-RECEPTOR complex formation which may limit the identification of spectral counts from the receptor. Prior to mass spectrometry analysis, the approaches could be cross-validated by co-immunoprecipitating BAK1 with the labelled peptide. Each of the approaches has limitations, which need to be assessed when choosing an approach to follow.

Studying ligand and receptor in parallel would greatly enhance conceptual advances that we could make in understanding JRP function.

5.4.4 Could JRP peptides contribute to *mik2* phenotypes?

Initially, I hypothesised that phytocytokines transcriptionally upregulated in *mik2* could explain some of the *mik2* phenotypes, such as constitutive elevated ROS production and defence gene expression. This led to the identification of a novel protein family with phytocytokine-like properties. However, as the ROS response to JRP4 is reduced in *mik2*, it is perhaps unlikely that JRPs are responsible for the elevated *mik2* background ROS. However, it must be considered that the reduced sensitivity could be due to a continuous low level of signalling leading to ligand-mediated desensitisation (Gully *et al.*, 2015; Smith *et al.*, 2017). It would be interesting to observe the effect of JRP overexpression and determine if this phenocopies *mik2*. Significantly, the reduced JRP4-induced ROS production in *mik2* breaks the endogenous/exogenous elicitor dichotomy that had been observed in Chapter 4,

with *mik2* showing enhanced ROS in response to DAMPs and reduced ROS in response to PAMPs.

5.4.5 Concluding remarks

Together, these results suggest that JRPs represent a novel family of phytocytokines. However, the role of JRPs in plant-microbe interactions remains to be established. Further work is required to elucidate the evolutionarily conservation of JRPs and the mechanisms of their putative processing and apoplastic release. Moreover, to understand JRP signalling it will be important to identify the JRP receptor in the future. Exploring the function of JRPs may help the understand how plants modulate danger signalling and integrate this into the complex network of existing pathways.

Chapter 6

The Arabidopsis SCOOP12 peptide represents a putative ligand for MIK2

6.1 Summary

SCOOP peptides are a novel family of plant phytocytokines, which are transcriptionally induced under biotic stress and contain a peptide motif capable of eliciting immune responses (Gully *et al.*, 2019). Whilst it has been shown that the response to SCOOP12 peptide is BAK1-dependent, the receptor remains elusive. Here I present genetic evidence supporting BAK1-dependency and demonstrating SOBIR1-independency, suggesting that the SCOOP12 receptor is an LRR-RK. Subsequently, I show that all assayed SCOOP12-induced responses are MIK2-dependent, and that expression of MIK2 is sufficient to confer responsivity to SCOOP12 in *Nicotiana benthamiana*. Taken together, these data intimate that MIK2 is the SCOOP12 receptor.

6.2 Introduction

Plants are able to recognise microbial-derived non-self elicitors to stimulate immune responses. In addition, they actively synthesise and release a plethora of small secreted peptides, known as phytocytokines, which act as secondary signals to amplify and enhance immune signalling, and thus act as phytocytokines (Gust *et al.*, 2017). These peptides are often produced as propeptides that undergo proteolytic processing to release bioactive peptides. These peptides are recognised by receptor complexes homologous to those recognising non-self elicitors. Generally, receptor complexes consist of a ligand-binding leucine-rich repeat-type receptor and a SERK co-receptor, with the peptides acting as the molecular glue to induce complex formation. Several families of such peptides have been described including Peps, PIPs and systemin that are recognised by the *At*PEPR1/2, *At*RLK7 and *Sl*SYR, respectively (Pearce *et al.*, 1991; Yamaguchi *et al.*, 2006, 2010; Krol *et al.*, 2010; Hou *et al.*, 2014; Wang *et al.*, 2018*a*).

Recently, Gully *et al.* (2019) used a bioinformatic approach to identity a novel family of 14 paralogous propeptides in the *Arabidopsis thaliana* genome, which they named PROSCOOPs. Within this family they noted that *PROSCOOP12* was transcriptionally highly responsive to

biotic and oxidative stress, suggesting a role as a phytocytokine. They subsequently identified 74 homologs within available *Brassicaceae* genomes and used these sequences to identify conserved regions, revealing a biologically-active 13-amino acid SCOOP motif. They were able to demonstrate that SCOOP12 could induce PTI responses, culminating in induced-resistance to *Pseudomonas syringae*.

As discussed in Chapter 4, the LRR-RK MIK2 differently regulates elicitor-induced ROS production, and I therefore wanted to test whether SCOOP12-induced ROS production was affected in *mik2*. Here I present data showing that all assayed SCOOP12-induced outputs are MIK2-dependent and SCOOP12 induces MIK2-BAK1 complex formation. Moreover, transient expression of MIK2 was sufficient to confer sensitivity to SCOOP12 in *N. benthamiana*. Combined these data provide preliminary evidence that MIK2 is the receptor for SCOOP12.

Furthermore, I identified amino acid sequences within *Fusarium* and *Streptomyces* proteomes that share a high degree of sequence similarity to SCOOP12. I hypothesise that that these motifs could also be recognised by MIK2. MIK2-dependent recognition of these peptides could explain the enhanced susceptibility to *Fusarium oxysporum* in *mik2* (Van der Does *et al.*, 2017), and the MIK2-dependent responses to the recently-reported *Fusarium*-derived extract EnFOE (Van der Does *et al.*, 2017; Coleman *et al.*, 2019). This raises the intriguing possibility that MIK2 may recognise a SCOOP12-like motif present in both plant and microbial proteomes.

6.3 Results

6.3.1 A subset of the *PROSCOOP* genes are transcriptionally responsive to elicitors

Gully et al. (2019) reported the identification of the PROSCOOP family of peptides; however, they focused on the characterisation of SCOOP12. Initially, I wanted to investigate whether other PROSCOOPs were transcriptionally responsive to biotic stress, as was shown for PROSCOOP12. Using in house RNAseq data generated by Marta Bjornson it is evident from cluster-based on expression analysis, that the 3 genes in cluster I (PROSCOOP4, 12 and 14) are highly transcriptionally responsive to diverse elicitors, while others showed limited and inconsistent responses (Fig 6.1a,b). Members of previously described peptide families have been shown to have distinct expression profiles despite being often recognised by the same receptor(s), presumably to fulfil different physiological roles in the plant (Jun et al., 2010; Bartels et al., 2013; Vie et al., 2015b; Campbell and Turner, 2017; Okuda et al., 2019). Therefore, it is not surprising that only a subset of the PROSCOOPs are upregulated by biotic elicitors.

6.3.2 Responses to SCOOP12 are BAK1-dependent but SOBIR1-independent

Gully et al. (2019) showed that seedling growth inhibition was impaired in response to SCOOP12 in the *bak1-4* mutant, suggesting that BAK1 positively regulates responses to SCOOP12; presumably as a co-receptor within the receptor complex. However, other components of the receptor complex remain elusive. Initially I sought to confirm this BAK1-dependency and determine SOBIR1-dependency to distinguish between LRR-RK- and LRR-RLP-based perception. To this end I performed ROS assays with the dominant negative *bak1-5* allele (Schwessinger et al., 2011) and the null *sobir1-13* mutant (Gao et al., 2009; Leslie et al., 2010) to test whether SCOOP12-induced ROS production was dependent upon these RKs. SCOOP12 was able to induce ROS production in Col-0 and *sobir1-13* to the same extent (Fig. 6.1a-b), indicating that the SCOOP12 receptor is not an LRR-RLP. However, ROS production was abolished in the *bak1-5* background (Fig. 6.1a-b), supporting BAK1-dependency.

In addition, I was able to demonstrate that SCOOP12 induces a strong and rapid influx of cytoplasm calcium using an aequorin calcium reporter line (Knight *et al.*, 1991) (Fig 6.1c). However, this influx was reduced and delayed in *bak1-4 35S::AEQ*.

Furthermore, Perraki et al. (2018) reported a BAK1 phosphosite, Ser612, which is critical for the function of BAK1 in immune signalling. This residue is phosphorylated during receptor complex activation. Probing with α-pSer612 (which specifically recognises this phosphorylated epitope) revealed SCOOP12-induced phosphorylation of this residue (Fig. 6.2 d) (Perraki et al., 2018). This provides further support for the role of BAK1 in SCOOP12 perception.

Together, my data indicates that the SCOOP12 receptor is an LRR-RK. Moreover, the *bak1-5* sensitivity suggests that the receptor has the conserved Tyr-VIa residue within its kinase domain (Perraki *et al.*, 2018)

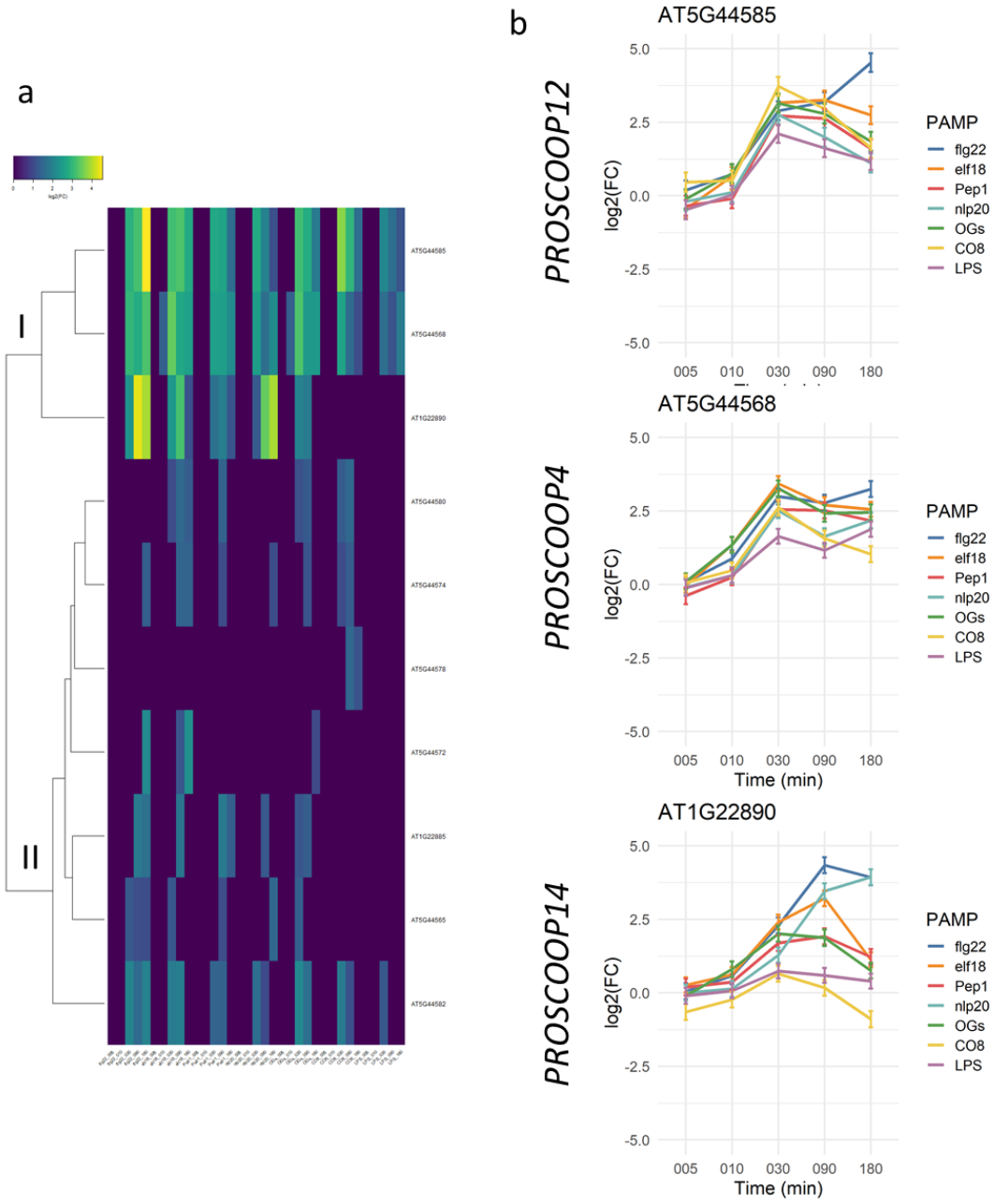

Figure 6. 1 Transcriptional responsivity of *PROSCOOP* genes to biotic elicitors

(a) Clustering of *PROSCOOP* genes based on transcriptional response of *MIK2* to a range of biotic elicitors in whole seedlings over a time course (5 to 180 min). Ch8 = 1 µM chitooctaose, elf18 = 1 µM elf18, flg22 = 1 µM flg22, LPS = 1 µM 3-hydroxydecanoic acid, nlp20 = 1 µM nlp20, OG =100µg/mL oligogalacturonides d.p. 14-16 , Pep1 = 1 µM Pep1. (Data from M. Bjornson) (b) Detailed transcriptomic profiles of *PROSCOOP* genes clustered in clade I. (This is the work of Marta. Bjornson)

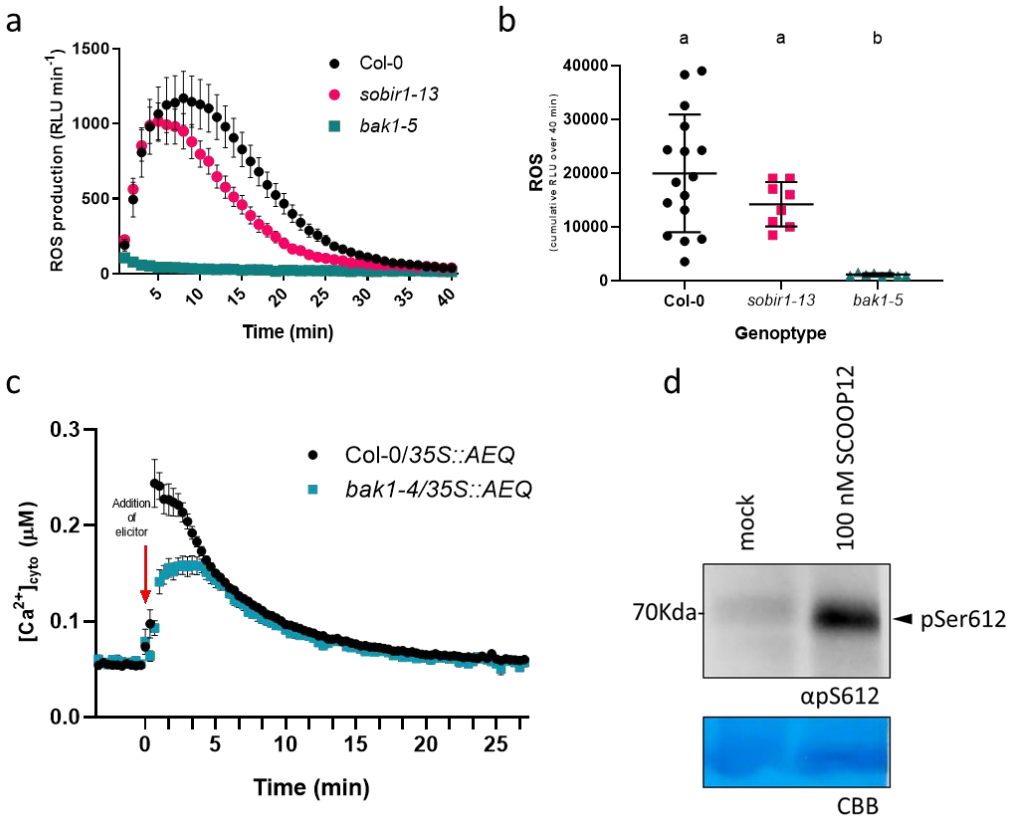

Figure 6. 2 SCOOP12-induced ROS production and cytoplasmic calcium influx are BAK1-dependent and SOBIR1-independent

(a) 1 µM SCOOP12-induced ROS production in leaf disks from six-week-old rosettes (n≥8). Error bars represent S.E.M. (b) Cumulative SCOOP12-induced ROS production over 40 min. Line indicates mean, error bars indicate S.D. Lower case letters represent significance groupings ($p<0.01$) following one-way ANOVA followed by Tukeys Post-hoc test. (c) Change in Cytoplasmic calcium concentration in response to 1 µM SCOOP12 in seven-day-old seedlings. Calcium concentration was calculated using the method developed by Knight *et al.* (1991). (n=8) This experiment was performed once. (d) 100 nM SCOOP12-induced phosphorylation of BAK1 Ser612 in 2-week-old Col-0 seedlings assessed by western-blot. CBB staining was used as a loading control.

6.3.3 Responses to SCOOP12 are MIK2-dependent

As reported in previous chapters, elicitor-induced ROS production is differentially affected by the loss of *MIK2*. I therefore sought to characterise SCOOP12-induced ROS production in *mik2*. Surprisingly, SCOOP12-induced ROS production was completely abolished in *mik2* mutants, both in Col-0 and Wassilewskija (Ws-2) backgrounds (Fig. 6.2a-d). The same loss of SCOOP12-induced cytoplasmic calcium influx could be seen in the *mik2* background (Fig. 6.2 e). The loss of ROS production in *mik2* seemed absolute; stronger than the response to any other elicitor tested. I therefore decided to investigate whether *mik2* mutants also had reduced SCOOP12-induced MAPK phosphorylation. No difference in flg22-, Pep1- and JRP4-induced MAPK phosphorylation had been seen between Col-0 and *mik2* (Chapter 4-5), however, there was a complete loss of SCOOP12-induced phosphorylation of MAPK3, MAPK4/11 and MAPK6 in *mik2-1* and *mik2-2* (Fig. 6.2 f). I could however observe MAPK phosphorylation in the *bak1-5* mutant in response to SCOOP12. This is probably due to the different threshold requirements for triggering the activation of ROS production and MAPK phosphorylation with other partially redundant SERKs sufficient to fulfil the role. Indeed, it has previously been shown that the kinetics of MAPK phosphorylation are delayed in *bak1-5* in response to other elicitors, but not abolished (Schwessinger *et al.*, 2011).

To further scrutinise the lack of SCOOP12 responses in *mik2*, I decided to assay seedling growth in the presence of SCOOP12. This is a response to long term exposure which can allow even weak responses to manifest. In both Col-0 and Ws-2 ecotypes I could observe strong seedling growth inhibition in the presence of 1 μM SCOOP12, and I was able to reproduced the previously observed impaired seedling growth inhibition in *bak1-4* (Gully *et al.*, 2019) (Fig. 6.2f-g). However, seedling growth inhibition was completely abolished in *mik2-1*, *mik2-2* and *mik2-4* lines, showing that MIK2 is also required for seedling growth inhibition.

Taken together, these results suggest that *mik2* mutants are completely insensitive to SCOOP12.

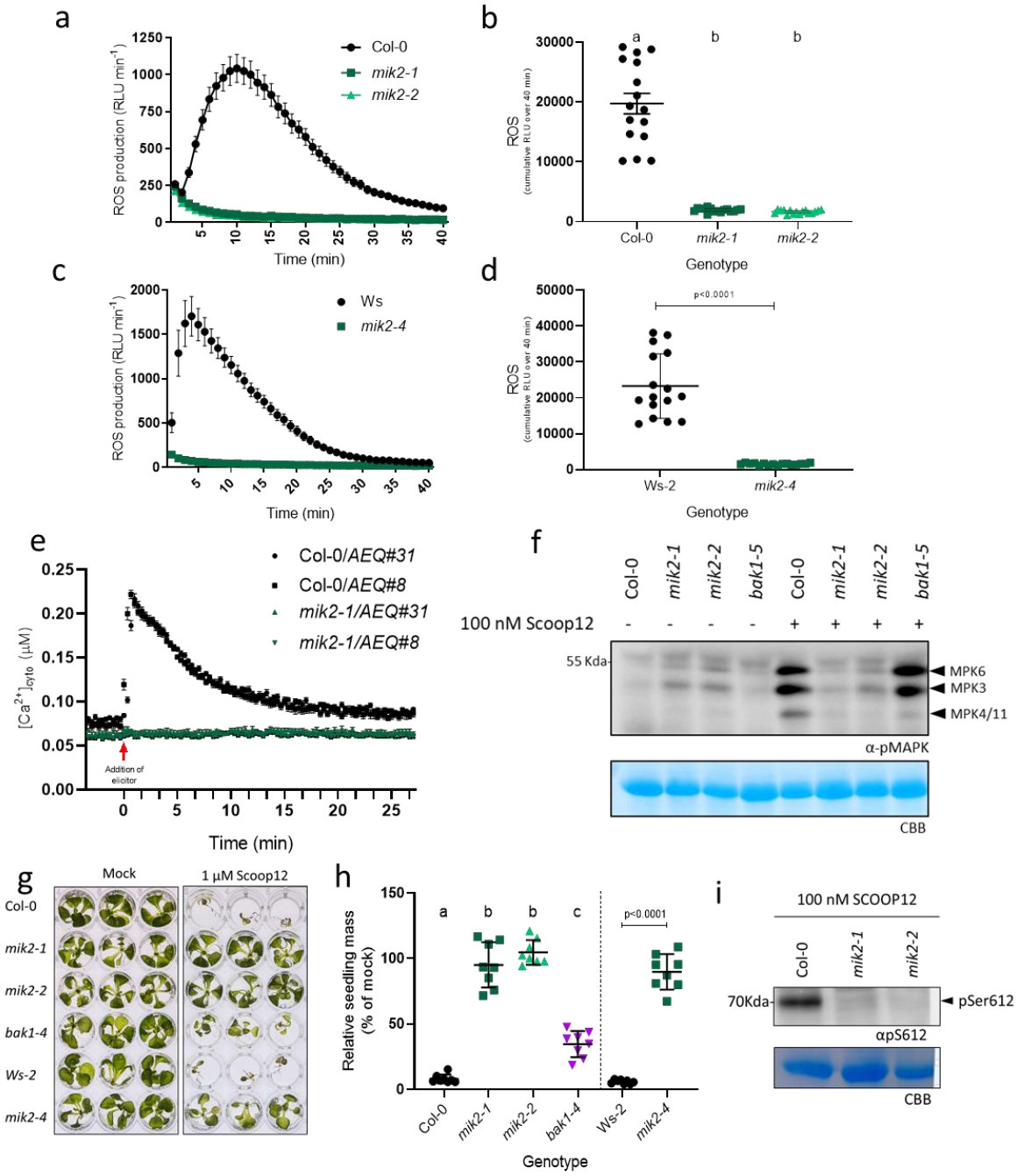

Figure 6. 3 SCOOP12-induced responses are MIK2-dependent

(a,c) 1 µM SCOOP12-induced ROS production in leaf disks (n=16) (b,d) Cumulative SCOOP12-induced ROS production over 40 min. (e) Change in Cytoplasmic calcium concentration in response to 1 µM SCOOP12 in seven-day-old seedlings. Calcium concentration was calculated using the method developed by Knight *et al.* (1991). (n=12) (f) MAPK and (i) BAK1 Ser612 phosphorylation in 2-week-old seedlings assessed by western blot following 15 min treatment with 100 nM SCOOP12 or mock. CBB staining was used to confirm equal loading. (g) Seedling growth in media with 1 µM SCOOP12 or without. (h) Mass of seedlings grown in media containing 1 µM SCOOP12 normalised to the mass of seedlings grown in the absence of the peptide.

Bars indicate mean, (a,c,e) error bars represent S.E.M. (b,d,h) error bars indicate S.D. Lower case letters represent significance groupings ($p<0.001$) following one-way ANOVA followed by Tukeys Post-hoc test. Where only 2 groups were being compared an unpaired T-test was performed.

6.3.4 MIK2 confers responsiveness to SCOOP12 in *N. benthamiana*

Having demonstrated that MIK2 is required for the perception of SCOOP12 in Arabidopsis, I wanted to test if MIK2 is sufficient to confer responsiveness to SCOOP12 by expressing it in the heterologous system *N. benthamiana*. In accordance with Gully *et al.* (2019) I was unable to observe any response to SCOOP12 in *N. benthamiana* (Fig 6.3a,b). There is no ortholog of MIK2 in *N. benthamiana*; however, transient expression of full length MIK2 in *N. benthamiana* was sufficient to confer sensitivity to SCOOP12 (Fig 6.3c; Fig. 6.4a,b). Furthermore, the paralog of MIK2, MIK2-like, is unable to confer this recognition, however this could be due to very low expression and requires repetition Fig. 6.4a,b).

Similarly, expression of a chimera between the MIK2 ectodomain and the cytoplasmic domain of EFR was sufficient to confer SCOOP12-induced ROS production (Fig. 6.4a,b). The reciprocal chimera was however unable to confer sensitivity to SCOOP12; yet, conferred elf18-induced ROS production (Fig. 6.4c-d). These results suggest that MIK2 is sufficient to confer sensitivity to SCOOP12 in *N. benthamiana*, providing further evidence that MIK2 is most likely the receptor for SCOOP12.

6.3.5 SCOOP12 induces MIK2-BAK1 complex formation

Given that SCOOP12 perception is MIK2- and BAK1-dependent, I sought to test if MIK2 and BAK1 could form a SCOOP12-induced complex. To investigate this, I performed Co-immunoprecipitation assays in stable transgenic *Arabidopsis* lines, *mik2-1/35S::MIK2-GFP* and *efr-1/35S*::*EFR-GFP*. As expected, elf18-induced EFR-BAK1 complex formation could clearly be observed (Fig. 6.6) (Roux *et al.*, 2011). BAK1 was not pulled-down with MIK2-GFP under mock conditions, or with elf18 treatment. However, SCOOP12 treatment resulted in the co-immunoprecipitation of BAK1 with MIK2-GFP (Fig 6.6). This suggests that SCOOP12-induces MIK2-BAK1 complex formation. The IP-GFP BAK1 band is weaker for MIK2-GFP with SCOOP12 treatment than for EFR-GFP with elf18 treatment. This could be because: 1/ the input pool of MIK2-GFP was larger, so only a small proportion was involved in BAK1 complex formation; 2/ MIK2 could use additional SERK co-receptors, thus only a proportion of complexes contain BAK1; or 3/ the interaction induced by SCOOP12 is weaker than that by elf18 thus more complexes dissociate during immunoprecipitation. It must be noted that this does not demonstrate a direct interaction, however, it supports the hypothesis that SCOOP12-induces MIK2-BAK1 complex formation.

6.3.6 MIK2 kinase activity is required for SCOOP12 responsivity

Previous results suggested that the MIK2 cytoplasmic domain requires kinase activity for function (Chapter 3). To test whether MIK2 kinase activity is required for SCOOP12 sensitivity complementation lines were generated with wild-type and kinase-dead MIK2 variants. Whilst the wild-type MIK2 was able to complement *mik2-1*, the kinase-dead variant

was only partially able to complement the response. It produced a delayed and weaker response. This suggests that the kinase activity of MIK2 plays an important role in MIK2 function.

6.3.7 Sequences with a high degree of similarity to SCOOP12 are present within pathogen proteomes

Whilst a substantial body of evidence now supports MIK2 as a candidate receptor for SCOOP12, the exact amino acid constraints required for SCOOP12 activity are unknown. I decided to BLAST the SCOOP12 amino acid sequence against all NCBI databases to look for other proteins containing the motif. The identical sequence is present in one other Arabidopsis protein, AT5G42830, an HXXXD-type acyl-transferase family protein with a predicted cytoplasmic localisation. Whether this protein could generate a biologically active peptide in the apoplast remains unknown.

Moreover, beyond *Brassicaceae* sequences with a high degree of similarity to SCOOP12 were identified in unrelated pathogen proteomes, specifically *Fusarium* Spp. and *Streptomyces* Spp. (Fig. 6.5). In *Streptomyces* the alignment falls within the extracellular N-terminus of an EamA transporter of unknown function. Meanwhile, in *Fusarium* the alignment is within the N-terminus of an RNA polymerase I-specific transcription-initiation factor. Going forward, it will be interesting to test whether these motifs are also able to induce PTI responses. This raises the intriguing possibility that the SCOOP12 motif could simultaneously be present in plant and microbial proteins. Indeed nlp20 has previously been shown to be present in three different kingdoms (Böhm *et al.*, 2014; Oome *et al.*, 2014). Based on these observations, it is tempting to speculate that the SCOOP12-like motif-containing protein could be the active component of the EnFOE extract from Fusarium that is recognised in a MIK2-dependent manner (Coleman et al., 2019). Moreover, it may explain the previously reported enhanced susceptibility to *Fusarium oxysporum* in mik2 (Van der Does et al., 2017).

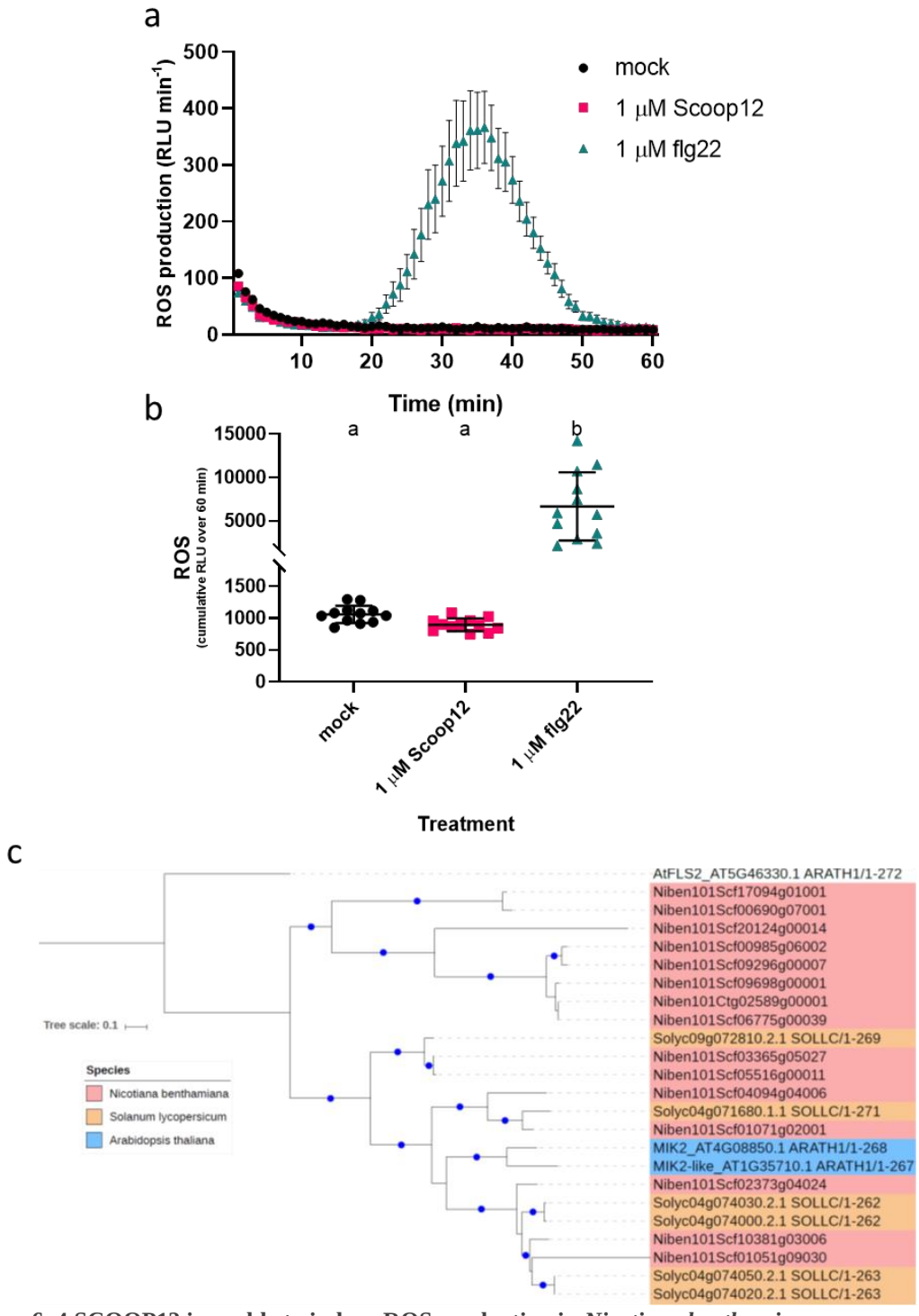

Figure 6. 4 SCOOP12 is unable to induce ROS production in *Nicotiana benthamiana*

(a) ROS production induced by the addition of 1 µM SCOOP12 or flg22 in *N. benthamiana* leaf disks. Error bars represent S.E.M. (n=8) (b) Cumulative peptide induced ROS production upon 1 µM SCOOP12, 1 µM flg22 or mock treatment in *N. benthamiana* leaf disks. Line indicates mean, error bars indicate S.D. Lower case letters represent significance groupings ($p<0.0001$) following one-way ANOVA followed by Tukeys Post-hoc test. (c) Phylogenetic tree showing LRR-RK subfamily XIIb from tomato, *N. benthamiana* and *Arabidopsis*. Sequences of the kinase domains were obtained from Dufayard *et al.* (2017) and Wang *et al.* (2018). The Sequences were aligned using MUSCLE and a tree was generated using using PhyML maximum likelihood with LG matrix. The tree was visualised using iTOL (Letunic and Bork, 2019). The kinase domain of *A. thaliana* FLS2 was used as an outgroup. Blue dots represent >80% bootstrapping support (100 iterations performed)

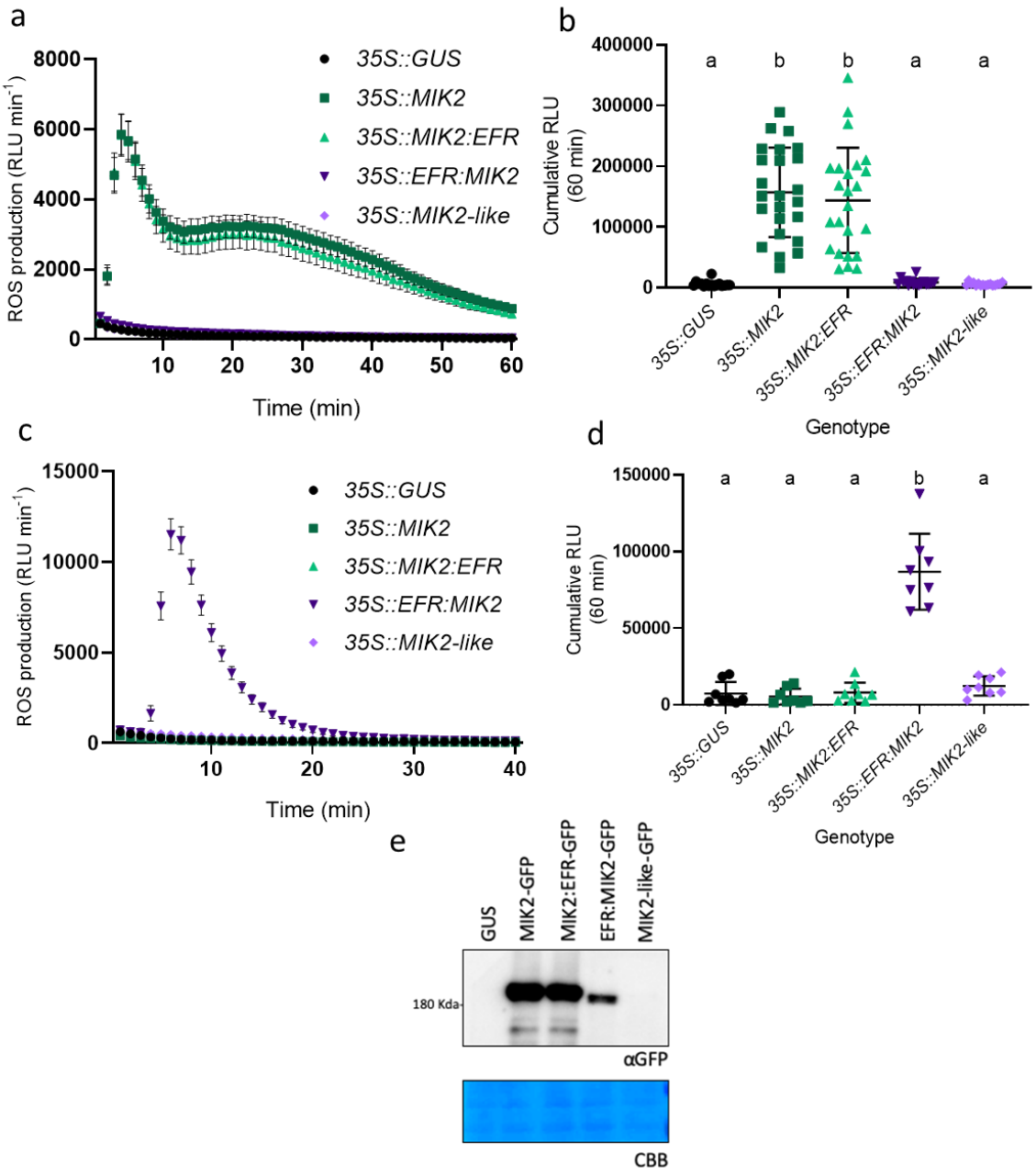

Figure 6. 5 Expression of MIK2 is sufficient to confer responsivity to SCOOP12 in *Nicotiana benthamiana*

(a-d) ROS production induced by the addition of 1 µM SCOOP12 to *N. benthamiana* leaf disks taken from four-week-old plants infiltrated two days previously with $O.D._{600}$=0.2 Agrobacterium containing respective construct. (a,c) Error bars represent S.E.M. (b,d) bar represents the mean, error bars represent S.D. Lower case letters represent significance groupings ($p<0.0001$) following one-way ANOVA followed by Tukeys Post-hoc test. (a-b) Leaf disks were treated with 1 µM SCOOP12 ($n\geq16$), (c-d) Leaf disks treated with 1 µM elf18 (n=8). (e) Western blot showing the expression of GFP constructs.

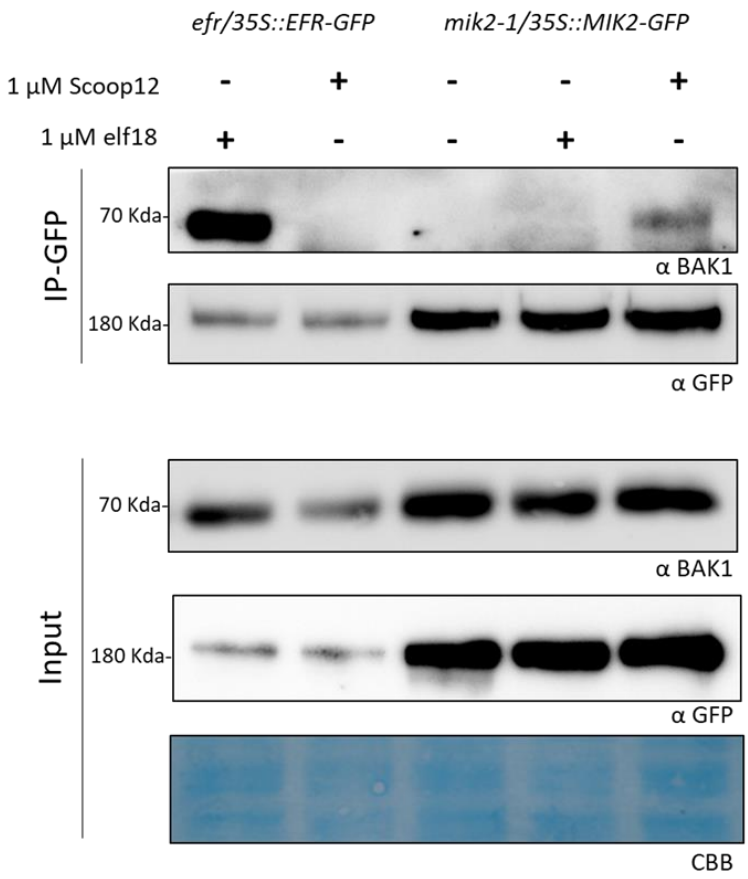

Figure 6. 6 SCOOP12 induces MIK2-BAK1 interaction

Co-immunoprecipitation of BAK1 with EFR-GFP and MIK2-GFP in *efr/35s::EFR-GFP* and *mik2-1/35S::MIK2-GFP* lines respectively. Twelve-day-old liquid grown seedlings were treated with mock, 1 µM SCOOP12 or 1 µM elf18 for 10 min. CBB staining was performed as a loading control. (Additional repeats have been performed by Huanjie Yang)

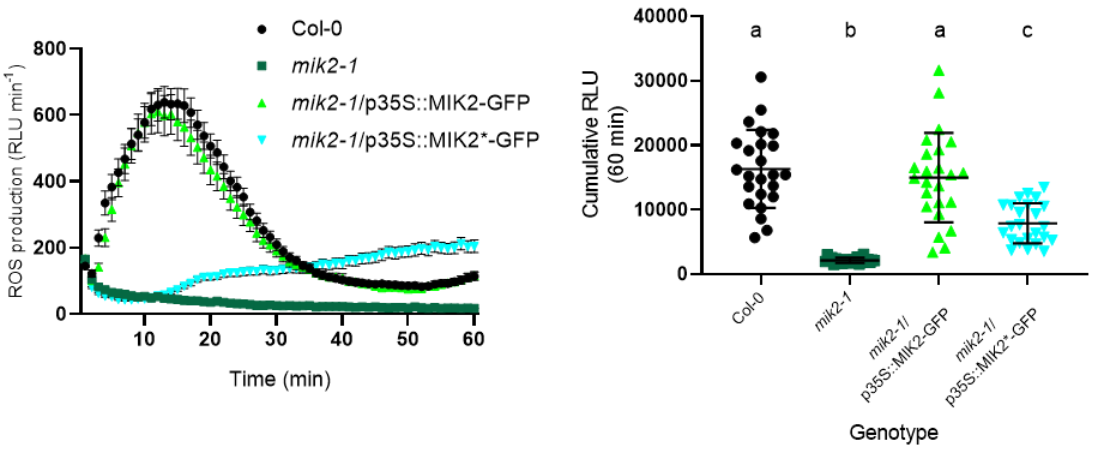

Figure 6. 7 MIK2 kinase activity is required for full SCOOP12-induced ROS production

(a) 1 µM SCOOP12-induced ROS production in leaf disks taken from five-week-old rosettes (n=24) Error bars represent S.E.M.. (b) Cumulative SCOOP12-induced ROS production over 60 min. Lower case letters represent significance groupings ($p<0.0005$) following one-way ANOVA followed by Tukeys Post-hoc test.

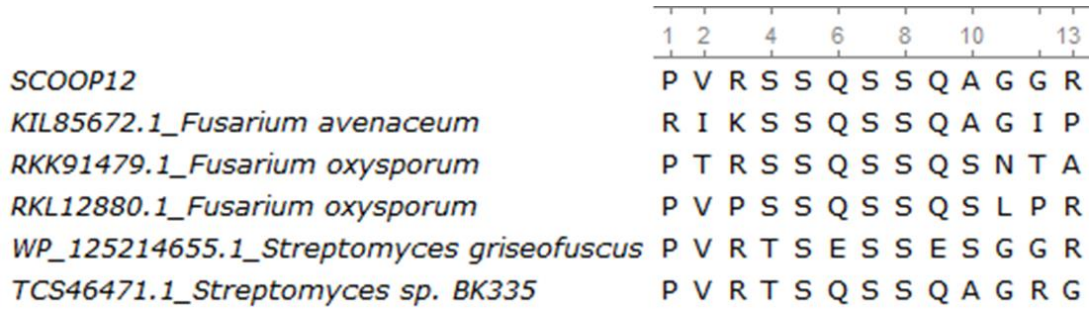

Figure 6. 8 Sequences with a high degree of sequence similarity to SCOOP12 are present in microbe genomes

Alignment of several of the strongest candidates from *Fusarium* and *Streptomyces* proteomes with SCOOP12 identified through BLAST.

6.4 Discussion

6.4.1 Is MIK2 the receptor for SCOOP12?

Currently, the genetic data available suggests that MIK2 is required and sufficient to confer SCOOP12 sensitivity. The complete loss of sensitivity observed in diverse bioassays such as MAPK activation and seedling growth inhibition is indicative of receptor function. Furthermore, SCOOP12 induces MIK2-BAK1 complex formation. This is consistent with the current paradigm of LRR-RK signalling, advocating that MIK2 is the SCOOP12 receptor. Nevertheless, this data does not demonstrate that MIK2 is indeed the ligand-binding receptor. In order to demonstrate this, we are now planning to perform ligand-binding assays to establish conclusively a direct, physical interaction between SCOOP12 and the MIK2 ectodomain. Moreover, it will be interesting to establish whether the presence of the BAK1 ectodomain will be able to enhance this binding affinity, as previously observed for the IDA-HAESA ligand-receptor pair (Santiago *et al.*, 2016) and whether SCOOP12 is sufficient to mediate the direct interaction between the MIK2 and BAK1 ectodomains.

6.4.2 SCOOP12 as a phytocytokine

There are currently 14 *PROSCOOP*s identified within the *Arabidopsis thaliana* genome. However, more may still be identified. Indeed, because of relaxed selection on regions of peptides not involved in binding, there is sometimes poor sequence conservation. It is therefore challenging to identify paralogs based on the short 13-amino acid active epitope. We currently have no information on the sequence constraints governing SCOOP activity. Structural data combined with peptide mutagenesis would allow us to more accurately predict peptides containing an active SCOOP motif, not necessarily evident based on the amino acid sequence. Recently, structural data facilitated the identification of CIF3 and CIF4 peptides,

which were not originally identified based on sequence alignment with CIF1/2 (Okuda *et al.*, 2019).

Moreover, the synthetic SCOOP12 peptide was identified using bioinformatic approaches. It is unclear whether this 13-amino acid peptide is physiologically relevant. It is notoriously challenging to investigate proteolytic processing of peptides due to redundancy between proteases and pleotropic phenotypes. Consequently, we have only recently begun to understand the proteolytic processing of some of the best characterised plant peptides (Srivastava *et al.*, 2009; Schardon *et al.*, 2016; Hander *et al.*, 2019; Olsson *et al.*, 2019*a*). Potentially a shorter peptide maybe sufficient, or more potent. Conversely, the same may be true for a longer peptide which may have a higher binding affinity. Indeed, it is tempting to speculate that the second conserved motif identified by in the PROSCOOPs may be required for processing of the peptide (Gully *et al.*, 2019); it is generally upstream of the SCOOP motif. Moreover, SCOOP12 contains a proline residue which could be hydroxylated, and subsequently arabinosylated to enhance activity and binding, as shown previously for other plant peptides (Ogawa-Ohnishi *et al.*, 2013; Xu *et al.*, 2015; Olsson *et al.*, 2019*a*). There is no evidence to support this idea currently.

Gully et al. (2019) reported that SCOOP12 was able to induce a range of PTI outputs, culminating in induced-resistance to Pseudomonas syringae. Some of these PTI-outputs have been corroborated here, such as seedling growth inhibition and ROS production, and new outputs have been demonstrated including cytoplasmic calcium influx and MAPK phosphorylation. Taken together these data suggest that SCOOP12 is an active elicitor and capable of potentiating immune signalling.

6.4.3 A SCOOP12-like motif is present in microbial proteins

The potential that the SCOOP motif is present in both DAMPs and PAMPs is an intriguing prospect. First, it needs to be established whether any of the microbial derived motifs are able to induce PTI responses and whether these are also MIK2-dependent. If these peptides are indeed recognised by *Arabidopsis* it would then be important to establish whether these epitopes are physiologically relevant during the infection process. For the *Streptomyces* peptides this is feasible as the active epitope is present in a region of the protein exposed to the apoplast. However, the *Fusarium spp.* proteins that contain the epitopes are predicted to be cytoplasmic. Nevertheless, the bacterial elongation-factor TU (EF-Tu) is mostly cytoplasmic; yet, sufficient protein seems present in the apoplast to facilitate immune recognition. It was however shown that EF-Tu is a non-classically secreted protein, can be involved in cell adhesion at the bacterial periplasm (Widjaja *et al.*, 2017), and can be found in extracellular vesicles (Bahar *et al.*, 2016), offering hypotheses to explain how EF-Tu may get exposed to the plant immune system, in addition to being simply made available upon bacterial

cell lysis. Moreover, it is becoming clear that plants actively attempt to expose PAMPs to the immune system (Buscaill *et al.*, 2019). In order to investigate the physiological role of these putative PAMPs, it would be preferable to mutate them within the pathogen and look for a gain of virulence. However, this may generate pleiotropic phenotypes as they may perform important functions in the pathogen. Assuming that the physiological relevance of these putative PAMP(s) can be demonstrated; the transfer of MIK2 into crops to confer genetic resistance would be promising. Several *Fusarium* and *Streptomyces* species cause economically important diseases, such as *Fusarium* wilt in banana and tomato; head blight and associated mycotoxin production in cereals, and potato scab (Loria *et al.*, 1997; Gordon, 2017).

6.4.4 The PROSCOOP family and MIK2 are both restricted to the *Brassicaceae*

The data presented here suggests that SCOOP12 sensitivity is MIK2-depdepdent with no apparent redundancy from the only other member of subfamily XIIb in *Arabidopsis*, MIK2-like. Only within *Brassicaceae* genomes are there sequences more similar to *MIK2* than *MIK2-like*, this in combination with the fact that no SCOOP12 sensitivity was reported outside *Brassicaceae*, suggests that MIK2, with its current function, evolved around the time of the *Brassicaceae* divergence (Fischer *et al.*, 2016; Van der Does *et al.*, 2017; Gully *et al.*, 2019). This coincides with the emergence of the PROSCOOP family which also appear to be *Brassicaceae* specific (Gully *et al.*, 2019). It is interesting to speculate how the putative MIK2-SCOOP signalling module arose. Could MIK2 have evolved to recognise a PAMP, which was subsequently mimicked by an endogenous elicitor (Coleman *et al.*, 2019)?

6.4.5 To what extent can the role of MIK2 in SCOOP12 perception explain the diverse *mik2* phenotypes?

Even if we demonstrate that MIK2 is the receptor for SCOOP12, this does not resolve the mechanistic basis of the *mik2* phenotypes described previously. However, it does provide additional hypotheses and approaches to address these questions. Ultimately it would be ideal to investigate if the *PROSCOOP12* loss-of-function phenocopies *mik2*. The challenge with this approach is the potential redundancy between *PROSCOOP12* and potential other *PROSCOOP* genes encoding peptides that may also be recognised by MIK2; a higher order mutant may have to be generated, especially with *PROSCOOP4* and *14* that are also up-regulated upon elicitor treatment. However, Gully *et al.* (2019) reported phenotypes in the single *scoop12* mutant. This would establish whether the *mik2* phenotypes and transcriptomic perturbations are as a result of its role in SCOOP-perception or independent of this. If the phenotypes were shared it could suggest that the SCOOP peptides play an important role in maintaining transcriptomic and ROS homeostasis. This would be puzzling as application of SCOOP12 induced ROS production and biotic stress responses, whilst *MIK2* genetically

appears to negatively regulate them. It is therefore perhaps more tempting to speculate that an indirect mechanism is responsible for the loss-of-function phenotypes. This could be similar to the role of BAK1 in negative regulation of cell death, which in contrast to the well-defined role of BAK1 in LRR-RK signalling, is poorly understood (Schwessinger *et al.*, 2011; de Oliveira *et al.*, 2016; Gao *et al.*, 2019). The plant may 'guard' against absence of MIK2, potentially not through a classical mechanism with a cytoplasmic immune receptor (Dangl and Jones, 2001; Rodriguez *et al.*, 2016).

NaCl has recently been shown to be sensed by the lipid glycosyl-inositol phosphorylceramide (Jiang et al., 2019). Overexpression of *PROPEP3*, and pre-treatment with synthetic Pep3, has been shown to enhance salt tolerance in *Arabidopsis* in a PEPR-dependent manner (Nakaminami *et al.*, 2018). This sets a precedent for intersection between peptide signalling in the context of immunity and salt stress tolerance. The impaired salt stress tolerance in *mik2* could be due to the role of MIK2 in SCOOP perception (Julkowska *et al.*, 2016; Van der Does *et al.*, 2017). Potentially, SCOOPs may act as part of a general danger response mechanism. It will be interesting to see if *PROSCOOP* mutants or overexpression lines are also more sensitive or tolerant to salt stress respectively.

Similarly, SCOOPs could positively regulate responses to inhibition of cellulose biosynthesis if their release or synthesis is triggered during cell wall or salt stress. It is possible that this may explain the role of MIK2 as a positive regulator of cell wall damage responses.

The differential regulation of ROS responses is more challenging to explain. Flg22 pre-treatment has been shown to positively regulate Pep1-induced ROS responses while this is not the case for elf18 (Flury *et al.*, 2013). This was shown to be independent of PEPR expression levels and was specific to ROS production (Flury *et al.*, 2013). This suggests possibility of pathway specific crosstalk upstream of ROS production. It would be interesting to investigate whether we observe this differential regulation in *proscoop* mutants, or whether pre-treatment with SCOOP12 is able to differentially regulate ROS responses.

6.4.6 Concluding remarks

In conclusion, MIK2 is an exciting candidate for the SCOOP12 receptor. If direct binding is established, it will be important to determine the constraints of MIK2 recognition to determine whether MIK2 could also recognise other SCOOP peptides within the *Arabidopsis* proteome or potentially microbial proteins carrying SCOOP-like motifs. If this were the case it would have exciting biotechnological implications. Furthermore, it will be important to unravel how the *mik2* phenotypes are linked to the role of MIK2 in SCOOP-perception.

Chapter 7

General Discussion

Plants rely on cell-surface localised pattern recognition receptors (PRRs) to perceive and amplify signals indicative of danger. Perception of these pathogen- or damage- associated molecular patterns (PAMPs/DAMPs) results in the induction of pattern-triggered immunity (PTI). Since the cloning of the first PRRs over two decades ago, our understanding developed substantially. We now understand the general mechanisms underlying elicitor perception by leucine-rich repeat receptor kinases, and receptor-like proteins, through elicitor-induced receptor-co-receptor heterodimerisation, resulting in cytoplasmic domain activation (Hohmann *et al.*, 2017). This activates cytoplasmic kinases which transduce the signal to executor proteins. These include transcription factors, ion channels and NADPH oxidases that either enhance resistance directly, or activate secondary signalling (Saijo *et al.*, 2018). The intricate regulatory mechanisms by which PRR complexes are governed is gradually being revealed (Couto and Zipfel, 2016). We are also beginning to explore the potential of deploying PRRs transgenically to engineer broad-spectrum, quantitative disease resistance in the field (Dangl *et al.*, 2013; Boutrot and Zipfel, 2017).

With the help of my colleagues, my PhD work has added to our understanding of this process. Here I will review some of the work in a wider context and consider future perspectives.

7.1 Identification of novel pattern recognition receptors to engineer resistance

Since the cloning of the first PRRs over two decades ago, our understanding has advanced significantly (Yu *et al.*, 2017; Saijo *et al.*, 2018). Whilst the number of known PRRs has increased considerably over recent years, fewer PRRs have been characterised than cytoplasmic immune receptors, and there is an incentive to identify novel, family-specific, PRRs to engineer resistance (Boutrot and Zipfel, 2017; Kourelis and Van Der Hoorn, 2018). PRR discovery has been a central theme of this thesis. Here I will discuss the merits and shortfalls of the approaches employed.

7.1.1 Chimeric receptors

The use of chimeric receptors to dissect ligand-binding from downstream signalling can provide valuable information when employing a reverse genetic approach to identify receptors. This information can validate the selection of clades of receptor-kinases which merit further investigation. However, the biological conclusions that can be drawn from such

an experiment are limited due to a range of assumptions. Indeed, the approach employed in this thesis assumes BAK1/SERK-dependency (BRASSINOSTROID INSENSITIVE1-ASSOCIATED KINASE1/ SOMATIC EMBRYOGENESIS RECEPTOR KINASE). Chimeric receptors with the EFR ectodomain will undergo BAK1 heterodimerisation upon elf18 application (Hohmann *et al.*, 2018*b*). This may result in outputs that are not usually associated with the respective cytoplasmic domain.

An advantage of this approach is that it gives an impression of receptor functionality in a heterologous system. It can reveal whether downstream signalling components are compatible with the cytoplasmic domain. In the work presented here the EFR (ELONGATION-FACTOR TU RECEPTOR) ectodomain is shape complementary with *Nicotiana benthamiana* SERK paralogs, this is not necessarily true of the ectodomains for the uncharacterised receptors. This may prevent heterodimerisation and function in a way that cannot be predicted by the chimeric receptors.

Moreover, the outputs assayed provide only limited information about the function of the receptor. I observed striking differences between the output of leucine-rich repeat (LRR) subfamily XII cytoplasmic domains, and that of BRASSINOSTEROID INSENSITIVE1 (LRR-RK subfamily X). However, I hypothesise that I would have been unable to distinguish the early outputs from the cytoplasmic domains of LRR-RK subfamily XII and XI (*e.g.* HAESA) as both induce ROS production and cytoplasmic calcium influx (Butenko *et al.*, 2014; Olsson *et al.*, 2019*b*). This is despite these RKs regulating distinct processes *in planta*, which may become apparent in later outputs from the chimeric receptors.

I believe the distinct dynamics of ROS outputs observed between the chimeric receptors merits further investigation. If increases in induced ROS production correlate with pattern triggered immunity, this could prove a valuable tool in PRR engineering allowing the development of modular assemblies to enhance PRR function. Indeed, chimeric receptors containing the *Os*CeBIP ectodomain (CHITIN ELICITOR-BINDING PROTEIN - an RLP from rice required for chitin perception) and the cytoplasmic domains from Xa21 and Pi-d2 (RKs known to induced a cell death response) resulted in enhanced resistance to *Magnaporthe grisea* (Kishimoto *et al.*, 2010, 2011; Kouzai *et al.*, 2013). However, the mechanism remains unclear as chitin perception is SERK independent, whilst Xa21 is a SERK-dependent PRR (Shan *et al.*, 2008; Chen *et al.*, 2014*b*).

7.1.2 Heterologous expression

In general it is accepted that LRR-RK PRRs retain functionality when expressed in heterologous angiosperm systems (Mendes *et al.*, 2010; Lacombe *et al.*, 2010; Afroz *et al.*, 2011; Tripathi *et al.*, 2014; Holton *et al.*, 2015; Schoonbeek *et al.*, 2015; Schwessinger *et al.*, 2015; Du *et al.*, 2015; Albert *et al.*, 2015; Lu *et al.*, 2015; Hao *et al.*, 2016; Hegenauer *et al.*,

2016; Wang *et al.*, 2016*a*; Boschi *et al.*, 2017; Kunwar *et al.*, 2018). Heterologous expression is therefore a viable approach to characterise putative LRR-RK PRRs. PRRs are often lineage specific making it feasible to test for a gain-of-function as explored in this thesis (Boller and Felix, 2009; Cook *et al.*, 2015). This gain-of-function can manifest itself as enhanced resistance. Pathogens of the heterologous system are unlikely to be under co-evolutionary pressure to evade recognition by the candidate PRR (as it originates from a non-host genome). This could result in stronger recognition and subsequence resistance.

A major limitation of this approach is that the source of a putative PAMP is unknown; therefore, multiple pathogens may have to be screened. Moreover, as resistance is likely to be quantitative it must be scored more precisely, creating a significant phenotyping workload. Nevertheless, an appropriate heterologous system can combine discovery and validation steps, streamlining a research and development pipeline. Generating transgenic lines is a significant cost associated with this approach.

7.1.3 Loss-of-function.

Loss-of-function can either follow forward or reverse genetic approaches. In this thesis I followed a reverse genetic approach, looking for loss-of-resistance in *Arabidopsis thaliana* LRR-RK subfamily XII. This is a challenging approach to due to the quantitative nature of the resistance and redundancy between PRRs. That is not to say redundancy in the recognition of one PAMP, but pathogens produce an assortment of PAMPs which likely contribute additively to host recognition and immunity. Whilst the loss of some PRRs have a striking impact on pathology, for example the *fls2* mutant is significantly more susceptible to spray inoculation with *Pseudomonas syringae* pv. *tomato* DC3000 Cor- (Chapter 3), others may only exert a small effect and would be difficult to identify in a screen.

The majority of PRRs identified through loss-of-function approaches were identified subsequent to the elicitor. This can allow either forward or reverse genetic screens for elicitor insensitivity.

The advent of modern genome editing techniques facilitates the production of higher order mutants which will speed the phenotyping process (Chapter 3). Higher order mutants can be screened with pathogens or pathogen extracts in order to identify enhanced susceptibility or insensitivity respectively this can significantly streamline phenotyping and overcome potentially redundancy issues.

7.1.4 Identification of PRR ligands

The majority of PRRs have been identified subsequent to their cognate ligand (Boutrot and Zipfel, 2017). Screening for response to a ligand or eliciting fraction dramatically reduces the biological complexity of the question with only the plants response being observed, rather

than the dynamic interaction between the plant and pathogen. Moreover, if the precise ligand is known it facilitates biochemical PRR identification approaches.

Non-self-derived elicitors

The identification of novel PAMPs has generally relied upon the successive purification of pathogen extracts with eliciting functions (Boller and Felix, 2009). Early examples include *Phytophthora* transglutaminase (Nürnberger *et al.*, 1994; Hahlbrock *et al.*, 1995; Brunner *et al.*, 2002), bacterial flagellin (Felix *et al.*, 1999), Elongation factor-TU (Kunze *et al.*, 2004) and Cold shock protein (Felix and Boller, 2003). Recently the same approach lead to the identification of a *Fusarium* extract, EnFoE, which lead to MIK2-depdendent pattern-triggered immune responses (Coleman *et al.*, 2019). When microbial extracts are purified to identify eliciting fractions, it is important to ensure that these are free from known, potent contaminant PAMPs. Moreover, even once an eliciting fraction is identified it can be challenging to identify the active epitope depending on its abundance (PAMPs can be active at nanomolar concentrations); biochemical properties for the PAMP; and genomic resources available for the pathogen. PAMP in plants have also been identified through rational consideration of abundant/conserved apoplastic molecules and homology with PAMPs recognised in metazoan systems.

Self-derived elicitors

In this thesis I have described the identification of a novel phytocytokine. Most known phytocytokines conform to similar general characteristics including elicitor-induced transcription, short length and a conserved, active C-terminal (Matsubayashi, 2014; Hou *et al.*, 2014; Olsson *et al.*, 2019*a*; Segonzac and Monaghan, 2019). Synthetic versions of these peptides can then be screened for activity, such as induced ROS production, cytoplasmic calcium influx or MAPK phosphorylation. This approach proved valuable in the identification the tentatively named JRP peptides in Chapter 6.

The transfer of the extracellular ATP receptor DOES NOT RESPOND TO NUCLEOTIDES1 from *Arabidopsis thaliana* to *Solanaceous* plants resulted in enhanced resistance to *Phytophthora infestans* demonstrating that DAMP receptors can also have biotechnological applications (Bouwmeester *et al.*, 2014). However, a whole phytocytokine signalling module has never been transferred between species. Expression of SYSTEMIN RECPTOR1 (SYR1) in *Nicotiana benthamiana* and *Arabidopsis thaliana* confers sensitivity to exogenously applied systemin (Wang *et al.*, 2018*a*). However, the PROSYSTEMIN ligand has never been co-transferred to determine whether the whole module could function heterologously. This would rely on appropriate expression and processing in the heterologous host. More speculatively, lineage specific phytocytokine-receptor ectodomain pairs could be used in

receptor engineering to engineer synthetic ligand-induced SERK-dimerization 'switches' in heterologous host.

The identification of BAK1-depdendent JRP4 raises the question: what is the JRP4 receptor? As discussed in Chapter 5 there are several ways to tackle this question. Due to the length of the peptide it is likely that N-terminal biotinylation will not affect function. Therefore, a streptavidin pull-down of biotinylated JRP4 may identify candidate JRP4-associated RKs through proteomics. This could be complemented by parallel identification of JRP4-induced BAK1-GFP-associated proteins by mass spectrometry. However, genetic approaches to look for loss-of-sensitivity could also be applied.

7.2 The role of MIK2

The evidence presented here suggests MIK2 is the SCOOP12 receptor. Assuming this is corroborated by binding studies, this represents a major advance in our understanding of MIK2 function. SCOOP12's role as a phytocytokine is supported by its transcriptional upregulation during biotic stress and ability to induce immune outputs (*i.e.* ROS production, cytoplasmic calcium influx, MAPK phosphorylation, defence gene expression, callose deposition, seedling growth inhibition and resistance to *Pseudomonas syringae*). Surprisingly, Gully *et al.* (2019) found that during infection with *Erwinia amylovora* a suite of defence related genes were upregulated in *proscoop12*, relative to Col-0. However, there were no transcriptomic differences under mock conditions. This suggests that SCOOP12 negatively regulates their expression during infection. This may explain a mild increase in resistance to *E. amylovora* and *Alternaria brassicicola* necrotrophic pathogens in *proscoop12* (Gully *et al.*, 2019). The different roles in resistance to necrotrophic and biotrophic pathogens could imply SCOOP12 mediates cross talk between jasmonic acid and salicylic acid (SA) pathways. Given the *proscoop12* infection phenotypes it is surprising that, other than *Fusarium oxysporum* susceptibility, we did not observed differences in infection assays in *mik2*. This may be due to the constitutive mild autoimmunity in *mik2*. Moving forward it is imperative to test whether the role of MIK2 in SCOOP perception can be uncoupled from constitutive *mik2* phenotypes.

One approach to this is determining whether loss-of-MIK2 phenocopies loss-of-SCOOP. There are 14 PROSCOOP peptides in Col-0. It would be a challenge to knock these all out genetically. It should be investigated whether other SCOOP peptides show MIK2-depdendent activity. Our data suggests that only a subset of 3 PROSCOOPs are transcriptionally responsive to elicitor application; these could be prioritised in future investigations. However, they may show transcriptional responsivity to other stresses, such as salt, or tissue specific expression patterns which are overlooked in the seedling transcriptomes analysed.

Structural information from the MIK2-SCOOP12-SERK complex would allow identification and mutation of residues in the MIK2 ectodomain required for SCOOP12-binding. These SCOOP12-binding deficient MIK2 alleles could be used to complement *mik2*. If constitutive ROS production and defence gene expression was supressed it would demonstrate the two processes can be uncoupled. If so, it would be informative to repeat the *mik2* phenotyping with these lines.

If some *mik2* phenotypes are found to be independent of SCOOP perception – what is causing these phenotypes? It is possible that a MIK2-associated protein functions aberrantly in the absence of MIK2. Several LRR-RK ectodomains have been shown to interact with the MIK2 *in vitro* (Smakowska-Luzan *et al.*, 2018). Potentially, MIK2 regulates the function of these receptors through direct interaction.

Moreover, the correlation between the transcriptomic differences in *mik2* and *bak1 bak1-like1* silenced plants is striking (Chapter 4). This combined with the dwarfism in the *mik2 bak1* lines suggests there are parallels between these mutants. *bak1 bkk1* autoimmunity is dependent upon endoplasmic reticulum quality control and glycosylation pathways as well as the plasma membrane localised calcium permeable channel CNGC20 (de Oliveira *et al.*, 2016; Yu *et al.*, 2019*b*). It would be logical to test if these components are also genetically required for *mik2* constitutive ROS and defence gene expression by creating double mutants. If this is the case it would support the hypothesis that *mik2* phenotypes may share a commonality with the autoimmunity seen in *bak1* mutants. It would be challenging to test elicitor induced responses in endoplasmic reticulum quality control and glycosylation pathway mutants as these processes are also important for the production of functional PRRs (Nekrasov *et al.*, 2009; Saijo *et al.*, 2009; Trempel *et al.*, 2016). *bak1 bkk1* autoimmunity is also SA-dependent (Gao *et al.*, 2017), however, constitutive background ROS could still be seen in *mik2-1 sid2-1*, (SALICYLIC ACID INDUCTION DEFICIENT 2 – a mutant in SA biosynthesis) suggesting background ROS is SA-independent. Whilst the constitutive ROS production and defence gene expression are consistent with autoimmunity, it more challenging to reconcile this with the differential regulation of elicitor-induced ROS production. Indeed, it may not be autoimmunity *per se* that is responsible for the phenotypes seen, but it could a consequence of one or more of the upregulated genes in *mik2*. Indeed recently activation of cytoplasmic immune receptors has been shown to modulate cell-surface immune signalling through the transcriptional upregulation of genes involved in cell-surface immune signalling leading to enhanced elicitor induced ROS production (Ngou *et al.*, 2020; Yuan *et al.*, 2020).

It would also be interesting to investigate the effect of SCOOP12 on cellulose biosynthesis-inhibition, salt stress tolerance and elicitor induced ROS production. This could either be done using synthetic peptide application, or over expression of *PROSCOOP12*. Indeed, Pep

treatment has been shown to negatively regulate cellulose biosynthesis inhibition responses (Engelsdorf *et al.*, 2018); it would be interesting if phytocytokines antagonistically regulated this process.

One finding that must be reconciled is the MIK2-depdendency of the response to the *Fusarium* elicitor EnFoE (Coleman *et al.*, 2019). As discussed in Chapter 7, a SCOOP12-like motif may also be present in *Fusarium*, which is recognised by MIK2. It would be interesting to test whether SCOOP12 pre-treatment could lead to ligand-induced desensitisation to the EnFoE extract, this would suggest that the same receptor was responsible for the recognition of both elicitors. It is possible that MIK2 recognises distinct ligands through independent mechanisms. However, there is the potential that EnFoE treatment induces the release of SCOOP peptides which are then perceived by MIK2 as a secondary signal, however, the response to EnFoE is very rapid, so this is unlikely.

The diverse phenotypes of the *mik2* mutant have made it challenging to understand the function of MIK2. The discovery that MIK2 is the likely ligand binding receptor for SCOOP12 represents a major advance in our understanding. We can leverage this information to explore how MIK2 regulates immune homeostasis and responses to diverse environmental stimuli. This may help explain the previously undescribed dichotomy in regulation of elicitor-induced ROS revealed in *mik2*.

7.3 Why so many phytocytokines?

Whilst the JRPs were the only peptides followed up from the *mik2* transcriptome, there are many other candidates that merit investigation as putative phytocytokines. Many small peptides genes are not present as probes on the microarray chips and many will not be upregulated in *mik2*. This highlights the potential for numerous phytocytokines.

Whilst historically phytocytokines were seen to have a predominantly positive role as potentiators of immune signalling. We are beginning to understand phytocytokine signalling has a much more complex architecture, regulating diverse aspects of plant physiology under pathogen invasion, including negatively regulating resistance (Gust *et al.*, 2017). Moving forward, the precise physiological relevance of individual phytocytokines needs to be established. This includes establishing where and when phytocytokines (and cognate receptors) are expressed and secreted. Many phytocytokines appear to have multiple roles in the plant. PATHOGEN-INDUCED PEPTIDE1/ TARGET OF LBD SIXTEEN2 signals through its cognate receptor RLK7 (Hou *et al.*, 2014). It acts as a phytocytokine to potentiate immune signalling, however, it is also expressed by lateral root founder cells (LRFCs) to supress LRFC identity in adjacent cells through RLK7 (Hou *et al.*, 2014; Toyokura *et al.*, 2019). Another example is the RALF peptides which are involved in diverse processes in

immunity, reproduction and development (Haruta *et al.*, 2014; Stegmann *et al.*, 2017; Mecchia *et al.*, 2017; Ge *et al.*, 2017; Gonneau *et al.*, 2018; Zhao *et al.*, 2018). It is important that the responses seen when high concentrations of peptide are applied exogenously are not overinterpreted; they may not correspond with the physiological role of the peptide. Moreover, there is likely considerable crosstalk between phytocytokines to fine-tune responses.

It is interesting that some phytocytokines, such as the SCOOPs and systemin, appear to have evolved recently and are lineage specific. Do these recent phytocytokines play a redundant role with more ancient phytocytokines, such as PROPEPs, or do they have novel functions or characteristic which confer an advantage to the plant?

It must be considered that most plant-microbe interactions are benign. Signalling peptides play important roles in regulating mycorrhization, nodulation and microbiome architecture both locally and systemically (De Bang *et al.*, 2017; Kereszt *et al.*, 2018). In this regard it is interesting that *JRP4* appears be positively transcriptionally regulated by biotic interactions and phosphate starvation (Chapter 5).

The expansion of phytocytokine gene families allows evolution of diverse cis regulatory elements. Thus the peptides can be expressed in multiple contexts, as can be seen with the *PROPEP* genes (Bartels *et al.*, 2013). The discovery that antimicrobial peptides can also be recognised as phytocytokines provides a mechanism for the evolution of novel phytocytokine signalling modules via sub/neofunctionalization of antimicrobial ancestors (Chen *et al.*, 2014*a*; Chien *et al.*, 2015). Indeed, it has been proposed that many of the cysteine-rich signalling peptides in reproduction and pollen tube guidance may have evolved from antimicrobial ancestors (Bircheneder and Dresselhaus, 2016).

In metazoan systems an inflammatory code has been proposed in which immune responses are governed by combinatorial, hierarchical interactions between PAMP and DAMP signalling (Escamilla-Tilch *et al.*, 2013). Indeed, it is apparent that the immune system responds to elicitors in the context of common patterns of pathogenesis (Vance *et al.*, 2009). It is therefore logical that plant may use a complex network of agonistic and antagonistic phytocytokines to govern immune responses.

7.4 Outlook and summary

The work presented in this thesis aimed at characterising the role of *Arabidopsis* LRR-RK subfamily XII in immune signalling. I have successfully demonstrated that the cytoplasmic domains of this RK family can generate early outputs indicative of immune signalling and merit further investigation as putative pattern-recognition receptors. Moreover, it was established that MIK2, a member of this subfamily is the likely ligand-binding receptor for the phytocytokine SCOOP12.

However, the absence of MIK2 at the plasma membrane leads to constitutive reactive oxygen species production, transcriptomic perturbations, and aberrant responses to a range of environmental stimuli. These transcriptomic perturbations in *mik2* led to the identification of a novel family of phytocytokines which can induce early immune outputs in a BAK1-depdendent manner.

Understanding how plant cells perceive and respond to apoplastic stimuli remains an interesting and important question. This is especially true in the context of disease resistance where the elegant co-evolutionary battle between host recognition and pathogen evasion can be unravelled at the molecular level. Ultimately a more intricate understanding of how plants perceive and respond to their biotic environment will allow us to rationally manipulate these responses to our benefit.

Bibliography

Abrash EB, Bergmann DC. 2010. Regional specification of stomatal production by the putative ligand CHALLAH. Development **137**, 447–455.

Abrash EB, Davies KA, Bergmann DC. 2011. Generation of Signaling Specificity in *Arabidopsis* by Spatially Restricted Buffering of Ligand–Receptor Interactions. The Plant Cell **23**, 2864–2879.

Acharya BR, Raina S, Maqbool SB, Jagadeeswaran G, Mosher SL, Appel HM, Schultz JC, Klessig DF, Raina R. 2007. Overexpression of CRK13, an Arabidopsis cysteine-rich receptor-like kinase, results in enhanced resistance to Pseudomonas syringae. The Plant Journal **50**, 488–499.

Afroz A, Chaudhry Z, Rashid U, Ali GM, Nazir F, Iqbal J, Khan MR. 2011. Enhanced resistance against bacterial wilt in transgenic tomato (Lycopersicon esculentum) lines expressing the Xa21 gene. Plant Cell, Tissue and Organ Culture **104**, 227–237.

Alassimone J, Fujita S, Doblas VG, *et al.* 2016. Polarly localized kinase SGN1 is required for Casparian strip integrity and positioning. Nature Plants **2**, 16113.

Albert I, Böhm H, Albert M, *et al.* 2015. An RLP23–SOBIR1–BAK1 complex mediates NLP-triggered immunity. Nature Plants **1**, 15140.

Albert M, Felix G. 2010. Chimeric receptors of the Arabidopsis thaliana pattern recognition receptors EFR and FLS2. Plant signaling & behavior **5**, 1430–2.

Albert M, Jehle AK, Fürst U, Chinchilla D, Boller T, Felix G. 2013. A two-hybrid-receptor assay demonstrates heteromer formation as switch-on for plant immune receptors. Plant Physiology **163**, 1504–1509.

Albert M, Jehle AK, Mueller K, Eisele C, Lipschis M, Felix G. 2010. Arabidopsis thaliana pattern recognition receptors for bacterial elongation factor Tu and flagellin can be combined to form functional chimeric receptors. The Journal of biological chemistry **285**, 19035–42.

Allen DG, Blinks JR, Prendergast FG. 1977. Aequorin luminescence: Relation of light emission to calcium concentration - A calcium-independent component. Science **195**, 996–998.

Almagro Armenteros JJ, Tsirigos KD, Sønderby CK, Petersen TN, Winther O, Brunak S, von Heijne G, Nielsen H. 2019. SignalP 5.0 improves signal peptide predictions using deep neural networks. Nature Biotechnology **37**, 420–423.

Alonso JM, Stepanova AN, Leisse TJ, *et al.* 2003. Genome-wide insertional mutagenesis of Arabidopsis thaliana. Science **301**, 653–657.

Amano Y, Tsubouchi H, Shinohara H, Ogawa M, Matsubayashi Y. 2007. Tyrosine-sulfated glycopeptide involved in cellular proliferation and expansion in Arabidopsis. Proceedings of the National Academy of Sciences of the United States of America **104**, 18333–8.

Amselem J, Cuomo CA, van Kan JAL, *et al.* 2011. Genomic Analysis of the Necrotrophic Fungal Pathogens Sclerotinia sclerotiorum and Botrytis cinerea (PM Richardson, Ed.). PLoS Genetics **7**, e1002230.

Anne P, Amiguet-Vercher A, Brandt B, Kalmbach L, Geldner N, Hothorn M, Hardtke CS. 2018. CLERK is a novel receptor kinase required for sensing of root-active CLE peptides in *Arabidopsis*. Development **145**, dev162354.

Aoki Y, Okamura Y, Tadaka S, Kinoshita K, Obayashi T. 2016. ATTED-II in 2016: A plant coexpression database towards lineage-specific coexpression. Plant and Cell Physiology **57**, e5.

Apel K, Hirt H. 2004. REACTIVE OXYGEN SPECIES: Metabolism, Oxidative Stress, and Signal Transduction. Annual Review of Plant Biology **55**, 373–399.

Arvidsson S, Kwasniewski M, Riaño-Pachón DM, Mueller-Roeber B. 2008. QuantPrime - A flexible tool for reliable high-throughput primer design for quantitative PCR. BMC Bioinformatics **9**, 465.

Asai T, Tena G, Plotnikova J, Willmann MR, Chiu WL, Gomez-Gomez L, Boller T, Ausubel FM, Sheen J. 2002. Map kinase signalling cascade in Arabidopsis innate immunity. Nature **415**, 977–983.

Asami T, Min YK, Nagata N, Yamagishi K, Takatsuto S, Fujioka S, Murofushi N, Yamaguchi I, Yoshida S. 2000. Characterization of brassinazole, a triazole-type brassinosteroid biosynthesis inhibitor. Plant Physiology **123**, 93–99.

Asami T, Mizutani M, Fujioka S, *et al.* 2001. Selective Interaction of Triazole Derivatives with DWF4, a Cytochrome P450 Monooxygenase of the Brassinosteroid Biosynthetic Pathway, Correlates with Brassinosteroid Deficiency in Planta. Journal of Biological Chemistry **276**, 25687–25691.

Bacete L, Mélida H, Miedes E, Molina A. 2018. Plant cell wall-mediated immunity: cell wall changes trigger disease resistance responses. Plant Journal **93**, 614–636.

Bahar O, Mordukhovich G, Luu DD, Schwessinger B, Daudi A, Jehle AK, Felix G, Ronald PC. 2016. Bacterial outer membrane vesicles induce plant immune responses. Molecular Plant-Microbe Interactions **29**, 374–384.

De Bang TC, Lundquist PK, Dai X, *et al.* 2017. Genome-wide identification of medicago peptides involved in macronutrient responses and nodulation. Plant Physiology **175**, 1669–1689.

Bartels S, Boller T. 2015. Quo vadis, Pep? Plant elicitor peptides at the crossroads of immunity, stress, and development. Journal of Experimental Botany **66**, 5183–5193.

Bartels S, Lori M, Mbengue M, van Verk M, Klauser D, Hander T, Boni R, Robatzek S, Boller T. 2013. The family of Peps and their precursors in Arabidopsis: differential expression and localization but similar induction of pattern-triggered immune responses. Journal of Experimental Botany **64**, 5309–5321.

Beardon EG. 2018. Discovery and analysis of novel resistance genes in rice to the parasitic weed Striga hermonthica. (PhD Thesis) University of Sheffield.

Beck M, Zhou J, Faulkner C, MacLean D, Robatzek S. 2012. Spatio-Temporal Cellular Dynamics of the *Arabidopsis* Flagellin Receptor Reveal Activation Status-Dependent Endosomal Sorting. The Plant Cell **24**, 4205–4219.

Bender CL, Stone HE, Sims JJ, Cooksey DA. 1987. Reduced pathogen fitness of Pseudomonas syringae pv. tomato Tn5 mutants defective in coronatine production. Physiological and Molecular Plant Pathology **30**, 273–283.

Bi G, Liebrand TWH, Bye RR, Postma J, van der Burgh AM, Robatzek S, Xu X, Joosten MHAJ. 2016. SOBIR1 requires the GxxxG dimerization motif in its transmembrane domain to form constitutive complexes with receptor-like proteins. Molecular plant pathology **17**, 96–107.

Bi G, Zhou Z, Wang W, Li L, Rao S, Wu Y, Zhang X, Menke FLHH, Chen S, Zhou J-MM. 2018. Receptor-like cytoplasmic kinases directly link diverse pattern recognition receptors to the activation of mitogen-activated protein kinase cascades in arabidopsis. Plant Cell **30**, 1543–1561.

Bircheneder S, Dresselhaus T. 2016. Why cellular communication during plant reproduction is particularly mediated by CRP signalling. Journal of Experimental Botany **67**, 4849–4861.

Bischoff V, Cookson SJ, Wu S, Scheible WR. 2009. Thaxtomin A affects CESA-complex density, expression of cell wall genes, cell wall composition, and causes ectopic lignification in Arabidopsis thaliana seedlings. Journal of Experimental Botany **60**, 955–965.

Blaum BS, Mazzotta S, Nöldeke ER, Halter T, Madlung J, Kemmerling B, Stehle T. 2014. Structure of the pseudokinase domain of BIR2, a regulator of BAK1-mediated immune signaling in Arabidopsis. Journal of Structural Biology **186**, 112–121.

Böhm H, Albert I, Oome S, Raaymakers TM, Van den Ackerveken G, Nürnberger T. 2014. A Conserved Peptide Pattern from a Widespread Microbial Virulence Factor Triggers Pattern-Induced Immunity in Arabidopsis (P Birch, Ed.). PLoS Pathogens **10**, e1004491.

Boisson-Dernier A, Lituiev DS, Nestorova A, Franck CM, Thirugnanarajah S, Grossniklaus U. 2013. ANXUR receptor-like kinases coordinate cell wall integrity with growth at the pollen tube tip via NADPH oxidases. PLoS biology **11**, e1001719.

Boisson-Dernier A, Roy S, Kritsas K, Grobei MA, Jaciubek M, Schroeder JI, Grossniklaus U. 2009. Disruption of the pollen-expressed FERONIA homologs ANXUR1 and ANXUR2 triggers pollen tube discharge. Development **136**, 3279–3288.

Boller T, Felix G. 2009. A Renaissance of Elicitors: Perception of Microbe-Associated Molecular Patterns and Danger Signals by Pattern-Recognition Receptors. Annual Review of Plant Biology **60**, 379–406.

Boschi F, Schvartzman C, Murchio S, *et al.* 2017. Enhanced Bacterial Wilt Resistance in Potato Through Expression of Arabidopsis EFR and Introgression of Quantitative Resistance from Solanum commersonii. Frontiers in plant science **8**, 1642.

Boudsocq M, Willmann MR, McCormack M, Lee H, Shan L, He P, Bush J, Cheng S-H, Sheen J. 2010. Differential innate immune signalling via Ca2+ sensor protein kinases. Nature **464**, 418–422.

Bourdais G, Burdiak P, Gauthier A, *et al.* 2015. Large-Scale Phenomics Identifies Primary and Fine-Tuning Roles for CRKs in Responses Related to Oxidative Stress. PLoS genetics **11**, e1005373.

Boutrot F, Zipfel C. 2017. Function, Discovery, and Exploitation of Plant Pattern Recognition Receptors for Broad-Spectrum Disease Resistance. Annual Review of Phytopathology **55**, 257–286.

Bouwmeester K, Han M, Blanco-Portales R, Song W, Weide R, Guo LY, van der Vossen EAG, Govers F. 2014. The Arabidopsis lectin receptor kinase LecRK-I.9 enhances resistance to Phytophthora infestans in Solanaceous plants. Plant Biotechnology Journal **12**, 10–16.

Bozsoki Z, Cheng J, Feng F, Gysel K, Vinther M, Andersen KR, Oldroyd G, Blaise M, Radutoiu S, Stougaard J. 2017. Receptor-mediated chitin perception in legume roots is functionally separable from Nod factor perception. Proceedings of the National Academy of Sciences of the United States of America **114**, E8118–E8127.

Brady SM, Orlando DA, Lee JY, Wang JY, Koch J, Dinneny JR, Mace D, Ohler U, Benfey PN. 2007. A high-resolution root spatiotemporal map reveals dominant expression patterns. Science **318**, 801–806.

Brooks DM, Hernández-Guzmán G, Kloek AP, Alarcón-Chaidez F, Sreedharan A, Rangaswamy V, Peñaloza-Vázquez A, Bender CL, Kunkel BN. 2004. Identification and characterization of a well-defined series of coronatine biosynthetic mutants of Pseudomonas syringae pv. tomato DC3000. Molecular Plant-Microbe Interactions **17**, 162–174.

Brunkard JO, Zambryski PC. 2017. Plasmodesmata enable multicellularity: new insights into their evolution, biogenesis, and functions in development and immunity. Current Opinion in Plant Biology **35**, 76–83.

Brunner F, Rosahl S, Lee J, Rudd JJ, Geiler C, Kauppinen S, Rasmussen G, Scheel D,

Nürnberger T. 2002. Pep-13, a plant defense-inducing pathogen-associated pattern from Phytophthora transglutaminases. EMBO Journal **21**, 6681–6688.

Brutus A, Sicilia F, Macone A, Cervone F, De Lorenzo G. 2010. A domain swap approach reveals a role of the plant wall-associated kinase 1 (WAK1) as a receptor of oligogalacturonides. Proceedings of the National Academy of Sciences of the United States of America **107**, 9452–7.

Bücherl CA, Jarsch IK, Schudoma C, Segonzac C, Mbengue M, Robatzek S, MacLean D, Ott T, Zipfel C. 2017. Plant immune and growth receptors share common signalling components but localise to distinct plasma membrane nanodomains. eLife **6**.

Buer CS, Masle J, Wasteneys GO. 2000. Growth Conditions Modulate Root-Wave Phenotypes in Arabidopsis. Plant and Cell Physiology **41**, 1164–1170.

Burkart RC, Stahl Y. 2017. Dynamic complexity: plant receptor complexes at the plasma membrane. Current Opinion in Plant Biology **40**, 15–21.

Burnet F. 1941. *The Production of Antibodies. A Review and a Theoretical Discussion.* Macmillan & Co.

Burr CA, Leslie ME, Orlowski SK, Chen I, Wright CE, Daniels MJ, Liljegren SJ. 2011. CAST AWAY, a Membrane-Associated Receptor-Like Kinase, Inhibits Organ Abscission in Arabidopsis. Plant Physiology **156**, 1837–1850.

Buscaill P, Chandrasekar B, Sanguankiattichai N, *et al.* 2019. Glycosidase and glycan polymorphism control hydrolytic release of immunogenic flagellin peptides. Science **364**, 748.

Butenko MA, Patterson SE, Grini PE, Stenvik G-E, Amundsen SS, Mandal A, Aalen RB. 2003. Inflorescence deficient in abscission controls floral organ abscission in Arabidopsis and identifies a novel family of putative ligands in plants. The Plant cell **15**, 2296–307.

Butenko MA, Wildhagen M, Albert M, Jehle A, Kalbacher H, Aalen RB, Felix G. 2014. Tools and Strategies to Match Peptide-Ligand Receptor Pairs. The Plant cell **26**, 1838–1847.

Campbell L, Turner SR. 2017. A Comprehensive Analysis of RALF Proteins in Green Plants Suggests There Are Two Distinct Functional Groups. Frontiers in Plant Science **8**, 37.

Campos ML, De Souza CM, De Oliveira KBS, Dias SC, Franco OL. 2018. The role of antimicrobial peptides in plant immunity. Journal of Experimental Botany **69**, 4997–5011.

Cao Y, Liang Y, Tanaka K, Nguyen CT, Jedrzejczak RP, Joachimiak A, Stacey G. 2014. The kinase LYK5 is a major chitin receptor in Arabidopsis and forms a chitin-induced complex with related kinase CERK1. eLife **3**.

Castells E, Casacuberta JM. 2007. Signalling through kinase-defective domains: The prevalence of atypical receptor-like kinases in plants. Journal of Experimental Botany **58**, 3503–3511.

Castrillo G, Teixeira PJPL, Paredes SH, *et al.* 2017. Root microbiota drive direct integration of phosphate stress and immunity. Nature **543**, 513–518.

Century KS, Shapiro AD, Repetti PP, Dahlbeck D, Holub E, Staskawicz BJ. 1997. NDR1, a pathogen-induced component required for Arabidopsis disease resistance. Science **278**, 1963–1965.

Chakraborty S, Pan H, Tang Q, Woolard C, Xu G. 2018. The Extracellular Domain of Pollen Receptor Kinase 3 is structurally similar to the SERK family of co-receptors. Scientific Reports **8**, 2796.

Chapman EJ, Greenham K, Castillejo C, Sartor R, Bialy A, Sun T ping, Estelle M. 2012. Hypocotyl transcriptome reveals auxin regulation of growth-promoting genes through GA-dependent and -independent pathways (MA Blazquez, Ed.). PLoS ONE **7**, e36210.

Chater C, Peng K, Movahedi M, *et al.* 2015. Elevated CO2-Induced Responses in Stomata Require ABA and ABA Signaling. Current Biology **25**, 2709–2716.

Chaudhary A, Chen X, Gao J, Leśniewska B, Hammerl R, Dawid C, Schneitz K. 2019. The Arabidopsis receptor kinase STRUBBELIG regulates the response to cellulose deficiency. bioRxiv, 775775.

Chen K, Du L, Chen Z. 2003. Sensitization of defense responses and activation of programmed cell death by a pathogen-induced receptor-like protein kinase in Arabidopsis. Plant Molecular Biology **53**, 61–74.

Chen K, Fan B, Du L, Chen Z. 2004. Activation of hypersensitive cell death by pathogen-induced receptor-like protein kinases from Arabidopsis. Plant Molecular Biology **56**, 271–283.

Chen Y-L, Lee C-Y, Cheng K-T, Chang W-H, Huang R-N, Nam HG, Chen Y-R. 2014*a*. Quantitative peptidomics study reveals that a wound-induced peptide from PR-1 regulates immune signaling in tomato. The Plant cell **26**, 4135–48.

Chen W, Lv M, Wang Y, Wang P-A, Cui Y, Li M, Wang R, Gou X, Li J. 2019. BES1 is activated by EMS1-TPD1-SERK1/2-mediated signaling to control tapetum development in Arabidopsis thaliana. Nature Communications **10**, 4164.

Chen X, Zuo S, Schwessinger B, *et al.* 2014*b*. An XA21-Associated Kinase (OsSERK2) Regulates Immunity Mediated by the XA21 and XA3 Immune Receptors. Molecular Plant **7**, 874–892.

Cheng C-Y, Krishnakumar V, Chan AP, Thibaud-Nissen F, Schobel S, Town CD. 2017. Araport11: a complete reannotation of the *Arabidopsis thaliana* reference genome. The Plant Journal **89**, 789–804.

Cheval C, Johnston M, Samwald S, Liu X, Bellandi A, Breakspear A, Kadota Y, Zipfel C, Faulkner C. 2019. Chitin perception in plasmodesmata identifies subcellular, context-specific immune signalling in plants. bioRxiv, 611582.

Chevalier D, Batoux M, Fulton L, Pfister K, Yadav RK, Schellenberg M, Schneitz K. 2005. STRUBBELIG defines a receptor kinase-mediated signaling pathway regulating organ development in Arabidopsis. Proceedings of the National Academy of Sciences of the United States of America **102**, 9074–9079.

Chezem WR, Memon A, Li F-SS, Weng J-KK, Clay NK. 2017. SG2-type R2R3-MYB transcription factor MYB15 controls defense-induced lignification and basal immunity in arabidopsis. Plant Cell **29**, 1907–1926.

Chien PS, Nam HG, Chen YR. 2015. A salt-regulated peptide derived from the CAP superfamily protein negatively regulates salt-stress tolerance in Arabidopsis. Journal of Experimental Botany **66**, 5301–5313.

Chinchilla D, Zipfel C, Robatzek S, Kemmerling B, Nürnberger T, Jones JDG, Felix G, Boller T. 2007. A flagellin-induced complex of the receptor FLS2 and BAK1 initiates plant defence. Nature **448**, 497–500.

Chitwood DH, Kumar R, Headland LR, *et al.* 2013. A Quantitative Genetic Basis for Leaf Morphology in a Set of Precisely Defined Tomato Introgression Lines. The Plant Cell **25**, 2465–2481.

Chiu CH, Choi J, Paszkowski U. 2018. Independent signalling cues underpin arbuscular mycorrhizal symbiosis and large lateral root induction in rice. New Phytologist **217**, 552–557.

Chivasa S, Murphy AM, Hamilton JM, Lindsey K, Carr JP, Slabas AR. 2009. Extracellular ATP is a regulator of pathogen defence in plants. The Plant Journal **60**, 436–448.

Choi HW, Manohar M, Manosalva P, Tian M, Moreau M, Klessig DF. 2016. Activation of Plant Innate Immunity by Extracellular High Mobility Group Box 3 and Its Inhibition by Salicylic Acid. PLoS pathogens **12**, e1005518.

Choi J, Tanaka K, Cao Y, Qi Y, Qiu J, Liang Y, Lee SY, Stacey G. 2014. Identification of a plant receptor for extracellular ATP. Science **343**, 290–294.

Chong ZS, Ohnishi S, Yusa K, Wright GJ. 2018. Pooled extracellular receptor-ligand interaction screening using CRISPR activation. Genome Biology **19**, 205.

Clark SE, Running MP, Meyerowitz EM. 1993. CLAVATA1, a regulator of meristem and flower development in Arabidopsis. Development (Cambridge, England) **119**, 397–418.

Clark SE, Running MP, Meyerowitz EM. 1995. CLAVATA3 is a specific regulator of shoot and floral meristem development affecting the same processes as CLAVATA1. Development **121**, 2057–2067.

Clark SE, Williams RW, Meyerowitz EM. 1997. The CLAVATA1 gene encodes a putative receptor kinase that controls shoot and floral meristem size in Arabidopsis. Cell **89**, 575–85.

Clarke CR, Chinchilla D, Hind SR, Taguchi F, Miki R, Ichinose Y, Martin GB, Leman S, Felix G, Vinatzer BA. 2013. Allelic variation in two distinct Pseudomonas syringae flagellin epitopes modulates the strength of plant immune responses but not bacterial motility. New Phytologist **200**, 847–860.

Claus LAN, Savatin D V., Russinova E. 2018. The crossroads of receptor-mediated signaling and endocytosis in plants. Journal of Integrative Plant Biology **60**, 827–840.

Clough SJ, Bent AF. 1998. Floral dip: A simplified method for Agrobacterium-mediated transformation of Arabidopsis thaliana. Plant Journal **16**, 735–743.

Coleman AD, Raasch L, Maroschek J, Ranf S, Hückelhoven R. 2019. The Arabidopsis leucine-rich repeat receptor kinase MIK2 is a crucial component of pattern-triggered immunity responses to Fusarium fungi. bioRxiv, 720037.

Consortium TTG. 2012. The tomato genome sequence provides insights into fleshy fruit evolution. Nature **485**, 635–641.

Cook DE, Mesarich CH, Thomma BPHJ. 2015. Understanding Plant Immunity as a Surveillance System to Detect Invasion. Annual Review of Phytopathology **53**, 541–563.

Couto D, Niebergall R, Liang X, *et al.* 2016. The Arabidopsis Protein Phosphatase PP2C38 Negatively Regulates the Central Immune Kinase BIK1. (L Shan, Ed.). PLoS pathogens **12**, e1005811.

Couto D, Zipfel C. 2016. Regulation of pattern recognition receptor signalling in plants. Nature Reviews Immunology **16**, 537–52.

Crooks GE, Hon G, Chandonia JM, Brenner SE. 2004. WebLogo: A sequence logo generator. Genome Research **14**, 1188–1190.

Cui Y, Hu C, Zhu Y, *et al.* 2018*a*. CIK Receptor Kinases Determine Cell Fate Specification during Early Anther Development in Arabidopsis. The Plant cell **30**, 2383–2401.

Cui Y, Li X, Yu M, Li R, Fan L, Zhu Y, Lin J. 2018*b*. Sterols regulate endocytic pathways during flg22-induced defense responses in Arabidopsis. Development (Cambridge, England) **145**, dev165688.

Dangl JL, Horvath DM, Staskawicz BJ. 2013. Pivoting the plant immune system from dissection to deployment. Science **341**, 746–751.

Dangl JL, Jones JD. 2001. Plant pathogens and integrated defence responses to infection. Nature **411**, 826–33.

Dardick C, Schwessinger B, Ronald P. 2012. Non-arginine-aspartate (non-RD) kinases are

associated with innate immune receptors that recognize conserved microbial signatures. Current Opinion in Plant Biology **15**, 358–366.

Davis KR, Darvill AG, Albersheim P, Dell A. 1986. Host-Pathogen Interactions : XXIX. Oligogalacturonides Released from Sodium Polypectate by Endopolygalacturonic Acid Lyase Are Elicitors of Phytoalexins in Soybean. Plant physiology **80**, 568–77.

Davis KR, Hahlbrock K. 1987. Induction of defense responses in cultured parsley cells by plant cell wall fragments. Plant physiology **84**, 1286–90.

Daxinger L, Hunter B, Sheikh M, Jauvion V, Gasciolli V, Vaucheret H, Matzke M, Furner I. 2008. Unexpected silencing effects from T-DNA tags in Arabidopsis. Trends in Plant Science **13**, 4–6.

Decreux A, Messiaen J. 2005. Wall-associated kinase WAK1 interacts with cell wall pectins in a calcium-induced conformation. Plant and Cell Physiology **46**, 268–278.

DeFalco TA, Bender KW, Snedden WA. 2010. Breaking the code: Ca2+ sensors in plant signalling. Biochemical Journal **425**, 27–40.

Delaux P-M, Radhakrishnan G V, Jayaraman D, *et al.* 2015. Algal ancestor of land plants was preadapted for symbiosis. Proceedings of the National Academy of Sciences of the United States of America **112**, 13390–5.

Delgado-Cerezo M, Sánchez-Rodríguez C, Escudero V, *et al.* 2012. Arabidopsis Heterotrimeric G-protein Regulates Cell Wall Defense and Resistance to Necrotrophic Fungi. Molecular Plant **5**, 98–114.

Denness L, McKenna JF, Segonzac C, Wormit A, Madhou P, Bennett M, Mansfield J, Zipfel C, Hamann T. 2011. Cell wall damage-induced lignin biosynthesis is regulated by a reactive oxygen species- and jasmonic acid-dependent process in arabidopsis. Plant Physiology **156**, 1364–1374.

DeYoung BJ, Bickle KL, Schrage KJ, Muskett P, Patel K, Clark SE. 2006. The CLAVATA1-related BAM1, BAM2 and BAM3 receptor kinase-like proteins are required for meristem function in Arabidopsis. The Plant Journal **45**, 1–16.

Dixon MS, Golstein C, Thomas CM, Van Der Biezen EA, Jones JDG. 2000. Genetic complexity of pathogen perception by plants: The example of Rcr3, a tomato gene required specifically by Cf-2. Proceedings of the National Academy of Sciences of the United States of America **97**, 8807–8814.

Doblas VG, Smakowska-Luzan E, Fujita S, Alassimone J, Barberon M, Madalinski M, Belkhadir Y, Geldner N. 2017. Root diffusion barrier control by a vasculature-derived peptide binding to the SGN3 receptor. Science **355**, 280–284.

Dodds PN, Rathjen JP. 2010. Plant immunity: towards an integrated view of plant–pathogen interactions. Nature Reviews Genetics **11**, 539–548.

Van der Does D, Boutrot F, Engelsdorf T, *et al.* 2017. The Arabidopsis leucine-rich repeat receptor kinase MIK2/LRR-KISS connects cell wall integrity sensing, root growth and response to abiotic and biotic stresses (A Cheung, Ed.). PLOS Genetics **13**, e1006832.

Domínguez-Ferreras A, Kiss-Papp M, Jehle AK, Felix G, Chinchilla D. 2015. An Overdose of the Arabidopsis Coreceptor BRASSINOSTEROID INSENSITIVE1-ASSOCIATED RECEPTOR KINASE1 or Its Ectodomain Causes Autoimmunity in a SUPPRESSOR OF BIR1-1-Dependent Manner. Plant physiology **168**, 1106–21.

Draeger C, Ndinyanka Fabrice T, Gineau E, *et al.* 2015. Arabidopsis leucine-rich repeat extensin (LRX) proteins modify cell wall composition and influence plant growth. BMC Plant Biology **15**, 155.

Dressano K, Ceciliato PHO, Silva AL, Guerrero-Abad JC, Bergonci T, Ortiz-Morea FA,

Bürger M, Silva-Filho MC, Moura DS. 2017. BAK1 is involved in AtRALF1-induced inhibition of root cell expansion (H Yu, Ed.). PLoS Genetics **13**, e1007053.

Du J, Verzaux E, Chaparro-Garcia A, *et al.* 2015. Elicitin recognition confers enhanced resistance to Phytophthora infestans in potato. Nature Plants **1**, 15034.

Duan Q, Kita D, Johnson EA, Aggarwal M, Gates L, Wu H-M, Cheung AY. 2014. Reactive oxygen species mediate pollen tube rupture to release sperm for fertilization in Arabidopsis. Nature communications **5**, 3129.

Duan Q, Kita D, Li C, Cheung AY, Wu H-M. 2010. FERONIA receptor-like kinase regulates RHO GTPase signaling of root hair development. Proceedings of the National Academy of Sciences of the United States of America **107**, 17821–6.

Dubiella U, Seybold H, Durian G, Komander E, Lassig R, Witte C-P, Schulze WX, Romeis T. 2013. Calcium-dependent protein kinase/NADPH oxidase activation circuit is required for rapid defense signal propagation. Proceedings of the National Academy of Sciences of the United States of America **110**, 8744–9.

Dufayard J-F, Bettembourg M, Fischer I, Droc G, Guiderdoni E, Périn C, Chantret N, Diévart A. 2017. New Insights on Leucine-Rich Repeats Receptor-Like Kinase Orthologous Relationships in Angiosperms. Frontiers in plant science **8**, 381.

Dünser K, Gupta S, Herger A, Feraru MI, Ringli C, Kleine-Vehn J. 2019. Extracellular matrix sensing by FERONIA and Leucine-Rich Repeat Extensins controls vacuolar expansion during cellular elongation in Arabidopsis thaliana . The EMBO Journal **38**.

Earley KW, Haag JR, Pontes O, Opper K, Juehne T, Song K, Pikaard CS. 2006. Gateway-compatible vectors for plant functional genomics and proteomics. Plant Journal **45**, 616–629.

Eckerstorfer MF, Engelhard M, Heissenberger A, Simon S, Teichmann H. 2019. Plants Developed by New Genetic Modification Techniques—Comparison of Existing Regulatory Frameworks in the EU and Non-EU Countries. Frontiers in Bioengineering and Biotechnology **7**, 26.

Eckshtain-Levi N, Weisberg AJ, Vinatzer BA. 2018. The population genetic test Tajima's D identifies genes encoding pathogen-associated molecular patterns and other virulence-related genes in Ralstonia solanacearum. Molecular Plant Pathology **19**, 2187–2192.

Ehrhardt DW, Wais R, Long SR. 1996. Calcium spiking in plant root hairs responding to Rhizobium nodulation signals. Cell **85**, 673–81.

Engelsdorf T, Gigli-Bisceglia N, Veerabagu M, McKenna JF, Vaahtera L, Augstein F, Does D Van der, Zipfel C, Hamann T. 2018. The plant cell wall integrity maintenance and immune signaling systems cooperate to control stress responses in Arabidopsis thaliana. Science Signaling **11**, eaao3070.

Engler C, Youles M, Gruetzner R, Ehnert T-M, Werner S, Jones JDG, Patron NJ, Marillonnet S. 2014. A Golden Gate Modular Cloning Toolbox for Plants. ACS Synthetic Biology **3**, 839–843.

Erwig J, Ghareeb H, Kopischke M, Hacke R, Matei A, Petutschnig E, Lipka V. 2017. Chitin-induced and CHITIN ELICITOR RECEPTOR KINASE1 (CERK1) phosphorylation-dependent endocytosis of Arabidopsis thaliana LYSIN MOTIF-CONTAINING RECEPTOR-LIKE KINASE5 (LYK5). New Phytologist **215**, 382–396.

Escamilla-Tilch M, Filio-Rodríguez G, García-Rocha R, Mancilla-Herrera I, Mitchison NA, Ruiz-Pacheco JA, Sánchez-García FJ, Sandoval-Borrego D, Vázquez-Sánchez EA. 2013. The interplay between pathogen-associated and danger-associated molecular patterns: An inflammatory code in cancer. Immunology and Cell Biology **91**, 601–610.

Escobar-Restrepo JM, Huck N, Kessler S, Gagliardini V, Gheyselinck J, Yang WC,

Grossniklaus U. 2007. The Feronia receptor-like kinase mediates male-female interactions during pollen tube reception. Science **317**, 656–660.

Eshed Y, Zamir D. 1995. An introgression line population of Lycopersicon pennellii in the cultivated tomato enables the identification and fine mapping of yield-associated QTL. Genetics **141**, 1147–62.

Espinoza C, Liang Y, Stacey G. 2017. Chitin receptor CERK1 links salt stress and chitin-triggered innate immunity in Arabidopsis. The Plant Journal **89**, 984–995.

Etchells JP, Turner SR. 2010. The PXY-CLE41 receptor ligand pair defines a multifunctional pathway that controls the rate and orientation of vascularcell division. Development **137**, 767–774.

Evans MJ, Choi W-G, Gilroy S, Morris RJ. 2016. A ROS-Assisted Calcium Wave Dependent on the AtRBOHD NADPH Oxidase and TPC1 Cation Channel Propagates the Systemic Response to Salt Stress. Plant Physiology **171**, 1771–1784.

Eves-Van Den Akker S, Lilley CJ, Yusup HB, Jones JT, Urwin PE. 2016. Functional C-TERMINALLY ENCODED PEPTIDE (CEP) plant hormone domains evolved *de novo* in the plant parasite *Rotylenchulus reniformis*. Molecular Plant Pathology **17**, 1265–1275.

Fabrice TN, Vogler H, Draeger C, Munglani G, Gupta S, Herger AG, Knox P, Grossniklaus U, Ringli C. 2018. LRX Proteins Play a Crucial Role in Pollen Grain and Pollen Tube Cell Wall Development. Plant physiology **176**, 1981–1992.

Falk A, Feys BJ, Frost LN, Jones JDG, Daniels MJ, Parker JE. 1999. EDS1, an essential component of R gene-mediated disease resistance in Arabidopsis has homology to eukaryotic lipases. Proceedings of the National Academy of Sciences of the United States of America **96**, 3292–3297.

Fan L. 2016. Identification of a novel receptor of bacterial PAMP RsE in Arabidopsis using genomic tools. Universität Tübingen.

Fan P, Wang H, Xue H, Rosas-Diaz T, Tang W, Zhang H, Xu L, Lozano-Duran R. 2019. The receptor-like kinases BAM1 and BAM2 promote the cell-to-cell movement of miRNA in the root stele to regulate xylem patterning. bioRxiv, 603415.

Faulkner C, Petutschnig E, Benitez-Alfonso Y, Beck M, Robatzek S, Lipka V, Maule AJ. 2013. LYM2-dependent chitin perception limits molecular flux via plasmodesmata. Proceedings of the National Academy of Sciences of the United States of America **110**, 9166–70.

Feijó JA, Wudick MM. 2018. 'Calcium is life'. Journal of Experimental Botany **69**, 4147–4150.

Felix G, Boller T. 2003. Molecular sensing of bacteria in plants: The highly conserved RNA-binding motif RNP-1 of bacterial cold shock proteins is recognized as an elicitor signal in tobacco. Journal of Biological Chemistry **278**, 6201–6208.

Felix G, Duran JD, Volko S, Boller T. 1999. Plants have a sensitive perception system for the most conserved domain of bacterial flagellin. Plant Journal **18**, 265–276.

Feng W, Kita D, Peaucelle A, *et al.* 2018. The FERONIA Receptor Kinase Maintains Cell-Wall Integrity during Salt Stress through Ca 2+ Signaling. Current Biology **28**, 666-675.e5.

Feng J, Li J, Gao Z, *et al.* 2015. SKIP Confers Osmotic Tolerance during Salt Stress by Controlling Alternative Gene Splicing in Arabidopsis. Molecular Plant **8**, 1038–1052.

Fernbach PM, Light N, Scott SE, Inbar Y, Rozin P. 2019. Extreme opponents of genetically modified foods know the least but think they know the most. Nature Human Behaviour **3**, 251–256.

Ferrari S, Savatin D V., Sicilia F, Gramegna G, Cervone F, De Lorenzo G. 2013.

Oligogalacturonides: Plant damage-associated molecular patterns and regulators of growth and development. Frontiers in Plant Science **4**, 49.

Fischer I, Diévart A, Droc G, Dufayard JF, Chantret N. 2016. Evolutionary dynamics of the leucine-rich repeat receptor-like kinase (LRR-RLK) subfamily in angiosperms. Plant Physiology **170**, 1595–1610.

Fisher K, Turner S. 2007. PXY, a Receptor-like Kinase Essential for Maintaining Polarity during Plant Vascular-Tissue Development. Current Biology **17**, 1061–1066.

Flannery S, Bowie AG. 2010. The interleukin-1 receptor-associated kinases: critical regulators of innate immune signalling. Biochemical pharmacology **80**, 1981–91.

Fletcher JC, Brand U, Running MP, Simon R, Meyerowitz EM. 1999. Signaling of Cell Fate Decisions by CLAVATA3 in Arabidopsis Shoot Meristems. Science **283**, 1911–1914.

Flury P, Klauser D, Schulze B, Boller T, Bartels S. 2013. The anticipation of danger: Microbe-associated molecular pattern perception enhances AtPep-triggered oxidative burst. Plant Physiology **161**, 2023–2035.

Foreman J, Demidchik V, Bothwell JHF, *et al.* 2003. Reactive oxygen species produced by NADPH oxidase regulate plant cell growth. Nature **422**, 442–446.

Fradin EF, Zhang Z, Juarez Ayala JC, Castroverde CDM, Nazar RN, Robb J, Liu C-M, Thomma BPHJ. 2009. Genetic dissection of Verticillium wilt resistance mediated by tomato Ve1. Plant physiology **150**, 320–32.

Fucile G, Di Biase D, Nahal H, La G, Khodabandeh S, Chen Y, Easley K, Christendat D, Kelley L, Provart NJ. 2011. Eplant and the 3D data display initiative: Integrative systems biology on the world wide web. PLoS ONE **6**, 15237.

Galindo-Trigo S, Blanco-Touriñán N, DeFalco TA, Wells ES, Gray JE, Zipfel C, Smith LM. 2019. CrRLK1L receptor-like kinases HERCULES RECEPTOR KINASE 1 and ANJEA are female determinants of pollen tube reception. bioRxiv, 428854.

Gamir J, Darwiche R, van't Hof P, Choudhary V, Stumpe M, Schneiter R, Mauch F. 2017. The sterol-binding activity of PATHOGENESIS-RELATED PROTEIN 1 reveals the mode of action of an antimicrobial protein. The Plant Journal **89**, 502–509.

Gao X, Ruan X, Sun Y, Wang X, Feng B. 2019. BAKing up to Survive a Battle: Functional Dynamics of BAK1 in Plant Programmed Cell Death. Frontiers in Plant Science **9**, 1913.

Gao M, Wang X, Wang D, *et al.* 2009. Regulation of Cell Death and Innate Immunity by Two Receptor-like Kinases in Arabidopsis. Cell Host and Microbe **6**, 34–44.

Gao Y, Wu Y, Du J, Zhan Y, Sun D, Zhao J, Zhang S, Li J, He K. 2017. Both light-induced SA accumulation and ETI mediators contribute to the cell death regulated by BAK1 and BKK1. Frontiers in Plant Science **8**, 622.

Gao L-L, Xue H-W. 2012. Global Analysis of Expression Profiles of Rice Receptor-Like Kinase Genes. Molecular Plant **5**, 143–153.

Ge Z, Bergonci T, Zhao Y, *et al.* 2017. Arabidopsis pollen tube integrity and sperm release are regulated by RALF-mediated signaling. Science **358**, 1596–1600.

Geisler M, Nadeau J, Sack FD. 2000. Oriented asymmetric divisions that generate the stomatal spacing pattern in arabidopsis are disrupted by the too many mouths mutation. The Plant cell **12**, 2075–86.

Geldner N, Hyman DL, Wang X, Schumacher K, Chory J. 2007. Endosomal signaling of plant steroid receptor kinase BRI1. Genes & Development **21**, 1598–1602.

Geng Y, Wu R, Wee CW, Xie F, Wei X, Chan PMY, Tham C, Duan L, Dinneny JR. 2013. A spatio-temporal understanding of growth regulation during the salt stress response in

Arabidopsis. Plant Cell **25**, 2132–2154.

Gigli-Bisceglia N, Engelsdorf T, Strnad M, *et al.* 2018. Cell wall integrity modulates Arabidopsis thaliana cell cycle gene expression in a cytokinin- and nitrate reductase-dependent manner. Development (Cambridge, England) **145**, dev166678.

Gimenez-Ibanez S, Hann DR, Ntoukakis V, Petutschnig E, Lipka V, Rathjen JP. 2009. AvrPtoB Targets the LysM Receptor Kinase CERK1 to Promote Bacterial Virulence on Plants. Current Biology **19**, 423–429.

Gish LA, Clark SE. 2011. The RLK/Pelle family of kinases. Plant Journal **66**, 117–127.

Göhre V, Spallek T, Häweker H, Mersmann S, Mentzel T, Boller T, de Torres M, Mansfield JW, Robatzek S. 2008. Plant Pattern-Recognition Receptor FLS2 Is Directed for Degradation by the Bacterial Ubiquitin Ligase AvrPtoB. Current Biology **18**, 1824–1832.

Gómez-Gómez L, Boller T. 2000. Fls2. Molecular Cell **5**, 1003–1011.

Gómez-Gómez L, Felix G, Boller T. 1999. A single locus determines sensitivity to bacterial flagellin in Arabidopsis thaliana. The Plant Journal **18**, 277–284.

Gonneau M, Desprez T, Martin M, *et al.* 2018. Receptor Kinase THESEUS1 Is a Rapid Alkalinization Factor 34 Receptor in Arabidopsis. Current Biology **28**, 2452-2458.e4.

Goodstein DM, Shu S, Howson R, *et al.* 2012. Phytozome: A comparative platform for green plant genomics. Nucleic Acids Research **40**, D1178-86.

Gordon TR. 2017. Fusarium oxysporum and the Fusarium Wilt Syndrome . Annual Review of Phytopathology **55**, 23–39.

Gou X, He K, Yang H, Yuan T, Lin H, Clouse SD, Li J. 2010. Genome-wide cloning and sequence analysis of leucine-rich repeat receptor-like protein kinase genes in Arabidopsis thaliana. BMC Genomics **11**, 19.

Grant SGN, Jessee J, Bloom FR, Hanahan D. 1990. Differential plasmid rescue from transgenic mouse DNAs into Escherichia coli methylation-restriction mutants. Proceedings of the National Academy of Sciences of the United States of America **87**, 4645–4649.

Grison MS, Kirk P, Brault ML, Wu XN, Schulze WX, Benitez-Alfonso Y, Immel F, Bayer EM. 2019. Plasma Membrane-Associated Receptor-like Kinases Relocalize to Plasmodesmata in Response to Osmotic Stress. Plant Physiology **181**, 142–160.

Gronnier J, Gerbeau-Pissot P, Germain V, Mongrand S, Simon-Plas F. 2018. *Divide and Rule: Plant Plasma Membrane Organization*.

Groom QJ, Torres MA, Fordham-Skelton AP, Hammond-Kosack KE, Robinson NJ, Jones JDG. 1996. rbohA, a rice homologue of the mammalian gp91phox respiratory burst oxidase gene. The Plant Journal **10**, 515–522.

Gully K, Hander T, Boller T, Bartels S. 2015. Perception of Arabidopsis At Pep peptides, but not bacterial elicitors, accelerates starvation-induced senescence. Frontiers in Plant Science **6**, 1–10.

Gully K, Pelletier S, Guillou M-C, *et al.* 2019. The SCOOP12 peptide regulates defense response and root elongation in *Arabidopsis thaliana*. Journal of Experimental Botany **70**, 1349–1365.

Gust AA, Felix G. 2014. Receptor like proteins associate with SOBIR1-type of adaptors to form bimolecular receptor kinases. Current Opinion in Plant Biology **21**, 104–111.

Gust AA, Pruitt R, Nürnberger T. 2017. Sensing Danger: Key to Activating Plant Immunity. Trends in Plant Science **22**, 779–791.

Hahlbrock K, Scheel D, Logemann E, Nürnberger T, Parniske M, Reinold S, Sacks WR, Schmelzer E. 1995. Oligopeptide elicitor-mediated defense gene activation in cultured

parsley cells. Proceedings of the National Academy of Sciences of the United States of America **92**, 4150–4157.

Halfon MS, Hashimoto C, Keshishian H. 1995. The Drosophila Toll gene functions zygotically and is necessary for proper motoneuron and muscle development. Developmental Biology **169**, 151–167.

Halter T, Imkampe J, Mazzotta S, *et al.* 2014. The Leucine-Rich Repeat Receptor Kinase BIR2 Is a Negative Regulator of BAK1 in Plant Immunity. Current Biology **24**, 134–143.

Hamann T, Bennett M, Mansfield J, Somerville C. 2009. Identification of cell-wall stress as a hexose-dependent and osmosensitive regulator of plant responses. The Plant Journal **57**, 1015–1026.

Han G. 2019. Origin and evolution of the plant immune system. New Phytologist **222**, 70–83.

Hanada K, Zou C, Lehti-Shiu MD, Shinozaki K, Shiu SH. 2008. Importance of lineage-specific expansion of plant tandem duplicates in the adaptive response to environmental stimuli. Plant Physiology **148**, 993–1003.

Hander T, Fernández-Fernández ÁD, Kumpf RP, *et al.* 2019. Damage on plants activates Ca 2+ -dependent metacaspases for release of immunomodulatory peptides. Science **363**, eaar7486.

Hao H, Fan L, Chen T, Li R, Li X, He Q, Botella MA, Lin J. 2014. Clathrin and membrane microdomains cooperatively regulate RbohD dynamics and activity in Arabidopsis. Plant Cell **26**, 1729–1745.

Hao G, Pitino M, Duan Y, Stover E. 2016. Reduced susceptibility to xanthomonas citri in transgenic citrus expressing the fls2 receptor from nicotiana benthamiana. Molecular Plant-Microbe Interactions **29**, 132–142.

Hara K, Kajita R, Torii KU, Bergmann DC, Kakimoto T. 2007. The secretory peptide gene EPF1 enforces the stomatal one-cell-spacing rule. Genes & development **21**, 1720–5.

Hara K, Yokoo T, Kajita R, Onishi T, Yahata S, Peterson KM, Torii KU, Kakimoto T. 2009. Epidermal Cell Density is Autoregulated via a Secretory Peptide, EPIDERMAL PATTERNING FACTOR 2 in Arabidopsis Leaves. Plant and Cell Physiology **50**, 1019–1031.

Haruta M, Sabat G, Stecker K, Minkoff BB, Sussman MR. 2014. A peptide hormone and its receptor protein kinase regulate plant cell expansion. Science **343**, 408–411.

Hazak O, Hardtke CS. 2016. CLAVATA 1-type receptors in plant development. Journal of Experimental Botany **67**, 4827–4833.

He Z-H, Cheeseman I, He D, Kohorn BD. 1996. A cluster of five cell wall-associated receptor kinase genes, Wak1–5, are expressed in specific organs of Arabidopsis. Plant Molecular Biology **39**, 1189–1196.

He K, Gou X, Yuan T, Lin H, Asami T, Yoshida S, Russell SD, Li J. 2007. BAK1 and BKK1 Regulate Brassinosteroid-Dependent Growth and Brassinosteroid-Independent Cell-Death Pathways. Current Biology **17**, 1109–1115.

He P, Shan L, Lin NC, Martin GB, Kemmerling B, Nürnberger T, Sheen J. 2006. Specific Bacterial Suppressors of MAMP Signaling Upstream of MAPKKK in Arabidopsis Innate Immunity. Cell **125**, 563–575.

He Z, Wang ZY, Li J, Zhu Q, Lamb C, Ronald P, Chory J. 2000. Perception of brassinosteroids by the extracellular domain of the receptor kinase BRI1. Science **288**, 2360–2363.

He Y, Zhou J, Shan L, Meng X. 2018. Plant cell surface receptor-mediated signaling - A common theme amid diversity. Journal of Cell Science **131**, jcs209353.

Heese A, Hann DR, Gimenez-Ibanez S, Jones AME, He K, Li J, Schroeder JI, Peck SC, Rathjen JP. 2007. The receptor-like kinase SERK3/BAK1 is a central regulator of innate immunity in plants. Proceedings of the National Academy of Sciences **104**, 12217–12222.

Hegenauer V, Furst U, Kaiser B, Smoker M, Zipfel C, Felix G, Stahl M, Albert M. 2016. Detection of the plant parasite Cuscuta reflexa by a tomato cell surface receptor. Science **353**, 478–481.

Hematy K, Sado P-E, Van Tuinen A, Rochange S, Desnos T, Balzergue S, Pelletier S, Renou J-P, Hofte H. 2007. A receptor-like kinase mediates the response of Arabidopsis cells to the inhibition of cellulose synthesis. Current Biology **17**, 922–931.

Herger A, Dünser K, Kleine-Vehn J, Ringli C. 2019. Leucine-Rich Repeat Extensin Proteins and Their Role in Cell Wall Sensing. Current Biology **29**, R851–R858.

Hernández-Blanco C, Feng DX, Hu J, *et al.* 2007. Impairment of cellulose synthases required for Arabidopsis secondary cell wall formation enhances disease resistance. Plant Cell **19**, 890–903.

Higashiyama T, Yang W-C. 2017. Gametophytic Pollen Tube Guidance: Attractant Peptides, Gametic Controls, and Receptors. Plant physiology **173**, 112–121.

Hillocks RJ. 2012. Farming with fewer pesticides: EU pesticide review and resulting challenges for UK agriculture. Crop Protection **31**, 85–93.

Hind SR, Strickler SR, Boyle PC, *et al.* 2016. Tomato receptor FLAGELLIN-SENSING 3 binds flgII-28 and activates the plant immune system. Nature Plants **2**, 16128.

Hirakawa Y, Kondo Y, Fukuda H. 2010. TDIF Peptide Signaling Regulates Vascular Stem Cell Proliferation via the *WOX4* Homeobox Gene in *Arabidopsis*. The Plant Cell **22**, 2618–2629.

Hirakawa Y, Shinohara H, Kondo Y, Inoue A, Nakanomyo I, Ogawa M, Sawa S, Ohashi-Ito K, Matsubayashi Y, Fukuda H. 2008. Non-cell-autonomous control of vascular stem cell fate by a CLE peptide/receptor system. Proceedings of the National Academy of Sciences of the United States of America **105**, 15208–15213.

Hiruma K, Gerlach N, Sacristán S, *et al.* 2016. Root Endophyte Colletotrichum tofieldiae Confers Plant Fitness Benefits that Are Phosphate Status Dependent. Cell **165**, 464–474.

Hogetsu T, Shibaoka H, Shimokoriyama M. 1974. Involvement of cellulose synthesis in actions of gibberellin and kinetin on cell expansion. 2,6-Dicholorobenzonitrile as a new cellulose-synthesis inhibitor. Plant and Cell Physiology **15**, 389–393.

Hohmann U, Hothorn M. 2019. Crystal structure of the leucine-rich repeat ectodomain of the plant immune receptor kinase SOBIR1. Acta Crystallographica Section D: Structural Biology **75**, 488–497.

Hohmann U, Lau K, Hothorn M. 2017. The Structural Basis of Ligand Perception and Signal Activation by Receptor Kinases. Annual Review of Plant Biology **68**.

Hohmann U, Nicolet J, Moretti A, Hothorn LA, Hothorn M. 2018*a*. Mechanistic analysis of the SERK3 elongated allele defines a role for BIR ectodomains in brassinosteroid signaling. Nature Plants, 1.

Hohmann U, Santiago J, Nicolet J, Olsson V, Spiga FM, Hothorn LA, Butenko MA, Hothorn M. 2018*b*. Mechanistic basis for the activation of plant membrane receptor kinases by SERK-family coreceptors. Proceedings of the National Academy of Sciences **115**.

Hok S, Allasia V, Andrio E, *et al.* 2014. The receptor kinase IMPAIRED OOMYCETE SUSCEPTIBILITY1 attenuates abscisic acid responses in Arabidopsis. Plant physiology **166**, 1506–18.

Hok S, Danchin EGJ, Allasia V, Panabières F, Attard A, Keller H. 2011. An Arabidopsis

(malectin-like) leucine-rich repeat receptor-like kinase contributes to downy mildew disease. Plant, Cell and Environment **34**, 1944–1957.

Holmes DR, Grubb LE, Monaghan J. 2018. The jasmonate receptor COI1 is required for AtPep1-induced immune responses in Arabidopsis thaliana. BMC Research Notes **11**, 555.

Holton N, Nekrasov V, Ronald PC, Zipfel C. 2015. The phylogenetically-related pattern recognition receptors EFR and XA21 recruit similar immune signaling components in monocots and dicots. PLoS pathogens **11**, e1004602.

Holzwart E, Huerta AI, Glöckner N, Garnelo Gómez B, Wanke F, Augustin S, Askani JC, Schürholz AK, Harter K, Wolf S. 2018. BRI1 controls vascular cell fate in the Arabidopsis root through RLP44 and phytosulfokine signaling. Proceedings of the National Academy of Sciences of the United States of America **115**, 11838–11843.

Hooper CM, Castleden IR, Tanz SK, Aryamanesh N, Millar AH. 2017. SUBA4: the interactive data analysis centre for Arabidopsis subcellular protein locations. Nucleic Acids Research **45**, D1064–D1074.

Horsch RB, Fry JE, Hoffmann NL, Eichholtz D, Rogers SG, Fraley RT. 1985. A simple and general method for transferring genes into plants.

Hothorn M, Belkhadir Y, Dreux M, Dabi T, Noel JP, Wilson IA, Chory J. 2011. Structural basis of steroid hormone perception by the receptor kinase BRI1. Nature **474**, 467–472.

Hou S, Liu Z, Shen H, Wu D. 2019. Damage-Associated Molecular Pattern-Triggered Immunity in Plants. Frontiers in Plant Science **10**, 646.

Hou S, Wang X, Chen D, Yang X, Wang M, Turrà D, Di Pietro A, Zhang W. 2014. The secreted peptide PIP1 amplifies immunity through receptor-like kinase 7. PLoS pathogens **10**, e1004331.

Hu H, Wang JJ, Shi C, *et al.* 2015. A receptor like kinase gene with expressional responsiveness on Xanthomonas oryzae pv. oryzae is essential for Xa21-mediated disease resistance. Rice **8**, 34.

Hu C, Zhu Y, Cui Y, *et al.* 2018. A group of receptor kinases are essential for CLAVATA signalling to maintain stem cell homeostasis. **4**.

Huang P-Y, Yeh Y-H, Liu A-C, Cheng C-P, Zimmerli L. 2014. The Arabidopsis LecRK-VI.2 associates with the pattern-recognition receptor FLS2 and primes *Nicotiana benthamiana* pattern-triggered immunity. The Plant Journal **79**, 243–255.

Huck N, Moore JM, Federer M, Grossniklaus U. 2003. The Arabidopsis mutant feronia disrupts the female gametophytic control of pollen tube reception. Development **130**, 2149–2159.

Huffaker A, Dafoe NJ, Schmelz EA. 2011. ZmPep1, an ortholog of arabidopsis elicitor peptide 1, regulates maize innate immunity and enhances disease resistance. Plant Physiology **155**, 1325–1338.

Huffaker A, Pearce G, Ryan CA. 2006. An endogenous peptide signal in Arabidopsis activates components of the innate immune response. Proceedings of the National Academy of Sciences of the United States of America **103**, 10098–103.

Humphry M, Bednarek P, Kemmerling B, *et al.* 2010. A regulon conserved in monocot and dicot plants defines a functional module in antifungal plant immunity. Proceedings of the National Academy of Sciences of the United States of America **107**, 21896–901.

Hunt L, Bailey KJ, Gray JE. 2010. The signalling peptide EPFL9 is a positive regulator of stomatal development. New Phytologist **186**, 609–614.

Hunt L, Gray JE. 2009. The Signaling Peptide EPF2 Controls Asymmetric Cell Divisions during Stomatal Development. Current Biology **19**, 864–869.

Hurst CH, Turnbull D, Myles SM, Leslie K, Keinath NF, Hemsley PA. 2018. Variable Effects of C-Terminal Fusions on FLS2 Function: Not All Epitope Tags Are Created Equal. Plant Physiology **177**, 522–531.

Hutten SJ, Hamers DS, Aan den Toorn M, van Esse W, Nolles A, Bücherl CA, de Vries SC, Hohlbein J, Borst JW. 2017. Visualization of BRI1 and SERK3/BAK1 Nanoclusters in Arabidopsis Roots (M Otegui, Ed.). PLOS ONE **12**, e0169905.

Igarashi D, Tsuda K, Katagiri F. 2012. The peptide growth factor, phytosulfokine, attenuates pattern-triggered immunity. The Plant Journal **71**, 194–204.

Imin N, Mohd-Radzman NA, Ogilvie HA, Djordjevic MA. 2013. The peptide-encoding CEP1 gene modulates lateral root and nodule numbers in Medicago truncatula. Journal of Experimental Botany **64**, 5395–5409.

Imin N, Patel N, Corcilius L, Payne RJ, Djordjevic MA. 2018. CLE peptide tri-arabinosylation and peptide domain sequence composition are essential for SUNN-dependent autoregulation of nodulation in *Medicago truncatula*. New Phytologist **218**, 73–80.

Irieda H, Inoue Y, Mori M, *et al.* 2019. Conserved fungal effector suppresses PAMP-triggered immunity by targeting plant immune kinases. Proceedings of the National Academy of Sciences of the United States of America **116**, 496–505.

Ito Y, Kaku H, Shibuya N. 1997. Identification of a high-affinity binding protein for N-acetylchitooligosaccharide elicitor in the plasma membrane of suspension-cultured rice cells by affinity labeling. The Plant Journal **12**, 347–356.

Ito Y, Nakanomyo I, Motose H, Iwamoto K, Sawa S, Dohmae N, Fukuda H. 2006. Dodeca-CLE as peptides as suppressors of plant stem cell differentiation. Science **313**, 842–845.

Jaillais Y, Hothorn M, Belkhadir Y, Dabi T, Nimchuk ZL, Meyerowitz EM, Chory J. 2011. Tyrosine phosphorylation controls brassinosteroid receptor activation by triggering membrane release of its kinase inhibitor. Genes and Development **25**, 232–237.

Janeway CA. 1992. The immune system evolved to discriminate infectious nonself from noninfectious self. Immunology Today **13**, 11–16.

Jehle AK, Lipschis M, Albert M, Fallahzadeh-Mamaghani V, Fürst U, Mueller K, Felix G. 2013. The receptor-like protein ReMAX of Arabidopsis detects the microbe-associated molecular pattern eMax from Xanthomonas. The Plant cell **25**, 2330–40.

Jia G, Liu X, Owen HA, Zhao D. 2008. Signaling of cell fate determination by the TPD1 small protein and EMS1 receptor kinase. Proceedings of the National Academy of Sciences **105**, 2220–2225.

Jiang Y, Han B, Zhang H, Mariappan KG, Bigeard J, Colcombet J, Hirt H. 2019*a*. MAP 4K4 associates with BIK 1 to regulate plant innate immunity . EMBO reports, e47965.

Jiang Z, Zhou X, Tao M, *et al.* 2019*b*. Plant cell-surface GIPC sphingolipids sense salt to trigger Ca2+ influx. Nature, 1–6.

Jinn TL, Stone JM, Walker JC. 2000. HAESA, an Arabidopsis leucine-rich repeat receptor kinase, controls floral organ abscission. Genes & development **14**, 108–17.

Jones JDG, Dangl JL. 2006. The plant immune system. Nature **444**, 323–9.

Jones D, Thomas C, Hammond-Kosack K, Balint-Kurti P, Jones J. 1994. Isolation of the tomato Cf-9 gene for resistance to Cladosporium fulvum by transposon tagging. Science **266**, 789–793.

De Jonge R, Van Esse HP, Kombrink A, Shinya T, Desaki Y, Bours R, Van Der Krol S, Shibuya N, Joosten MHAJ, Thomma BPHJ. 2010. Conserved fungal LysM effector Ecp6 prevents chitin-triggered immunity in plants. Science **329**, 953–955.

Jordá L, Sopeña-Torres S, Escudero V, Nuñez-Corcuera B, Delgado-Cerezo M, Torii KU, Molina A. 2016. ERECTA and BAK1 receptor like kinases interact to regulate immune responses in Arabidopsis. Frontiers in Plant Science **7**, 897.

Julkowska MM, Klei K, Fokkens L, Haring MA, Schranz ME, Testerink C. 2016. Natural variation in rosette size under salt stress conditions corresponds to developmental differences between Arabidopsis accessions and allelic variation in the LRR-KISS gene. Journal of experimental botany **67**, 2127–2138.

Jun J, Fiume E, Roeder AHK, *et al.* 2010. Comprehensive analysis of CLE polypeptide signaling gene expression and overexpression activity in Arabidopsis. Plant physiology **154**, 1721–36.

Jupe F, Rivkin AC, Michael TP, *et al.* 2019. The complex architecture and epigenomic impact of plant T-DNA insertions (J Schmutz, Ed.). PLoS Genetics **15**, e1007819.

Kadota Y, Goh T, Tomatsu H, Tamauchi R, Higashi K, Muto S, Kuchitsu K. 2004. Cryptogein-Induced Initial Events in Tobacco BY-2 Cells: Pharmacological Characterization of Molecular Relationship among Cytosolic Ca2+ Transients, Anion Efflux and Production of Reactive Oxygen Species. Plant and Cell Physiology **45**, 160–170.

Kadota Y, Shirasu K, Zipfel C. 2015. Regulation of the NADPH Oxidase RBOHD During Plant Immunity. Plant and Cell Physiology **56**, 1472–1480.

Kadota Y, Sklenar J, Derbyshire P, *et al.* 2014. Direct regulation of the NADPH oxidase RBOHD by the PRR-associated kinase BIK1 during plant immunity. Molecular cell **54**, 43–55.

Kaku H, Nishizawa Y, Ishii-Minami N, Akimoto-Tomiyama C, Dohmae N, Takio K, Minami E, Shibuya N. 2006. Plant cells recognize chitin fragments for defense signaling through a plasma membrane receptor. Proceedings of the National Academy of Sciences of the United States of America **103**, 11086–91.

Karlova R, Boeren S, van Dongen W, Kwaaitaal M, Aker J, Vervoort J, de Vries S. 2009. Identification of in vitro phosphorylation sites in the Arabidopsis thaliana somatic embryogenesis receptor-like kinases. PROTEOMICS **9**, 368–379.

Katz C, Levy-Beladev L, Rotem-Bamberger S, Rito T, Rüdiger SGD, Friedler A. 2011. Studying protein-protein interactions using peptide arrays. Chemical Society Reviews **40**, 2131–2145.

Kawaharada Y, Kelly S, Nielsen MW, *et al.* 2015. Receptor-mediated exopolysaccharide perception controls bacterial infection. Nature **523**, 308–312.

Kawamoto N, Carpio DP Del, Hofmann A, *et al.* 2019. A peptide pair coordinates regular ovule initiation patterns with seed number and fruit size. bioRxiv, 736439.

Kaya H, Iwano M, Takeda S, Kanaoka MM, Kimura S, Abe M, Kuchitsu K. 2015. Apoplastic ROS production upon pollination by RbohH and RbohJ in Arabidopsis. Plant Signaling & Behavior **10**, e989050.

Kaya H, Nakajima R, Iwano M, *et al.* 2014. Ca $^{2+}$ -Activated Reactive Oxygen Species Production by *Arabidopsis* RbohH and RbohJ Is Essential for Proper Pollen Tube Tip Growth. The Plant Cell **26**, 1069–1080.

Keegstra K. 2010. Plant Cell Walls: Figure 1. Plant Physiology **154**, 483–486.

Kelly SJ, Muszyński A, Kawaharada Y, Hubber AM, Sullivan JT, Sandal N, Carlson RW, Stougaard J, Ronson CW. 2013. Conditional Requirement for Exopolysaccharide in the *Mesorhizobium–Lotus* Symbiosis. Molecular Plant-Microbe Interactions **26**, 319–329.

Kemmerling B, Schwedt A, Rodriguez P, *et al.* 2007. The BRI1-Associated Kinase 1, BAK1, Has a Brassinolide-Independent Role in Plant Cell-Death Control. Current Biology

17, 1116–1122.

Kereszt A, Mergaert P, Montiel J, Endre G, Kondorosi É. 2018. Impact of plant peptides on symbiotic nodule development and functioning. Frontiers in Plant Science **9**, 1026.

Kessler SA, Shimosato-Asano H, Keinath NF, Wuest SE, Ingram G, Panstruga R, Grossniklaus U. 2010. Conserved molecular components for pollen tube reception and fungal invasion. Science **330**, 968–971.

Kilby NJ, Leyser HM, Furner IJ. 1992. Promoter methylation and progressive transgene inactivation in Arabidopsis. Plant molecular biology **20**, 103–12.

Kilian J, Whitehead D, Horak J, Wanke D, Weinl S, Batistic O, D'Angelo C, Bornberg-Bauer E, Kudla J, Harter K. 2007. The AtGenExpress global stress expression data set: protocols, evaluation and model data analysis of UV-B light, drought and cold stress responses. The Plant Journal **50**, 347–363.

Kim TW, Guan S, Burlingame AL, Wang ZY. 2011. The CDG1 Kinase Mediates Brassinosteroid Signal Transduction from BRI1 Receptor Kinase to BSU1 Phosphatase and GSK3-like Kinase BIN2. Molecular Cell **43**, 561–571.

Kim J, Yang R, Chang C, Park Y, Tucker ML. 2018. The root-knot nematode Meloidogyne incognita produces a functional mimic of the Arabidopsis INFLORESCENCE DEFICIENT IN ABSCISSION signaling peptide. Journal of Experimental Botany **69**, 3009–3021.

Kimura S, Hunter K, Vaahtera L, *et al.* 2019. CRK2 and C-terminal phosphorylation of NADPH oxidase RBOHD regulate ROS production in Arabidopsis. bioRxiv, 618819.

Kishimoto K, Kouzai Y, Kaku H, Shibuya N, Minami E, Nishizawa Y. 2010. Perception of the chitin oligosaccharides contributes to disease resistance to blast fungus Magnaporthe oryzae in rice. Plant Journal **64**, 343–354.

Kishimoto K, Kouzai Y, Kaku H, Shibuya N, Minami E, Nishizawa Y. 2011. Enhancement of MAMP signaling by chimeric receptors improves disease resistance in plants. Plant Signaling and Behavior **6**, 449–451.

Knight MR, Campbell AK, Smith SM, Trewavas AJ. 1991. Transgenic plant aequorin reports the effects of touch and cold-shock and elicitors on cytoplasmic calcium. Nature **352**, 524–526.

Kock C, Dufrêne YF, Heinisch JJ. 2015. Up against the wall: Is yeast cell wall integrity ensured by mechanosensing in plasma membrane microdomains? Applied and Environmental Microbiology **81**, 806–811.

Kohorn BD, Kobayashi M, Johansen S, Riese J, Huang LF, Koch K, Fu S, Dotson A, Byers N. 2006. An Arabidopsis cell wall-associated kinase required for invertase activity and cell growth. Plant Journal **46**, 307–316.

Komis G, Šamajová O, Ovečka M, Šamaj J. 2018. Cell and Developmental Biology of Plant Mitogen-Activated Protein Kinases. Annual Review of Plant Biology **69**, 237–265.

Komori R, Amano Y, Ogawa-Ohnishi M, Matsubayashi Y. 2009. Identification of tyrosylprotein sulfotransferase in Arabidopsis. Proceedings of the National Academy of Sciences of the United States of America **106**, 15067–72.

Koncz C, Schell J. 1986. The promoter of TL-DNA gene 5 controls the tissue-specific expression of chimaeric genes carried by a novel type of Agrobacterium binary vector. MGG Molecular & General Genetics **204**, 383–396.

Kondo T, Kajita R, Miyazaki A, *et al.* 2010. Stomatal density is controlled by a mesophyll-derived signaling molecule. Plant and Cell Physiology **51**, 1–8.

Kong Q, Sun T, Qu N, Ma J, Li M, Cheng Y, Zhang Q, Wu D, Zhang Z, Zhang Y. 2016. Two redundant receptor-like cytoplasmic kinases function downstream of pattern recognition

receptors to regulate activation of SA biosynthesis in Arabidopsis. Plant Physiology **171**, pp.01954.2015.

Kourelis J, Van Der Hoorn RAL. 2018. Defended to the nines: 25 years of resistance gene cloning identifies nine mechanisms for R protein function. Plant Cell **30**, 285–299.

Kouzai Y, Kaku H, Shibuya N, Minami E, Nishizawa Y. 2013. Expression of the chimeric receptor between the chitin elicitor receptor CEBiP and the receptor-like protein kinase Pi-d2 leads to enhanced responses to the chitin elicitor and disease resistance against Magnaporthe oryzae in rice. Plant Molecular Biology **81**, 287–295.

Krogh A, Larsson B, Von Heijne G, Sonnhammer ELL. 2001. Predicting transmembrane protein topology with a hidden Markov model: Application to complete genomes. Journal of Molecular Biology **305**, 567–580.

Krol E, Mentzel T, Chinchilla D, *et al.* 2010. Perception of the Arabidopsis danger signal peptide 1 involves the pattern recognition receptor AtPEPR1 and its close homologue AtPEPR2. The Journal of biological chemistry **285**, 13471–9.

Kruijt M, De Kock MJD, De Wit PJGM. 2005. Receptor-like proteins involved in plant disease resistance. Molecular Plant Pathology **6**, 85–97.

Kumar S, Stecher G, Suleski M, Hedges SB. 2017. TimeTree: A Resource for Timelines, Timetrees, and Divergence Times. Molecular Biology and Evolution **34**, 1812–1819.

Kumpf RP, Shi C-L, Larrieu A, Stø IM, Butenko MA, Péret B, Riiser ES, Bennett MJ, Aalen RB. 2013. Floral organ abscission peptide IDA and its HAE/HSL2 receptors control cell separation during lateral root emergence. Proceedings of the National Academy of Sciences of the United States of America **110**, 5235–40.

Kunwar S, Iriarte F, Fan Q, *et al.* 2018. Transgenic expression of EFR and Bs2 genes for field management of bacterial wilt and bacterial spot of tomato. Phytopathology **108**, 1402–1411.

Kunze G, Zipfel C, Robatzek S, Niehaus K, Boller T, Felix G. 2004. The N terminus of bacterial elongation factor Tu elicits innate immunity in Arabidopsis plants. Plant Cell **16**, 3496–3507.

Kutschera A, Dawid C, Gisch N, *et al.* 2019. Bacterial medium-chain 3-hydroxy fatty acid metabolites trigger immunity in Arabidopsis plants. Science **364**, 178–181.

Kwaaitaal MACJ, De Vries SC, Russinova E. 2005. Arabidopsis thaliana Somatic Embryogenesis Receptor Kinase 1 protein is present in sporophytic and gametophytic cells and undergoes endocytosis. Protoplasma **226**, 55–65.

Kwak JM, Mori IC, Pei ZM, *et al.* 2003. NADPH oxidase AtrbohD and AtrbohF genes function in ROS-dependent ABA signaling in arabidopsis. EMBO Journal **22**, 2623–2633.

Lacombe S, Rougon-Cardoso A, Sherwood E, *et al.* 2010. Interfamily transfer of a plant pattern-recognition receptor confers broad-spectrum bacterial resistance. Nature Biotechnology **28**, 365–369.

Lal NK, Nagalakshmi U, Hurlburt NK, *et al.* 2018. The Receptor-like Cytoplasmic Kinase BIK1 Localizes to the Nucleus and Regulates Defense Hormone Expression during Plant Innate Immunity. Cell Host and Microbe **23**, 485-497.e5.

Van Larebeke N, Engler G, Holsters M, Van Den Elsacker S, Zaenen I, Schilperoort RA, Schell J. 1974. Large plasmid in agrobacterium tumefaciens essential for crown gall-inducing ability. Nature **252**, 169–170.

Le MH, Cao Y, Zhang X-C, Stacey G. 2014. LIK1, a CERK1-interacting kinase, regulates plant immune responses in Arabidopsis. PloS one **9**, e102245.

Lee JY, Colinas J, Wang JY, Mace D, Ohler U, Benfey PN. 2006. Transcriptional and

posttranscriptional regulation of transcription factor expression in Arabidopsis roots. Proceedings of the National Academy of Sciences of the United States of America **103**, 6055–6060.

Lee IC, Hong SW, Whang SS, Lim PO, Nam HG, Koo JC. 2011. Age-dependent action of an ABA-inducible receptor kinase, RPK1, as a positive regulator of senescence in arabidopsis leaves. Plant and Cell Physiology **52**, 651–662.

Lee DS, Kim YC, Kwon SJ, Ryu C-M, Park OK. 2017. The Arabidopsis Cysteine-Rich Receptor-Like Kinase CRK36 Regulates Immunity through Interaction with the Cytoplasmic Kinase BIK1. Frontiers in Plant Science **8**, 1856.

Lee JS, Kuroha T, Hnilova M, Khatayevich D, Kanaoka MM, McAbee JM, Sarikaya M, Tamerler C, Torii KU. 2012. Direct interaction of ligand-receptor pairs specifying stomatal patterning. Genes & development **26**, 126–36.

Lee Y, Rubio MC, Alassimone J, Geldner N. 2013. A Mechanism for Localized Lignin Deposition in the Endodermis. Cell **153**, 402–412.

Lee Y, Yoon TH, Lee JHJ, *et al.* 2018. A Lignin Molecular Brace Controls Precision Processing of Cell Walls Critical for Surface Integrity in Arabidopsis. Cell **173**, 1468-1480.e9.

Lehti-Shiu MD, Zou C, Hanada K, Shiu S-H. 2009. Evolutionary history and stress regulation of plant receptor-like kinase/pelle genes. Plant physiology **150**, 12–26.

Lehti-Shiu MD, Zou C, Shiu S-H. 2012. *Origin, Diversity, Expansion History, and Functional Evolution of the Plant Receptor-Like Kinase/Pelle Family* (F Tax and B Kemmerling, Eds.). Springer Berlin Heidelberg.

Lemaitre B, Nicolas E, Michaut L, Reichhart J-M, Hoffmann JA. 1996. The Dorsoventral Regulatory Gene Cassette spätzle/Toll/cactus Controls the Potent Antifungal Response in Drosophila Adults. Cell **86**, 973–983.

Leslie ME, Lewis MW, Youn JY, Daniels MJ, Liljegren SJ. 2010. The EVERSHED receptor-like kinase modulates floral organ shedding in Arabidopsis. Development **137**, 467–476.

Letunic I, Bork P. 2019. Interactive Tree Of Life (iTOL) v4: recent updates and new developments. Nucleic Acids Research **47**, W256–W259.

Levin DE. 2011. Regulation of cell wall biogenesis in Saccharomyces cerevisiae: the cell wall integrity signaling pathway. Genetics **189**, 1145–1175.

Leyser HMO, Furner IJ. 1992. Characterisation of three shoot apical meristem mutants of Arabidopsis thaliana. Development **116**, 397–403.

Li J, Chory J. 1997. A Putative Leucine-Rich Repeat Receptor Kinase Involved in Brassinosteroid Signal Transduction. Cell **90**, 929–938.

Li L, Kim P, Yu L, Cai G, Chen S, Alfano JR, Zhou JM. 2016. Activation-Dependent Destruction of a Co-receptor by a Pseudomonas syringae Effector Dampens Plant Immunity. Cell Host and Microbe **20**, 504–514.

Li L, Li M, Yu L, *et al.* 2014. The FLS2-associated kinase BIK1 directly phosphorylates the NADPH oxidase RbohD to control plant immunity. Cell Host and Microbe **15**, 329–338.

Li J, Wen J, Lease KA, Doke JT, Tax FE, Walker JC. 2002. BAK1, an Arabidopsis LRR receptor-like protein kinase, interacts with BRI1 and modulates brassinosteroid signaling. Cell **110**, 213–222.

Li C, Yeh FL, Cheung AY, *et al.* 2015. Glycosylphosphatidylinositol-anchored proteins as chaperones and co-receptors for FERONIA receptor kinase signaling in Arabidopsis. eLife **4**, 1–21.

Liang X, Ding P, Lian K, *et al.* 2016. Arabidopsis heterotrimeric G proteins regulate immunity by directly coupling to the FLS2 receptor. eLife **5**, e13568.

Liang P, Stratil TF, Popp C, Marín M, Folgmann J, Mysore KS, Wen J, Ott T. 2018. Symbiotic root infections in Medicago truncatula require remorin-mediated receptor stabilization in membrane nanodomains. Proceedings of the National Academy of Sciences of the United States of America **115**, 5289–5294.

Liang X, Zhou J-M. 2018. Receptor-Like Cytoplasmic Kinases: Central Players in Plant Receptor Kinase–Mediated Signaling. Annual Review of Plant Biology **69**, 267–299.

Liao D, Cao Y, Sun X, Espinoza C, Nguyen CT, Liang Y, Stacey G. 2017. Arabidopsis E3 ubiquitin ligase PLANT U-BOX13 (PUB13) regulates chitin receptor LYSIN MOTIF RECEPTOR KINASE5 (LYK5) protein abundance. New Phytologist **214**, 1646–1656.

Liebrand TWH, van den Berg GCM, Zhang Z, *et al.* 2013. Receptor-like kinase SOBIR1/EVR interacts with receptor-like proteins in plant immunity against fungal infection. Proceedings of the National Academy of Sciences of the United States of America **110**, 10010–5.

Liebrand TWH, van den Burg HA, Joosten MHAJ. 2014. Two for all: receptor-associated kinases SOBIR1 and BAK1. Trends in plant science **19**, 123–32.

Lin J-X, Leonard WJ. 2019. Fine-Tuning Cytokine Signals. Annual Review of Immunology **37**, 295–324.

Lin Z-JD, Liebrand TWH, Yadeta KA, Coaker G. 2015. PBL13 Is a Serine/Threonine Protein Kinase That Negatively Regulates Arabidopsis Immune Responses. Plant physiology **169**, 2950–62.

Lin W, Ma X, Shan L, He P. 2013. Big Roles of Small Kinases: The Complex Functions of Receptor-Like Cytoplasmic Kinases in Plant Immunity and Development. Journal of Integrative Plant Biology **55**, 1188–1197.

Lin W, Tang W, Anderson CT, Yang Z. 2018. FERONIA's sensing of cell wall pectin activates ROP GTPase signaling in Arabidopsis. bioRxiv, 269647.

Lin G, Zhang L, Han Z, Yang X, Liu W, Li E, Chang J, Qi Y, Shpak ED, Chai J. 2017. A receptor-like protein acts as a specificity switch for the regulation of stomatal development. Genes & development **31**, 927–938.

Lindner H, Müller LM, Boisson-Dernier A, Grossniklaus U. 2012. CrRLK1L receptor-like kinases: Not just another brick in the wall. Current Opinion in Plant Biology **15**, 659–669.

Liu T, Liu Z, Song C, *et al.* 2012. Chitin-induced dimerization activates a plant immune receptor. Science **336**, 1160–1164.

Liu Z, Wu Y, Yang F, Zhang Y, Chen S, Xie Q, Tian X, Zhou J-M. 2013*a*. BIK1 interacts with PEPRs to mediate ethylene-induced immunity. Proceedings of the National Academy of Sciences of the United States of America **110**, 6205–10.

Liu J, Zhong S, Guo X, *et al.* 2013*b*. Membrane-bound RLCKs LIP1 and LIP2 are essential male factors controlling male-female attraction in Arabidopsis. Current Biology **23**, 993–998.

De Lorenzo G, Brutus A, Savatin DV, Sicilia F, Cervone F. 2011. Engineering plant resistance by constructing chimeric receptors that recognize damage-associated molecular patterns (DAMPs). FEBS letters **585**, 1521–8.

Lori M, Van Verk MC, Hander T, Schatowitz H, Klauser D, Flury P, Gehring CA, Boller T, Bartels S. 2015. Evolutionary divergence of the plant elicitor peptides (Peps) and their receptors: Interfamily incompatibility of perception but compatibility of downstream signalling. Journal of Experimental Botany **66**, 5315–5325.

Loria R, Bukhalid RA, Fry BA, King RR. 1997. PLANT PATHOGENICITY IN THE GENUS *STREPTOMYCES*. Plant Disease **81**, 836–846.

Lozano-Torres JL, Wilbers RHP, Gawronski P, *et al.* 2012. Dual disease resistance mediated by the immune receptor Cf-2 in tomato requires a common virulence target of a fungus and a nematode. Proceedings of the National Academy of Sciences of the United States of America **109**, 10119–10124.

Lu S-W, Chen S, Wang J, Yu H, Chronis D, Mitchum MG, Wang X. 2009. Structural and Functional Diversity of *CLAVATA3/ESR* (*CLE*)-Like Genes from the Potato Cyst Nematode *Globodera rostochiensis*. Molecular Plant-Microbe Interactions **22**, 1128–1142.

Lu D, Lin W, Gao X, Wu S, Cheng C, Avila J, Heese A, Devarenne TP, He P, Shan L. 2011. Direct ubiquitination of pattern recognition receptor FLS2 attenuates plant innate immunity. Science **332**, 1439–1442.

Lu F, Wang H, Wang S, Jiang W, Shan C, Li B, Yang J, Zhang S, Sun W. 2015. Enhancement of innate immune system in monocot rice by transferring the dicotyledonous elongation factor Tu receptor EFR. Journal of Integrative Plant Biology **57**, 641–652.

Lu D, Wu S, Gao X, Zhang Y, Shan L, He P. 2010. A receptor-like cytoplasmic kinase, BIK1, associates with a flagellin receptor complex to initiate plant innate immunity. Proceedings of the National Academy of Sciences of the United States of America **107**, 496–501.

Van Der Luit AH, Olivari C, Haley A, Knight MR, Trewavas AJ. 1999. Distinct calcium signaling pathways regulate calmodulin gene expression in tobacco. Plant Physiology **121**, 705–714.

Luo L. 2012. Plant cytokine or phytocytokine. Plant Signaling and Behavior **7**, 1513–4.

Luu DD, Joe A, Chen Y, *et al.* 2019. Biosynthesis and secretion of the microbial sulfated peptide RaxX and binding to the rice XA21 immune receptor. Proceedings of the National Academy of Sciences of the United States of America **116**, 8525–8534.

Ma S, Gong Q, Bohnert HJ. 2006. Dissecting salt stress pathways. Journal of experimental botany **57**, 1097–107.

Ma C, Liu Y, Bai B, Han Z, Tang J, Zhang H, Yaghmaiean H, Zhang Y, Chai J. 2017*a*. Structural basis for BIR1-mediated negative regulation of plant immunity. Cell Research **27**, 1521–1524.

Ma X, Xu G, He P, Shan L. 2016. SERKing Coreceptors for Receptors. Trends in Plant Science **21**, 1017–1033.

Ma Y, Zhao Y, Berkowitz GA. 2017*b*. Intracellular Ca2+ is important for flagellin-triggered defense in Arabidopsis and involves inositol polyphosphate signaling. Journal of Experimental Botany **68**, 3617–3628.

Macho AP, Boutrot F, Rathjen JP, Zipfel C. 2012. Aspartate oxidase plays an important role in Arabidopsis stomatal immunity. Plant physiology **159**, 1845–56.

Macho AP, Schwessinger B, Ntoukakis V, *et al.* 2014. A bacterial tyrosine phosphatase inhibits plant pattern recognition receptor activation. Science **343**, 1509–1512.

Mahmood K, Kannangara R, Jørgensen K, Fuglsang AT. 2014. Analysis of peptide PSY1 responding transcripts in the two Arabidopsis plant lines: wild type and psy1r receptor mutant. BMC Genomics **15**, 441.

Majhi BB, Sreeramulu S, Sessa G. 2019. Brassinosteroid-signaling kinase5 associates with immune receptors and is required for immune responses1. Plant Physiology **180**, 1166–1184.

Mang H, Feng B, Hu Z, *et al.* 2017. Differential Regulation of Two-Tiered Plant Immunity and Sexual Reproduction by ANXUR Receptor-Like Kinases. The Plant cell **29**, 3140–3156.

Martins S, Dohmann EMN, Cayrel A, *et al.* 2015. Internalization and vacuolar targeting of the brassinosteroid hormone receptor BRI1 are regulated by ubiquitination. Nature Communications **6**, 6151.

Masachis S, Segorbe D, Turrà D, *et al.* 2016. A fungal pathogen secretes plant alkalinizing peptides to increase infection. Nature Microbiology **1**, 16043.

Matsubayashi Y. 2014. Posttranslationally Modified Small-Peptide Signals in Plants. Annual Review of Plant Biology **65**, 385–413.

Matsubayashi Y, Ogawa M, Kihara H, Niwa M, Sakagami Y. 2006. Disruption and overexpression of Arabidopsis phytosulfokine receptor gene affects cellular longevity and potential for growth. Plant physiology **142**, 45–53.

Matsubayashi Y, Ogawa M, Morita A, Sakagami Y. 2002. An LRR receptor kinase involved in perception of a peptide plant hormone, phytosulfokine. Science **296**, 1470–1472.

Matsubayashi Y, Sakagami Y. 1996. Phytosulfokine, sulfated peptides that induce the proliferation of single mesophyll cells of Asparagus officinalis L. Proceedings of the National Academy of Sciences of the United States of America **93**, 7623–7627.

Matsuzaki Y, Ogawa-Ohnishi M, Mori A, Matsubayashi Y. 2010. Secreted Peptide Signals Required for Maintenance of Root Stem Cell Niche in Arabidopsis. Science **329**, 1065–1067.

Matzinger P. 1994. Tolerance, Danger, and the Extended Family. Annual Review of Immunology **12**, 991–1045.

Matzinger P. 2002. The danger model: A renewed sense of self. Science **296**, 301–305.

Matzke MA, Kanno T, Matzke AJM. 2015. RNA-Directed DNA Methylation: The Evolution of a Complex Epigenetic Pathway in Flowering Plants. Annual Review of Plant Biology **66**, 243–267.

Mbengue M, Bourdais G, Gervasi F, *et al.* 2016. Clathrin-dependent endocytosis is required for immunity mediated by pattern recognition receptor kinases. Proceedings of the National Academy of Sciences of the United States of America **113**, 11034–11039.

McCann HC, Nahal H, Thakur S, Guttman DS. 2012. Identification of innate immunity elicitors using molecular signatures of natural selection. Proceedings of the National Academy of Sciences of the United States of America **109**, 4215–20.

McGurl B, Ryan CA. 1992. The organization of the prosystemin gene. Plant molecular biology **20**, 405–9.

McKenna JF, Rolfe DJ, Webb SED, Tolmie AF, Botchway SW, Martin-Fernandez ML, Hawes C, Runions J. 2019. The cell wall regulates dynamics and size of plasma-membrane nanodomains in Arabidopsis. Proceedings of the National Academy of Sciences of the United States of America **116**, 12857–12862.

Mecchia MA, Santos-Fernandez G, Duss NN, *et al.* 2017. RALF4/19 peptides interact with LRX proteins to control pollen tube growth in Arabidopsis. Science **358**, 1600–1603.

Medzhitov R, Janeway CA. 1997. Innate Immunity: The Virtues of a Nonclonal System of Recognition. Cell **91**, 295–298.

Medzhitov R, Janeway CA. 2002. Decoding the patterns of self and nonself by the innate immune system. Science **296**, 298–300.

Mélida H, Sopeña-Torres S, Bacete L, Garrido-Arandia M, Jordá L, López G, Muñoz-Barrios A, Pacios LF, Molina A. 2018. Non-branched β-1,3-glucan oligosaccharides trigger immune responses in Arabidopsis. The Plant Journal **93**, 34–49.

Mendes BMJ, Cardoso SC, Boscariol-Camargo RL, Cruz RB, Mourão Filho FAA, Bergamin Filho A. 2010. Reduction in susceptibility to Xanthomonas axonopodis pv. citri in

transgenic Citrus sinensis expressing the rice Xa21 gene. Plant Pathology **59**, 68–75.

Meng L, Buchanan BB, Feldman LJ, Luan S. 2012. CLE-like (CLEL) peptides control the pattern of root growth and lateral root development in Arabidopsis. Proceedings of the National Academy of Sciences **109**, 1760–1765.

Meng X, Chen X, Mang H, Liu C, Yu X, Gao X, Torii KU, He P, Shan L. 2015. Differential Function of Arabidopsis SERK Family Receptor-like Kinases in Stomatal Patterning. Current Biology **25**, 2361–2372.

Meng X, Zhang S. 2013. MAPK Cascades in Plant Disease Resistance Signaling. Annual Review of Phytopathology **51**, 245–266.

Mentlak TA, Kombrink A, Shinya T, *et al.* 2012. Effector-mediated suppression of chitin-triggered immunity by Magnaporthe oryzae is necessary for rice blast disease. Plant Cell **24**, 322–335.

Mersmann S, Bourdais G, Rietz S, Robatzek S. 2010. Ethylene signaling regulates accumulation of the FLS2 receptor and is required for the oxidative burst contributing to plant immunity. Plant physiology **154**, 391–400.

Mi H, Muruganujan A, Ebert D, Huang X, Thomas PD. 2019. PANTHER version 14: more genomes, a new PANTHER GO-slim and improvements in enrichment analysis tools. Nucleic Acids Research **47**, D419–D426.

Miller G, Schlauch K, Tam R, Cortes D, Torres MA, Shulaev V, Dangl JL, Mittler R. 2009. The plant NADPH oxidase RBOHD mediates rapid systemic signaling in response to diverse stimuli. Science Signaling **2**, ra45.

Min YK, Asami T, Fujioka S, Murofushi N, Yamaguchi I, Yoshida S. 1999. New lead compounds for brassinosteroid biosynthesis inhibitors. Bioorganic and Medicinal Chemistry Letters **9**, 425–430.

Mitchum MG, Wang X, Wang J, Davis EL. 2012. Role of Nematode Peptides and Other Small Molecules in Plant Parasitism. Annual Review of Phytopathology **50**, 175–195.

Mithöfer A, Mazars C. 2002. Aequorin-based measurements of intracellular Ca2+-signatures in plant cells. Biological Procedures Online **4**, 105–118.

Mittler R. 2017. ROS Are Good. Trends in Plant Science **22**, 11–19.

Miya A, Albert P, Shinya T, Desaki Y, Ichimura K, Shirasu K, Narusaka Y, Kawakami N, Kaku H, Shibuya N. 2007. CERK1, a LysM receptor kinase, is essential for chitin elicitor signaling in Arabidopsis. Proceedings of the National Academy of Sciences of the United States of America **104**, 19613–19618.

Mohd-Radzman NA, Laffont C, Ivanovici A, Patel N, Reid DE, Stougaard J, Frugier F, Imin N, Djordjevic MA. 2016. Different pathways act downstream of the peptide receptor CRA2 to regulate lateral root and nodule development. Plant Physiology **171**, pp.00113.2016.

Monaghan J, Matschi S, Romeis T, Zipfel C. 2015. The calcium-dependent protein kinase CPK28 negatively regulates the BIK1-mediated PAMPinduced calcium burst. Plant Signaling and Behavior **10**, 1–5.

Monaghan J, Matschi S, Shorinola O, *et al.* 2014. The calcium-dependent protein kinase CPK28 buffers plant immunity and regulates BIK1 turnover. Cell Host and Microbe **16**, 605–615.

Monshausen GB, Bibikova TN, Messerli MA, Shi C, Gilroy S. 2007. Oscillations in extracellular pH and reactive oxygen species modulate tip growth of Arabidopsis root hairs. Proceedings of the National Academy of Sciences of the United States of America **104**, 20996–1001.

Monshausen GB, Haswell ES. 2013. A force of nature: Molecular mechanisms of

mechanoperception in plants. Journal of Experimental Botany **64**, 4663–4680.

Moore WC. 1952. *'Plant Pathology'*. San Diego, California: Academic Press Inc.

Morales J, Kadota Y, Zipfel C, Molina A, Torres M-A. 2016. The Arabidopsis NADPH oxidases *RbohD* and *RbohF* display differential expression patterns and contributions during plant immunity. Journal of Experimental Botany **67**, 1663–1676.

Morita J, Kato K, Nakane T, Kondo Y, Fukuda H, Nishimasu H, Ishitani R, Nureki O. 2016. Crystal structure of the plant receptor-like kinase TDR in complex with the TDIF peptide. Nature Communications **7**, 12383.

Mosher S, Kemmerling B. 2013. PSKR1 and PSY1R-mediated regulation of plant defense responses. Plant signaling & behavior **8**, e24119.

Mosher S, Seybold H, Rodriguez P, *et al.* 2013. The tyrosine-sulfated peptide receptors PSKR1 and PSY1R modify the immunity of Arabidopsis to biotrophic and necrotrophic pathogens in an antagonistic manner. The Plant Journal **73**, 469–482.

Mott GA, Thakur S, Smakowska E, Wang PW, Belkhadir Y, Desveaux D, Guttman DS. 2016. Genomic screens identify a new phytobacterial microbe-associated molecular pattern and the cognate Arabidopsis receptor-like kinase that mediates its immune elicitation. Genome Biology **17**, 98.

Mou S, Zhang X, Han Z, Wang J, Gong X, Chai J. 2017. CLE42 binding induces PXL2 interaction with SERK2. Protein and Cell **8**, 612–617.

Moussu S, Broyart C, Santos-Fernandez G, Augustin S, Wehrle S, Grossniklaus U, Santiago J. 2019. Structural basis for recognition of RALF peptides by LRX proteins during pollen tube growth. bioRxiv, 695874.

Moussu S, Santiago J. 2019. Structural biology of cell surface receptor–ligand interactions. Current Opinion in Plant Biology **52**, 38–45.

Müller K, Carstens AC, Linkies A, Torres MA, Leubner-Metzger G. 2009. The NADPH-oxidase AtrbohB plays a role in Arabidopsis seed after-ripening. New Phytologist **184**, 885–897.

Müller LM, Flokova K, Schnabel E, Sun X, Fei Z, Frugoli J, Bouwmeester HJ, Harrison MJ. 2019. A CLE–SUNN module regulates strigolactone content and fungal colonization in arbuscular mycorrhiza. Nature Plants **5**, 933–939.

Murphy E, De Smet I. 2014. Understanding the RALF family: A tale of many species. Trends in Plant Science **19**, 664–671.

Murphy E, Vu LD, Van den Broeck L, *et al.* 2016. RALFL34 regulates formative cell divisions in Arabidopsis pericycle during lateral root initiation. Journal of Experimental Botany **67**, 4863–4875.

Nadeau JA, Sack FD. 2002. Control of stomatal distribution on the Arabidopsis leaf surface. Science **296**, 1697–1700.

Nagata N, Min YK, Nakano T, Asami T, Yoshida S. 2000. Treatment of dark-grown Arabidopsis thaliana with a brassinosteroid-biosynthesis inhibitor, brassinazole, induces some characteristics of light-grown plants. Planta **211**, 781–790.

Nakaminami K, Okamoto M, Higuchi-Takeuchi M, *et al.* 2018. AtPep3 is a hormone-like peptide that plays a role in the salinity stress tolerance of plants. Proceedings of the National Academy of Sciences **115**, 5810–5815.

Nakamura A, Higuchi K, Goda H, Fujiwara MT, Sawa S, Koshiba T, Shimada Y, Yoshida S. 2003. Brassinolide Induces IAA5, IAA19, and DR5, a Synthetic Auxin Response Element in Arabidopsis, Implying a Cross Talk Point of Brassinosteroid and Auxin Signaling. Plant Physiology **133**, 1843–1853.

Nakayama T, Shinohara H, Tanaka M, Baba K, Ogawa-Ohnishi M, Matsubayashi Y. 2017. A peptide hormone required for Casparian strip diffusion barrier formation in Arabidopsis roots. Science **355**.

Nasrallah JB, Stein JC, Kandasamy MK, Nasrallah ME. 1994. Signaling the arrest of pollen tube development in self-incompatible plants. Science **266**, 1505–1508.

Nawrath C, Métraux JP. 1999. Salicylic acid induction-deficient mutants of Arabidopsis express PR-2 and PR-5 and accumulate high levels of camalexin after pathogen inoculation. Plant Cell **11**, 1393–1404.

Nekrasov V, Li J, Batoux M, *et al.* 2009. Control of the pattern-recognition receptor EFR by an ER protein complex in plant immunity. EMBO Journal **28**, 3428–3438.

Neukermans J, Inzé A, Mathys J, De Coninck B, van de Cotte B, Cammue BPA, Van Breusegem F. 2015. ARACINs, brassicaceae-specific peptides exhibiting antifungal activities against necrotrophic pathogens in Arabidopsis. Plant Physiology **167**, 1017–1029.

Ngou B, Ahn H-K, Ding P, Jones J. 2020. Mutual Potentiation of Plant Immunity by Cell-surface and Intracellular Receptors. bioRxiv.

Nimchuk ZL, Tarr PT, Ohno C, Qu X, Meyerowitz EM. 2011. Plant stem cell signaling involves ligand-dependent trafficking of the CLAVATA1 receptor kinase. Current Biology **21**, 345–352.

Nishiyama T, Sakayama H, de Vries J, *et al.* 2018. The Chara Genome: Secondary Complexity and Implications for Plant Terrestrialization. Cell **174**, 448-464.e24.

Ntoukakis V, Schwessinger B, Segonzac C, Zipfel C. 2011. Cautionary notes on the use of C-terminal BAK1 fusion proteins for functional studies. The Plant cell **23**, 3871–8.

Nürnberger T, Nennstiel D, Jabs T, Sacks WR, Hahlbrock K, Scheel D. 1994. High affinity binding of a fungal oligopeptide elicitor to parsley plasma membranes triggers multiple defense responses. Cell **78**, 449–460.

Ogasawara Y, Kaya H, Hiraoka G, *et al.* 2008. Synergistic activation of the Arabidopsis NADPH oxidase AtrbohD by Ca2+ and phosphorylation. The Journal of biological chemistry **283**, 8885–92.

Ogawa-Ohnishi M, Matsushita W, Matsubayashi Y. 2013. Identification of three hydroxyproline O-arabinosyltransferases in Arabidopsis thaliana. Nature Chemical Biology **9**, 726–730.

Oh M-H, Wang X, Kota U, Goshe MB, Clouse SD, Huber SC. 2009. Tyrosine phosphorylation of the BRI1 receptor kinase emerges as a component of brassinosteroid signaling in Arabidopsis. Proceedings of the National Academy of Sciences of the United States of America **106**, 658.

Ohkubo Y, Tanaka M, Tabata R, Ogawa-Ohnishi M, Matsubayashi Y. 2017. Shoot-to-root mobile polypeptides involved in systemic regulation of nitrogen acquisition. Nature Plants **3**, 17029.

Okamoto S, Shinohara H, Mori T, Matsubayashi Y, Kawaguchi M. 2013. Root-derived CLE glycopeptides control nodulation by direct binding to HAR1 receptor kinase. Nature Communications **4**, 2191.

Okonechnikov K, Golosova O, Fursov M, *et al.* 2012. Unipro UGENE: A unified bioinformatics toolkit. Bioinformatics **28**, 1166–1167.

Okuda S, Fujita S, Moretti A, Hohmann U, Doblas VG, Ma Y, Pfister A, Brandt B, Geldner N, Hothorn M. 2019. Molecular mechanism for the recognition of sequence-divergent CIF peptides by the plant receptor kinases GSO1/SGN3 and GSO2. bioRxiv, 692228.

Okuda S, Tsutsui H, Shiina K, *et al.* 2009. Defensin-like polypeptide LUREs are pollen tube attractants secreted from synergid cells. Nature **458**, 357–361.

Oldroyd GED. 2013. Speak, friend and enter: signalling systems that promote beneficial symbiotic associations in plants. Nature Reviews Microbiology **11**, 252–263.

de Oliveira MV V., Xu G, Li B, *et al.* 2016. Specific control of Arabidopsis BAK1/SERK4-regulated cell death by protein glycosylation. Nature Plants **2**, 15218.

Olsson V, Joos L, Zhu S, Gevaert K, Butenko MA, De Smet I. 2019*a*. Look Closely, the Beautiful May Be Small: Precursor-Derived Peptides in Plants. Annual Review of Plant Biology **70**, 153–186.

Olsson V, Smakowska-Luzan E, Breiden M, Marhavy P, Schneeweiss R, Belkhadir Y, Simon R, Butenko MA. 2019*b*. The IDA cell separation pathway connects developmental and defense responses. bioRxiv, 761346.

Oome S, Raaymakers TM, Cabral A, Samwel S, Böhm H, Albert I, Nürnberger T, Van Den Ackerveken G. 2014. Nep1-like proteins from three kingdoms of life act as a microbe-associated molecular pattern in Arabidopsis. Proceedings of the National Academy of Sciences of the United States of America **111**, 16955–16960.

Ortiz-Morea FA, Savatin D V, Dejonghe W, *et al.* 2016. Danger-associated peptide signaling in Arabidopsis requires clathrin. Proceedings of the National Academy of Sciences of the United States of America **113**, 11028–33.

Ott T. 2017. Membrane nanodomains and microdomains in plant–microbe interactions. Current Opinion in Plant Biology **40**, 82–88.

Ou Y, Lu X, Zi Q, *et al.* 2016. RGF1 INSENSITIVE 1 to 5, a group of LRR receptor-like kinases, are essential for the perception of root meristem growth factor 1 in Arabidopsis thaliana. Cell Research **26**, 686–698.

Patharkar OR, Gassmann W, Walker JC. 2017. Leaf shedding as an anti-bacterial defense in Arabidopsis cauline leaves (G Coaker, Ed.). PLoS Genetics **13**, e1007132.

Pearce G, Moura DS, Stratmann J, Ryan CA. 2001. RALF, a 5-kDa ubiquitous polypeptide in plants, arrests root growth and development. Proceedings of the National Academy of Sciences of the United States of America **98**, 12843–12847.

Pearce G, Strydom D, Johnson S, Ryan CA. 1991. A Polypeptide from Tomato Leaves Induces Wound-Inducible Proteinase Inhibitor Proteins. Science **253**, 895–897.

Perraki A, DeFalco TA, Derbyshire P, *et al.* 2018. Phosphocode-dependent functional dichotomy of a common co-receptor in plant signalling. Nature **561**, 248–252.

Petutschnig EK, Jones AME, Serazetdinova L, Lipka U, Lipka V. 2010. The Lysin Motif Receptor-like Kinase (LysM-RLK) CERK1 is a major chitin-binding protein in Arabidopsis thaliana and subject to chitin-induced phosphorylation. Journal of Biological Chemistry **285**, 28902–28911.

Pfister A, Barberon M, Alassimone J, *et al.* 2014. A receptor-like kinase mutant with absent endodermal diffusion barrier displays selective nutrient homeostasis defects. eLife **3**, e03115.

Planas-Riverola A, Gupta A, Betegoń-Putze I, Bosch N, Ibaneş M, Cano-Delgado AI. 2019. Brassinosteroid signaling in plant development and adaptation to stress. Development (Cambridge) **146**, dev151894.

Plomion C, Aury J-M, Amselem J, *et al.* 2018. Oak genome reveals facets of long lifespan. Nature Plants **4**, 440–452.

Pruitt RN, Joe A, Zhang W, Feng W, Stewart V, Schwessinger B, Dinneny JR, Ronald PC. 2017. A microbially derived tyrosine-sulfated peptide mimics a plant peptide hormone. New Phytologist **215**, 725–736.

Pruitt RN, Schwessinger B, Joe A, *et al.* 2015. The rice immune receptor XA21 recognizes a tyrosine-sulfated protein from a Gram-negative bacterium. Science advances **1**, e1500245.

Qi X, Han S-K, Dang JH, Garrick JM, Ito M, Hofstetter AK, Torii KU. 2017. Autocrine regulation of stomatal differentiation potential by EPF1 and ERECTA-LIKE1 ligand-receptor signaling. eLife **6**.

Qi B, Zheng H. 2013. Modulation of root-skewing responses by *KNAT1* in *Arabidopsis thaliana*. The Plant Journal **76**, 380–392.

Qian P, Song W, Yokoo T, Minobe A, Wang G, Ishida T, Sawa S, Chai J, Kakimoto T. 2018. The CLE9/10 secretory peptide regulates stomatal and vascular development through distinct receptors. Nature Plants **4**, 1071–1081.

Qiu P, Pan P, Govind S. 1998. A role for the Drosophila Toll/Cactus pathway in larval hematopoiesis. Development **125**, 1909–1920.

Ranf S, Eschen-Lippold L, Fröhlich K, Westphal L, Scheel D, Lee J. 2014. Microbe-associated molecular pattern-induced calcium signaling requires the receptor-like cytoplasmic kinases, PBL1 and BIK1. BMC Plant Biology **14**, 374.

Ranf S, Eschen-Lippold L, Pecher P, Lee J, Scheel D. 2011. Interplay between calcium signalling and early signalling elements during defence responses to microbe- or damage-associated molecular patterns. The Plant Journal **68**, 100–113.

Ranf S, Gisch N, Schäffer M, *et al.* 2015. A lectin S-domain receptor kinase mediates lipopolysaccharide sensing in Arabidopsis thaliana. Nature Immunology **16**, 426–433.

Ranf S, Grimmer J, Pöschl Y, Pecher P, Chinchilla D, Scheel D, Lee J. 2012. Defense-related calcium signaling mutants uncovered via a quantitative high-throughput screen in arabidopsis thaliana. Molecular Plant **5**, 115–130.

Ratcliffe OJ, Kumimoto RW, Wong BJ, Riechmann JL. 2003. Analysis of the Arabidopsis MADS AFFECTING FLOWERING gene family: MAF2 prevents vernalization by short periods of cold. Plant Cell **15**, 1159–1169.

Refrégier G, Pelletier S, Jaillard D, Höfte H. 2004. Interaction between wall deposition and cell elongation in dark-grown hypocotyl cells in Arabidopsis. Plant Physiology **135**, 959–968.

Reid DE, Ferguson BJ, Gresshoff PM. 2011. Inoculation- and Nitrate-Induced CLE Peptides of Soybean Control NARK-Dependent Nodule Formation. Molecular Plant-Microbe Interactions **24**, 606–618.

Ren S, Song X, Chen W, Lu R, Lucas WJ, Liu C. 2019*a*. CLE25 peptide regulates phloem initiation in *Arabidopsis* through a CLERK-CLV2 receptor complex. Journal of Integrative Plant Biology, jipb.12846.

Ren H, Willige BC, Jaillais Y, Geng S, Park MY, Gray WM, Chory J. 2019*b*. BRASSINOSTEROID-SIGNALING KINASE 3, a plasma membrane-associated scaffold protein involved in early brassinosteroid signaling (GP Copenhaver, Ed.). PLoS Genetics **15**, e1007904.

Replogle A, Wang J, Paolillo V, Smeda J, Kinoshita A, Durbak A, Tax FE, Wang X, Sawa S, Mitchum MG. 2013. Synergistic interaction of clavata1, clavata2, and receptor-like protein kinase 2 in cyst nematode parasitism of arabidopsis. Molecular Plant-Microbe Interactions **26**, 87–96.

Rhyasen GW, Starczynowski DT. 2015. IRAK signalling in cancer. British Journal of Cancer **112**, 232–237.

Ripke S, Neale BM, Corvin A, *et al.* 2014. Biological insights from 108 schizophrenia-associated genetic loci. Nature **511**, 421-+.

Robatzek S, Chinchilla D, Boller T. 2006. Ligand-induced endocytosis of the pattern

recognition receptor FLS2 in Arabidopsis. Genes and Development **20**, 537–542.

Robatzek S, Somssich IE. 2002. Targets of AtWRKY6 regulation during plant senescence and pathogen defense. Genes and Development **16**, 1139–1149.

Rodriguez E, El Ghoul H, Mundy J, Petersen M. 2016. Making sense of plant autoimmunity and 'negative regulators'. The FEBS Journal **283**, 1385–1391.

Rooney HCE, Van't Klooster JW, Van Der Hoorn RAL, Joosten MHAJ, Jones JDG, De Wit PJGM. 2005. Plant science: Cladosporium Avr2 inhibits tomato Rcr3 protease required for Cf-2-dependent disease resistance. Science **308**, 1783–1786.

Rosas-Diaz T, Zhang D, Fan P, *et al.* 2018. A virus-targeted plant receptor-like kinase promotes cell-to-cell spread of RNAi. Proceedings of the National Academy of Sciences of the United States of America **115**, 1388–1393.

Ross A, Somssich IE. 2016. A DNA-based real-time PCR assay for robust growth quantification of the bacterial pathogen Pseudomonas syringae on Arabidopsis thaliana. Plant Methods **12**, 48.

Rotman N, Rozier F, Boavida L, Dumas C, Berger F, Faure JE. 2003. Female control of male gamete delivery during fertilization in Arabidopsis thaliana. Current Biology **13**, 432–436.

Roux M, Schwessinger B, Albrecht C, Chinchilla D, Jones A, Holton N, Malinovsky FG, Tör M, de Vries S, Zipfel C. 2011. The Arabidopsis leucine-rich repeat receptor-like kinases BAK1/SERK3 and BKK1/SERK4 are required for innate immunity to hemibiotrophic and biotrophic pathogens. Plant Cell **23**, 2440–2455.

Russinova E, Borst J-W, Kwaaitaal M, Caño-Delgado A, Yin Y, Chory J, de Vries SC. 2004. Heterodimerization and Endocytosis of Arabidopsis Brassinosteroid Receptors BRI1 and AtSERK3 (BAK1). The Plant Cell **16**, 3216–3229.

Rutherford R, Masson PH. 1996. Arabidopsis thaliana sku mutant seedlings show exaggerated surface-dependent alteration in root growth vector. Plant physiology **111**, 987–98.

Ryan CA, Pearce G. 1998. SYSTEMIN: A Polypeptide Signal for Plant Defensive Genes. Annual Review of Cell and Developmental Biology **14**, 1–17.

Saffer AM, Carpita NC, Irish VF, Correspondence VFI, Irish VF. 2017. Rhamnose-Containing Cell Wall Polymers Suppress Helical Plant Growth Independently of Microtubule Orientation. Current Biology **27**, 2248-2259.e4.

Sager RE, Lee JY. 2018. Plasmodesmata at a glance. Journal of Cell Science **131**, jcs209346.

Saijo Y, Loo EP, Yasuda S. 2018. Pattern recognition receptors and signaling in plant-microbe interactions. The Plant Journal **93**, 592–613.

Saijo Y, Tintor N, Lu X, Rauf P, Pajerowska-Mukhtar K, Häweker H, Dong X, Robatzek S, Schulze-Lefert P. 2009. Receptor quality control in the endoplasmic reticulum for plant innate immunity. EMBO Journal **28**, 3439–3449.

Saintenac C, Lee W-S, Cambon F, *et al.* 2018. Wheat receptor-kinase-like protein Stb6 controls gene-for-gene resistance to fungal pathogen Zymoseptoria tritici. Nature Genetics **50**.

Sakamoto T, Deguchi M, Brustolini OJB, Santos AA, Silva FF, Fontes EPB. 2012. The tomato RLK superfamily: Phylogeny and functional predictions about the role of the LRRII-RLK subfamily in antiviral defense. BMC Plant Biology **12**, 229.

Sánchez-Vallet A, Mesters JR, Thomma BPHJ. 2015. The battle for chitin recognition in plant-microbe interactions. FEMS Microbiology Reviews **39**, 171–183.

Sánchez-Vallet A, Saleem-Batcha R, Kombrink A, Hansen G, Valkenburg DJ, Thomma

BPHJ, Mesters JR. 2013. Fungal effector Ecp6 outcompetes host immune receptor for chitin binding through intrachain LysM dimerization. eLife **2013**, e00790.

Santiago J, Brandt B, Wildhagen M, Hohmann U, Hothorn LA, Butenko MA, Hothorn M. 2016. Mechanistic insight into a peptide hormone signaling complex mediating floral organ abscission. eLife **5**.

Saur IML, Kadota Y, Sklenar J, Holton NJ, Smakowska E, Belkhadir Y, Zipfel C, Rathjen JP. 2016. NbCSPR underlies age-dependent immune responses to bacterial cold shock protein in Nicotiana benthamiana. Proceedings of the National Academy of Sciences of the United States of America.

Savary S, Ficke A, Aubertot JN, Hollier C. 2012. Crop losses due to diseases and their implications for global food production losses and food security. Food Security **4**, 519–537.

Schallus T, Jaeckh C, Fehér K, *et al.* 2008. Malectin: a novel carbohydrate-binding protein of the endoplasmic reticulum and a candidate player in the early steps of protein N-glycosylation. Molecular biology of the cell **19**, 3404–14.

Schardon K, Hohl M, Graff L, Pfannstiel J, Schulze W, Stintzi A, Schaller A. 2016. Precursor processing for plant peptide hormone maturation by subtilisin-like serine proteinases. Science **354**, 1594–1597.

Scheible W-R, Fry B, Kochevenko A, Schindelasch D, Zimmerli L, Somerville S, Loria R, Somerville CR. 2003. An Arabidopsis mutant resistant to thaxtomin A, a cellulose synthesis inhibitor from Streptomyces species. The Plant cell **15**, 1781–94.

Scheid OM, Paszkowski J, Potrykus I. 1991. Reversible inactivation of a transgene in Arabidopsis thaliana. MGG Molecular & General Genetics **228**, 104–112.

Schindelin J, Arganda-Carreras I, Frise E, *et al.* 2012. Fiji: An open-source platform for biological-image analysis. Nature Methods **9**, 676–682.

Schnabel E, Journet EP, De Carvalho-Niebel F, Duc G, Frugoli J. 2005. The Medicago truncatula SUNN gene encodes a CLV1-like leucine-rich repeat receptor kinase that regulates nodule number and root length. Plant Molecular Biology **58**, 809–822.

Schoonbeek H jan, Wang HH, Stefanato FL, Craze M, Bowden S, Wallington E, Zipfel C, Ridout CJ. 2015. Arabidopsis EF-Tu receptor enhances bacterial disease resistance in transgenic wheat. New Phytologist **206**, 606–613.

Schopfer CR, Nasrallah ME, Nasrallah JB. 1999. The male determinant of self-incompatibility in Brassica. Science **286**, 1697–1700.

Schultz ER, Zupanska AK, Sng NJ, Paul AL, Ferl RJ. 2017. Skewing in Arabidopsis roots involves disparate environmental signaling pathways. BMC Plant Biology **17**, 31.

Schulze B, Mentzel T, Jehle AK, Mueller K, Beeler S, Boller T, Felix G, Chinchilla D. 2010. Rapid heteromerization and phosphorylation of ligand-activated plant transmembrane receptors and their associated kinase BAK1. The Journal of biological chemistry **285**, 9444–51.

Schwessinger B, Bahar O, Thomas N, *et al.* 2015. Transgenic Expression of the Dicotyledonous Pattern Recognition Receptor EFR in Rice Leads to Ligand-Dependent Activation of Defense Responses. PLoS pathogens **11**, e1004809.

Schwessinger B, Ronald PC. 2012. Plant Innate Immunity: Perception of Conserved Microbial Signatures. Annual Review of Plant Biology **63**, 451–482.

Schwessinger B, Roux M, Kadota Y, Ntoukakis V, Sklenar J, Jones A, Zipfel C. 2011. Phosphorylation-Dependent Differential Regulation of Plant Growth, Cell Death, and Innate Immunity by the Regulatory Receptor-Like Kinase BAK1 (DS Guttman, Ed.). PLoS Genetics **7**, e1002046.

Sede AR, Borassi C, Wengier DL, Mecchia MA, Estevez JM, Muschietti JP. 2018. Arabidopsis pollen extensins LRX are required for cell wall integrity during pollen tube growth. FEBS Letters **592**, 233–243.

Segonzac C, Feike D, Gimenez-Ibanez S, Hann DR, Zipfel C, Rathjen JP. 2011. Hierarchy and roles of pathogen-associated molecular pattern-induced responses in nicotiana benthamiana. Plant Physiology **156**, 687–699.

Segonzac C, Monaghan J. 2019. Modulation of plant innate immune signaling by small peptides. Current Opinion in Plant Biology **51**, 22–28.

Sessions A, Burke E, Presting G, *et al.* 2002. A high-throughput arabidopsis reverse genetics system. Plant Cell **14**, 2985–2994.

Shan L, He P, Li J, Heese A, Peck SC, Nürnberger T, Martin GB, Sheen J. 2008. Bacterial Effectors Target the Common Signaling Partner BAK1 to Disrupt Multiple MAMP Receptor-Signaling Complexes and Impede Plant Immunity. Cell Host and Microbe **4**, 17–27.

Sharon M, Sharon M. 2015. Identification and Characterization of Graphene. Graphene.

She J, Han Z, Kim T-WW, *et al.* 2011. Structural insight into brassinosteroid perception by BRI1. Nature **474**, 472–477.

Shen W, Liu J, Li J-F. 2019. Type-II Metacaspases Mediate the Processing of Plant Elicitor Peptides in Arabidopsis. Molecular Plant.

Shi H, Shen Q, Qi Y, Yan H, Nie H, Chen Y, Zhao T, Katagiri F, Tang D. 2013. BR-signaling kinase1 physically associates with flagellin SENSING2 and regulates plant innate immunity in Arabidopsis. Plant Cell **25**, 1143–1157.

Shi C-L, von Wangenheim D, Herrmann U, *et al.* 2018. The dynamics of root cap sloughing in Arabidopsis is regulated by peptide signalling. Nature Plants **4**, 596–604.

Shih HW, Miller ND, Dai C, Spalding EP, Monshausen GB. 2014. The receptor-like kinase FERONIA is required for mechanical signal transduction in Arabidopsis seedlings. Current Biology **24**, 1887–1892.

Shimizu T, Nakano T, Takamizawa D, *et al.* 2010. Two LysM receptor molecules, CEBiP and OsCERK1, cooperatively regulate chitin elicitor signaling in rice. The Plant Journal **64**, 204–214.

Shinohara H, Matsubayashi Y. 2007. Functional immobilization of plant receptor-like kinase onto microbeads towards receptor array construction and receptor-based ligand fishing. Plant Journal **52**, 175–184.

Shinohara H, Matsubayashi Y. 2017. Expression of plant receptor kinases in tobacco By-2 cells. Methods in Molecular Biology. Humana Press, New York, NY, 29–35.

Shinohara H, Mori A, Yasue N, Sumida K, Matsubayashi Y. 2016. Identification of three LRR-RKs involved in perception of root meristem growth factor in Arabidopsis. Proceedings of the National Academy of Sciences of the United States of America **113**, 3897–3902.

Shinohara H, Yasue N, Onuki T, Kondoh Y, Yoshida M, Matsubayashi Y. 2019. Screening and identification of a non-peptide antagonist for the peptide hormone receptor in Arabidopsis. Communications Biology **2**, 61.

Shiu SH, Bleecker AB. 2001*a*. Receptor-like kinases from Arabidopsis form a monophyletic gene family related to animal receptor kinases. Proceedings of the National Academy of Sciences of the United States of America **98**, 10763–8.

Shiu S-H, Bleecker AB. 2001*b*. Plant Receptor-Like Kinase Gene Family: Diversity, Function, and Signaling. Science Signaling **2001**, re22–re22.

Shiu S-H, Karlowski WM, Pan R, Tzeng Y-H, Mayer KFX, Li W-H. 2004. Comparative

analysis of the receptor-like kinase family in Arabidopsis and rice. The Plant cell **16**, 1220–34.

Shoji T, Suzuki K, Abe T, Kaneko Y, Shi H, Zhu JK, Rus A, Hasegawa PM, Hashimoto T. 2006. Salt stress affects cortical microtubule organization and helical growth in Arabidopsis. Plant and Cell Physiology **47**, 1158–1168.

Shpak ED. 2013. Diverse Roles of *ERECTA* Family Genes in Plant Development. Journal of Integrative Plant Biology **55**, 1238–1250.

Shpak ED, Berthiaume CT, Hill EJ, Torii KU. 2004. Synergistic interaction of three ERECTA-family receptor-like kinases controls Arabidopsis organ growth and flower development by promoting cell proliferation. Development **131**, 1491–1501.

Shpak ED, McAbee JM, Pillitteri LJ, Torii KU. 2005. Plant science: Stomatal patterning and differentiation by synergistic interactions of receptor kinases. Science **309**, 290–293.

Sierla M, Hõrak H, Overmyer K, *et al.* 2018. The Receptor-like Pseudokinase GHR1 Is Required for Stomatal Closure. The Plant cell **30**, 2813–2837.

Sijen T, Vijn I, Rebocho A, Van Blokland R, Roelofs D, Mol JNM, Kooter JM. 2001. Transcriptional and posttranscriptional gene silencing are mechanistically related. Current Biology **11**, 436–440.

Singh P, Kuo Y-C, Mishra S, *et al.* 2012. The Lectin Receptor Kinase-VI.2 Is Required for Priming and Positively Regulates Arabidopsis Pattern-Triggered Immunity. The Plant Cell **24**, 1256–1270.

Smakowska-Luzan E, Mott GA, Parys K, *et al.* 2018. An extracellular network of Arabidopsis leucine-rich repeat receptor kinases. Nature **553**, 342–346.

Smith JM, Salamango DJ, Leslie ME, Collins CA, Heese A. 2017. Correction to: Sensitivity to Flg22 is modulated by ligand-induced degradation and de novo synthesis of the endogenous flagellin-receptor FLAGELLIN-SENSING2 (Plant Physiology, (2014) 164(1), (440-454), 10.1104/pp.113.229179). Plant Physiology **174**, 2549.

Somssich M, Je B Il, Simon R, Jackson D. 2016. CLAVATA-WUSCHEL signaling in the shoot meristem. Development (Cambridge) **143**, 3238–3248.

Song W, Liu L, Wang J, *et al.* 2016. Signature motif-guided identification of receptors for peptide hormones essential for root meristem growth. Cell research **26**, 674–85.

Song WY, Wang GL, Chen LL, *et al.* 1995. A receptor kinase-like protein encoded by the rice disease resistance gene, Xa21. Science **270**, 1804.

Souza C de A, Li S, Lin AZ, Boutrot F, Grossmann G, Zipfel C, Somerville SC. 2017. Cellulose-Derived Oligomers Act as Damage-Associated Molecular Patterns and Trigger Defense-Like Responses. Plant physiology **173**, 2383–2398.

Sreekanta S, Haruta M, Minkoff BB, Glazebrook J. 2015. Functional characterization of PCRK1, a putative protein kinase with a role in immunity. Plant Signaling and Behavior **10**, e1063759.

Sreeramulu S, Mostizky Y, Sunitha S, *et al.* 2013. BSKs are partially redundant positive regulators of brassinosteroid signaling in Arabidopsis. Plant Journal **74**, 905–919.

Srivastava R, Liu J-X, Guo H, Yin Y, Howell SH. 2009. Regulation and processing of a plant peptide hormone, AtRALF23, in Arabidopsis. The Plant Journal **59**, 930–939.

Stahl Y, Grabowski S, Bleckmann A, *et al.* 2013. Moderation of Arabidopsis Root Stemness by CLAVATA1 and ARABIDOPSIS CRINKLY4 Receptor Kinase Complexes. Current Biology **23**, 362–371.

Stegmann M, Monaghan J, Smakowska-Luzan E, Rovenich H, Lehner A, Holton N,

Belkhadir Y, Zipfel C. 2017. The receptor kinase FER is a RALF-regulated scaffold controlling plant immune signaling. Science **355**.

Stein JC, Howlett B, Boyes DC, Nasrallah ME, Nasrallah JB. 1991. Molecular cloning of a putative receptor protein kinase gene encoded at the self-incompatibility locus of Brassica oleracea. Proceedings of the National Academy of Sciences of the United States of America **88**, 8816–20.

Stenvik G-E, Tandstad NM, Guo Y, Shi C-L, Kristiansen W, Holmgren A, Clark SE, Aalen RB, Butenko MA. 2008. The EPIP peptide of INFLORESCENCE DEFICIENT IN ABSCISSION is sufficient to induce abscission in arabidopsis through the receptor-like kinases HAESA and HAESA-LIKE2. The Plant cell **20**, 1805–17.

Stührwohldt N, Dahlke RI, Steffens B, Johnson A, Sauter M. 2011. Phytosulfokine-α controls hypocotyl length and cell expansion in Arabidopsis thaliana through phytosulfokine receptor 1. PloS one **6**, e21054.

Sugano SS, Shimada T, Imai Y, Okawa K, Tamai A, Mori M, Hara-Nishimura I. 2010. Stomagen positively regulates stomatal density in Arabidopsis. Nature **463**, 241–4.

Sun Y, Han Z, Tang J, Hu Z, Chai C, Zhou B, Chai J. 2013*a*. Structure reveals that BAK1 as a co-receptor recognizes the BRI1-bound brassinolide. Cell Research **23**, 1326–1329.

Sun Y, Li L, Macho AP, Han Z, Hu Z, Zipfel C, Zhou JM, Chai J. 2013*b*. Structural basis for flg22-induced activation of the Arabidopsis FLS2-BAK1 immune complex. Science **342**, 624–628.

Swarbreck SM, Guerringue Y, Matthus E, Jamieson FJC, Davies JM. 2019. Impairment in karrikin but not strigolactone sensing enhances root skewing in *Arabidopsis thaliana*. The Plant Journal **98**, 607–621.

Szymczak LC, Kuo HY, Mrksich M. 2018. Peptide Arrays: Development and Application. Analytical Chemistry **90**, 266–282.

Tabata R, Sumida K, Yoshii T, Ohyama K, Shinohara H, Matsubayashi Y. 2014. Perception of root-derived peptides by shoot LRR-RKs mediates systemic N-demand signaling. Science **346**, 343–346.

Takahashi F, Suzuki T, Osakabe Y, Betsuyaku S, Kondo Y, Dohmae N, Fukuda H, Yamaguchi-Shinozaki K, Shinozaki K. 2018. A small peptide modulates stomatal control via abscisic acid in long-distance signalling. Nature **556**, 1.

Takayama S, Shiba H, Iwano M, Shimosato H, Che FS, Kai N, Watanabe M, Suzuki G, Hinata K, Isogai A. 2000. The pollen determinant of self-incompatibility in Brassica campestris. Proceedings of the National Academy of Sciences of the United States of America **97**, 1920–5.

Takeda S, Gapper C, Kaya H, Bell E, Kuchitsu K, Dolan L. 2008. Local positive feedback regulation determines cell shape in root hair cells. Science **319**, 1241–1244.

Takeuchi H, Higashiyama T. 2012. A species-specific cluster of defensin-like genes encodes diffusible pollen tube attractants in Arabidopsis. PLoS biology **10**, e1001449.

Takeuchi H, Higashiyama T. 2016. Tip-localized receptors control pollen tube growth and LURE sensing in Arabidopsis. Nature **531**, 245–8.

Taleski M, Imin N, Djordjevic MA. 2018. CEP peptide hormones: key players in orchestrating nitrogen-demand signalling, root nodulation, and lateral root development. Journal of Experimental Botany **69**, 1829–1836.

Tang J, Han Z, Sun Y, Zhang H, Gong X, Chai J. 2015. Structural basis for recognition of an endogenous peptide by the plant receptor kinase PEPR1. Cell research **25**, 110–20.

Tang W, Kim TW, Oses-Prieto JA, Sun Y, Deng Z, Zhu S, Wang R, Burlingame AL,

Wang ZY. 2008. BSKs mediate signal transduction from the receptor kinase BRI1 in Arabidopsis. Science **321**, 557–560.

Tateno M, Brabham C, Debolt S. 2016. Cellulose biosynthesis inhibitors - A multifunctional toolbox. Journal of Experimental Botany **67**, 533–542.

Thynne E, Saur IML, Simbaqueba J, *et al.* 2017. Fungal phytopathogens encode functional homologues of plant rapid alkalinization factor (RALF) peptides. Molecular Plant Pathology **18**, 811–824.

Tian W, Hou C, Ren Z, *et al.* 2019. A calmodulin-gated calcium channel links pathogen patterns to plant immunity. Nature **572**, 131–135.

Toal TW, Ron M, Gibson D, *et al.* 2018. Regulation of root angle and gravitropism. G3: Genes, Genomes, Genetics **8**, 3841–3855.

Torii KU, Mitsukawa N, Oosumi T, Matsuura Y, Yokoyama R, Whittier RF, Komeda Y. 1996. The Arabidopsis ERECTA gene encodes a putative receptor protein kinase with extracellular leucine-rich repeats. The Plant Cell **8**, 735–746.

Torres MA, Dangl JL. 2005. Functions of the respiratory burst oxidase in biotic interactions, abiotic stress and development. Current Opinion in Plant Biology **8**, 397–403.

Torres MA, Dangl JL, Jones JDG. 2002. Arabidopsis gp91phox homologues AtrbohD and AtrbohF are required for accumulation of reactive oxygen intermediates in the plant defense response. Proceedings of the National Academy of Sciences **99**, 517–522.

Toyokura K, Goh T, Shinohara H, *et al.* 2019. Lateral Inhibition by a Peptide Hormone-Receptor Cascade during Arabidopsis Lateral Root Founder Cell Formation. Developmental Cell **48**, 64-75.e5.

Toyota M, Spencer D, Sawai-Toyota S, Jiaqi W, Zhang T, Koo AJ, Howe GA, Gilroy S. 2018. Glutamate triggers long-distance, calcium-based plant defense signaling. Science **361**, 1112–1115.

Trempel F, Kajiura H, Ranf S, Grimmer J, Westphal L, Zipfel C, Scheel D, Fujiyama K, Lee J. 2016. Altered glycosylation of exported proteins, including surface immune receptors, compromises calcium and downstream signaling responses to microbe-associated molecular patterns in Arabidopsis thaliana. BMC Plant Biology **16**, 31.

Tripathi JN, Lorenzen J, Bahar O, Ronald P, Tripathi L. 2014. Transgenic expression of the rice Xa21 pattern-recognition receptor in banana (Musa sp.) confers resistance to Xanthomonas campestris pv. musacearum. Plant Biotechnology Journal **12**, 663–673.

Tsuwamoto R, Fukuoka H, Takahata Y. 2007. GASSHO1 and GASSHO2 encoding a putative leucine-rich repeat transmembrane-type receptor kinase are essential for the normal development of the epidermal surface in Arabidopsis embryos. The Plant Journal **54**, 30–42.

Tucker ML, Yang R. 2013. A gene encoding a peptide with similarity to the plant IDA signaling peptide (AtIDA) is expressed most abundantly in the root-knot nematode (Meloidogyne incognita) soon after root infection. Experimental Parasitology **134**, 165–170.

Ullah H, Chen JG, Temple B, Boyes DC, Alonso JM, Davis KR, Ecker JR, Jones AM. 2003. The β-subunit of the arabidopsis G protein negatively regulates auxin-induced cell division and affects multiple developmental processes. Plant Cell **15**, 393–409.

Vaahtera L, Schulz J, Hamann T. 2019. Cell wall integrity maintenance during plant development and interaction with the environment. Nature Plants **5**, 924–932.

Vance RE, Isberg RR, Portnoy DA. 2009. Patterns of Pathogenesis: Discrimination of Pathogenic and Nonpathogenic Microbes by the Innate Immune System. Cell Host and Microbe **6**, 10–21.

Vaughn LM, Masson PH. 2011. A QTL study for regions contributing to Arabidopsis

thaliana root skewing on tilted surfaces. G3: Genes, Genomes, Genetics **1**, 105–115.

Veluchamy S, Hind SR, Dunham DM, Martin GB, Panthee DR. 2014. Natural Variation for Responsiveness to flg22, flgII-28, and csp22 and Pseudomonas syringae pv. tomato in Heirloom Tomatoes (D Arnold, Ed.). PLoS ONE **9**, e106119.

Vetter MM, Kronholm I, He F, Häweker H, Reymond M, Bergelson J, Robatzek S, De Meaux J. 2012. Flagellin perception varies quantitatively in arabidopsis thaliana and its relatives. Molecular Biology and Evolution **29**, 1655–1667.

Vie AK, Najafi J, Liu B, Winge P, Butenko MA, Hornslien KS, Kumpf R, Aalen RB, Bones AM, Brembu T. 2015*a*. The *IDA/IDA-LIKE* and *PIP/PIP-LIKE* gene families in *Arabidopsis* : phylogenetic relationship, expression patterns, and transcriptional effect of the PIPL3 peptide. Journal of Experimental Botany **66**, 5351–5365.

Vie AK, Najafi J, Liu B, Winge P, Butenko MA, Hornslien KS, Kumpf R, Aalen RB, Bones AM, Brembu T. 2015*b*. The IDA/IDA-LIKE and PIP/PIP-LIKE gene families in Arabidopsis: phylogenetic relationship, expression patterns, and transcriptional effect of the PIPL3 peptide. Journal of experimental botany **66**, 5351–65.

Vie AK, Najafi J, Winge P, Cattan E, Wrzaczek M, Kangasjärvi J, Miller G, Brembu T, Bones AM. 2017. The IDA-LIKE peptides IDL6 and IDL7 are negative modulators of stress responses in Arabidopsis thaliana. Journal of Experimental Botany **68**, 3557–3571.

Waese J, Fan J, Pasha A, *et al.* 2017. ePlant: Visualizing and Exploring Multiple Levels of Data for Hypothesis Generation in Plant Biology. The Plant Cell **29**, 1806–1821.

Walker JC, Zhang R. 1990. Relationship of a putative receptor protein kinase from maize to the S-locus glycoproteins of Brassica. Nature **345**, 743–6.

Wan J, Tanaka K, Zhang X-C, Son GH, Brechenmacher L, Nguyen THN, Stacey G. 2012. LYK4, a lysin motif receptor-like kinase, is important for chitin signaling and plant innate immunity in Arabidopsis. Plant physiology **160**, 396–406.

Wan J, Zhang XC, Neece D, Ramonell KM, Clough S, Kim SY, Stacey MG, Stacey G. 2008. A LysM receptor-like kinase plays a critical role in chitin signaling and fungal resistance in Arabidopsis. Plant Cell **20**, 471–481.

Wan W, Zhang L, Pruitt R, *et al.* 2019. Comparing Arabidopsis receptor kinase and receptor protein-mediated immune signaling reveals BIK1-dependent differences. New Phytologist **221**, 2080–2095.

Wang L, Albert M, Einig E, Fürst U, Krust D, Felix G. 2016*a*. The pattern-recognition receptor CORE of Solanaceae detects bacterial cold-shock protein. Nature Plants **2**, 16185.

Wang X, Chory J. 2006. Brassinosteroids Regulate Dissociation of BKI1, a Negative Regulator of BRI1 Signaling, from the Plasma Membrane. Science **313**, 1118–1122.

Wang L, Einig E, Almeida-Trapp M, Albert M, Fliegmann J, Mithöfer A, Kalbacher H, Felix G. 2018*a*. The systemin receptor SYR1 enhances resistance of tomato against herbivorous insects. Nature Plants **4**, 152–156.

Wang J, Grubb LE, Wang J, *et al.* 2018*b*. A Regulatory Module Controlling Homeostasis of a Plant Immune Kinase. Molecular Cell **69**, 493-504.e6.

Wang X, Hou S, Wu Q, Lin M, Acharya BR, Wu D, Zhang W. 2017*a*. IDL6-HAE/HSL2 impacts pectin degradation and resistance to *Pseudomonas syringae* pv tomato DC3000 in Arabidopsis leaves. The Plant Journal **89**, 250–263.

Wang J, Jiang J, Wang J, Chen L, Fan S-L, Wu J-W, Wang X, Wang Z-X. 2014. Structural insights into the negative regulation of BRI1 signaling by BRI1-interacting protein BKI1. Cell Research **24**, 1328–1341.

Wang X, Kota U, He K, Blackburn K, Li J, Goshe MB, Huber SC, Clouse SD. 2008.

Sequential Transphosphorylation of the BRI1/BAK1 Receptor Kinase Complex Impacts Early Events in Brassinosteroid Signaling. Developmental Cell **15**, 220–235.

Wang J, Lee C, Replogle A, Joshi S, Korkin D, Hussey R, Baum TJ, Davis EL, Wang X, Mitchum MG. 2010. Dual roles for the variable domain in protein trafficking and host-specific recognition of Heterodera glycines CLE effector proteins. New Phytologist **187**, 1003–1017.

Wang J, Li H, Han Z, Zhang H, Wang T, Lin G, Chang J, Yang W, Chai J. 2015. Allosteric receptor activation by the plant peptide hormone phytosulfokine. Nature **525**, 265–268.

Wang C, Li J, Yuan M. 2007. Salt tolerance requires cortical microtubule reorganization in Arabidopsis. Plant and Cell Physiology **48**, 1534–1547.

Wang T, Liang L, Xue Y, Jia P-F, Chen W, Zhang M-X, Wang Y-C, Li H-J, Yang W-C. 2016*b*. A receptor heteromer mediates the male perception of female attractants in plants. Nature **531**, 241–4.

Wang X, Mitchum MG, Gao B, Li C, Diab H, Baum TJ, Hussey RS, Davis EL. 2005. A parasitism gene from a plant-parasitic nematode with function similar to CLAVATA3/ESR (CLE) of Arabidopsis thaliana. Molecular Plant Pathology **6**, 187–191.

Wang YY, Xu Y, Sun Y, *et al.* 2018*c*. Leucine-rich repeat receptor-like gene screen reveals that Nicotiana RXEG1 regulates glycoside hydrolase 12 MAMP detection. Nature Communications **9**, 594.

Wang C, Zhou M, Zhang X, Yao J, Zhang Y, Mou Z. 2017*b*. A lectin receptor kinase as a potential sensor for extracellular nicotinamide adenine dinucleotide in arabidopsis thaliana. eLife **6**.

Wang ZY, Zhu JY, Sae-Seaw J. 2013. Brassinosteroid signaling. Development (Cambridge) **140**, 1615–1620.

Waszczak C, Carmody M, Kangasjärvi J. 2018. Reactive Oxygen Species in Plant Signaling. Annual Review of Plant Biology **69**, 209–236.

Weber E, Engler C, Gruetzner R, Werner S, Marillonnet S. 2011. A modular cloning system for standardized assembly of multigene constructs (J Peccoud, Ed.). PLoS ONE **6**, e16765.

Whitford R, Fernandez A, Tejos R, *et al.* 2012. GOLVEN Secretory Peptides Regulate Auxin Carrier Turnover during Plant Gravitropic Responses. Developmental Cell **22**, 678–685.

Widjaja M, Harvey KL, Hagemann L, *et al.* 2017. Elongation factor Tu is a multifunctional and processed moonlighting protein. Scientific Reports **7**, 11227.

Wilkins O, Nahal H, Foong J, Provart NJ, Campbell MM. 2009. Expansion and diversification of the Populus R2R3-MYB family of transcription factors. Plant Physiology **149**, 981–993.

Willmann R, Lajunen HM, Erbs G, *et al.* 2011. Arabidopsis lysin-motif proteins LYM1 LYM3 CERK1 mediate bacterial peptidoglycan sensing and immunity to bacterial infection. Proceedings of the National Academy of Sciences **108**, 19824–19829.

Winter D, Vinegar B, Nahal H, Ammar R, Wilson G V, Provart NJ. 2007. An 'Electronic Fluorescent Pictograph' browser for exploring and analyzing large-scale biological data sets. PloS one **2**, e718.

Wolf S. 2017. Plant cell wall signalling and receptor-like kinases. Biochemical Journal **474**, 471–492.

Wolf S, van der Does D, Ladwig F, *et al.* 2014. A receptor-like protein mediates the response

to pectin modification by activating brassinosteroid signaling. Proceedings of the National Academy of Sciences of the United States of America **111**, 15261–6.

Wolf S, Hématy K, Höfte H. 2012*a*. Growth control and cell wall signalling in plants. Annual review of plant biology **63**, 381–407.

Wolf S, Höfte H. 2014. Growth control: A saga of cell walls, ROS, and peptide receptors. Plant Cell **26**, 1848–1856.

Wolf S, Mravec J, Greiner S, Mouille G, Höfte H. 2012*b*. Plant cell wall homeostasis is mediated by brassinosteroid feedback signaling. Current Biology **22**, 1732–1737.

Wong JEMM, Nadzieja M, Madsen LH, *et al.* 2019. A Lotus japonicus cytoplasmic kinase connects Nod factor perception by the NFR5 LysM receptor to nodulation. Proceedings of the National Academy of Sciences of the United States of America **116**, 14339–14348.

Wu A, Allu AD, Garapati P, *et al.* 2012. JUNGBRUNNEN1, a reactive oxygen species-responsive NAC transcription factor, regulates longevity in Arabidopsis. Plant Cell **24**, 482–506.

Wu Y, Xun Q, Guo Y, Zhang J, Cheng K, Shi T, He K, Hou S, Gou X, Li J. 2016. Genome-Wide Expression Pattern Analyses of the Arabidopsis Leucine-Rich Repeat Receptor-Like Kinases. Molecular plant **9**, 289–300.

Xi L, Wu XN, Gilbert M, Schulze WX. 2019. Classification and Interactions of LRR Receptors and Co-receptors Within the Arabidopsis Plasma Membrane – An Overview. Frontiers in Plant Science **10**, 472.

Xiao Y, Stegmann M, Han Z, DeFalco TA, Parys K, Xu L, Belkhadir Y, Zipfel C, Chai J. 2019. Mechanisms of RALF peptide perception by a heterotypic receptor complex. Nature **572**, 270–274.

Xin X-F, Nomura K, Aung K, Velásquez AC, Yao J, Boutrot F, Chang JH, Zipfel C, He SY. 2016. Bacteria establish an aqueous living space in plants crucial for virulence. Nature **539**, 524–529.

Xu C, Liberatore KL, MacAlister CA, *et al.* 2015. A cascade of arabinosyltransferases controls shoot meristem size in tomato. Nature Genetics **47**, 784–792.

Xu S-L, Rahman A, Baskin TI, Kieber JJ. 2008. Two leucine-rich repeat receptor kinases mediate signaling, linking cell wall biosynthesis and ACC synthase in Arabidopsis. The Plant cell **20**, 3065–79.

Xue D-X, Li C-L, Xie Z-P, Staehelin C. 2019. LYK4 is a component of a tripartite chitin receptor complex in Arabidopsis thaliana. Journal of Experimental Botany.

Yadeta KA, Elmore JM, Creer AY, Feng B, Franco JY, Rufian JS, He P, Phinney B, Coaker G. 2017. A cysteine-rich protein kinase associates with a membrane immune complex and the cysteine residues are required for cell death. Plant Physiology **173**, 771–787.

Yamada K, Yamaguchi K, Shirakawa T, *et al.* 2016*a*. The Arabidopsis CERK 1-associated kinase PBL 27 connects chitin perception to MAPK activation . The EMBO Journal **35**, 2468–2483.

Yamada K, Yamashita-Yamada M, Hirase T, *et al.* 2016*b*. Danger peptide receptor signaling in plants ensures basal immunity upon pathogen-induced depletion of BAK1. The EMBO Journal **33**, 1438–1453.

Yamada K, Yamashita-Yamada M, Hirase T, *et al.* 2016*c*. Danger peptide receptor signaling in plants ensures basal immunity upon pathogen-induced depletion of BAK1. The EMBO Journal **33**, 1438–1453.

Yamaguchi Y, Huffaker A, Bryan AC, Tax FE, Ryan CA. 2010. PEPR2 Is a Second Receptor for the Pep1 and Pep2 Peptides and Contributes to Defense Responses in

Arabidopsis. The Plant Cell **22**, 508–522.

Yamaguchi Y, Pearce G, Ryan CA. 2006. The cell surface leucine-rich repeat receptor for AtPep1, an endogenous peptide elicitor in Arabidopsis, is functional in transgenic tobacco cells. Proceedings of the National Academy of Sciences of the United States of America **103**, 10104–9.

Yan L, Ma Y, Liu D, *et al.* 2012. Structural basis for the impact of phosphorylation on the activation of plant receptor-like kinase BAK1. Cell Research **22**, 1304–1308.

Yan H, Zhao Y, Shi H, Li J, Wang Y, Tang D. 2018. BRASSINOSTEROID-SIGNALING kinase1 phosphorylates MAPKKK5 to regulate immunity in arabidopsis. Plant Physiology **176**, 2991–3002.

Yang X, Wang B, Farris B, Clark G, Roux SJ. 2015. Modulation of Root Skewing in Arabidopsis by Apyrases and Extracellular ATP. Plant and Cell Physiology **56**, 2197–2206.

Yeh Y-H, Panzeri D, Kadota Y, *et al.* 2016. The Arabidopsis Malectin-Like/LRR-RLK IOS1 Is Critical for BAK1-Dependent and BAK1-Independent Pattern-Triggered Immunity. The Plant cell **28**, 1701–21.

Yin Y, Wang Z-Y, Mora-Garcia S, Li J, Yoshida S, Asami T, Chory J. 2002. BES1 Accumulates in the Nucleus in Response to Brassinosteroids to Regulate Gene Expression and Promote Stem Elongation. Cell **109**, 181–191.

Yu M, Cui Y, Zhang X, Li R, Lin J. 2019*a*. Organization and dynamics of functional plant membrane microdomains. Cellular and Molecular Life Sciences.

Yu X, Feng B, He P, Shan L. 2017. From Chaos to Harmony: Responses and Signaling upon Microbial Pattern Recognition. Annual Review of Phytopathology **55**, 109–137.

Yu X, Xu G, Li B, *et al.* 2019*b*. The Receptor Kinases BAK1/SERK4 Regulate Ca2+ Channel-Mediated Cellular Homeostasis for Cell Death Containment. Current Biology **29**, 3778-3790.e8.

Yuan M, Jiang Z, Bi G, Nomura K, Liu M, He S, Zhou J-M, Xin X-F. 2020. Pattern-recognition receptors are required for NLR-mediated plant immunity. bioRxiv.

Yun HS, Bae YH, Lee YJ, Chang SC, Kim S-K, Li J, Nam KH. 2009. Analysis of phosphorylation of the BRI1/BAK1 complex in arabidopsis reveals amino acid residues critical for receptor formation and activation of BR signaling. Molecules and Cells **27**, 183–190.

Zhang M, Chiang YH, Toruño TY, *et al.* 2018*a*. The MAP4 Kinase SIK1 Ensures Robust Extracellular ROS Burst and Antibacterial Immunity in Plants. Cell Host and Microbe **24**, 379-391.e5.

Zhang W, Fraiture M, Kolb D, Löffelhardt B, Desaki Y, Boutrot FFG, Tör M, Zipfel C, Gust AA, Brunner F. 2013. Arabidopsis receptor-like protein30 and receptor-like kinase suppressor of BIR1-1/EVERSHED mediate innate immunity to necrotrophic fungi. The Plant cell **25**, 4227–41.

Zhang L, Kars I, Essenstam B, Liebrand TWH, Wagemakers L, Elberse J, Tagkalaki P, Tjoitang D, van den Ackerveken G, van Kan JAL. 2014. Fungal endopolygalacturonases are recognized as microbe-associated molecular patterns by the arabidopsis receptor-like protein RESPONSIVENESS TO BOTRYTIS POLYGALACTURONASES1. Plant physiology **164**, 352–64.

Zhang J, Li W, Xiang T, *et al.* 2010. Receptor-like cytoplasmic kinases integrate signaling from multiple plant immune receptors and are targeted by a Pseudomonas syringae effector. Cell Host and Microbe **7**, 290–301.

Zhang Q, Li Y, Xu T, *et al.* 2016*a*. The chromatin remodeler DDM1 promotes hybrid vigor

by regulating salicylic acid metabolism. Cell Discovery **2**, 16027.

Zhang H, Lin X, Han Z, Qu L-J, Chai J. 2016*b*. Crystal structure of PXY-TDIF complex reveals a conserved recognition mechanism among CLE peptide-receptor pairs. Cell Research **26**, 543–555.

Zhang X, Liu W, Nagae TT, Takeuchi H, Zhang H, Han Z, Higashiyama T, Chai J. 2017. Structural basis for receptor recognition of pollen tube attraction peptides. Nature Communications **8**.

Zhang X, Mou Z. 2009. Extracellular pyridine nucleotides induce *PR* gene expression and disease resistance in Arabidopsis. The Plant Journal **57**, 302–312.

Zhang L, Shi X, Zhang Y, *et al.* 2019. CLE9 peptide-induced stomatal closure is mediated by abscisic acid, hydrogen peroxide, and nitric oxide in Arabidopsis thaliana. Plant Cell and Environment **42**, 1033–1044.

Zhang N, Zhang D, Chen SL, Gong BQ, Guo Y, Xu L, Zhang XN, Li JF. 2018*b*. Engineering artificial microRNAs for multiplex gene silencing and simplified transgenic screen. Plant Physiology **178**, 989–1001.

Zhao C, Zayed O, Yu Z, Jiang W, Zhu P, Hsu CC, Zhang L, Andy Tao W, Lozano-Durán R, Zhu JK. 2018. Leucine-rich repeat extensin proteins regulate plant salt tolerance in Arabidopsis. Proceedings of the National Academy of Sciences of the United States of America **115**, 13123–13128.

Zheng B, Bai Q, Wu L, Liu H, Liu Y, Xu W, Li G, Ren H, She X, Wu G. 2019. EMS1 and BRI1 control separate biological processes via extracellular domain diversity and intracellular domain conservation. Nature Communications **10**, 4165.

Zhong S, Liu M, Wang Z, *et al.* 2019. Cysteine-rich peptides promote interspecific genetic isolation in Arabidopsis. Science **364**, eaau9564.

Zhou F, Guo Y, Qiu L-J. 2016. Genome-wide identification and evolutionary analysis of leucine-rich repeat receptor-like protein kinase genes in soybean. BMC Plant Biology **16**.

Zhou J, Liu D, Wang P, *et al.* 2018. Regulation of Arabidopsis brassinosteroid receptor BRI1 endocytosis and degradation by plant U-box PUB12/PUB13-mediated ubiquitination. Proceedings of the National Academy of Sciences of the United States of America **115**, E1906–E1915.

Zhou P, Silverstein KAT, Gao L, Walton JD, Nallu S, Guhlin J, Young ND. 2013. Detecting small plant peptides using SPADA (Small Peptide Alignment Discovery Application). BMC Bioinformatics **14**, 335.

Zhou J, Wu S, Chen X, Liu C, Sheen J, Shan L, He P. 2014. The Pseudomonas syringae effector HopF2 suppresses Arabidopsis immunity by targeting BAK1. Plant Journal **77**, 235–245.

Ziemann S, Van Der Linde K, Lahrmann U, *et al.* 2018. An apoplastic peptide activates salicylic acid signalling in maize. Nature Plants **4**, 172–180.

Zimmermann P, Hirsch-Hoffmann M, Hennig L, Gruissem W. 2004. GENEVESTIGATOR. Arabidopsis microarray database and analysis toolbox. Plant physiology **136**, 2621–32.

Zipfel C. 2014. Plant pattern-recognition receptors. Trends in Immunology **35**, 345–351.

Zipfel C, Kunze G, Chinchilla D, Caniard A, Jones JDG, Boller T, Felix G. 2006. Perception of the bacterial PAMP EF-Tu by the receptor EFR restricts Agrobacterium-mediated transformation. Cell **125**, 749–60.

Zipfel C, Oldroyd GED. 2017. Plant signalling in symbiosis and immunity. Nature **543**, 328–336.

Zipfel C, Robatzek S, Navarro L, Oakeley EJ, Jones JDG, Felix G, Boller T. 2004. Bacterial disease resistance in Arabidopsis through flagellin perception. Nature **428**, 764–767.

Zoulias N, Harrison EL, Casson SA, Gray JE. 2018. Molecular control of stomatal development. Biochemical Journal **475**, 441–454.

Appendices

Chimeric	Primer	Purpose
EFRecto:MIK2	GCCTCTGTCAGTTAGAAAGAAAATCATCTACATACTAGTTCCGATCATCG	Chimeric receptors
	CGATGATCGGAACTAGTATGTAGATGATTTTCTTTCTAACTGACAGAGGC	Chimeric receptors
EFRecto:MIK2-like	GCCTCTGTCAGTTAGAAAGAAACTTGTTGTGTGGATATTAGTGCC	Chimeric receptors
	GGCACTAATATCCACACAACAAGTTTCTTTCTAACTGACAGAGGC	Chimeric receptors
EFRecto:AT5G39390	GCCTCTGTCAGTTAGAAAGAAAAAAGTTGCCGTTGGTGTAGGTGTAGC	Chimeric receptors
	GCTACACCTACACCAACGGCAACTTTTTTCTTTCTAACTGACAGAGGC	Chimeric receptors
EFRecto:XII2	GCCTCTGTCAGTTAGAAAGAAAGTTCTTCTACCGGTTCTGTTATCG	Chimeric receptors
	CGATAACAGAACCGGTAGAAGAACTTTCTTTCTAACTGACAGAGGC	Chimeric receptors
EFRecto:XPS1	GCCTCTGTCAGTTAGAAAGAAAATTTGTGTCAGTGCAGTTATGGCAGC	Chimeric receptors
	GCTGCCATAACTGCACTGACACAAATTTTCTTTCTAACTGACAGAGGC	Chimeric receptors
EFRecto:XII3	GCCTCTGTCAGTTAGAAAGAAAGTTGCGATTGGGGTCAGCGTAGGC	Chimeric receptors
	GCCTACGCTGACCCCAATCGCAACTTTCTTTCTAACTGACAGAGGC	Chimeric receptors
EFRecto:XII5	GCCTCTGTCAGTTAGAAAGAAAATTGGAGTTAGCGTAGGCATAACTTTGC	Chimeric receptors
	GCAAAGTTATGCCTACGCTAACTCCAATTTTCTTTCTAACTGACAGAGGC	Chimeric receptors
EFRecto:XII6	CCTCTGTCAGTTAGAAAGAAAATTTTAGTAAGCATAGGCATAGCTTTGC	Chimeric receptors
	GCAAAGCTATGCCTATGCTTACTAAAATTTTCTTTCTAACTGACAGAGG	Chimeric receptors
EFRecto:BRI1	GCCTCTGTCAGTTAGAAAGAAAGCTGGTAGTGTGGCGATGGGATTG	Chimeric receptors
	CAATCCCATCGCCACACTACCAGCTTTCTTTCTAACTGACAGAGGC	Chimeric receptors
EFRecto:FLS2	GCCTCTGTCAGTTAGAAAGAAAGTCATCCTGATTATTCTTGGATCAGC	Chimeric receptors
	GCTGATCCAAGAATAATCAGGATGACTTTCTTTCTAACTGACAGAGGC	Chimeric receptors
MIK2:EFR	CACAAGGATCGAAACCTAGTTGTCAGTGGTATTTGTATAGGTATAGC	Chimeric receptors
	CCACTGACAACTAGGTTTCGATCCTTGTGTGATTTCTTTGAGG	Chimeric receptors
sobir1-13	TAGGGCATACAATGCTGAAGC	PCR
	TCAAGAACTAATGTGGCCAGC	PCR

bak1-4	TCAGGTTTTGCATCCTGCTCC	PCR
	TCATCATTCGCGAGGCGAGC	PCR
bak1-5€	AAGAGGGCTTGCGTATTTACATGATCATC	PCR
	GACCAATTGTCCCACGCACTG	PCR
bak1-1	GCAACTTGGTCAGCTTCCAAACTTGC	PCR
	GCTCACCAATTCCGTCAGATTTCC	PCR
bak1-3	GCACTGAAAAACAGTTTAGCCGACCC	PCR
	GAATTTCATTCTTCCAGAACCAAATCG	PCR
mik2-1	ATGAACCGTTTCTCTGGAACC	PCR
	TTTGACTTTGTTCCCAGTTGG	PCR
mik2-2	CAAAGGGAATAGTTTCTCCGG	PCR
	TTTGTAGACTTTGCCGTGTCC	PCR
mik2-3	AATATCACGGTGAACAATCGC	PCR
	GATTCAGTTCCGAAATACCCC	PCR
mik2-4	CTTGGGTCAATCCAAACACAAGCAGC	PCR
	TTTGACTTTGTTCCCAGTTGG	PCR
efr-1	TTGCCAATATCTCAAGCCTTG	PCR
	AAACACTCCTGTTGTTGGCAC	PCR
fls2c	TATGGCTGGAGACAGAACACC	PCR
	TCCATCAAGACAGCTAATGAGC	PCR
mik2-like-1	AAGGAAGAAGGAATTGAACCG	PCR
	ATTTTGTTACGGAAAGTTGCG	PCR
mik2-like-2	AGACTTTGCTGTATCCTCCGG	PCR
	TCGTGTTAACCACCTCTCTGG	PCR
xii2-1	ACCACACGGCAATTATAAACG	PCR
	ACTGAAGTTGTGGCATCTTGC	PCR
xii2-4	GAATAATCACCTAACCGGCGAAATCC	PCR
	CGTAGTGATGATCCTGATCAAGTTCC	PCR
xii3-1	TAGGCATTTTGCAATTGCTTC	PCR
	TGCAAATGGGAGCAATTAGTC	PCR
xps1-2	CTAACAGGGAAGTTTCCTGCC	PCR
	TCTTATATCTGGAATGGGCCC	PCR
xps1-3	GAATAATCTGCATACCGCAGG	PCR
	TGGAAAGTGTCTCTGGAATGG	PCR
xps1-4	CCAAGTCTAATGTTTGCAGGC	PCR
	GACTCCCTGCCTCTCTGTAGC	PCR
xii5-1	ATGCTTCTTCACCACAGATGG	PCR
	GGAGGGAATTATTTCACAGGG	PCR
xii5-2	AGAAAAACATACCCATTCCCG	PCR
	GCTTGCCTATCAGTTTCATCG	PCR
xii6-1	CAATGAACAAATTCTTTGGCG	PCR
	TGAAAATTTCCTTTGGAAGGC	PCR
xii6-2	GTGAAGAATCGCTTTGTCTGC	PCR
	TGCTGTTGGTCATAGCTTCG	PCR
pepr1-1	TTTCACCTGTCAATCCGTTTC	PCR

	TCGTTTCGGATCACCTAATTG	PCR
pepr2-3	ACGGTGAACAAAATACGAACG	PCR
	TCTCAGATCTGCGGATAGCTC	PCR
sid2-1$	GCTCTGCAGCTTCAATGC	PCR
	CGAAGAAATGAAGAGCTTGG	PCR
ndr1-1	GTGTGTCCTACTGAGTC	PCR
	AGGTGAGACCAGCTGTGA	PCR
eds1-2¥	ACACAAGGGTGATGCGAGACA	PCR
	GGCTTGTATTCATCTTCTATCC	PCR
	GTGGAAACCAAATTTGACATTAG	PCR
SALK_LB	ATTTTGCCGATTTCGGAAC	PCR
SAIL_LB	TAGCATCTGAATTTCATAACCAATCTCGATACAC	PCR
GABI_LB	CCCATTTGGACGTGAATGTAGACAC	PCR
FLAG_LB	CGTGTGCCAGGTGCCCACGGAATAGT	PCR
M13 Fw	GTAAAACGACGGCCAG	PCR
M13 Rv	CAGGAAACAGCTATGAC	PCR
At2g24130	CACCATGGATTATTGTTCTTTGTTGGTTGTCTCG	gateway entry cloning
	TGAACTAGCTTCTCCTTGTGTTTCTTGAG	gateway entry cloning
AT3G47110	CACCATGGGGGTTCCTTGTATTGTTATGAGAC	gatway entry cloning
	AGTCTCCTCGTCTCTGAAAAAACTTTCTCTG	gatway entry cloning

Appendix table 1 Oligonucleotides used in this study for non qRT-PCR purposes

€ CAPS marker NruI (WT =149bp *bak1-5* =179bp)

$ CAPS marker TruI1

¥ PCR genotyping of *eds1-2*, multiplex PCR Wt: 1500 bp + 750 bp Mut: 1500 bp + 600 np

Target	Primer sequence	Reference
UBOX	TGCGCTGCCAGATAATACACTATT	(Segonzac *et al.*, 2011)
	TGCTGCCCAACATCAGGTT	
FRK1	ATCTTCGCTTGGAGCTTCTC	(He *et al.*, 2006)
	TGCAGCGCAAGGACTAGAG	
AT1G51890	CCAGTTTGTTCTGTAATACTCAGG	(He *et al.*, 2006)
	CTAGCCGACTTTGGGCTATC	
CYP81F2	AATGGAGAGAGCAACACAATG	(He *et al.*, 2006)
	ATACTGAGCATGAGCCCTTTG	
PROPEP3	CTCTTGAAGTGTTCCGGTCTCG	(Wu *et al.*, 2012)
	TCTTCCTCGCTGTGTGATGACG	
WRKY30	TCTCGGAGCCAAATTTCCAAGAGG	(Zhang *et al.*, 2016*a*)
	TCCTCGGTAACTGATCTCAAGGAG	
AT3G02840	ACGCTTTGATCGTTCCTCTTCTGG	(Wu *et al.*, 2012)
	CGAACATTGTGTCGCGAGATCC	
PEPR2	TCGGATTGGCTCGGATTCTAGATG	This publication
	TCTGGTGCAATGTACCCAGTTG	
PEPR1	ATTCTCGTGGACGAGCTTCTGG	(Zhang *et al.*, 2018*b*)
	TGCCAGTTCCGTCACTTGCATC	
AT1G58225	CCACTGGAGGTTTCTTTGCTGTCG	This publication
	CCGTTTGCCAAATTTCCACTGAGG	
AT5G24240	GGACAGCCTGTTTCAGTAGATGGC	This publication
	AGCTCCTTCACCAACCTGTGTG	
SAUR15	TTGAGGAGTTTCTTGGGTGCTAAG	(Chapman *et al.*, 2012)
	GCCATGAATCCTCTTGGTGTCG	
OPRF	AACTGAAAAACACCTTGGGC	(Ross and Somssich, 2016)
	CCTGGGTTGTTGAAGTGGTA	
AT4G26410	GAGCTGAAGTGGCTTCCATGAC	(Ross and Somssich, 2016)
	GGTCCGACATACCCATGATCC	
UBC21	AAAGGACCTTCGGAGACTCCTTACG	(Delgado-Cerezo *et al.*, 2012)
	GGTCAAGAATCGAACTTGAGGAGGTT	
PCB-TUBULIN	CAAGTATGTTCCCCGAGCCGT	(Delgado-Cerezo *et al.*, 2012)
	GGTCCCTTCGGTCAGCTCTTC	
AT3G47570	GGCATTGCCGGAAAGAATATTGG	This publication
	CAACAACAGGGAAACCGACTCTG	
AT3G47090	CATGTTAGCGACTTCGGTCTCG	This publication
	TTCCATATTCTGGTGCGGCATAC	
AT3G47580	TTTGGTCTGGCTCGGCTTCTAC	This publication
	CCGGCTGAGCTTAGTTGGTTAAGG	

Appendix table 2 Primers used for qRT-PCR

Probe	AGI	pvalue	FC log2	Gene symbol	Gene description ARAPORT11
A_84_P 19804	AT5G19880	0.000	5.1		Peroxidase superfamily protein;(source:Araport11)
A_84_P 544532	AT1G58225	0.000	5.0		hypothetical protein;(source:Araport11)
A_84_P 826417	AT5G24110	0.000	4.8	WRKY DNA-BINDING PROTEIN 30 (WRKY30)	member of WRKY Transcription Factor; Group III
A_84_P 848499	AT5G35935	0.000	4.7		transposable_element_gene
A_84_P 786320	AT5G35935	0.000	4.6		transposable_element_gene
A_84_P 76184	AT5G24110	0.000	4.5	WRKY DNA-BINDING PROTEIN 30 (WRKY30)	member of WRKY Transcription Factor; Group III
A_84_P 764897	AT4G28420	0.000	4.5		Tyrosine transaminase family protein;(source:Araport11)
A_84_P 558934	AT3G12910	0.000	4.2		NAC (No Apical Meristem) domain transcriptional regulator superfamily protein;(source:Araport11)
A_84_P 23967	AT2G29100	0.000	3.8	GLUTAMATE RECEPTOR 2.9 (GLR2.9)	member of Putative ligand-gated ion channel subunit family
A_84_P 10997	AT4G23310	0.000	3.7	CRK23	Encodes a cysteine-rich receptor-like protein kinase.
A_84_P 24055	AT3G28890	0.000	3.7	RECEPTOR LIKE PROTEIN 43 (RLP43)	receptor like protein 43;(source:Araport11)
A_84_P 553463	AT2G19405	0.000	3.6		transmembrane protein;(source:Araport11)
A_84_P 15382	AT2G30770	0.001	3.6	CYP71A13	putative cytochrome P450
A_84_P 1465049	AT1G14880	0.007	3.5	PLANT CADMIUM RESISTANCE 1(PCR1)	PLANT CADMIUM RESISTANCE 1;(source:Araport11)
A_84_P 10728	AT2G29110	0.000	3.5	GLUTAMATE RECEPTOR 2.8 (GLR2.8)	member of Putative ligand-gated ion channel subunit family
A_84_P 555128	AT1G59915	0.000	3.5		cryptdin protein-like protein;(source:Araport11)
A_84_P 857638	AT2G30770	0.002	3.4	CYP71A13	putative cytochrome P450
A_84_P 16454	AT1G26410	0.001	3.4	(ATBBE6)	FAD-binding Berberine family protein;(source:Araport11)
A_84_P 753747	AT1G51913	0.000	3.4		transmembrane protein;(source:Araport11)
A_84_P 13831	AT4G23150	0.000	3.4	CRK7	Encodes a cysteine-rich receptor-like protein kinase.
A_84_P 19697	AT1G47890	0.000	3.3	RECEPTOR LIKE PROTEIN 7 (RLP7)	receptor like protein 7;(source:Araport11)
A_84_P 179234	AT5G46770	0.017	3.2		hypothetical protein;(source:Araport11)
A_84_P 12162	AT1G29680	0.010	3.1		histone acetyltransferase (DUF1264);(source:Araport11)
A_84_P 22793	AT1G15610	0.015	3.1		transmembrane protein;(source:Araport11)
A_84_P 18663	AT5G05340	0.000	3.0	PEROXIDASE 52 (PRX52)	Encodes a protein with sequence similarity to peroxidases that is involved in lignin biosynthesis.
A_84_P 16574	AT3G57260	0.000	3.0	PATHOGENESIS-RELATED PROTEIN 2 (PR2)	beta-1,3-glucanase
A_84_P 16401	AT2G25440	0.002	3.0	RECEPTOR LIKE PROTEIN 20 (RLP20)	receptor like protein 20;(source:Araport11)
A_84_P 10034	AT4G18990	0.000	3.0	XYLOGLUCAN ENDOTRANSGLUCOSYLASE/HYDROLASE 29	xyloglucan endotransglucosylase/hydrolase 29;(source:Araport11)
A_84_P 12057	AT5G08250	0.002	2.9		Cytochrome P450 superfamily protein;(source:Araport11)
A_84_P 14898	AT5G10760	0.000	2.9	APOPLASTIC, EDS1-DEPENDENT 1(AED1)	Eukaryotic aspartyl protease family protein;(source:Araport11)
A_84_P 848817	AT5G10760	0.000	2.9	APOPLASTIC, EDS1-DEPENDENT 1(AED1)	Eukaryotic aspartyl protease family protein;(source:Araport11)
A_84_P 20402	AT4G04510	0.000	2.8	CRK38	Encodes a cysteine-rich receptor-like protein kinase.
A_84_P 507017	AT5G44990	0.004	2.8		Glutathione S-transferase family protein;(source:Araport11)
A_84_P 541841	AT1G51920	0.000	2.8		transmembrane protein;(source:Araport11)
A_84_P 10439	AT1G09080	0.000	2.7	BINDING PROTEIN 3 (BIP3)	Heat shock protein 70 (Hsp 70) family protein;(source:Araport11)

Appendix table 3 Microarray probes showing >4 fold upregulation of cognate transcripts in *mik2*

Probe	AGI	pvalue	FC log2	Gene symbol	Gene description ARAPORT11
A_84_P12174	AT5G54010	0.009	2.7	UDP-GLYCOSYLTRANSFERASE 79B6 (UGT79B6)	Encodes a flavonoid 3-O-glucoside
A_84_P700126	AT2G24165	0.015	2.7		pseudogene of receptor like protein 30;(source:Araport11)
A_84_P23919	AT2G35980	0.000	2.7	YELLOW-LEAF-SPECIFIC GENE 9 (YLS9)	Encodes a protein whose sequence is similar to Arabidopsis non-race specific disease resistance gene (NDR1).
A_84_P757951	AT2G31335	0.005	2.7		hypothetical protein;(source:Araport11)
A_84_P613251	AT3G18250	0.000	2.7		Putative membrane lipoprotein;(source:Araport11)
A_84_P66214	AT3G02840	0.000	2.7		ARM repeat superfamily protein;(source:Araport11)
A_84_P788781	AT1G09080	0.001	2.6	BINDING PROTEIN 3 (BIP3)	Heat shock protein 70 (Hsp 70) family protein;(source:Araport11)
A_84_P502843	AT1G59865	0.000	2.6		transmembrane protein;(source:Araport11)
A_84_P55910	AT4G11070	0.000	2.6	(WRKY41)	member of WRKY Transcription Factor; Group III
A_84_P18466	AT3G57270	0.001	2.6	BETA-1,3-GLUCANASE 1 (BG1)	encodes a member of glycosyl hydrolase family 17
A_84_P22344	AT4G23280	0.000	2.6	CRK20	Encodes a cysteine-rich receptor-like protein kinase.
A_84_P99776	AT3G25010	0.000	2.6	RECEPTOR LIKE PROTEIN 41 (RLP41)	receptor like protein 41;(source:Araport11)
A_84_P18100	AT1G69930	0.000	2.6	GLUTATHIONE S-TRANSFERASE TAU 11 (GSTU11)	Encodes glutathione transferase belonging to the tau class of GSTs.
A_84_P19013	AT1G32960	0.001	2.6	(SBT3.3)	Subtilase family protein;(source:Araport11)
A_84_P16844	AT5G38250	0.000	2.6		Protein kinase family protein;(source:Araport11)
A_84_P850889	AT1G36622	0.000	2.5		transmembrane protein;(source:Araport11)
A_84_P596516	AT4G14450	0.000	2.5	(PH1)	. It interacts with defense related MAP kinase MPK6. It's expression is induced by PAMP elicitors.
A_84_P17305	AT2G40740	0.000	2.5	WRKY DNA-BINDING PROTEIN 55 (WRKY55)	member of WRKY Transcription Factor; Group III
A_84_P737368	AT1G36622	0.000	2.5		transmembrane protein;(source:Araport11)
A_84_P11446	AT1G15520	0.003	2.5	ATP-BINDING CASSETTE G40 (ABCG40)	ABC transporter family involved in ABA transport and resistance to lead. Localizes to plasma membrane.
A_84_P502299	AT3G57100	0.001	2.5		transmembrane protein, putative (DUF677);(source:Araport11)
A_84_P826986	AT4G23140	0.000	2.4	CRK6	Arabidopsis thaliana receptor-like protein kinase. Naming convention from Chen et al 2003 (PMID 14756307)
A_84_P19456	AT4G04500	0.006	2.4	CRK37	Encodes a cysteine-rich receptor-like protein kinase.
A_84_P15041	AT5G61890	0.000	2.4	(ERF114)	encodes a member of the ERF (ethylene response factor) subfamily B-4 of ERF/AP2 transcription factor family.
A_84_P188254	AT4G23140	0.000	2.4	CRK6	Arabidopsis thaliana receptor-like protein kinase. Naming convention from Chen et al 2003 (PMID 14756307)
A_84_P559351	AT5G55460	0.000	2.4	(ATLTP4.5)	Bifunctional inhibitor/lipid-transfer protein/seed storage 2S albumin superfamily protein;(source:Araport11)
A_84_P10141	AT5G01550	0.000	2.4	L-TYPE LECTIN RECEPTOR KINASE VI.3 (LECRK-VI.3)	Encodes LecRKA4.2, a member of the lectin receptor kinase subfamily A4
A_84_P22467	AT5G11140	0.002	2.4		phospholipase-like protein (PEARLI 4) family protein;(source:Araport11)
A_84_P23016	AT2G03290	0.008	2.4		emp24/gp25L/p24 family/GOLD family protein;(source:Araport11)
A_84_P836180	AT2G32680	0.001	2.4	RECEPTOR LIKE PROTEIN 23 (RLP23)	receptor like protein 23;(source:Araport11)
A_84_P759766	AT3G42471	0.025	2.4		transposable_element_gene
A_84_P20114	AT2G32680	0.001	2.4	RECEPTOR LIKE PROTEIN 23 (RLP23)	receptor like protein 23;(source:Araport11)
A_84_P837351	AT5G61890	0.000	2.4	(ERF114)	encodes a member of the ERF (ethylene response factor) subfamily B-4 of ERF/AP2 transcription factor family.
A_84_P21007	AT2G43570	0.001	2.4	CHITINASE, PUTATIVE (CHI)	chitinase;(source:Araport11)
A_84_P56360	AT5G57010	0.000	2.4		calmodulin-binding family protein;(source:Araport11)

Probe	AGI	pvalue	FC log2	Gene symbol	Gene description ARAPORT11
A_84_P19294	AT1G26380	0.026	2.1	FAD-LINKED OXIDOREDUCTASE 1(FOX1)	Functions in the biosynthesis of 4-hydroxy indole-3-carbonyl nitrile (4-OH-ICN), a cyanogenic phytoalexin in Arabidopsis.
A_84_P854733	AT3G18250	0.012	2.1		Putative membrane lipoprotein;(source:Araport11)
A_84_P15036	AT5G60900	0.000	2.0	RECEPTOR-LIKE PROTEIN KINASE 1(RLK1)	Encodes a receptor-like protein kinase.
A_84_P842764	AT3G29610	0.004	2.0		transposable_element_gene;(source:Araport11);similar to unknown protein [Arabidopsis thaliana] (TAIR:AT3G31406.1);(source:TAIR10)
A_84_P20237	AT1G26420	0.000	2.0	(ATBBE7)	FAD-binding Berberine family protein;(source:Araport11)
A_84_P21525	AT5G12030	0.006	2.0	HEAT SHOCK PROTEIN 17.6A (HSP17.6A)	Encodes a cytosolic small heat shock protein with chaperone activity that is induced by heat and osmotic stress and is also expressed late in seed development.
A_84_P600850	AT3G28540	0.003	2.0		P-loop containing nucleoside triphosphate hydrolases superfamily protein;(source:Araport11)
A_84_P506229	AT3G22350	0.001	2.0		F-box and associated interaction domains-containing protein;(source:Araport11)
A_84_P800250	AT5G47400	0.002	2.0		sphingomyelin phosphodiesterase;(source:Araport11)
A_84_P553120	AT5G48400	0.001	2.0	(ATGLR12)	member of Putative ligand-gated ion channel subunit family
A_84_P532349	AT3G09520	0.001	2.0	EXOCYST SUBUNIT EXO70 FAMILY PROTEIN H4 (EXO70H4)	A member of EXO70 gene family, putative exocyst subunits, conserved in land plants.

Probe	AGI	pvalue	FC log2	Gene symbol	Gene description ARAPORT11
A_84_P11800	AT3G46340	0.000	-2.00058		Leucine-rich repeat protein kinase family protein;(source:Araport11)
A_84_P21896	ATMG72570	0.003	-2.01111		Integrase-type DNA-binding superfamily protein;(source:Araport11)
A_84_P14420	AT2G41580	0.000	-2.02589		transposable_element_gene
A_84_P23740	ATMG28450	0.039	-2.06708	AGAMOUS-LIKE 58	AGAMOUS-like 58;(source:Araport11)
A_84_P223699	AT3G16580	0.004	-2.07407		F-box and associated interaction domains-containing protein;(source:Araport11)
A_84_P763378	AT4G06635	0.022	-2.07693		transposable_element_gene;(source:Araport11);pseudogene, hypothetical protein;(source:TAIR10)
A_84_P753806	ATMG80183	0.023	-2.10429	ATEFL8	EPIDERMAL PATTERNING FACTOR-like protein;(source:Araport11)
A_84_P839786	AT3G49300	0.029	-2.10497		proline-rich family protein;(source:Araport11)
A_84_P845171	AT5G42800	0.014	-2.11172	DIHYDROFLAVONOL 4-REDUCTASE	dihydroflavonol reductase. Catalyzes the conversion of dihydroquercetin to leucocyanidin in the biosynthesis of anthocyanins.
A_84_P584570	ATMG76210	0.005	-2.12296		DUF241 domain protein, putative (DUF241);(source:Araport11)
A_84_P577086	AT5G38270	0.000	-2.13798	F-BOX/DUF295 BRASSICEAE-SPECIFIC 37	F-box family protein;(source:Araport11)
A_84_P570322	AT2G05915	0.025	-2.18623		hypothetical protein;(source:Araport11)
A_84_P11928	AT4G19800	0.001	-2.22936		Glycosyl hydrolase family protein with chitinase insertion domain-containing protein;(source:Araport11)
A_84_P729072	AT4G14300	0.031	-2.22807	RNA-BINDING GLYCINE-RICH PROTEIN D4	Belongs to a member of the RNA-binding glycine-rich (RBG) gene superfamily.
A_84_P14079	AT5G58460	0.007	-2.22888	CATION/H+ EXCHANGER 25	member of Putative Na+/H+ antiporter family
A_84_P583283	AT5G16330	0.036	-2.29779		NC domain-containing protein-like protein;(source:Araport11)
A_84_P583738	AT2G21450	0.001	-2.37489	CHROMATIN REMODELING 34	chromatin remodeling 34;(source:Araport11)
A_84_P804223	AT5G40260	0.023	-2.44844	SWEET8	Encodes RPG1(RUPTURED POLLEN GRAIN 1), a member of the MtN3/saliva gene family.
A_84_P17198	ATMG71690	0.000	-2.45987		glucuronoxylan 4-O-methyltransferase-like protein (DUF579);(source:Araport11)
A_84_P526497	AT5G35945	0.005	-2.65152		F-box/LRR protein;(source:Araport11)
A_84_P545044	AT5G03090	0.000	-3.19222		Mto 1 responding down protein;(source:Araport11)
A_84_P820294	AT5G67540	0.001	-3.32648		Arabinanase/levansucrase/invertase;(source:Araport11)
A_84_P754704	ATMG53801	0.003	-3.65569		Natural antisense transcript overlaps with AT1G53800;(source:Araport11)
A_84_P19658	AT5G24240	0.000	-4.39813	ATPI4Kgamma3	Encodes PI4Kγ3, localizes to the nucleus and has autophosphorylation activity, but no lipid kinase activity.

Appendix table 4 Microarray probes showing >4 fold down regulation of cognate transcripts in *mik2*